Universitat Autònoma de Barcelona

Departament de Bioquímica i Biologia Molecular
Unitat de Medicina

INc Institut de Neurociències

THE ROLE OF THE PDK1/PKB KINASES IN REGULATING NEURONAL SURVIVAL AND DIFFERENTIATION: CHARACTERIZATION OF THE PDK1 K465E KNOCK-IN MICE

Tinatin Zurashvili

TESIS DOCTORAL

Bellaterra, 2013

Universitat Autònoma de Barcelona

Departament de Bioquímica i Biologia Molecular
Unitat de Medicina

INc Institut de Neurociències

THE ROLE OF THE PDK1/PKB KINASES IN REGULATING NEURONAL SURVIVAL AND DIFFERENTIATION: CHARACTERIZATION OF THE PDK1 K465E KNOCK-IN MICE

Memoria de tesis doctoral presentada por Tinatin Zurashvili para optar al grado de Doctora en Bioquímica y Biología Molecular por la Universitat Autònoma de Barcelona.

Este trabajo ha sido realizado bajo la dirección del Doctor José Ramón Bayascas en la Unitat de Medicina del Departament de Bioquímica i Biologia Molecular y en el Institut de Neurociències de la Universitat Autònoma de Barcelona.

El director, La doctoranda,

Dr. José Ramón Bayascas Tinatin Zurashvili

Bellaterra, 2013

Oh profundidad de las riquezas de la sabiduría y de la ciencia de Dios!
¡Cuán incomprensibles son sus juicios, e inescrutables sus caminos!

(San Pablo, Romanos 11:33)

Acknowledgements

First I would like to express my deepest gratitude to my supervisor Dr. José Bayascas for giving me the opportunity to do my PhD studies in his lab. He has created an excellent environment in the lab and has shared his insights as I hurdle all the obstacles in the completion this research work. His professionalism has been invaluable for my development. I want to thank him for his inspiring guidance, continued support and encouragement throughout my PhD and finally, lots of thanks for the critical and proof-reading of this thesis.

To my present and past lab members who in one way or another contributed and extended their assistance in this work. Special thanks to Lluís Cordón Barris for his collaboration and his huge contribution to my work and Xiang Yu Zhou for many funny times. Lots of thanks to the past lab; Juuli Lamberg, Patricia Ortega, Esther Cabañas, Natalia Gorska, Laura Kempainnen and Anna Santaella for making a friendly working atmosphere.

I am indebted to many people who have helped me technically during my PhD, including Mar Castillo at the Histology Service, Nuria Barba at the Microscopy Service and special thanks to Cristina Gutierrez for the productive work and pleasant company during the long hours spent in the primary cell culture room. Thanks to Roser Pane and Jessica Pairada from the animal facility of the Universitat de Lleida for animal care.

To every investigator and group leader of our department. In particular, I want to thank Victor Yuste, José Lizcano, Carlos Saura for always being welcome on my frequent visits to their labs. I would like to thank all the members of the research groups. Especial thanks to Arnaldo, Sergi for their expert advices to Elsa for Spanish lessons. Lots of thanks, to Gerard for many useful recommendations, to Tatiana and Arantza for their readiness in difficult moments. Thanks to Nabil and the girls of Yuste´s group for making lab and desk lively and cheerful place. Thanks to Alfredo, Bruna, Rut, Mireia and all the former as well as current PhD students of the department for their kindness, understanding and hospitability. Thanks a lot!

I would also like to extend my thanks to the administrative staff of the Institut de Neurociències & Departament de Bioquímica i Biologia Molecular. Thanks for facilitating those administrative tasks which were always ambiguous for me.

During these years I have been supported by a UAB predoctoral fellowship without which this thesis would not have been possible. Throughout the entire process of my PhD studies in UAB I received a lot of support from many people around me who I cannot mention but I express my sincere gratefulness. Joan X. Comella deserves my deep gratitude for his help and the opportunity which he gave to me at the very beginning of my PhD studies.

I would also like to thank my thesis committee for their precious time.

Finally, I wish to thank my family for their support and encouragement throughout my study.

Moltes gràcies a tots!

TABLE OF CONTENTS

SUMMARY

Neuronal cell death programmes are counteracted by survival signals during development in order to maintain the tissue homeostasis. Neuronal differentiation is a mechanism generating functionally integrated neuronal cells from their progenitors. These processes appear to be mediated via activation of the Ras/Raf/MAPK and the PI3K/PDK1/PKB signaling pathways and are associated with a selective increase in protein translation. Protein kinase B (PKB/Akt) is a serine/threonine protein kinase which is claimed to be the critical transducer for several extracellular signals provided by different neurotransmitters, growth factors and hormones that promote phosphoinositide 3-kinase (PI3K) activation. PI3K is a lipid kinase characterized by its ability to phosphorylate the 3-OH group in the inositol ring of phospholipids at the inner side of the plasma membrane to generate phosphatidylinositol-3,4,5-trisphosphate (PtdIns(3,4,5)P3 or PIP3), which is a potent second messenger. PKB regulation by its activator PDK1 precisely relies on a PtdIns(3,4,5)P_3 binding domain, named Pleckstrin Homology domain (PH-domain). Both PDK1 and PKB are protein kinases of the AGC family containing PH-domains which mediate their recruitment to the plasma membrane, where PKB is activated by phosphorylation at two regulatory residues, namely Thr308 at the T-loop by PDK1, and Ser473 at the hydrophobic motif by mTORC2. In fact, PDK1 was shown to be a master kinase also playing an essential role in the activation of a number of AGC family members by phosphorylating their T-loops by means of a PH domain-independent mechanism. Activated PKB modulates the function of numerous substrates involved in the regulation of cell metabolism, survival, proliferation and growth, which deregulation has consequences in pathologies such as diabetes, cancer and neurodegeneration.

The crystal structure high resolution of the PDK1 PH domain revealed that the positively-charged lateral chain of Lysine at position 465 within the PH domain crystal establishes fundamental interactions with the negatively-charged phosphate groups of PIP3. Targeted mutagenesis of Lysine 465 to the negatively-charged aminoacid Glutamic acid abolished binding of PDK1 to PIP3 by disrupting the phosphoinositide binding pocket. Therefore, it was thought that this mutation could be instrumental in ablating this part of the PDK1 signaling pathway. In order to analyze the role of the PDK1-PIP3 interaction in vivo, PDK1$^{K465E/K465E}$ knock-in mice were generated which physiologically express from the endogenous locus a mutant form of PDK1 incapable of phosphoinositide binding. This knock-in mice model was shown to be a good tool to analyse the contributory role of the PKB signaling pathway to

glucose metabolism. The PDK1$^{K465E/K465E}$ mice were shown to be viable but smaller, with a modest reduction in PKB activity compared with the wild type littermates, and prone to diabetes. The importance of this pathway in tumourogenesis has been highlighted by introducing the PDK1 PH domain knock-in mutation into cancer-prone PTEN$^{+/-}$ mice, which resulted in the delayed tumour onset, suggesting that even moderate reduction of PKB activity can significantly delay tumour initiation and development. This makes the PDK1$^{K465E/K465E}$ mutant mouse model an excellent tool to explore the contribution of PKB to different human pathologies and to identify downstream substrates that could provide targets for therapeutic intervention. In particular, I aimed to use this genetic model to unravel the role of PKB on different aspects of brain development and function.

Stereological analysis of embryonic brain sections showed that the PDK1$^{K465E/K465E}$ mice displayed reduced brain size due to a reduction in neuronal cell size rather than cell number, since the number of cortical and hippocampal neuronal populations between PDK1$^{K465E/K465E}$ and PDK1$^{+/+}$ mice was not significantly different, whereas the volume of the mutant neuronal soma was approximately 80% of the volume of the wild type neuronal soma.

Stimulation of cortical neurons with BDNF induced a robust phosphorylation of Trk receptors followed by the phosphorylation of PKB at Thr308 in the PDK1$^{+/+}$ cells, which is blunted in the PDK1$^{K465E/K465E}$ neurons, whereas PKB phosphorylation at the mTORC2 site (Ser473) proceeded normally in both type of cells. The moderate reduction of PKB activation was not rate-limiting for the phosphorylation of those PKB substrates governing neuronal survival and apoptosis such as FOXO and GSK3. Then, it was questioned whether such mutation could affect survival responses in primary neuronal cultures. The findings from this study illustrate that the integrity of the PDK1 PH domain is not essential to support the survival of different embryonic neuronal populations analyzed. Cell viability is compromised after trophic factor deprivation, whilst BDNF treatment rescues cells from death to the same extent in both PDK1$^{+/+}$ and PDK1$^{K465E/K465E}$ neurons.

In contrast, the moderate reduction of PKB activity in the PDK1$^{K465E/K465E}$ neurons markedly reduced phosphorylation of the PRAS40 and TSC2 substrates, leading to decreased mTORC1/S6K activation and also reduced BRSK protein synthesis. The PDK1$^{K465E/K465E}$ neurons in culture showed reduced neurite outgrowth, delayed polarization and deficient axonogenesis. To establish the possible causal relation between the PKB pathway defects and axon formation, the impact of specific pharmacological treatments with PKB and mTORC1 inhibitors on neuronal differentiation were assessed, which provided strong evidence that the

differentiation defects were due to reduced PKB activity and inefficient activation of the mTORC1 signaling. Moreover, the overexpression of BRSK isoforms rescued the axonogenesis defects of the PDK1$^{K465E/K465E}$ hippocampal cells. Altogether, these findings illustrate how the binding of PDK1 to PIP3 creates a PKB signaling threshold which is sufficient to support survival, but not differentiation of neuronal cells. In this regard, there is increasing evidence that PI3K/PDK1 dependent, PKB independent pathways might be responsible for the control of essential cellular processes, for example cell survival, which rely on other members of the AGC family activated by PDK1.

These other PDK1-regulated members of the AGC family include SGK1, S6K and RSK. The activation of these kinases is not dependent on PDK1 binding to PIP3 and therefore they should be normally phosphorylated in the PDK1$^{K465E/K465E}$ knock-in mice neurons. However, I observed decreased phosphorylation of the SGK substrate NDRG1. This study clearly states for the first time, that NDRG1 is regulated by PKB, at least in neurons. Activation of S6K was found also incomplete in the PDK1$^{K465E/K465E}$ neurons due to reduced mTORC1 PKB-dependent activation, which could be overcome by nutrients. In fact, the only PDK1 substrate analyzed that appears to not to be affected by the PDK1 K465E mutation is RSK, which serves as a control of the specificity of this knock-in mutation.

In summary, the data allow to conclude that full activation of PKB is not essential in controlling neuronal survival. In marked contrast, reduced PKB-mediated, mTORC1-dependent, BRSK expression resulting from lack of PDK1-phosphoinositide binding prevents neuronal differentiation.

ABBREVIATIONS

AGC	cAMP-dependent kinase, cGMP-dependent kinase and protein kinase C family of kinases
Bad	Bcl-1/Bcl-XL-associated death domain protein
Bak	Bcl-2 homologous antagonist-killer protein
Bax	Bcl-2-associated X protein
Bcl-2	B-cell CLL/Lymphoma-2
Bcl-xl	Bcl-2 related gene, long isoform
Bim	Bcl-2-interacting mediator of cell death
BDNF	Brain-derived neurotrophic factor
4EBP1	4E-binding protein 1
ERK	extracellular-signal-regulated kinase
IGF1	Insulin-like growth factor 1
IRS	Insulin receptor substrate
IκB	Inhibitor of NF-κB
IKK	IκB kinase
MAPK	Mitogen-activated protein kinase
MCL-1	Myeloid cell leukaemia 1
MDM2	Murine double minute 2
mTOR	mammalian target of rapamycin
NF-κB	Nuclear factor-κ type B
NTs	Neurotrophins
PCD	Programmed cell death
PDK1	3-phosphoinositide-dependent protein kinase 1
PH	Pleckstrin Homology
PI3K	Phosphoinositide 3-kinase (also PI 3-kinase)
PIP2	Phosphatidylinositol-4,5-bisphosphate (also PtdIns(3,4,5)P_2)
PIP3	Phosphatidylinositol-3,4,5-trisphosphate (also PtdIns(3,4,5)P_3)
PKB/Akt	Protein kinase B

PKC	Protein kinase C
PLC-γ	Phospholipase C-γ
PRAS40	Proline-rich Akt Substrate of 40 kD
Raptor	Regulatory-associated protein of mTOR
Rheb	Ras homologue enriched in brain
Rictor	Rapamycin-insensitive companion of mTOR
S6K	p-70 ribosomal S6 protein kinase
Trk	Tropomyosin-related kinase
TSC	Tuberous sclerosis complex

Less frequently used abbreviations are defined upon their first use in the text.

INTRODUCTION

Neurons are fundamental building blocks with a complex morphology that represent an essential functional unit within the nervous system. In higher vertebrates, neuronal cells are generated in excess early during development, and die by programmed cell death, namely apoptosis, which leads to the elimination of as much as half of the originally produced cells. Only the cells that have access to sufficient amount of particular neurotrophic factors will survive into the adulthood. Thus, the final number of neurons is determined during the embryonic development (Oppenheim, 1989). Formation of axon and multiple dendrites is the first critical step in neuronal polarization, an initial process of differentiation which is terminated with synaptic specializations and establishment of functional networks (Craig *et al.*, 1992). Cell-extrinsic and intrinsic programs control the survival and differentiation of neurons. Both processes are directed to adjust the cell number and size of neuronal populations in order to innervate their targets in an appropriate manner. Any alteration on neuronal cell survival or differentiation during development can be translated into different clinical manifestations. Mature neurons have the ability to sustain cell survival in response to neurotrophic factors via mastering intracellular signaling processes that connect the transmembrane survival receptors to the molecular mechanisms that control the expression of genes that are critical for cell death. Neurodegenerative diseases are characterized by the progressive loss of functional neurons in adulthood, whereas the proper development of neurons is vital for the mental health of individuals and perturbations in their connectivity or morphology result in cognitive impairments. Despite the significant progress in the area of characterizing the signaling cascades supporting neuronal cell survival and differentiation, it still remains an interesting and important challenge.

1. NEURONAL CELL FATE DETERMINATION AND DIFFERENTIATION

Morphogenesis of mammalian nervous system requires cell proliferation, death/survival, differentiation and migration. Coordinated regulation of these processes lead to the generation of functionally integrated neurons from progenitor cells. The regulated balance between cell life and death decisions is a mechanism that determines the architecture of the developing nervous system. Programmed cell death (PCD) occurs in many developmental systems including the developing nervous system, where this naturally occurring cell death results in the elimination of poorly differentiated neurons while migrating toward their target locations (de la Rosa and de Pablo, 2000), thereby contributing to critical functions such as removal of damaged and harmful cells with inappropriate synaptic connections and regulation of the number of precursor

populations, which in turn will affect the size and morphology of the resulting neuronal structures (Oppenheim, 1991).

Neurons rely on a highly specialized network of signaling molecules that control development and survival. Both central and peripheral nervous systems employ multiple molecular mechanisms to shape and meet their specific functional demands. Neuronal differentiation is comprised of neuritogenesis, neurite outgrowth, polarization and synaptogenesis. All these processes together set up a broad pattern of neural connectivity and their disruption cause neurodevelopmental disorders. Neuritogenesis begins with the activation of membrane receptors by extracellular cues. An early event in the differentiation process is the sprouting of neurites which will lately become axons and dendrites.

Neuronal polarization involves the initial specification of the axon/dendrite identity of the undifferentiated neurites (Arimura and Kaibuchi, 2007). Establishment of polarity depends greatly on the proteins that interact with key regulators of the actin and microtubule cytoskeletons, since the reorganisation of the cytoskeleton and its asymmetric localization is essential in polarized cells. The polarized morphology of the neuron is crucial for its function, allowing unidirectional neuronal stimuli. Better understanding the molecular mechanisms responsible for neuronal cell fate and differentiation will surely make progenitor cells more suitable for replacement therapies.

1.1. NEURONAL CELL DEATH: APOPTOSIS

Apoptosis or programmed cell death was described in the early 1970`s (Kerr *et al.*, 1972). Apoptosis is the most studied and significant form of programmed cell death (PCD) that relies on a highly regulated process which, together with the generation of new cells, homeostatically maintains tissues and organ size and function within all the multicellular organisms (Buss *et al.*, 2006).

Apoptotic cell death distinguishes from necrosis, a form of traumatic cell death. Apoptotic cells display several morphological features that include cytoplasmic shrinkage, chromatin condensation and nuclear fragmentation (Kerr *et al.*, 1972). Other modes of programmed cell death include autophagy, which involves the degradation of intracellular components through the lysosome (He and Klionsky, 2009). Apoptosis is indispensable for normal embryonic development, which obvious example is vertebrate limb bud development during which apoptosis removes the cells between developing digits (Saunders, Jr., 1966).

Apoptosis occurs during development of the vertebrate nervous system within most populations of proliferating neuronal precursors and has a variety of adaptive functions. About half of the neurons originally generated during development will be lost before completion of the neural architecture (Miguel-Aliaga and Thor, 2009). It also acts as part of a quality control and repair mechanism by eliminating unwanted cells (Davies, 2003). Thus, apoptosis of neuronal progenitor cells is essential for brain formation. A few reports have demonstrated that in some species and regions of the nervous system the mature neurons are likely to undergo programmed cell death that serves for the renewing of the neuronal circuits. This programmed cell death is categorized as compensatory neurogenesis. Perturbation of this process leads to disease and pathology (Buss *et al.*, 2006;Miguel-Aliaga *et al.*, 2009). Increasing evidence suggests that neuronal apoptosis is a prominent feature in the dysfunction and death of neurons in a variety of degenerative diseases including Alzheimer`s disease, Parkinson disease and amyotrophic lateral sclerosis (Mattson, 2006). Additionally, apoptosis is one of the mechanisms by which neurons die following an acute traumatic brain injury or stroke (Becker and Bonni, 2004). Developmental cell death does not exactly mirror homeostatic or accidental cell death in the mechanisms by which apoptosis is triggered. During adult life, neuronal death is mainly related to pathological conditions, such as trauma, ischemia and neurodegenerative diseases. Neuronal apoptosis in these pathological disorders is thought to be caused by different stressors including energy failure, oxidative stress, irradiation, abnormal protein aggregates and free-radical generation, whereas commitment of developing neurons towards survival or death is mostly neurotrophic factor-dependent (Pettmann and Henderson, 1998;Snider, 1994). Furthermore, several important neurotrophic factors are described that support survival during development of various classes of neurons. Neurotrophic hypothesis states that growth factors are produced in limited amounts, and the neurons that successfully compete for these factors survive, but the less competitive ones die. Nevertheless, intracellular molecular mechanisms in both the developmentally regulated and the disease-related neuronal apoptosis appear to be similar. Many apoptotic signaling pathways converge at the mitochondria where signals are processed through molecular events culminating in the release of death factors.

The apoptotic cascade can be initiated via two distinct, but eventually converging signaling pathways such as transmembrane “extrinsic” and mitochondrial “intrinsic” pathways (Fig. 1) (Basu *et al.*, 2006). The extrinsic one involves the activation of death receptors such as Fas, tumour necrosis factor (TNF) receptor 1, DR (death receptor) 4 or DR5 (Danial and Korsmeyer, 2004). These death receptors have an extracellular domain which interacts with their respective

ligands such as Fas ligand (FasL), Tumour Necrosis Factor (TNF) and TNF-related apoptosis-inducing ligand (TRAIL).

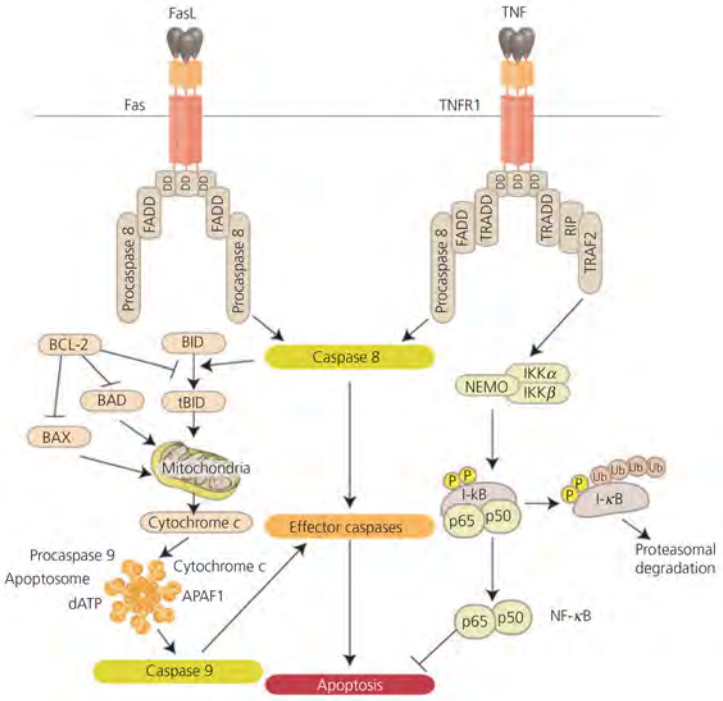

FIGURE 1. Schematic representation of the apoptotic signaling pathways. The extrinsic pathway is triggered by the interaction of specific pro-apoptotic ligands to death receptors, which are members of the tumour necrosis factor receptor family (TNFR) with an intracellular death domain (DD). The Fas associated death domain (FADD) adaptor mediates the recruitment of procaspase-8, which results activated and activates in turns the downstream effector caspases, triggering apoptosis. The initiator caspase-8 cleaves also the Bcl-2 family member Bid. Protease-cleaved Bid (tBid) translocates to the mitochondria, where it induces the permeabilization of the mitochondrial membrane, thereby providing a link to the intrinsic pathway. The intrinsic apoptotic signaling pathway relies on mitochondrial outer membrane permeabilization, resulting in the release of cytochrome *c*, which in association with Apaf-1 activates caspase-9. Activated caspase-9 in turn triggers once again the activation of effector caspases in a positive amplification loop. The intrinsic pathway is mainly controlled by pro-apoptotic and anti-apoptotic members of the Bcl-2 family. Bcl-2 and Bcl-XL are anti-apoptotic proteins that protect the cell from apoptotic insults, whereas Bax and Bad promote apoptosis. TNFR can also play an anti-apoptotic role by inducing the activation of the inhibitor of kB (I-kB) kinase (IKK) complex. This complex leads to I-kB degradation and consequently nuclear factor-kappa B (NF-kB) liberation that inhibit apoptosis at the transcriptional level. Figure is adapted from (Seilicovich, 2010).

Binding of the ligand to its receptor stimulates the recruitment of adaptor proteins such as Fas associated death domain (FADD) to an intracellular death domain in the receptor that is required for the activation of the initiator caspases -8 and -10, which in turns activate the effector caspase-3 and -7. Moreover, Caspase-8 also cleaves the pro-apoptotic protein Bid, thereby providing a link to the intrinsic pathway (Movassagh and Foo, 2008). Indeed, the cleavage of Bid initiates mitochondrial outer membrane permeabilization (MOMP) through the pro-apoptotic molecules Bak, Bax and Bad. The intrinsic pathway is characterized by mitochondrial dysfunction resulting in the release of mitochondrial death effectors under the control of the Bcl-2 family of proteins (Wang, 2001).

Among them, cytochrome *c* induces the binding of apoptosis protease-activating factor-1 (Apaf-1) to caspase-9 in a complex named apoptosome, which result in the activation of caspase-9 and

further activation of caspase-3 and -7. Another mitochondrial death effector is Smac/DIABLO, which releases caspases -3 and -7 from the inhibitor of apoptosis proteins (IAP). These effector caspases-3 and -7, and to some extent caspase-6, play fundamental roles as executors of the cell, by specifically degrading a huge number of cellular proteins and are ultimately responsible for an organized and innocuous disassembly of the cell (Earnshaw *et al.*, 1999). Mitochondria can also release caspase-independent death factors, such as apoptosis-induced factor (AIF) and endonuclease-G, which causes DNA fragmentation (Wang, 2001). That molecular program is accompanied by highly characteristic and easily identified morphological cellular changes such as cell shrinkage and rounding, membrane blebbing, chromatin condensation and nuclear fragmentation (Earnshaw, 1995). Cells which undergo apoptosis are packed into small vesicles so called apoptotic bodies which are phagocyted by neighbouring cells, often macrophages (Savill and Fadok, 2000).

The central core of this apoptotic cell death machinery is therefore this family of cysteine proteases so called caspases. 13 different caspases have been isolated in mammals so far. Null-mutant caspase-3 and caspase-9 mice models have shown similar phenotypes, with profound defects of programmed cell death in the developing nervous system, displaying hyperplasias and disorganized brain development (Cecconi *et al.*, 1998;Kuida *et al.*, 1996). These studies elegantly have shown that caspase-9 is a critical upstream activator of caspase-3 in vivo (Kuida *et al.*, 1998). In contrast with caspase-9, which mediates apoptosis after mitochondrial damage, caspase-12 is activated by endoplasmic-reticulum stress. Mice deficient in caspase-12 are resistant to stress-induced apoptosis and cytotoxicity induced by amyloid-beta (Nakagawa *et al.*, 2000). Thus genetic studies successfully demonstrated that eliminating caspase activity slow down or even prevent apoptosis.

Bcl-2, Bax and Bid are all members of the Bcl-2 (B cell lymphoma-2) large gene family of proteins, which share structural similarity in the so called BH (Bcl-2 homology) domains 1 to 4. Bcl-2 family members are divided into pro-apoptotic and anti-apoptotic proteins with regard to whether they promote or repress programmed cell death. Several members of the Bcl-2 family are expressed within the nervous system and are shown to act as developmental regulators. The subgroup comprised of Bcl-2, Bcl-XL, Bcl-Xs, Bcl-w, Bcl2-a1a and MCL1 are all proteins exhibiting pro-survival properties. With the exception of Bcl-Xs, all of these family-members possess four BH1 to BH4 domains and will be further discussed in section 1.3. Another subclass of proteins within the Bcl-2 family containing only BH3-domain is termed as BH3-only proteins. Proteins of this group have strong pro-apoptotic features, since it has been shown that

BH3-domain alone can induce apoptosis by sensing developmental death cues and intracellular damage (Ray *et al.*, 2000). This subgroup of pro-apoptotic proteins includes Bik, Bid and Bim (Boyd *et al.*, 1995;O'Connor *et al.*, 1998;Wang *et al.*, 1996). Finally, the subgroup of Bcl-2 family members containing Bax, Bak, and Bad proteins are characterized by possessing only three BH-domains (BH1-3) and are required downstream of BH3-only proteins to induce apoptosis (Hsu *et al.*, 1997;Kiefer *et al.*, 1995;Oltvai *et al.*, 1993;Yang *et al.*, 1995).

The pro-apoptotic molecule Bax is expressed at high levels both in the developing and in the adult brain and its deletion resulted in profound effects on survival in spinal cord motor neurons after growth factor deprivation in culture, and in neonatal sympathetic neurons after disconnection from their targets by axotomy (Deckwerth *et al.*, 1996). The $Bax^{-/-}$ knockout mice demonstrated the enrolment of Bax in naturally occurring cell death during neuronal development. Apoptotic cell death was remarkably reduced in various regions of the central and peripheral nervous systems in both developmental and early postnatal mutant mice with the resultant increased neuronal cell number.

Pro-apoptotic Bax and Bak differ in their localization. Bak mostly resides in the outer membrane of mitochondria, whereas Bax is characterized with diffuse cytosolic distribution. Like Bax, pro-apoptotic Bak enhances apoptotic cell death following appropriate stimuli. Bak-deficient mice showed no severe developmental abnormalities; however Bax/Bak double-deficient mice died prenatally and displayed multiple defects including accumulation of surplus cells in the nervous system (Lindsten *et al.*, 2000). The cells isolated from these animals were resistant to a variety of apoptotic stimuli (Wei *et al.*, 2001), indicating that either Bax or Bak is crucial for apoptosis signaling.

As mentioned before, BH3-only pro-apoptotic protein Bid was shown to function as a link between cell extrinsic, death receptor signaling pathway and intrinsic, cell death mitochondrial machinery. Bid is cleaved and activated by caspase-8 which itself is activated by cell surface death receptors. Truncated Bid then translocates onto mitochondria and triggers cytochrome *c* release (Luo *et al.*, 1998). However, Bid does not appear to play a major role in promoting programmed cell death of developmental neurons, since Bid-deficient mice show no neuronal developmental abnormalities (Leonard *et al.*, 2001).

Bad, a BH3-only pro-apoptotic protein was originally isolated as a binding partner for Bcl-XL and Bcl-2. Bad exerts its death-promoting effects by heterodimerizing with and inactivating death antagonists such are Bcl-XL and Bcl-2 (Yang *et al.*, 1995). In response to growth factor signals, certain kinases phosphorylate Bad. Phosphorylation of Bad results in its binding to 14-

3-3, which keeps it in an inactive state complex. In the absence of kinase–mediated survival signals, dephosphorylation of Bad disrupts its complex with 14-3-3 after which Bad is able to interact with anti-apoptotic Bcl-XL and promote apoptosis (Zha *et al.*, 1996). Bad-deficient mice grow to adulthood and develop B-cell lymphoma. Histological study of Bad-deficient mice organs showed no growth developmental abnormalities in brain, or alteration in neuronal programmed cell death (Ranger *et al.*, 2003).

1.2. CELL SURVIVAL MECHANISMS

After the identification of neurotrophic factors (Levi-Montalcini, 1983) the great interest of researchers was to figure out how trophic factor support preserves the survival of neurons. One of the first approaches was done by EM Johnson's group who showed that neurotrophic factors maintain neuronal survival by suppressing an endogenous, active death program in the cell (Martin *et al.*, 1988). The balance between cell apoptosis and survival in developing neurons is determined by the competition for the limited amount of neurotrophic factors which can be synthesised by target neuronal or non-neuronal cells. These factors comprise different families acting through different tyrosine kinase receptors. Among them the neurotrophins are part of the neurotrophic factor family and are involved in a wide variety of cellular processes including survival, neurite growth, differentiation, proliferation, synapse formation, neurotransmitter release and myelination. Neurotrophin-family ligands found in mammals are nerve growth factor (NGF), brain-derived neurotrophic factor (BDNF), NT-3 and NT-4/5. They signal through two types of receptors: tropomyosin kinase receptor (Trks) and pan-neurotrophin receptor p75. The most important intracellular signaling cascades that lead to survival of neurons are PI3K (phosphoinositide 3-kinase)/PKB (protein kinase B) and on the other hand Ras/Raf (Ras-activated factor)/MAPK (mitogen-activated protein kinase) pathways. These survival signaling pathways are directed to inhibit apoptosis at both transcriptional and post-translational levels, as discussed in the next section.

1.3. THE INTERPLAY BETWEEN SURVIVAL AND APOPTOTIC MECHANISMS

The anti-apoptotic Bcl-2 protein is a major mediator of the effects of neurotrophic factors on neuronal cell survival (Garcia *et al.*, 1992). There are five pro-survival members of the Bcl-2 family including Bcl-2, Bcl-XL, Bcl-w, Bcl2a1a and MCL-1 containing the four BH domains BH1 to BH4, numbered in their order of discovery. The Bcl-2 gene was originally identified as a

translocated gene in follicular lymphoma (Tsujimoto *et al.,* 1984) and its overexpression has been shown to protect different cell types from a wide range of apoptotic insults (Ibrado *et al.,* 1997;Shimizu *et al.,* 1995). The Bcl-2 family members are engaged in cell death prevention mostly by interacting with pro-apoptotic Bax or Bak (Willis *et al.,* 2007). Cristal structure resolution of the Bcl-XL and Bcl-2 BH1-4 motifs (Muchmore *et al.,* 1996;Petros *et al.,* 2001) allowed the design of site-directed mutagenesis within the BH domains, which blocked the anti-apoptotic functions of these proteins (Hirotani *et al.,* 1999).

The anti-apoptotic Bcl-2 family members are mainly mitochondrial outer membrane-associated proteins and functionally maintain the outer mitochondrial membrane integrity by opposing the pro-apoptotic Bcl-2 family members, which in turn compromise the mitochondrial membrane and allow the passage of apoptogenic proteins to the cytosol. Anti-apoptotic Bcl-2 family members restrain the caspase activation, thereby maintaining the neuronal survival during embryonic development and in the adult.

Mouse genetic models suggest that the survival of the cell requires protection by at least one Bcl-2 homologue. Despite the functional redundancy and the overlapping expression patterns, individual Bcl-2 genes inactivation results in diverse phenotypes. Bcl-2 overexpression reduced naturally occurring cell death, which led to hypertrophy of the nervous system (Martinou *et al.,* 1994). Furthermore, overexpression of Bcl-2 protected from apoptosis nerve growth factor (NGF)-deprived neurons (Gagliardini *et al.,* 1994). Mice deficient in Bcl-2 (Bcl-$2^{-/-}$) complete embryonic development, but displayed growth retardation and early postnatal mortality and exhibited significant loss of sympathetic, motor and sensory neurons (Michaelidis *et al.,* 1996;Veis *et al.,* 1993). Consistent with these findings, Bcl-2 expression determines whether a neuron dies or survives.

The fact that Bcl-2 deficient mice apparently complete normal development exhibiting only mild defects within the nervous system might be explained by the functional redundancy with other anti-apoptotic Bcl-2 family members. Pro-survival Bcl-XL is specifically expressed in the developing brain, and it was nominated as an important pro-survival neuronal factor. It was demonstrated that the Bcl-XL expression decreases after birth but is retained in the adult central nervous system. The Bcl-$XL^{-/-}$ mice were embryonic lethal at E13 displaying strongly enhanced apoptosis of postmitotic differentiating neurons of the developing brain (Gonzalez-Garcia *et al.,* 1995). In addition, Bcl-XL deficient neurons demonstrated increased susceptibility to serum deprivation (Roth *et al.,* 1996). The lack of neuronal survival caused by Bcl-XL deficiency *in vitro* and *in vivo* identified Bcl-XL as a critical anti-apoptotic factor in maintaining neuronal

survival during brain development. Thus, Bcl-XL might complement Bcl-2 in promoting cell survival within the developing nervous system.

The observation about the fact that none of the pro-apoptotic BH3-only proteins can kill the cell lacking Bax and Bak (Cheng *et al.*, 2001) encouraged the idea of Bcl-2 and its homolog Bcl-XL promoting cell survival via interacting with pro-apoptotic Bax and Bak. Consistent with the finding that Bcl-2 and Bcl-XL promote cell survival, while BH3-only proteins abrogate this function, the consequence of Bax and Bak deletion must presumably display an enhanced Bcl-2 and Bcl-XL promoted cell survival. Remarkably, several studies established the protein-protein interactions within the Bcl-2 family of proteins which is a key event in the regulation of programmed cell death. The α-helical BH3 domain of the pro-apoptotic proteins interacts with the hydrophobic groove within the BH1-3 domains of the anti-apoptotic Bcl-2 proteins (Sattler *et al.*, 1997). Indeed, anti-apoptotic Bcl-2 and Bcl-XL heterodimerize with pro-apoptotic Bax and this heterodimerization is required for the repression of apoptosis and cell fate decision (Sedlak *et al.*, 1995). Double deficient Bax/Bcl-XL embryos demonstrated that Bax deficiency could attenuate the increased apoptosis of Bcl-XL deficient neurons (Shindler *et al.*, 1997). Consistent with this finding, the relative levels of interaction between Bax and Bcl-XL appears to regulate neuronal survival.

In order to understand whether the pro-survival function of Bcl-XL is mediated by specifically inhibiting the pro-apoptotic effects of the Caspase-3, the null-mutation Bcl-XL and caspase-3 phenotypes were compared. A dramatic increase of activated caspase-3 was observed in Bcl-XL deficient nervous system, indicating that caspase-3 activation depends on Bcl-XL in the developing brain (Roth *et al.*, 2000). The observed neuronal cell death in Bcl-XL null embryos was completely abolished by concomitant deletion of caspase-3 and caspase-9 (Roth *et al.*, 2000;Zaidi *et al.*, 2001).

Synthesis of MCL-1 (Myeloid cell leukaemia 1), an anti-apoptotic Bcl-2 homologue, is blocked and MCL-1 protein rapidly degraded following the cellular stress (Nijhawan *et al.*, 2003). On the other hand, inhibition of MEK or PI3K independently resulted in the reduction of MCL-1 expression and loss of cell viability, since both MEK/MAPK and PI3K/Akt cell survival signaling pathways are essential in the regulation of MCL-1 expression and apoptosis prevention (Huang *et al.*, 2000;Liu *et al.*, 2001). MCL-1 deficient mice resulted in severe phenotype, with embryos dying at around embryonic day 3,5-4 and showing increased apoptotic activity (Rinkenberger *et al.*, 2000). In order to understand the function of the anti-apoptotic MCL-1 in neuronal development, since MCL-1 deletion resulted in peri-implantation lethality, conditional

knockout MCL-1 mutant mice were generated targeting the MCL-1 deficiency specifically to the neuronal lineage. Loss of MCL-1 in the brain resulted in widespread apoptotic death of both neural progenitors and newly committed neurons during the development of the nervous system (Arbour *et al.*, 2008). Moreover, both MCL-1 and Bcl-XL have been shown to block Bax and Bak-mediated apoptosis (Nijhawan *et al.*, 2003;Roth *et al.*, 2000).

Anti-apoptotic Bcl-2 family member Bcl-w was shown to be expressed in axons of sensory neurons and its regulation by target-derived neurotrophin stimulation suggests that Bcl-w might be involved in the promotion of neuronal cell survival in the phase of establishing synaptic connections (Pazyra-Murphy *et al.*, 2009). Furthermore, Bcl-w deletion caused abnormalities in size and function of axonal mitochondria of sensory neurons, manifested in progressive small fibber sensory degeneration and neuropathy, thereby suggesting that the absence of this protein may play a critical role in the viability of axonal processes (Courchesne *et al.*, 2011).

Another Bcl-2 super family member, which is directly regulated by PKB, is Bad. The BH3-only apoptotic factor Bad binds to Bcl-2 or Bcl-XL anti-apoptotic factors through their BH3 domains. Under conditions when no survival or growth factors are present, Bad remains unphosphorylated. The unphosphorylated form of Bad associates with Bcl-2 members and prevents their anti-apoptotic functions, which would normally lead to cytochrome *c* release and subsequent activation of the caspase cascade. In response to growth factors, PKB is activated and directly phosphorylates Bad at Ser136. The consequence of Bad phosphorylation by PKB is the dissociation of Bad from Bcl-XL and Bcl-2. The dissociated Bad binds to the adaptor protein 14-3-3 which firstly sequesters Bad from the mitochondria and also prevents the binding of Bad to Bcl-2 and Bcl-XL (Datta *et al.*, 1997). PKB can also phosphorylate Bax on Ser184, which leads to the inhibition of the conformational change required for Bax translocation to mitochondria and thus blocks the pore formation and release of cytochrome *c* (Yamaguchi and Wang, 2001). Taken together, there is abundant evidence that PKB controls Bcl-2 family proteins which ensure that mitochondrial integrity is preserved against stress.

PKB may also inhibit the expression of genes whose products act within the cell to control the apoptotic machinery. Indeed, many studies indicate that PKB promote cell survival by co-ordinately regulating FOXO transcription factors (Brunet *et al.*, 1999). When they are not phosphorylated, FOXOs induce apoptosis in a transcription dependent manner by upregulating death cytokines as well as their cognate receptors. In the presence of survival factors, when PKB is activated, it phosphorylates FOXOs at several regulatory sites and elicits the relocalization of FOXOs from the nucleus to the cytoplasm, away from their target genes. A search of the

promoter database using FOXO binding sites reveals that the genes encoding FasL and Fas receptor, TRAIL (TNF-related apoptosis inducing ligand), TNFα and TNF receptor contain FOXO binding sites in their promoters, indicating that these genes are regulated by FOXOs (Brunet *et al.*, 2001). The regulation of FOXO by PKB and its role in neuronal survival will be further discussed in section 2.3.1.

1.4. NEURONAL CELL DIFFERENTIATION: NEURONAL POLARIZATION

Neuronal development and the formation of the neuronal circuits during development is a highly regulated process which comprises the coordination of multiple cellular events which can be generally divided into three steps: neurogenesis, neuronal morphogenesis and synaptogenesis. In the process of neurogenesis, neuronal progenitors undergo proliferation and differentiation to generate neurons. Self-renewing radial glial cells (RGCs) constitute one major class of the progenitors. They undergo two phases of coordinated cell division which are critical in determining the overall number of self-renewing progenitors and thereby, in determining the brain size. The first is a proliferative phase of cell division during which RGCs divide symmetrically to generate similar progenitor cells to expand their progenitor pool, whilst the second phase is neurogenic in which RGCs divide asymmetrically and generate one self-renewing progenitor and one post-mitotic neuron or one intermediate progenitor cell (IPC). IPCs migrate and divide symmetrically to form neurons (Fig. 2) (Shitamukai and Matsuzaki, 2012).

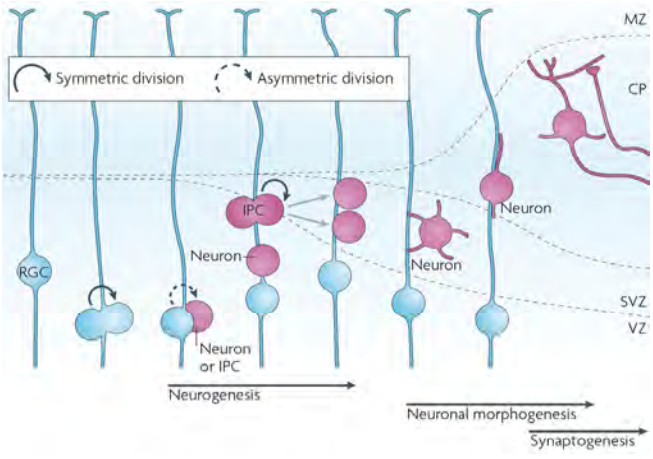

FIGURE 2. Schematic representation of neuronal development of the mammalian neocortex. The first step in neurogenesis, during which a cohort of neuronal progenitors undergoes two phases of highly coordinated cell divisions: In the first-proliferative- phase, which occurs early in development, the radial glial cells (RGCs) mainly divide symmetrically in the ventricular zone (VZ) and thus expand their pool. In the second-neurogenic-phase, most of the RGCs divide asymmetrically giving origin to one self-renewing progenitor, equivalent to mother cell (blue) and one post-mitotic neuron which is committed to be differentiated or one intermediate progenitor cell (IPC) which does not re-new but migrate to the subventricular zone (SVZ) and divide symmetrically to form neurons (purple). The second step is morphogenesis during which differentiated neurons migrate towards their final destination. During migration they polarize and acquire axon and dendrites. The third step is synaptogenesis during which axon ceases to grow but instead form synapses with their innervating targets. CP, cortical plate; MZ, marginal zone. Figure adapted from (Hur and Zhou, 2010).

The second step in neuronal development is the neuronal morphogenesis, which involves a highly regulated process such as neuronal cell differentiation, encompassing neuritogenesis, neurite outgrowth, polarization, pathfinding and synaptogenesis, which is the final step during which mature neurons establish synaptic integration in the central nervous system environment (Barnes and Polleux, 2009). Perturbation of any of these processes can cause defects in cortical development.

Polarization lies in the heart of several aspects of neuronal development. Neurons can inherit their axon/dendrite identity directly from the apico/basal polarity of their progenitors. This is the case for bipolar cells in the developing retina (Morgan *et al.*, 2006). However, most of the neuronal cell populations undergo morphological changes leading to the polarized outgrowth of their axon and dendrites. Differentiation of axon and dendrites is a critical step in neuronal cell development. Polarity refers to the asymmetric sides of the main axis of the cell. Neuron is a classical example of highly polarized cell. The polarized morphology of the neuron consists on a single long axon and many short and highly branched dendrites. The axon transmits the information to the target, whereas dendrites receive the incoming information. Thus, this polarized structure is essential for two primary functions of the neuron: reception of the synaptic input by dendrites and delivery of the output signals to the other target cells via the axon. How a neuron acquires its polarity and what mechanisms are responsible for to break out its symmetry during the development still remains an outstanding question. Neuronal polarization process was shown by the studies in 1980s based on the use of isolated embryonic hippocampal neuronal cultures and has far been studied most extensively nowadays. Shortly after plating, during the first few hours, the spherical neuronal cells extend lamellipodia around the cell periphery (stage 1). After 12-16 hours, lamellipodia clusters at particular sites and minor neurites appear with similar morphology (stage 2). In stage 3, one of the neurites emerges and differentiates as an axon. During stage 4 the remaining minor neurites develop as dendrites at around the fourth day in culture. Finally, in stage 5, the axon and dendrites develop different characteristics of mature neuron, such as establishment of synaptic specializations and contact (Fig. 3 and Table 1) (Craig *et al.*, 1992;Dotti *et al.*, 1988). In general, neuron polarization can be categorized into three phases. First phase involves the generation of the first neurite from a defined site. Second phase is the generation of axon and dendrites from minor neurites; this phase is regulated by growth-promoting and growth-inhibitory mechanisms controlling axon formation. During the third phase the nascent axon and dendrites determine their identity and acquire the molecular organization that allows proper electrical vectorial function (Caceres *et al.*, 2012)

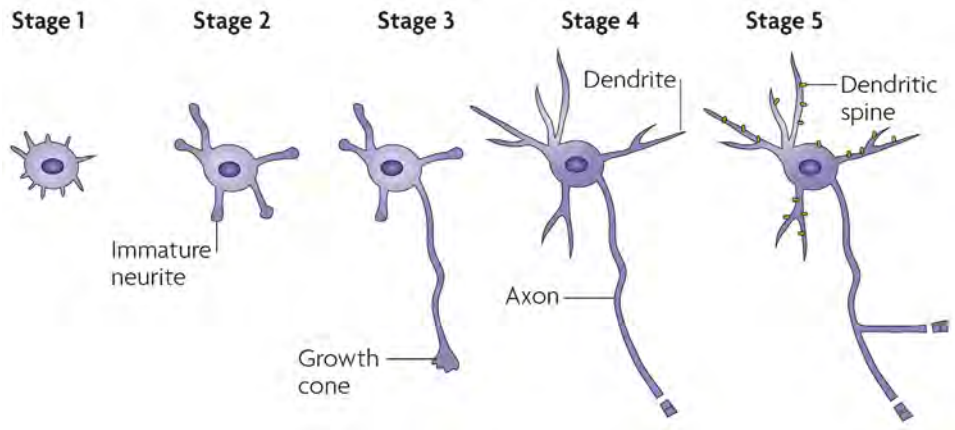

FIGURE 3. Schematic representation of neuronal polarization in cultured embryonic hippocampal neurons. Stage 1 is characterized by the presence of small cellular protrusions, called lamellipodia. Shortly after plating, neurites begin to sprout. In stage 2 these neurites extend and retract without net elongation, thus immature neurites with similar length are generated. Transformation of the most dominant minor neurite into fast-growing axon-like neurite is characteristic for the stage 3. In stage 4 the remaining neurites initiate subsequent growth and mature into dendrites. The terminal stage 5 encompasses the maturation of neurons onto a neuronal network through the formation of dendritic spines and axon terminals. Figure adapted from (Arimura and Kaibuchi, 2007).

STAGE	DIV	DIFFERENTIATION STEP
1	0,25	Development of membrane protrusions forming lamellipodia
2	0,5	Formation and extension of multiple neurites which are not yet committed (cells remain un-polarized and symmetric)
3	1,5	Cells start to polarize and the fast growing neurite becomes an axon
4	4	Complete polarization by differentiating the remaining neurites into dendrites followed by growth and branching
5	≥7	Synapse formation and further neuron maturation

TABLE 1. Staging differentiation steps of cultured hippocampal neurons *in vitro*.

Dissociated hippocampal neuronal cultures are widely used in the study of neuronal polarity. Using this system many intrinsic and extrinsic factors were defined that control neuronal polarization. Newborn neurons from the last mitotic division may have inherited cytoplasmic asymmetry that lately influences on axon/dendrite formation. The spherical symmetry of a cell is broken by centrosomes, the Golgi apparatus and endosomes that cluster together near the initiation site of the neurite in the case of hippocampal neurons (de Anda *et al.*, 2005). Many signaling molecules were found to be essential in neuron polarization and perturbing the activity of these molecules abolishes axon differentiation or causes multiple axon formation. Although many signaling pathways evoked by extracellular signals were identified that govern neuronal

polarization, this process still remains largely unknown. Activation of several components in the growth cone of the prospective axon appears to be essential for axon formation at the molecular level. BDNF and other extracellular factors that elevate the activity of intracellular signaling cascades which promote the initial breakdown of the cell symmetry and support polarization indeed serve as neuronal polarization factors (Matsuda *et al.*, 2009). Selection of the future axon requires accumulation and activation of many signaling molecules that are essential for neuronal polarization. Among these various components, mammalian partitioning-defective proteins mPAR-3 and mPAR-6 were shown to regulate neuronal polarization (Shi *et al.*, 2003). Several groups demonstrated that activation of PI3K by growth factors and accumulation of its product PIP3 at the tip of one of the immature neurites is important in axon specification process (Menager *et al.*, 2004;Shi *et al.*, 2003;Yoshimura *et al.*, 2006). Conversely, overexpression of the constitutively active PI3K catalytic subunit caused the formation of multiple axons (Yoshimura *et al.*, 2006). It was also reported that increases in the local concentration and activation of the Rho GTPase signaling modules is crucial in neurite extension (Arimura and Kaibuchi, 2007). The requirement of active LKB1 for axon initiation during neuronal polarization was demonstrated *in vivo* in embryonic cortex and *in vitro* in cultured embryonic hippocampal neurons. LKB1 does so by acting upstream of the SAD kinases (Barnes *et al.*, 2007;Shelly *et al.*, 2007). Activated LKB1 phosphorylates and modulates the catalytic activity of SAD-A and SAD-B (also called BRSK2 and BRSK1) which are serine-threonine kinases related to the *C. elegans* Par1 polarity determinant (Drewes *et al.*, 1997;Kishi *et al.*, 2005;Lizcano *et al.*, 2004;Wodarz, 2002). BRSKs are especially expressed in brain (Rodriguez-Asiain *et al.*, 2011) and were reported to be essential for axon/dendrite specification in vivo since BRSK1/2 double knockout mice neurons lack axon and dendrites and die within two hours after birth. Phenotypical features of BRSK double knockout mice were noticeably small forebrain and thinner cortex compared with control littermates (Kishi *et al.*, 2005). BRSK1/2 control polarization by phosphorylating microtubule-associated proteins such as Tau, which is involved in the growth and differentiation of axons and dendrites. Altogether, these evidences put LKB1 as a master regulator of neuronal polarization.

2. SIGNALING IN THE CENTRAL NERVOUS SYSTEM

2.1. NEUROTROPHINS AND THEIR RECEPTORS

Neurotrophins are a family of polypeptidic growth factors that are structurally related and perform a wide range of roles in the developing and mature nervous system. Indeed, neurotrophins are known to control cell fate, neurite elongation and guidance and synaptic plasticity. Neurotrophins are synthesised as precursors that can either be cleaved intracellularly by different pro-convertases to produce the mature proteins, or can be secreted as pro-neurotrophins (Lee *et al.*, 2001). Four neurotrophins are expressed in mammals: Nerve growth factor (NGF), brain derived neurotrophic factor (BDNF), neurotrophin 3 (NT3) and neurotrophin 4/5 (NT4/5). Nerve growth factor (NGF) was identified initially as a survival factor for motor and sensory neurons (Levi-Montalcini, 1987). Brain-derived neurotrophic factor (BDNF) was the second neurotrophin which was characterized as a survival factor for different neuronal populations (Barde *et al.*, 1982). BDNF is more abundantly expressed and distributed in the central nervous system than NGF and furthermore, BDNF has a higher degree of sequence conservation across species. Mature neurotrophins exert their biological function by binding two entirely distinct classes of cell transmembrane receptors; the high-affinity tropomyosin-related kinase (Trk) receptor and the low-affinity p75 neurotrophin receptor (p75NTR), a member of the tumour necrosis factor (TNF) receptor superfamily. Neurotrophins directly bind and promote the dimerization of Trk receptors, leading to their activation and triggering independent downstream signal transduction pathways that ultimately promote similar or different biological outcomes *in vivo*. Neurotrophins and their receptors exhibit a complex diversity of expression patterns in different cell types. For example, BDNF and TrkB are highly expressed in the brain, where they control many cellular functions in the neuron including survival, differentiation and plasticity. Neurotrophins show binding specificity for each particular receptor. Each neurotrophin is able to bind and activate p75NTR with low affinity, whereas they exhibit specific interaction abilities with Trk receptors. NGF binds to tyrosine kinase receptor A (TrkA), whereas BDNF and NT4/5 to TrkB and NT3 binds to TrkC. NT3 can also be a ligand for TrkA and TrkB (Fig. 4) (Chao, 2003). Neurotrophins regulate cell survival, proliferation and differentiation during the nervous system development and control synaptic strength and plasticity in the adult via binding and activating their receptors.

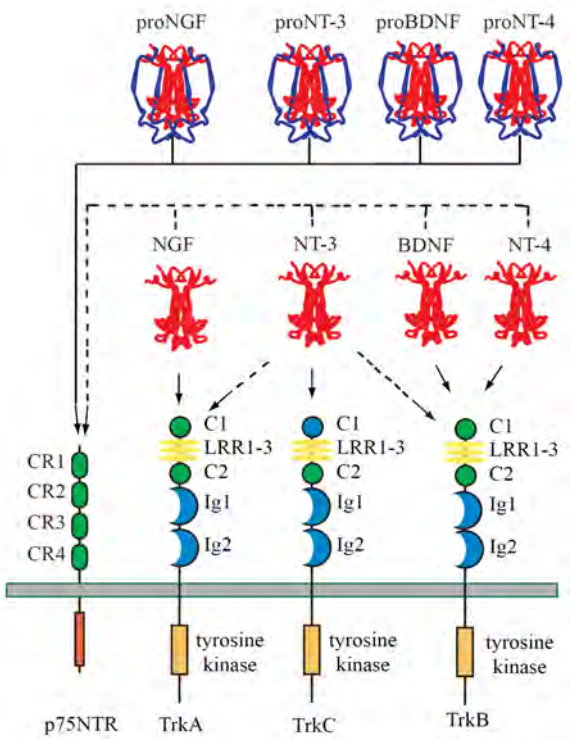

FIGURE 4. Neurotrophin and receptor interactions. Trk receptors contain extracellular IgG domains for ligand binding and the catalytic tyrosine kinase domain in the intracellular region. Each neurotrophin (NGF, BDNF, NT-3 and NT4/5) is derived from its respective precursor (proNGF, proBDNF, proNT-3, and proNT-4/5). Each mature neurotrophin is able to bind p75NTR with low affinity, but exhibits more specific interactions with Trk receptors. NGF binds specifically TrkA, BDNF and NT4/5 interact with TrkB and NT3 recognizes TrkC. In some cells types NT3 is able to activate TrkA and TrkB to a lesser extend. C, cysteine cluster; CR, cystein rich motif; Ig, immunoglobulin-like domain; LRRR, Leucine-rich repeat region. Figure adapted from (Reichardt, 2006).

The Trk family of receptors are transmembrane glycoproteins of ~140 kD with an extracellular ligand-binding domain containing multiple repeats of leucine-rich motifs, two cysteine clusters and two immunoglobulin-like domains; a single transmembrane domain, and an intracellular tyrosine kinase domain which is highly related (~80% amino acid identity) among the different Trk receptors. The most proximal immunoglobulin (Ig) domain is the major interface for neurotrophin interaction, although each of the extracellular domains of the receptor contributes to ligand binding. The p75 receptor is a transmembrane receptor of ~75 kD, with four cysteine-rich motifs at the extracellular domain, a single transmembrane domain and a cytoplasmic region containing a death domain similar to those present in other members of the TNF receptor super-family. There are no sequence similarities between Trks and p75 receptors neither in the extracellular ligand binding nor in the intracellular domains. Binding of neurotrophins to their Trk receptors induces the activation of three major signaling pathways, commonly referred as Ras/Raf/ERK, PI3K/PKB and PLC-γ signaling pathways, which are mainly involved in neuronal survival and differentiation. An additional level of complexity comes from the binding of neurotrophins to p75 receptor. The most defined role of p75 receptor is in signaling to apoptotic cell death. Activation of p75 triggers a different set of signaling cascades, such as the NF-kB and c-Jun N-terminal kinase-p53-Bax signaling pathways (Kaplan and Miller, 2000). The p75 receptor has a short intracellular domain lacking catalytic activity. However, this

receptor can bind neurotrophins and form complexes with other co-receptors to mediate diverse cellular functions depending on the cellular context (Murray *et al.*, 2004b) that can be synergistic or antagonistic to those activated by Trk receptors (Friedman, 2000). The interaction of neurotrophins with the p75 receptor can also induce cell death in the absence of Trk receptors. For instance, the endogenous NGF caused the death of chicken retinal neurons that express p75 but does not express the TrkA, NGF-specific receptor (Frade *et al.*, 1996) suggesting that neurotrophins might act as death ligands in a cell context-dependent manner.

Cellular localization of Trk receptor activation and the direction of the signal can further specify responses of neurotrophins. The nature of responses differs depending on whether the receptor is on the axon of the presynaptic cell, on the dendrite of the postsynaptic targets, or on the plasma membrane of the cellular soma. Abundant data now indicate that receptors are present on the presynaptic axon terminals and on postsynaptic dendrites, respectively. There is a specialized mechanism for retrograde signaling initiated by neurotrophins that stimulate the presynaptic cells. Binding of ligands can trigger the internalization of the ligand-receptor complex forming a signaling endosome which in turn can be transported from the nerve terminal to the cell body to mediate a particular biological response (Huang and Reichardt, 2003;Kaplan and Miller, 2000). There are however differences in the signaling initiated by stimulation of axon terminals or cell bodies. For instance, the site of stimulation determines the differential activation of individual mitogen-activated protein kinases (MAPK) in sensory neurons. Neurotrophin stimulation of cell body receptors induces the activation of the ERK1/2 MAPK signaling pathways. By contrast, neurotrophin stimulation of receptors of the distal axon activates ERK5 but not the ERK1/2 classical pathway, leading to changes in gene expression and cell survival (Watson *et al.*, 2001). The effects of neurotrophins on neuronal cell survival depend on which receptor complex is engaged and which signaling pathways are activated. Neurotrophins bind as dimers to Trk receptors, leading to the dimerization of the receptor and transphosphorylation of the tyrosine residues at positions 706/707 for human TrkB, which is located within the activation loop of the catalytic domain, potentiating in this way their tyrosine kinase activity. Phosphorylation of additional tyrosine residues including Tyr516 and Tyr816 in the TrkB sequence creates the binding sites for scaffolding proteins which possess either phosphotyrosine-binding (PTB) or Src-homology-2 (SH2) domains. Scaffold proteins function as intermediate adaptors coupling Trk receptors to intracellular signaling cascades. The effectors of Trk receptors cause the translocation and binding of various sets of adaptor proteins giving raise to the initiation of distinct signaling events. The roles of Trk receptors in mediating neuronal survival,

differentiation and synaptic function have been extensively studied and are mainly mediated through the activation of three major signaling pathways: PI3K-PKB, Ras/Raf/MAPK and PLCγ signaling pathways (Fig. 5). However, novel survival pathways beyond the classical MAPK, PI3K and PLCγ have been delineated, for example for NGF and GDNF-mediated responses of sympathetic neurons linking B-Raf to IKKs, independently of both PI3K and MEK-1/2 pathways (Encinas *et al.*, 2008).

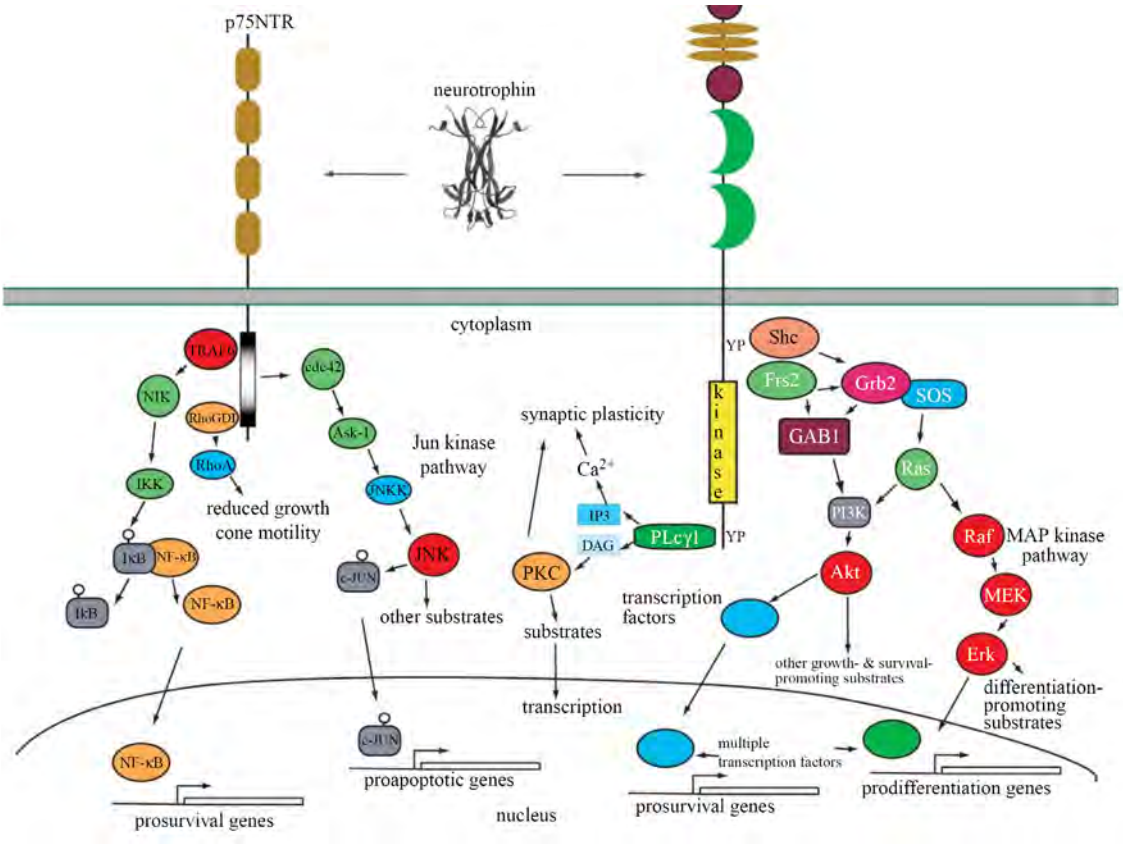

FIGURE 5. BDNF activated signaling cascades. The image depicts the interaction of neurotrophins with Trk receptors and the three major signalling pathways activated through the receptor. These pathways are (1) mitogen-activated protein kinase (MAPK), (2) phosphoinositide 3-kinase (PI3K) and (3) phospholipase Cγ (PLCγ) through activation of various adaptor proteins. Figure adapted from (Reichardt, 2006).

Phosphorylation of the tyrosine 516 residue located at the N-terminus of the TrkB kinase domain accelerates recruitment of the Src homology domain-containing proteins (Shc). Shc is an adaptor protein that participates in the enrolment of different intermediate molecules promoting Ras activation. Coupling of Shc to receptor creates the phosphotyrosine site for adaptor Grb2, which is bound to Ras exchange factor SOS (son of sevenless) and that finally leads to Ras/Raf/MAPK signaling cascade activation.

The Ras/Raf/MAPK pathway mediates signaling from various extracellular stimuli to the nucleus and has a pivotal role in the regulation of gene expression, cell proliferation, differentiation and early embryonic development (Robinson and Cobb, 1997). Activation of ERK1/2 requires sequential phosphorylation of MEK1/2 by Raf, and then phosphorylation of ERK1/2 by MEK1/2. ERK1/2 signaling transduction pathway is of particular interest because its activation is involved in the process of neuronal cell differentiation (Yang *et al.*, 2012). Experiments demonstrated that the ERK/STAT3 pathway was required for the development of ES cell-derived neurons *in vitro*. STAT proteins are activated by phosphorylation at a specific tyrosine residue which is required for dimer-formation, nuclear translocation, DNA binding and transcriptional activity. MAP kinase cascade negatively regulates STAT activity by decreasing its tyrosine phosphorylation (Li *et al.*, 2006). The sustained activation of ERK by NGF appears to be crucial in neuronal differentiation of PC12 cells, as blocking of ERK activation inhibits neurite induction, and constitutive activation of ERK is sufficient for inducing neurite outgrowth. ERK induces the expression of the p35, neuron specific activator of cyclin-dependent kinase 5, which is required for NGF-induced neurite outgrowth and thus determines PC12 cell fate (Harada *et al.*, 2001). Sustained ERK activation is involved in synaptic plasticity as well as differentiation in the dendrites of cultured hippocampal cells (Wu *et al.*, 2001).

Phosphorylation of TrkB in a tyrosine residue at position 816 serves as a specific recognition site for phospholipase Cγ (PLCγ) which catalyzes phosphoinositide turnover. PLCγ directly recruits to this site via its SH2 domain, where it becomes phosphorylated and activated. Following PLCγ activation, inositol (1,4,5) trisphosphate (IP3) and diacylgrycerol (DAG) are produced. DAG activates PKC, which is involved in synaptic plasticity. Accumulation of intracellular IP3 stimulates Ca^{2+} release from internal Ca^{2+} stores via interaction with IP3 receptors on the endoplasmic reticulum. Increased intracellular Ca^{2+} levels results in Ca^{2+}/calmoduline-dependent protein kinases (CaMKII, CaMKK and CaMKIV) activation, which are thought to be involved in activity-dependent plasticity (Tompa and Friedrich, 1998).

On the other hand, phosphoinositide 3-kinase (PI3K) does not directly interact with Trk receptors, but activation of PI3K/PKB signaling pathway occurs rather after the formation of a variety of adaptor protein complexes. Adaptor proteins such as GRB-associated binder-1 (GAB-1) and insulin receptor substrate-1 (IRS1) are recruited to activated TrkB through GRB2 and mediate the activation of PI3K (Holgado-Madruga *et al.*, 1997;Reichardt, 2006). Activated PI3K promotes the generation of D3-phosphorylated phosphoinositides, which accumulate at the plasma membrane and promote the recruitment of proteins containing phosphoinositide-binding

domains. These include the PH domain-containing kinases PDK1 and PKB, which play fundamental roles in promoting neuronal survival and differentiation (Brunet *et al.*, 2001;Huang and Reichardt, 2003).

In addition to dissimilarities between Trk receptors, individual receptors may respond differently depending on the nature of the ligand. Also, various subsets of the adaptor proteins compete with each other for the binding to activated Trk receptors (Segal, 2003). Intracellular signaling controlled by Trks are meant to be essential in controlling cell survival and differentiation. In most neuronal cell populations ligand engagement with Trk receptors promotes survival. However, neurotrophic factors have been shown over the years to exert many other functions that are determined by the cellular context. Among the diverse signaling pathways which transduce the signal of neurotrophic factors, the PI3K-PKB pathway has emerged during the past decade as a central mediator required for the neurotrophic factor-induced neuronal survival.

2.2. PI3K REGULATED SIGNALING PATHWAY

The interaction of growth factors with their receptors leads to activation of phosphoinositide 3-kinase (PI3K) and phosphorylation of phosphatidylinositol-4,5-bisphosphate (PtdIns(4,5)P_2) at D3 position of the inositol ring to generate the phosphaidylinositol-3,4,5-trisphosphate (PtdIns(3,4,5)P_3, or PIP3) second messenger. PI3Ks are a family of intracellular lipid kinases that phosphorylate the 3'-OH group of phosphatidylinositols. They are classified based on their own lipid substrate specificity into class-I, class-II and class-III. As mentioned before, classical class-I PI3Ks convert PIP2 into PIP3, whereas class-II and class-III PI3Ks act on phosphatidylinositols (PIs) and generate phosphatidylinositol 3-phosphate (PI-3-P). Class-I PI3Ks are divided into class-Ia and class-Ib PI3Ks. Class-Ia PI3K encompasses p85 adapter/regulatory subunit and p110 catalytic subunit and is activated by receptors with protein tyrosine kinase activity (RPTK), whereas class-Ib is activated by G-protein coupled receptors (Vanhaesebroeck *et al.*, 2001;Vanhaesebroeck *et al.*, 1997). Class-Ia PI3K are activated following their recruitment to the corresponding receptor through the interaction of the p85 regulatory subunit with phospho-tyrosine residues presented by adaptor proteins such as IRS1 or GAB1 (Holgado-Madruga *et al.*, 1997). PI3K activation results in production of phosphoinositides which take a role in propagation of the signal acting as the second messengers. This function of phosphoinositides is mediated by the specific interaction with lipid-binding domain containing proteins, such as proteins containing pleckstrin-homology (PH)

domains. Among them, the PDK1 and PKB kinases are key effectors of the PI3K signaling pathway.

2.2.1. The AGC family

Both PDK1 and PKB belong to the AGC family of protein kinases, which encompasses about 60 members out of the 518 kinases of the human kinome and are highly conserved throughout eukaryotic evolution (Manning *et al.*, 2002b). This AGC family was originally named after the cAMP-dependent kinase (PKA), cGMP-dependent kinase (PKG) and protein kinase C (PKC) family members. Protein kinases of the AGC family share the structural similarity and the most remarkable feature relying on the mechanism controlling their activity. This activation mechanism involves the dual phosphorylation at two regulatory motifs which are highly conserved: the activation segment also termed activation loop or T-loop located in the catalytic domain, and the hydrophobic motif found within the non-catalytic region following the kinase domain (Pearce *et al.*, 2010). AGC kinases are activated downstream of a wide range of extracellular stimuli by different mechanisms. The 3-phosphoinositide-dependent protein kinase 1 (PDK1) acts as the upstream activator phosphorylating a specific Thr or Ser residue located at the T-loop of the kinase domain of at least 23 members of the AGC family (Bayascas, 2010). This subgroup includes all the three PKB/Akt isoforms (Alessi *et al.*, 1997b;Walker *et al.*, 1998), the p70 ribosomal S6 protein kinases (S6K) -1 and -2 (Alessi *et al.*, 1998;Lee-Fruman *et al.*, 1999;Pullen *et al.*, 1998), the three serum and glucocorticoid inducible kinase (SGK) isoforms (Kobayashi and Cohen, 1999;Kobayashi *et al.*, 1999;Park *et al.*, 1999), p90 ribosomal S6 protein kinases (RSK) -1,-2 and -3 (Jensen *et al.*, 1999;Richards *et al.*, 1999), nine protein kinase C (PKC) isoforms (Chou *et al.*, 1998;Dutil *et al.*, 1998;Le Good *et al.*, 1998) and the three PKC related kinase (PRK) isoforms (Dettori *et al.*, 2009;Flynn *et al.*, 2000;Leenders *et al.*, 2004).

PDK1 was originally identified as the kinase capable of phosphorylating PKB at Thr308 in a phosphoinositide dependent manner. PDK1 is one of the few kinases present in the vertebrate genome as a single copy gene which is expressed ubiquitously. PDK1 is synthesized as a constitutively active enzyme which is activated following the trans-autophosphorylation of its own activation segment residue Ser241 (Casamayor *et al.*, 1999), but it is still able to co-ordinately regulate the activation of the different downstream substrates in response to different stimuli.

PDK1 consists of two functional domains, the N-terminal serine-threonine domain of the AGC family and the C-terminal Pleckstrin Homology (PH) domain which binds to PtdIns(3,4,5)P_3 with high affinity. Among the numerous AGC family-members, PDK1 and PKB are the only ones possessing phosphoinositides-binding PH domains, which lead to quite a distinctive mechanism of activation (Currie *et al.*, 1999). The PH domains act as specific recruitment modules controlling the translocation of both PDK1 and PKB to the part of the plasma membrane in which PtdIns(3,4,5)P_3 is synthesized (Anderson *et al.*, 1998). The binding of the PH domain to the phospholipid induces a major conformational change in PKB that enables the phosphorylation of the Thr308 at the T-loop by membrane-localized PDK1, causing partial activation. Phosphorylation of PKB on residue Ser473 within the hydrophobic motif results in a further increase in PKB activity (Fig. 6A). This is mediated by mammalian target of rapamycin complex 2 (mTORC2) (Sarbassov *et al.*, 2005b).

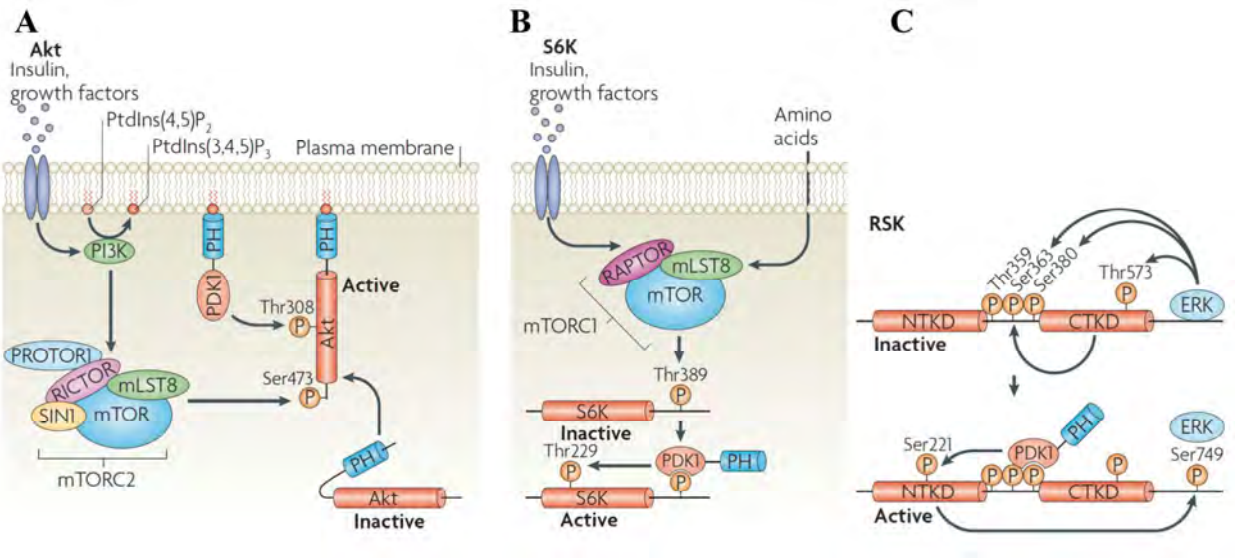

FIGURE 6. Mechanisms of activation of PKB/Akt, S6K and RSK. (A) PI3K is activated downstream of receptor tyrosine kinases. The generation of PtdIns(3,4,5)P_3 from PtdIns(4,5)P_2 by PI3K recruits PKB to the plasma membrane, where it is phosphorylated by PDK1 and mTORC2. (B) mTORC1 is activated downstream of growth factors and also by amino acids. It subsequently phosphorylates the hydrophobic motif of S6K providing a docking site for PDK1 which then can phosphorylate the activation segment. (C) ERK phosphorylates RSK carboxy-terminal kinase domain (CTKD) which phosphorylates the hydrophobic motif of the amino-terminal kinase domain (NTKD). This creates a docking site for the PIF pocket of PDK1 which activates RSK by phosphorylating the activation segment. Figure is adapted from (Pearce *et al.*, 2010)

However, the rest of PDK1 substrates lack PH domains to directly sense PtdIns(3,4,5)P_3 levels. Instead, these AGC kinases are phosphorylated at the hydrophobic motif that is not sufficient for their activation but creates a docking site that can be recognized by a groove within the PDK1 catalytic domain, termed PIF pocket, which functions as a phospho-docking site recognition motif. Once bound to the substrate, PDK1 then is able to phosphorylate the T-loop and activate targets such as S6K, RSK and SGK isoforms (Collins *et al.*, 2003). Phosphorylation of the S6K hydrophobic motif residue (Thr389) is mediated by mammalian target of rapamycin complex 1 (mTORC1) (Fig. 6B) (Hara *et al.*, 2002; Kim *et al.*, 2002). RSK isoforms are characterized by the presence of an N-terminus kinase domain (NTKD) of the AGC family and a C-terminus kinase domain (CTKD) of the CAMK family which is activated downstream of ERK1/2. The CTKB autophosphorylates then the hydrophobic motif, which is located in the linker region (Fig. 6C) (Dalby *et al.*, 1998). Recent work has established that mTORC2 regulates the hydrophobic motif phosphorylation and activity of SGK1 (Garcia-Martinez and Alessi, 2008). Deregulation of the activity of these enzymes and mutations in the enzyme encoded genes contribute to pathogenesis of many human disorders including neurodegenerative diseases (Table 2). Much effort is being applied in the development of drugs that target AGC kinases to treat these conditions. Despite intensive studies, still many basic questions remain.

Kinase	Substrates	Consensus motif for substrate*	Reported disease implications	Specific inhibitors
PDK1	Akt, PKC, PKN, RSK, S6K and SGK	Thr–Phe–Cys–Gly–Thr	Cancer	NA
Akt (also known as PKB)	AS160, BAD, BRAF, FOXO3, GSK3, HDM2, $p27^{KIP}$, PFK2, PGC1α, PDCD4, PRAS40, SKP2, TSC2 and WNK1	Arg–X–Arg–X–X–Ser/Thr–φ	Cancer, diabetes, schizophrenia, stroke and Huntington's disease	AKTI1/2 and MK2206
PKC	Adducin 1, gp130, GRK2, GSK3, IRS1, MARCKs, PKD, PDE3a, RAF1 and SHP1	Arg–Lys–X–Ser/Thr–X–Arg/Lys (for PKCα)	Cancer, cardiac disease, stroke and spinocerebellar ataxia type 14 (PKCγ)	NA
RSK	ATF4, BAD, DAPK, EEF2K, EIF4B, GSK3β, STK11, NFAT3, MAD1, $p27^{KIP}$, RAPTOR, RPS6, TSC2 and CCT	Arg/Lys–X–Arg–X–X–Ser/Thr	Cancer and Coffin–Lowry syndrome (RSK2)	BI-D1870 and SL-0101
S6K	CCT, EEF2K, EIF4B, GSK3β, IRS1, MAD1, mTOR, PDCD4, RPS6 and SKAR	Arg/Lys–X–Arg–X–X–Ser/Thr	Cancer, diabetes, Alzheimer's disease	NA
SGK	ENaC, FOXO3, MEKK2, NDRG1 and NEDD4L	Arg/Lys–X–Arg–X–X–Ser/Thr	Cancer, hypertension and Huntington's disease	GSK650394

TABLE 2. Substrates of some AGC kinases and their links to disease. AGC kinases phosphorylate a large number of substrates, a selection of which is shown. Consensus sequences for substrate phosphorylation that have been determined are indicated along with diseases in which AGC kinases have been implicated. *In which X denotes any amino acid and ϕ is a bulky hydrophobic residue. Table is modified from (Pearce *et al.*, 2010)

2.3. PKB/Akt: MAJOR EFFECTOR OF PI3K PATHWAY

PKB/Akt is a serine/threonine protein kinase of 60kD encoded by the cellular homologue of the transforming v-Akt oncogene, which was found in a retrovirus termed as Akt8 (Staal, 1987). PKB was first described by three different groups which demonstrated its high degree of homology with PKC and PKA (Bellacosa *et al.*, 1993;Coffer and Woodgett, 1991;Jones *et al.*, 1991). In mammals PKB/Akt exists as three closely and evolutionally related isoforms (termed as PKBα/Akt1, PKBβ/Akt2 and PKBγ/Akt3) with highly conserved domain structure. PKB/Akt isoforms are encoded by distinct genes, but exhibit more than 85% sequence identity. PKBα/Akt1 is ubiquitously expressed at high levels, whereas PKBβ/Akt2 is mostly expressed in insulin-responsive tissues such as liver, muscle and adipose tissue and PKBγ/Akt3 is highly expressed in brain and testis. PKB/Akt isoforms possess an amino-terminal Pleckstrin Homology domain (PH-domain), a central catalytic domain and a carboxy-terminal regulatory domain containing a hydrophobic motif. All three isoforms have two specific sites corresponding to Thr308 in the kinase domain and Ser473 in the hydrophobic motif of PKBα (Vanhaesebroeck and Alessi, 2000). As mentioned before, PKB is inactive in unstimulated cells and upon activation of PI3K and generation of PIP3, it translocates to the plasma membrane, where it becomes activated (Andjelkovic *et al.*, 1997). Down-regulation of PIP3 levels is specifically mediated by phosphatase and tensin homolog deleted on chromosome 10 (PTEN). Dephosphorylation of the hydrophobic motif of PKB by PH domain leucine-rich repeat protein phosphatase (PHLPP) and dephosphorylation of Thr308 site by protein phosphatase 2A (PP2A) leads PKB signaling to the end (Brognard *et al.*, 2007;Gao *et al.*, 2005).

PKB regulates many cellular processes including metabolism, proliferation, survival, growth and angiogenesis. Activated PKB phosphorylates serine/threonine residues on target proteins at a recognition sequence Arg-X-Arg-X-X- Ser/Thr-Hyd, where X is any amino acid and Hyd is a bulky hydrophobic residue (Alessi *et al.*, 1996). PKB manages to regulate the physiological functions through inhibitory or stimulatory phosphorylation of downstream substrates. The requirement of Arg residues at the -3 and -5 positions on peptides phosphorylated by PKB distinguishes it from other AGC kinases, which prefer the Lysine residue at these positions (Manning and Cantley, 2007).

2.3.1. PKB in neuronal survival

The PI3K/PKB signaling pathway has been proposed to contribute to diverse processes in the cell among which the prominent function in cell survival (Fig. 7). PKB as a major downstream target of growth factors enhances the cell survival by different mechanisms. Glycogen synthase kinase-3 (GSK3) is a bona fide, first characterised physiological substrate of PKB which activity is negatively regulated downstream of the PI3K pathway. GSK3 play essential roles in regulating neurogenesis, neuronal survival and neuronal plasticity and it is believed to be deregulated in a number of psychiatric disorders (Beaulieu *et al.*, 2009). Initially, GSK3 was found to be an important component of the apoptotic response occurring after growth factor withdrawal in cultured cortical neurons (Hetman *et al.*, 2000). Indeed, PKB inactivates GSK3 isoforms by phosphorylating them on an inhibitory site, namely Ser21 in GSK3α and Ser9 in GSK3β (Cross *et al.*, 1995). Inhibition of GSK3 is one of the mechanisms by which PKB kinase protects cells from programmed cell death. GSK3 promote cell death through the mitochondrial intrinsic apoptotic pathway by targeting several key proteins that regulate signals leading to the disruption of the mitochondria membrane. For example, GSK3 can directly phosphorylate the pro-apoptotic Bcl-2 family member Bax on Ser-163, which results in its activation (Linseman *et al.*, 2004). Also, stress-induced expression of pro-apoptotic Bim requires GSK3 activity, which can be counteracted by lithium (Hongisto *et al.*, 2003). Additionally, it has been reported that GSK3 exerts its pro-apoptotic function by phosphorylation and degradation of the anti-apoptotic Bcl-2 family member MCL-1 (Maurer *et al.*, 2006). Apart from the direct regulation of proteins implicated in mitochondrial function during apoptosis, GSK3 also regulates the expression of other components of the apoptotic signaling. The important tumour suppressor transcription factor p53 is regulated by GSK3, which binds directly to p53 and promotes p53-mediated transcription of specific genes (Watcharasit *et al.*, 2003). In addition to regulation of gene expression, GSK3 also regulates translation by phosphorylating and inhibiting elF2B, which appears to contribute to the control of cell survival by the PKB signaling pathway (Pap and Cooper, 2002).

PKB was also meant to inactivate human caspase-9 by phosphorylating Ser196, thereby providing a new mechanism for its anti-apoptotic role (Cardone *et al.*, 1998). However, the fact that the anti-apoptotic properties of PKB activation downstream of cytochrome c release were also observed in species such as mouse and monkey, in spite that the Ser196 phosphorylation site of caspase-9 is not conserved in these species (Fujita *et al.*, 1999), strongly argue against the notion of PKB directly regulating caspase-9 inactivation. By contrast, a prominent role of

ERK1/2 in promoting caspase-9 inactivation by phosphorylating Thr125 (Allan *et al.*, 2003), a well conserved site which become an integration point for multiple signaling pathways, is nowadays widely accepted (Allan and Clarke, 2009).

PKB directly regulates the cytoplasmic apoptotic machinery by regulating Bcl-2 family members activity. Upon growth factor stimulation, PKB enhances the cell survival by different mechanisms, one of which is blocking the function of pro-apoptotic proteins (Dudek *et al.*, 1997). PKB phosphorylates the Bcl-2 homology domain 3 (BH3)-only protein Bad at Ser136 thereby inhibiting its pro-apoptotic effect (Datta *et al.*, 1997). As described before, Bad pro-apoptotic function involves the binding with pro-survival Bcl-2 family members such as Bcl-XL resulting in their inactivation (Yang *et al.*, 1995). PKB-mediated phosphorylation of Bad at Ser136 is essential for the accessibility of other survival-promoting kinases at the Bad Ser155 phospho-site within the BH3 domain, which results in the binding of 14-3-3 proteins and disruption of Bad/Bcl-XL complex (Datta *et al.*, 2000). The survival effect of PKB among different cell types was also validated in primary neurons (Datta *et al.*, 2002).

PKB contributes to cell survival not only by directly inhibiting the pro-apoptotic BH3-only proteins, but also by regulating different transcription factors such are Forkhead, NF-kB and CREB that control the expression of survival or apoptotic genes. PKB phosphorylates the Forkhead transcription factor FOXO1 on Thr24 and Ser256, as well as FOXO3 and FOXO4 on their equivalent sites. PKB phosphorylation of FOXOs occurs in the nucleus and once phosphorylated they are sequester by 14-3-3 proteins, which triggers the release of FOXO transcription factors from the promoter of target pro-apoptotic genes, after which FOXO is exported from the nucleus. Among the gene promoters regulated by FOXO transcription factors, FasL and its receptor Fas, TRAIL (TNF-related apoptosis inducing ligand), TNFα and its receptor (Birkenkamp and Coffer, 2003) as well as Bim-1 (Dijkers *et al.*, 2000) represent relevant transcriptional targets that accounts for PKB-induced cell survival.

In addition to PKB function as a suppressor of critical death genes, it also triggers the expression of survival genes. PKB has the capacity to phosphorylate and activate IKKα and IKKβ, which are the upstream kinases that regulate the activation of the NF-κB family of transcription factors. IKKs directly phosphorylate IκB on a serine residue thereby targeting it for proteosomal degradation. As a result, NF-κB translocates into the nucleus where it activates transcription of pro-survival genes such as cIAP-1 and cIAP-2 (Dan *et al.*, 2008).

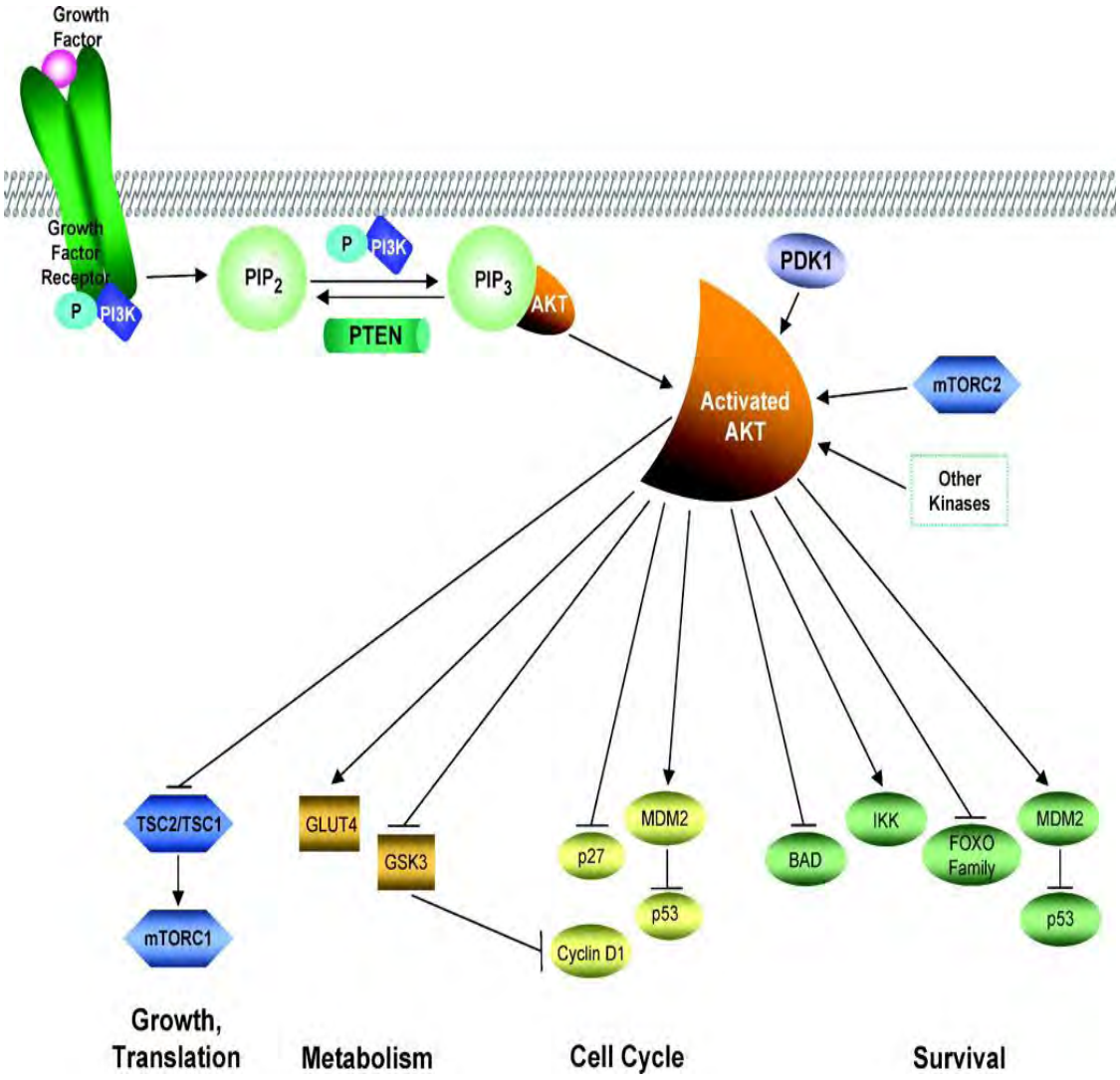

FIGURE 7. PKB substrates controlling cell survival (marked in green). Through the phosphorylation of a diverse set of substrates PKB mediate some of these biological processes, which are indicated on the figure (Crowell *et al.*, 2007).

The PKB signaling pathway also promotes survival by inhibiting the activity of the tumour suppressor protein p53. PKB activation initiated by survival factors promotes nuclear entry of the oncoprotein MDM-2 by phosphorylating it on Ser-166 and Ser-186. Once in the nucleus, MDM-2 promotes the ubiquitination and subsequent inactivation of p53 (Mayo and Donner, 2001), which is a major regulator of apoptosis. This function of p53 was mostly notable when chromosomal aberrations were detected due to DNA damage induced by environmental stresses. MDM-2 binds to the transactivation domain of p53, thereby blocking recruitment of factors necessary for the induction of gene expression. MDM-2, which forms a tight complex with p53, controls its function not only through inhibition of p53-mediated transcriptional activity, but also by promoting p53 degradation acting as an E3 ligase to maintain low protein levels of p53

under non-stressed conditions. Conversely, MDM-2 is positively regulated by p53 in an autoregulatory feedback loop in which p53 positively regulates MDM-2 expression and MDM-2 negatively regulates p53 (Momand *et al.*, 1992). MDM-2 has been also shown to be associated with MDMX, which is considered to be a direct substrate of PKB. PKB phosphorylates MDMX on Ser 367 generating a 14-3-3 binding site and the resultant association with 14-3-3 stabilizes MDM-2. The molecular details may need to be worked out but it is clear that PKB activity is important in keeping MDM-2 active and thus suppressing p53 activity (Lopez-Pajares *et al.*, 2008).

The other transcription factors which may account in part for the survival effects of the PKB pathway are CREB/CBP and E2F. In response to growth factor stimulation, PKB promotes the direct phosphorylation of CREB at Ser133, which stimulates the recruitment of CBP (CREB binding protein) to the promoter thereby activating cellular gene expression of pro-survival genes via the CRE-dependent mechanism. Several studies indicate that CREB and its paralog CREM are indeed important in cell survival. Overexpression of a dominant-negative CREB transgene enhances apoptosis (Du and Montminy, 1998) whereas targeted disruption of CREM gene causes a defect in germ cell apoptosis (Blendy *et al.*, 1996). The transcription factor E2F is known to have an important role in the regulation of apoptosis (Field *et al.*, 1996). It was shown that active PKB induces E2F inactivation, thereby promoting survival (Brennan *et al.*, 1997).

2.3.2. PKB in cell growth

One of the most conserved functions of PKB is promoting cell growth, which is a fundamental process of eukaryotic cell life. Nutrients and growth factors control cell growth by activating sensory signaling pathways. PKB contributes to this process by activating mTORC1 downstream of PI3K through the inhibitory phosphorylation of two mTORC1 inhibitory proteins, namely PRAS40 and TSC2. In response to growth factors TSC2, also called tuberin, is phosphorylated and functionally inactivated by active PKB (Inoki *et al.*, 2002). TSC2 is a negative regulator of the GTP binding protein Rheb (Ras homolog enriched in brain) which turns out as a main regulator of mTORC1 activation. In the GTP-bound state, Rheb binds directly to the kinase domain within the mTOR complex-1 and activates its kinase activity. TSC2 contains a GTP-ase activating protein domain at its C-terminus and in complex with TSC1, also named hamartin, is characterized with enhanced GAP activity towards Rheb, leading to its inactivation. In fact, TSC1 does not have any recognizable functional domain, but in complex with TCS2 prevents its degradation. Once TSC2 is phosphorylated by PKB it does not

have the functional GAP domain and can no longer convert GTP-bound active Rheb into GDP-bound inactive form, whereas functionally active TSC1/2 complex maintains Rheb in an inactive state (Castro *et al.*, 2003). In cells lacking either TSC1 or TSC2, the functional TSC1/2 complex is disrupted and consequently the levels of Rheb-GTP are elevated. This leads to deregulated mTORC1 activity and disorganized overgrowth within many organs that are seen in tuberous sclerosis hamartomas (Kwiatkowski and Manning, 2005). PKB also phosphorylates and inhibits PRAS40, a mTORC1 binding protein that inhibits mTOR activity, thereby allowing mTORC1 activation (Sancak *et al.*, 2007;Vander *et al.*, 2007).

2.3.3. mTORC1 and its downstream effectors

mTOR (mammalian target of rapamycin) is a serine/threonine kinase that belongs to the phosphoinositide 3-kinase (PI3K) related kinase (PIKK) family. mTOR plays a vital role in cell growth signaling pathways. mTOR exist in two huge functionally distinct complexes: mTOR complex-1 (mTORC1) and mTOR complex-2 (mTORC2) (Sarbassov *et al.*, 2005a). The unique proteins that distinguish these complexes are RAPTOR (regulatory-associated protein mTOR) within mTOR complex-1 that may have a role in substrate binding and in rapamycin-FKBP12 binding and sensitivity, and RICTOR (rapamycin-insensitive companion of mTOR) within mTOR complex-2 (Sarbassov *et al.*, 2005a). Another distinguishable set of components are PRAS40 (proline-rich Akt substrate 40kD) for mTORC1 which is a negative regulator of the whole complex (Sancak *et al.*, 2007) and PROTOR for mTORC2 which is likely to help in assembly the other mTORC2 subunits inside the complex (Pearce *et al.*, 2007). Besides that, mTORC2 contains mSIN1 (mammalian stress-activated protein kinase interacting protein 1) which is absent in the complex 1. mLST8 (the mammalian lethal with Sec13 protein8), also known as GβL, and DEPTOR (DEP domain-containing mTOR interacting protein) are shared components for both mTOR complexes.

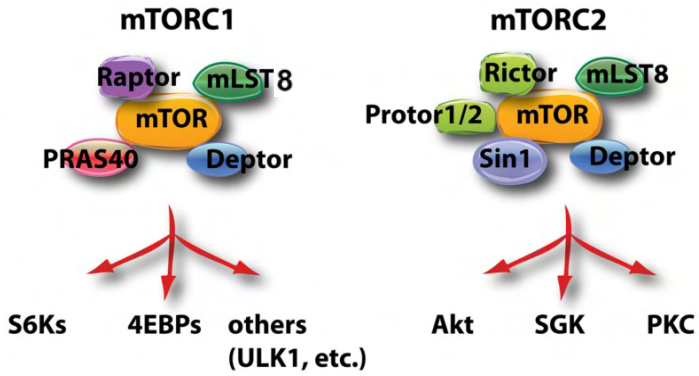

FIGURE 8. mTOR complexes. The diagram shows the components of mTORC1 and mTORC2 and their well-known substrates. Figure adapted from (Limon and Fruman, 2012)

mTORC1 is a major driver of cell growth in response to both growth factors and nutrients by regulating its downstream effectors S6 kinase-1 (S6K1) and 4EBP1. mTORC1 controls mRNA translation through activation of S6K1 and inactivation of eukaryotic translation initiation factor 4E (eIF4E) binding protein 1 (4EBP1), which is a translation suppressor that associates with and inhibits eIF4E. mTORC1 phosphorylates 4EBP1 at specific serine and threonine residues, which leads to release of eIF4E from 4EBP1 and permits its participation in translation initiation complex (Hara *et al.*, 1997). mTORC1 phosphorylates S6K at the hydrophobic motif (Thr389) allowing the phosphorylation by PDK1 in the S6K activation loop (Thr229). mTORC1 is also activated by amino acids in a PKB-independent manner. When phosphorylated by mTORC1, S6K promotes mRNA translation initiation and progression by phosphorylating multiple proteins. Several S6K targets have been described, including the S6 ribosomal protein (Kozma *et al.*, 1989), eEF2K (eukaryotic elongation factor 2 kinase) (Wang *et al.*, 2001) and eIF4B (eukaryotic translation initiation factor 4B) (Holz *et al.*, 2005). It is worth to mention that aside from the ability of mTORC1 to enhance protein synthesis through its downstream targets, active mTORC1 phosphorylates the Ulk1 kinase at Ser757 thereby inhibiting its autophagy induction activity (Kim *et al.*, 2011).

Unlike mTORC1, mTORC2 is the hydrophobic kinase for PKB, which is widely implicated in cell survival and differentiation (Sarbassov *et al.*, 2005b); mTORC2 is also the hydrophobic motif regulator for serum-and glucocorticoid-regulated kinase (SGK) (Garcia-Martinez *et al.*, 2008) and also, mTORC2 promotes the regulation of PKC isoforms which regulate cell cycle progression (Ikenoue *et al.*, 2008). All these findings collectively put mTORC2 upstream of important cellular processes such as survival or cell cycle progression.

2.3.4. mTORC1 in neuronal polarization

The majority of mammalian neurons are polarized, typically having multiple dendrites but only a single axon that ensures that information flows directionally within a neuronal circuit. Some extrinsic factors are identified as regulators of neuronal polarity. However, the main drive towards polarity in this system is cell-intrinsic. Several molecules including BRSK/SAD and LKB1/PAR-4 have been shown to play fundamental roles in neuronal polarization in the developing murine brain (Barnes *et al.*, 2007;Kishi *et al.*, 2005). Also, reduced TSC2 levels in cultured hippocampal neurons resulted in neurons with multiple axons, whereas its overexpression inhibits axon growth (Choi *et al.*, 2008). The TSC1/2 complex antagonizes axonogenesis by inhibiting mTORC1, which in turn phosphorylates ribosomal S6 kinase (S6K)

and the translational regulator 4EBP1, thereby stimulating the synthesis of selected proteins that promote cell growth (Wullschleger *et al.*, 2006) and also modulates the amount of BRSK/SAD protein within the neuron (Choi *et al.*, 2008). The BRSK/SAD kinases together with the LKB1/PAR-4 kinase are the best characterized and conserved regulators of neuronal polarity *in vivo*. Knockout studies demonstrated that BRSK1/SAD-B and BRSK2/SAD-A are required for neuronal polarity in mice (Kishi *et al.*, 2005). Although it is not clear how BRSK/SAD kinases regulate neuronal polarity, it is believed that part of this effect is mediated by phosphorylation of microtubule-associated proteins (MAPs) such as Tau (Kishi *et al.*, 2005).

Acting upstream of mammalian BRSK/SAD kinases, the mammalian homologue of polarity protein PAR-4, the LKB1 kinase, is required for neuronal polarity and axon formation in mouse brain (Barnes *et al.*, 2007). LKB1 phosphorylates and activates BRSK/SAD kinases in the presumptive axon leading to polarization and axon formation (Barnes *et al.*, 2007;Shelly *et al.*, 2007).

Studies of phospho-TSC2 localization in hippocampal primary cultures at early stages, before and at the onset on neuronal polarization, have revealed a pattern which may reflect the polarization process by which a single neurite will develop into an axon. Indeed, phosphorylated and thus inactivated TSC2 was specifically localized along the axon, whereas total TSC2 was distributed throughout the neuron. The downstream marker of the TSC2/mTORC1 signaling pathway, phospho-S6K (Thr389), was shown to be enriched in the axon but not in the dendrites, indicating that inactivation of TSC2 and activation of mTORC1 pathway occur specifically in the axon in the polarized neuron. Moreover, the PI3K inhibitor LY294002, which blocks PKB activation and thus TSC2 phosphorylation, significantly reduced phospho-TSC2 staining (Choi *et al.*, 2008) Although the authors of this work argue that phosphorylation/inactivation of TSC2 in the axon is mediated by the PI3K/PKB pathway, the rational argument for PKB standing upstream of TSC2 in newly polarized axons still remains to be elucidated.

3. PDK1/PKB GENETIC MODELS

3.1. PDK1 KNOCKOUT MUTATION IS INCOMPATIBLE WITH LIFE

To gain further insights into the roles that PDK1 play in activating the AGC kinases, mouse embryonic stem (ES) cells were generated in which both copies of the PDK1 gene were disrupted. Stimulation of the mutant ES cells lacking PDK1 with insulin-like growth factor (IGF1) induced PI3K activation. Although growth factors failed to activate PKB, S6K and RSK (Williams *et al.*, 2000) mutant cells proliferated at similar rates as control ones, what was unexpected as far as these members of the AGC kinase family regulate survival and proliferation in budding or fission yeast. Moreover, the studies *in vivo* about PDK1 regulating cell growth and apoptosis in *Drosophila* (Cho *et al.*, 2001c;Rintelen *et al.*, 2001) and in *C.elegans* (Paradis *et al.*, 1999) revealed that PDK1 is required for the normal development and viability of these organisms.

To learn more about the functions of PDK1 in mammals, PDK1 knockout mice were produced and analyzed. No $PDK1^{-/-}$ postnatal mice were ever recovered after the mating between the heterozygous $PDK1^{+/-}$ mice, which were themselves healthy and fertile. This indicated that the deletion of the PDK1 gene resulted in an embryonic lethal phenotype. Genotypic analysis of embryos from day E7 to E12,5 revealed the presence of $PDK1^{-/-}$ embryos at the expected Mendelian distribution, which were characterised by the absence of somites and the presence of a less developed head region. All this together indicated that PDK1 is indispensable in development, as germline deletion causes embryonic lethality (Lawlor *et al.*, 2002).

3.2. PDK1 HYPOMORPHIC MICE

The observed prenatal lethality of the PDK1 knockout embryos was rescued by generating PDK1 hypomorphic ($PDK1^{fl/fl}$) mutant mice. The $PDK1^{fl/fl}$ hypomorphic ES cells had markedly low levels of PDK1 protein and PDK1 kinase activity compared with the $PDK1^{+/+}$ wild type cells. The $PDK1^{fl/fl}$ mice were born viable at low than expected Mendelian frequency and were characterized by 40-50% reduced body size and proportionally reduced organ volumes compared with control littermates. Stereological estimation revealed that the reduced organ size was due to reduced cell cytoplasm volume rather than cell number. All these observations emphasize the importance of PDK1 for normal development and growth in a mammalian system (Lawlor *et al.*, 2002).

3.3. PDK1 CONDITIONAL KNOCKOUT MICE

However, the essentiality of PDK1 during embryonic development precluded the analysis of the PDK1 function in the adult tissues and organs. To bypass the lethal period, a number of tissue-specific conditional knockout mice were generated. Thus, the PDK1 muscle-specific knockout mice, in which PDK1 was specifically excised in skeletal and cardiac muscles, died suddenly from heart failure between 5 to 11 weeks of age and exhibited dilated cardiomyopathy resulting from cardyomyocites that were smaller and more sensitive to hypoxia (Mora *et al.*, 2003). Conditional deletion of PDK1 on T lineage development leads to impaired T cell differentiation (Hinton *et al.*, 2004). Liver specific PDK1 knockout mice lacking PDK1 in hepatocytes displayed post-pandrial glucose intolerance and died between 4-16 weeks of age due to liver failure (Mora *et al.*, 2005), whereas deletion of the PDK1 gene specifically in pancreatic β cells developed progressive hyperglycemia and reduction in islet density due to both reduced cell number and size (Hashimoto *et al.*, 2006).

Cells lacking PTEN, the lipid phosphatase that breaks down PdtIns(3,4,5)P_3 to PdtIns(4,5)P_2, are characterised by elevated levels of the downstream components of the phosphoinositide 3-kinase (PI3K) signaling, including up-regulation of the PdtIns(3,4,5)P_3 levels and hyperactivation of PKB and S6K activities. Loss of PTEN causes brain hypertrophy, resulting in disruption of the normal nervous system development (Fraser *et al.*, 2004;Marino *et al.*, 2002). To explore the importance of PDK1 and its contribution to abnormalities in the PTEN-deficient brain, the PTEN and PDK1 double knockout brain-specific mice were generated. The conditional deletion of PDK1 in brain caused microcephaly, but rescued the hypertrophy in PTEN-deficient brains (Chalhoub *et al.*, 2009) indicating that PDK1 is a key regulator in mediating brain size that antagonize the phenotype of the brain-specific PTEN knockout mice, which is in agreement with genetic studies showing epistasis between PTEN and PDK1 in fly and mice (Bayascas *et al.*, 2005;Rintelen *et al.*, 2001). Altogether, these studies provided novel insights onto the physiological roles of PDK1 in regulating organ and tissue homeostasis.

3.4. SITE-DIRECTED MUTAGENESIS DESIGN BASED ON STRUCTURAL DATA

A drawback of the tissue-specific PDK1 knockout models was that it was impossible to identify which of the downstream AGC kinase signal transduction pathways was responsible for the resultant phenotype. The crystal structure high resolution of the PDK1 catalytic domain first and the PDK1 PH domain soon after defined at molecular level the presence in the PDK1 protein of

a phospho-docking site binding pocket and a phosphoinositide binding pocket, respectively. This in combination with exhaustive mutational analyses studies revealed important features that increased the understanding of the mechanisms of regulation by PDK1 and allowed the rational design of single aminoacid mutations impairing the function of each of these binding pockets. These new genetic tools were called to become instrumental in defining the physiological roles that the PDK1 PIF pocket and the PDK1 PH domain play in the activation of diverse PDK1 substrates and in indentifying the contribution of the different PDK1-regulated kinases to the observed mice phenotypes.

3.4.1. PDK1 PIF pocket knock-in genetic models

The absence of the C-terminal hydrophobic motif in PDK1 distinguishes it from the other AGC kinases; however, PDK1 possesses a hydrophobic pocket in a small lobe within its catalytic domain similar to that found in PKA. Mutation of a residue that was predicted to form the central part of this pocket, Leu155, abolished the interaction of PDK1 with S6K and SGK1, and therefore the phosphorylation of S6K at Thr229 and SGK at Ser256, whereas the ability of PDK1 to phosphorylate either PKB or a short peptide that encompasses the Thr308 region at the activation loop of PKB was totally preserved (Biondi *et al.*, 2000).

The hydrophobic pocket on the kinase domain of PDK1, termed as PIF-pocket (PDK1-interacting fragment pocket) plays thus a key role in mediating the interaction and phosphorylation of S6K and SGK1 at their T-loops by PDK1. Furthermore, there is evidence that the prior phosphorylation of S6K, SGK1 (Biondi *et al.*, 2001) and RSK (Frodin *et al.*, 2000) at their corresponding hydrophobic motifs promotes their interaction with the PDK1 PIF-binding pocket and their PDK1-mediated T-loop phosphorylation, suggesting that the PIF pocket on PDK1 functions as a docking site recognition motif that enables PDK1 to bind the substrate once phosphorylated, thereby gaining the access for phosphorylation of its T-loop (Biondi *et al.*, 2001).

The elucidation of the crystal structure of the catalytic domain of PDK1 defined the residues performing the hydrophobic-groove within the PIF pocket. Mutagenesis of these residues indicated that they form a binding site for PDK1 substrates which are phosphorylated at Ser/Thr residues within their hydrophobic motifs (Biondi *et al.*, 2002). This observation was clearly explaining why the prior phosphorylation of PDK1 substrates at their hydrophobic motif was greatly enhancing their interaction with PDK1 (Biondi *et al.*, 2002).

In order to assess the role of the PDK1 PIF-binding pocket in regulating the specificity of activation of AGC kinases *in vivo*, knock-in embryonic stem (ES) cells were generated in which Leu155 was changed to Glutamic acid in both copies of the endogenous PDK1 gene. The PDK1 PIF-pocket was functionally disrupted by this approach. Expression of PDK1 was maintained at similar levels in both $PDK1^{L155E/L155E}$ and $PDK1^{+/+}$ ES cells. Growth factor activated only PKB, which is a PDK1 substrate that was not meant to require hydrophobic motif phosphorylation to be phosphorylated by PDK1. In contrast, growth factor failed to activate S6K, RSK, and SGK in the knock-in ES cells, demonstrating that the PDK1 PIF pocket plays a crucial role in enabling PDK1 to activate those substrates lacking PH domains (Collins *et al.*, 2003).

The $PDK1^{L155E/L155E}$ mice failed to develop to term. No $PDK1^{L155E/L155E}$ mice were ever isolated at E12,5 or later, indicating that the mutant embryos died and reabsorbed after this prenatal age. $PDK1^{L155E/L155E}$ embryos were retarded compared to control littermates of the same age. The mutant embryos displayed multiple abnormalities, including reduction in forebrain size and body axis defects.

To circumvent this prenatal lethality and to further dissect the contribution of the different PDK1 substrates in the regulation of cellular responses *in vivo* in tissues, a new strategy of transgenesis named tissue-specific conditional knock-in mice was engineered in which the mutant form of PDK1 is expressed in tissues expressing the Cre-recombinase under the control of a tissue-specific promoter. Thus, conditional knock-in mice expressing the PDK1 L155E mutation specifically in muscle were generated. The tissue-specific knock-in strategy worked successfully and, as it was expected, insulin induced phosphorylation and activation of PKB, but not S6K, in Cre-targeted tissues, whereas the activation of both PKB and S6K proceeded normally in non Cre-expressing tissues. The muscle specific $PDK1^{L155E/L155E}$ conditional knock-in mice were viable and of normal size and displayed no abnormality in glucose homeostasis (Bayascas *et al.*, 2006). Recently, PDK1 L155E neuronal-specific conditional knock-in mice have been generated, which are born alive and exhibit no overt phenotype (Lluis Cordon Barris, personal communication, ongoing project in JR Bayascas`lab).

3.4.2. PDK1 PH domain knock-in genetic models

PDK1 also contains a PH domain that binds PtdIns(3,4,5,)P_3 with high affinity and PtdIns(4,5)P_2 and PtdIns(3,4)P_2 with less affinity. This interaction does not affect PDK1 catalytic activity, but enhances its ability to activate PKB by co-localising both PDK1 and PKB to the plasma membrane (Currie *et al.*, 1999;Stokoe *et al.*, 1997). Triple mutation of three consecutive Arg residues to Leu (R472L/R473L/R474L) in the PH domain of PDK1 was shown to abolish the ability of PDK1 to interact with phosphoinositides (Currie *et al.*, 1999). This observation prompted to the generation of PDK1 (RRR472-474LLL) knock-in mutation in order to abolish PDK1-PtdIns(3,4,5,)P_3 binding and PKB activation. In response to insulin-like growth factor (IGF1), PDK1$^{R472,473,474L/\ R472,473,474L}$ knock-in ES cells showed normal activation of RSK, whereas PKB phosphorylation at Thr308 was significantly reduced. However, in homozygous knock-in ES cells as well as in mouse embryos, the PDK1 (RRR472-474LLL) mutant protein was only expressed at 20% of the normal levels, and resulted in embryonic lethality. Analysing the genotype of embryos revealed the presence of homozygous knock-in embryos at near Mendelian distribution between E7,5 and E10,5. At day E8, knock-in embryos were of similar size to their heterozygous or wild type littermates. However, the only phenotypic difference that became apparent between PDK1$^{R472,473,474L/R472,473,474L}$ and PDK1$^{+/+}$ mice embryos was head blood vessel and placental development defects (McManus *et al.*, 2004). Reduced expression of the mutant PDK1 protein could have contributed to the effects seen on PKB activation in ES cells as well as the embryonic lethality. Since the homozygous PDK1$^{R472,473,474L/\ R472,473,474L}$ have never ever developed to term, no much could be learned about the role of the PH domain of PDK1 in an animal model.

Lately, structural studies of the PDK1 PH domain-PIP3 complex suggested that the mutation of Arg473 to Leu could destabilize the PDK1 PH domain fold, which might explain the decreased expression or stability of the mutant PDK1 (RRR472-474LLL) protein (Komander *et al.*, 2004). Thus, it was impossible to determine whether the resultant phenotype was caused by the mutation or changes in protein expression or by the combination of both of these. Subsequent to this study, a knock-in point mutation (K465E) was designed that abrogated phosphoinositide binding without affecting the stability of the PDK1 PH domain (Fig. 9). Based on this, the PDK1$^{K465E/K465E}$ mice were generated. Homozygous PDK1$^{K465E/K465E}$ mice were found to be viable, born at the expected Mendelian frequency and being fertile.

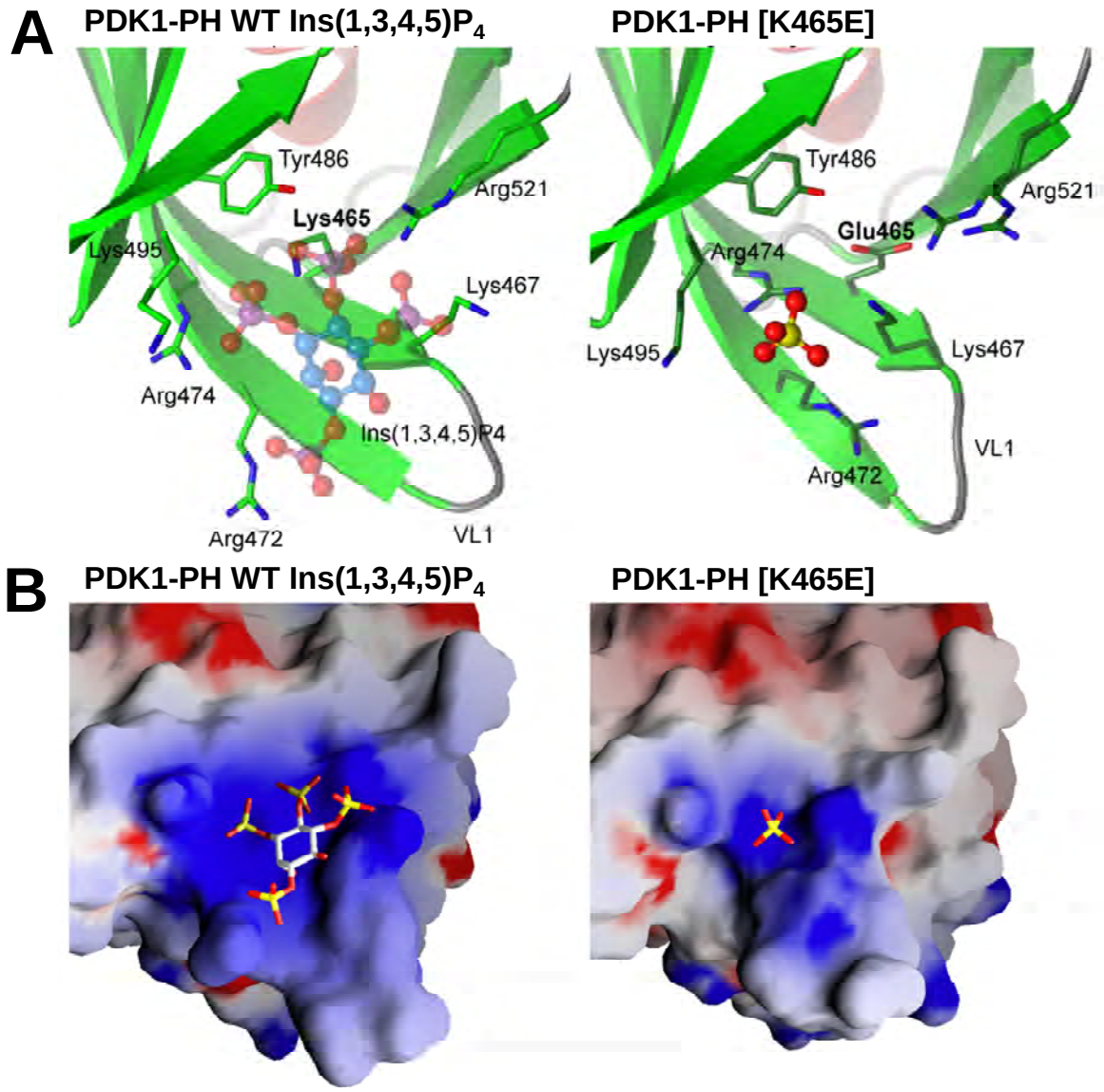

Figure 9. Crystal structure of the isolated PDK1[K465E] PH domain. (A) Comparison of the phosphoinositide-binding site of the wild-type PDK1 (left) with that of the PDK1 K465E mutant (right). A stick representation of the interactions of Ins(1,3,4,5)P_4 (blue, inositol ring; purple/red, phosphate groups) with protein residues (green) in the phosphoinositide binding site of the PDK1-PH domain is shown. Lys465 is the central residue in the back of the pocket, and its mutation to Glu does not affect the overall structure of the PH domain but leads to reorganization of the phosphoinositide-binding site by attracting surrounding positively charged residues. B) An electrostatic surface potential of the phosphoinositide binding site. Mutation of Lys465 to Glu alters the surface charge destroying the shape of the binding pocket (Bayascas *et al.*, 2008).

The significance that the interaction of the PDK1 PH domain with phosphoinositides plays in the activation of PKB has been evaluated *in vivo* in the PDK1$^{K465E/K465E}$ knock-in mouse model (Bayascas *et al.*, 2008), which expresses this rationally-designed point mutant form of PDK1 that retains catalytic activity but is incapable of phosphoinositide binding (Komander *et al.*, 2004). The inability of the mutant form of PDK1 to bind phosphoinositides was further confirmed by the experiment in which PDK1$^{K465E/K465E}$ protein did not interact with PIP3-coated beads, whereas wild type PDK1 interacted with this resin. Furthermore, in lysates derived from six different tissues from wild type and PDK1$^{K465E/K465E}$ mice, PDK1 was immunoprecipitated and assayed employing the T308tide peptide, encompassing the PDK1 phosphorylation site on the PKB T-loop, as a substrate and the extracts were immunoblotted with a specific PDK1 antibody. The results drawn from this experiment provided a clear evidence that the PDK1 protein is expressed in PDK1$^{K465E/K465E}$ knock-in mice at normal levels and moreover the catalytic activity of PDK1 is unaffected by the K465E mutation, as judged by the ability of PDK1 to phosphorylate the T308tide peptide (Bayascas *et al.*, 2008). In tissues derived from these mice, activation of PKB by growth factors is significantly reduced, whereas activation of the rest of PDK1 substrates proceeds normally. These mice are smaller and prone to diabetes. Deficient activation of PKB resulted in incomplete phosphorylation of some of its substrates, for example PRAS40 and TSC2 proteins. As a consequence, the growth factor-induced release of mTORC1 activation was significantly damaged, leading to reduced mTORC1 and S6K activities, which most likely explains the small size phenotype of the PDK1$^{K465E/K465E}$ mice (Bayascas *et al.*, 2008;Waugh *et al.*, 2009;Wullschleger *et al.*, 2011). Moreover, the PDK1$^{K465E/K465E}$ mice are protected from PTEN-induced tumourogenesis (Wullschleger *et al.*, 2011). The PDK1$^{K465E/K465E}$ mouse is a genuine model in which activation of PKB is only moderately reduced but not ablated, that has been proved instrumental in dissecting the PDK1 signaling (Bayascas, 2008). This has permitted to establish that in T-cells a PKB/Akt signaling threshold depending on PDK1-phosphoinositide interaction dictates specific cellular responses, such as cell migration, but not cell proliferation (Waugh *et al.*, 2009).

Thus, the above described PDK1(K465E) knock-in and PDK1(L155E) muscle-specific conditional knock-in genetic animal models have been successfully used in dissecting the role of the two major branches of the PDK1 signaling pathways in regulating some physiological processes. In glucose metabolism, the PDK1 K465E mice were shown to be viable and exhibited glucose intolerance and insulin resistance, which are the main hallmarks of diabetes (Bayascas

et al; 2008). By contrast, the PDK1 L155E muscle-specific conditional knock-in mice were shown to be normal regarding glucose homeostasis (Bayascas *et al.*, 2006).

3.5. INSIGHTS FROM PKB ISOFORM KNOCKOUT MICE MODELS

Targeted deletion of PKB isoforms in mice enabled the identification of biological processes controlled by individual PKB isoforms. PKB is implicated in the regulation of metabolism, cell survival, growth and migration. To understand the specific physiological functions of the individual isoforms, animal models deficient in PKBα, PKBβ and PKBγ were generated. Mice lacking PKBα, the most ubiquitously expressed member of the PKB family, demonstrated defects in fetal and postnatal growth and increased apoptosis compared with the control littermates (Chen *et al.*, 2001;Cho *et al.*, 2001b). In addition, PKBα$^{-/-}$ displayed placental insufficiency and as a consequence fetal growth impairment and neonatal mortality (Yang *et al.*, 2003). Also, PKBα is specifically required for thymus normal development (Fayard *et al.*, 2007). In contrast, PKBβ deficient mice displayed impaired ability of insulin to lower blood glucose levels. These mice are insulin resistant, with mild growth retardation and exhibit age-dependent loss of adipose tissue (Cho *et al.*, 2001a;Garofalo *et al.*, 2003). These observations establish PKBβ as the main regulator in maintaining normal glucose homeostasis. However, in contrast to diabetic PKBβ$^{-/-}$ mouse phenotype, PKBγ$^{-/-}$ mice display normal glucose metabolism, but reduced brain size by significant reduction in both cell volume and number. PKBγ deficiency in mouse brain was accompanied with a considerable reduction in total phosphorylated/activated PKB without any compensatory increase of other PKB isoforms, suggesting that PKB total activity failure was due to the loss of PKBγ isoform and further demonstrating that PKBγ is highly expressed in the nervous system (Easton *et al.*, 2005;Tschopp *et al.*, 2005). According to these genetic models, all three PKB isoforms appear to have some differential, non-redundant physiological functions. Further studies were required to complete the understanding of the spectrum of common and isoform-specific roles of the PKB kinases. Phenotypic analysis of double PKB isoform knockout mice revealed some overlap among the function of individual isoforms.

To address the issues of PKB isoform redundancy, mice with combined PKB deficiencies were generated. Double PKBα and PKBβ knockout mice develop to term but die shortly after birth by respiratory failure. These mice exhibit severe growth retardation with a very significant reduction in body weight, approximately 50% less than normal. They also showed skeletal muscle atrophy, impaired skin development and adipogenesis (Peng *et al.*, 2003). By contrast,

double PKBα and PKBγ knockout mice were embryonic lethal. They died around embryonic day 12 with severe impairments of growth and cardiovascular development. However, $PKB\alpha^{-/-}$ $PKB\gamma^{+/-}$ mice were born alive, but died several days after birth. Anatomic organ analysis of viable $PKB\alpha^{-/-}PKB\gamma^{+/-}$ mice at day 3 of age revealed hypotrophic thymus, heart and skin, which was much thinner than in the wild type (Yang *et al.*, 2005).

On the other hand, the PKBβ and PKBγ double knockout phenotype resulted in particular organ size reduction, 35 % in brain and 40% in testis weights compared to wild types, whereas the organ/body weight ratio was not changed in all the rest analysed tissues (heart, lung, thymus, liver, spleen, and kidney) which were proportionally decreased in size (Dummler *et al.*, 2006). Mice with a single functional allele of PKBα ($PKB\alpha^{+/-}PKB\beta^{-/-}PKB\gamma^{-/-}$) were born alive despite the severe reduction of body weight and insulin intolerance (Dummler *et al.*, 2006).

Single knockout PKB isoform mice models have no survival disadvantages in the adulthood; however PKBα knockout mice demonstrated increased neonatal mortality shortly after birth and displayed multiple developmental abnormalities. Furthermore, the pancreas-specific constitutively active PKBα mouse model showed an increase in pancreas cell and organ size accompanied by improved glucose tolerance (Bernal-Mizrachi *et al.*, 2001;Tuttle *et al.*, 2001). All this together is raising the intriguing possibility that the PKBα is the most critical isoform for fetal development and postnatal survival in mammals. This notion was further corroborated by the double $PKB\beta^{-/-}PKB\gamma^{-/-}$ knockout mice phenotype, which is fully viable with no growth abnormalities, as well as the $PKB\alpha^{+/-}PKB\beta^{-/-}PKB\gamma^{-/-}$ which were born alive in spite of having only a single PKBα isoform, in contrast to the $PKB\alpha^{-/-}PKB\beta^{-/-}PKB\gamma^{-/-}$ triple knockout mice which is embryonic lethal (Dummler *et al.*, 2006)

The PKBβ knockout mouse model was shown to be diabetic, whereas nor PKBα neither PKBγ seem to contribute to glucose homeostasis. As far as combined deficiency of PKBβ and PKBγ isoforms manifested glucose and insulin intolerance, this strongly suggested the enrolment of PKBβ isoform in glucose homeostasis.

However, it was reported that the double knockout $PKB\alpha^{-/-}PKB\beta^{-/-}$ mice with only PKBγ isoform retained, developed to term but died after birth with different severe abnormalities. The analogous phenotypical behaviour was found in $PKB\alpha^{-/-}PKB\gamma^{+/-}$ mice, whereas mice which were lacking both PKBα and PKBγ died approximately at day E11 displaying multiple embryonic developmental defects. These observations provide the strong genetic evidence about PKBγ isoform playing more critical role in early development and survival than PKBβ. Reduction in brain size was characteristic for PKBγ knockout mouse model, similar to this phenotype the

simultaneous deletion of PKBβ and PKBγ isoforms led to brain size reduction. This argues for the PKBγ isoform preference to regulate the brain size.

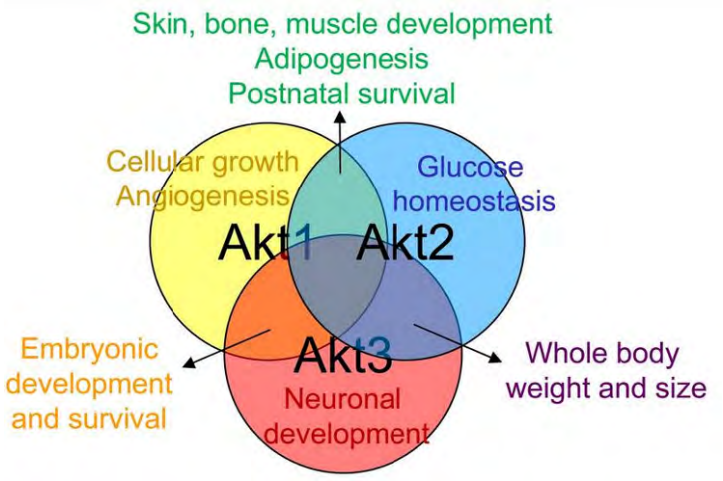

Figure 10. Overlapping and specific functions of PKB/Akt family members. PKB isoform-regulated common and distinct physiological functions, summarized from the phenotypic analysis of single and double PKB isoform knockout mice models. Figure adapted from (Gonzalez and McGraw, 2009)

PKB isoform single and double knockout mice genetic studies demonstrated different phenotypes, indicating that PKB isoforms play over-lapping but also differential roles in development and physiology (Fig. 10). Since PKB isoforms are structurally highly similar, the critical question raises how PKB activity is specified to discrete cellular functions in response to extracellular stimuli. It is considered that substrate specificity of PKB, abundance of each PKB isoform in a given type of tissue and specific cellular localizations may also in part account for PKB isoform specificity and the resultant phenotypes observed in the PKB isoform mutant mice. The understanding of PKB isoform individual or combinatorial contribution to distinct physiological functions is further required to facilitate the development of therapeutic approaches directed to interfere with PKB kinase functions. However, the PDK1 K465E mutation, which specifically and partially impairs the activation of all the three PKB isoforms by PDK1, could be a good alternative to define the physiological roles that the PKB kinases might play in adult tissues and in particular in the central nervous system, when compared to other PDK1 substrates.

Genotype	Targeted tissues	Viability	General findings and reference(s)
PDK1$^{-/-}$	All	Embryonic lethal E9,5	Lack of somites, forebrain and neural crest-derived tissue (Lawlor *et al.*, 2002)
PDK1$^{flox/flox}$	All	Viable	Reduced size (Lawlor *et al.*, 2002)
PDK1$^{-/-}$	Muscle	Lethality 5-11 weeks	Dilated cardiomyopathy (Mora *et al.*, 2003)
PDK1$^{-/-}$	Liver	Lethality 4-16 weeks	Postpandrial glucose intolerance and liver failure (Mora *et al.*, 2005)
PDK1$^{-/-}$	Pancreas	Viable	Hyperglycemia, islet mass loss (Hashimoto *et al.*, 2006)
PDK1$^{-/-}$	T-cells	Viable	Impaired T-cell differentiation (Hinton *et al.*, 2004)
PDK1(L155E)	All	Embryonic lethal E12	Developmental defects, forebrain reduction (Collins *et al.*, 2003;McManus *et al.*, 2004)
PDK1(R131E)	All	Embryonic lethal E19,5	General growth retardation (Collins *et al.*, 2005)
PDK1(RRR/LLL)	All	Embryonic lethal E10,5	Head blood vessel defects, lack of placental development (McManus *et al.*, 2004)
PDK1(L155E)	Muscle	Viable	Normal glucose homeostasis (Bayascas *et al.*, 2006)
PDK1(K465E)	All	Viable	Small, insulin-resistant, hyperinsulinemic (Bayascas *et al.*, 2008)
PKBα$^{-/-}$	All	Partial neonatal mortality	Small body size, increased apoptosis, placental defects, thymus developmental defects (Chen *et al.*, 2001;Cho *et al.*, 2001b;Fayard *et al.*, 2007;Yang *et al.*, 2003)
PKBβ$^{-/-}$	All	Viable	Insulin resistance, hyperglycemia, age-dependent lipoatrophy (Cho *et al.*, 2001a;Garofalo *et al.*, 2003)
PKBγ$^{-/-}$	All	Viable	Reduced brain weight (Easton *et al.*, 2005;Tschopp *et al.*, 2005)
PKBα$^{-/-}$PKBβ$^{-/-}$	All	Neonatal lethality	Small size, impaired skin, skeletal muscle, bone development and adipogenesis (Peng *et al.*, 2003)
PKBα$^{-/-}$PKBγ$^{-/-}$	All	Embryonic lethal E11	Severe impairments in growth, cardiovascular and nervous system development (Yang *et al.*, 2005)
PKBβ$^{-/-}$PKBγ$^{-/-}$	All	Viable	Impaired glucose homeostasis, reduced body size, reduced brain and testis weights (Dummler *et al.*, 2006)

TABLE 3. Genetically modified PDK1 and PKB mouse models. The table includes the information about phenotypes of genetically modified mouse models.

AIMS

AIM 1.-To analyze the intracellular signaling pathways induced by neurotrophic factors in the PDK1$^{K465E/K465E}$ mutant primary cultures of cortical neurons

1.1- To analyze the activation of PKB induced by neurotrophic factors in the primary cultures of PDK1$^{K465E/K465E}$ mutant and PDK1$^{+/+}$ wild type cortical neurons

1.2- To analyze the activation of the other PDK1 substrates rather than PKB, which regulation does not rely on a PtdIns(3,4,5)P_3 binding domain, in the primary cultures of PDK1$^{K465E/K465E}$ mutant and PDK1$^{+/+}$ wild type cortical neurons

AIM 2.-To study whether the PDK1 K465E mutation can affect neuronal responses in primary cultures of different neuronal cell populations

2.1-To investigate the role of PKB in survival of neuronal primary cultures upon stimulation with neurotrophic factors

2.2-To investigate the influence of the PDK1 K465E mutation on neuronal morphogenesis of primary cultures of cortical and hippocampal neurons

METHODS

1. EXPERIMENTAL ANIMAL MODEL

For the development of the objectives of this thesis, I have used the $PDK1^{K465E/K465E}$ knock-in mice, which express a rationally-designed point-mutant form of the PDK1 protein kinase which is incapable of phosphoinositide binding but with preserved catalytic activity. The generation and genotyping of the $PDK1^{K465E/K465E}$ knock-in mice expressing this single-aminoacid substitution of Lysine 465 for Glutamic acid in the PDK1 PH domain have been described previously (Bayascas *et al.*, 2008). Mice were transferred from the University of Dundee, Scotland, and maintained in the Animal House Facility Estabulari de Rosegadors de la Universitat de Lleida under standard husbandry conditions. Animals were housed with access to food and water *ad libitum* in a colony room kept at a constant temperature in between 19-22ºC and at 40-60% humidity, under a 12/12 hours light/dark cycle.

Mice homozygous for the knock-in allele expressing the PDK1 mutation in the whole body including brain have always been obtained from heterozygous breedings. To obtain embryonic primary cultures, experimental matings were set in which the day of pregnancy was determined after the appearance of the vaginal plug. At the appropriate day, pregnant mice were euthanized by cervical dislocation and embryos dissected out from the uterus. Genotype determination was carried out from the tail of each individual embryo. In this study I have used the homozygous $PDK1^{K465E/K465E}$ knock-in mice and cells for all the experiments, and the results were compared to control $PDK1^{+/+}$ wild type littermates.

All animal-related procedures were performed in compliance with the 214/1997 Act for the care and use of laboratory animals, and approved by the Universitat Autònoma de Barcelona ethical committee of animal care under a Generalitat de Catalunya project license.

2. PRIMARY CELL CULTURES

Primary cortical and hippocampal neuronal cultures were prepared from $PDK1^{+/+}$ and $PDK1^{K465E/K465E}$ littermate mice at embryonic day 15.5, whereas cerebellar granule neurons were obtained at postnatal day 8. Cerebral cortical or hippocampal tissues were dissected and the cells were enzymatically dissociated for 10 min at 37ºC in Solution 2 that consist on Krebs Ringer Buffer (120 mM NaCl, 4.8 mM KCl, 1.2 mM KH_2PO_4, 25 mM $NaHCO_3$, 14.3 mM glucose) containing 0.3% BSA, 0.03% $MgS0_4$ and 0.25 mg/ml of trypsin. The enzymatic digestion was stopped by adding solution 4 (see Table 4).

SOLUTION	REAGENTS	QUANTITY
PBS (1X)	H_2O	430 ml
	PBS 10X	50 ml
	Glucose 30%	10 ml
	Penicillin 10000U/ml-Streptomycin 10mg/ml	12.5 ml
Krebs-Ringer Buffer (KRB) 10X	NaCl	70.70 g
	KCl	3.60 g
	KH_2PO_4	1.66 g
	$NaHCO_3$	21.40 g
	Glucose	25.70 g
	H_2O	till 1000 ml
Magnesium Stock 3.8%	$MgSO_4 \cdot 7H_2O$	19 g
	H_2O	to 50 ml
Calcium Stock 1.2%	$CaCl_2 \cdot 2H_2O$	0.12 g
	H_2O	to 10ml
CELL CULTURE SOLUTIONS, FRESHLY PREPARED		
Solution 1	KRB 1X	50 ml
	BSA Fraction V	0.15 g
	Magnesium Stock 3.8%	0.4 ml
Solution 2	Solution 1	10 ml
	Trypsin	2.5 mg
Solution 3	Solution 1	10 ml
	DNase	0.8 mg
	Trypsin Inhibitor	5.2 mg
	Magnesium Stock 3.8%	0.1 ml
Solution 4	Solution 1	8.4 ml
	Solution 3	1.6 ml
Solution 5	Solution 1	5 ml
	Magnesium Stock 3.8%	40 µl
	Calcium Stock 1.2%	6 µl

TABLE 4. Solutions and media used for primary culture preparation and maintenance. A list of recipes for the preparation of solutions and mediums used in the primary cultures is provided.

The disaggregated tissue was then pelleted by centrifugation for 0.5 min at 1500 rpm, the supernatant was discarded and the pellets were mechanically dissociated in Solution 3 consisting on Krebs Ringer Buffer containing 0.3% BSA, 0.03% $MgS0_4$, 0.08 mg/ml DNase and 0.52 mg/ml trypsin inhibitor by gentle pipetting using a fire-polished Pasteur pipette to

produce a single cell suspension. Cells were collected and added to solution 5 consisting on Krebs Ringer Buffer containing 0.3% BSA, 0.03% $MgS0_4$ and 0.0014% $CaCl_2$. Cells were then centrifuged for 5 min at 1000 rpm and resuspended, then counted with the Scepter™ 2.0 Handheld Automated Cell Counter (Millipore) and finally diluted in DMEM (Dulbecco´s Modified Eagle Medium, Sigma Aldrich #D5796) complemented with 30 mM glucose, 2 mM L-Glutamine, 250 U/ml penicillin-0.25 mg/ml streptomycin and 10% FBS (Fetal Bovine Serum, GIBCO #10270). The cortical cells were plated onto poly-D-Lysine (50 µg/ml) coated 24-well plates for cell viability studies, or 6-well plates for Western blot analysis, at a density of 15 x 10^4 cells/ml, whereas hippocampal cells were plated onto poly-D-Lysine (150 µg/ml) coated 12-mm diameter glass cover slips in 24-well plates at a density of 5 x 10^4 cells/ml. The cells were allowed to attach to the plate for two hours and then the medium replaced by Neurobasal™ medium (GIBCO #21103) complemented with 30 mM glucose, 2 mM L-Glutamine, 250 U/ml penicillin-0.25 mg/ml streptomycin and 2% B27 Supplement (GIBCO #17504). Cells were maintained at 37°C in a humidified incubator containing 5% CO2 in normoxia conditions. Cerebellar granule cell cultures were prepared from dissociated cerebella of 8-day old mice by mechanically chopping up the cerebellum followed by trypsin digestion and trituration as described in the previous paragraph. Cells were plated in BME (Basal Medium Eagle, Sigma Aldrich #B1522) supplemented with 25 mM KCl, 10% FBS, 250 U/ml penicillin-0.25 mg/ml streptomycin. 10 µM Cytosine-β-D-arabinofuranoside was added to the culture after 24 h of seeding to prevent the proliferation of non-neuronal cells. Cells were plated onto 48-well culture plates coated with 10 µg/ml Poly-L-Lysine at a density of 1.35 x 10^6 cells/ml.

3. TROPHIC DEPRIVATION, STIMULATION AND DRUG TREATMENT

Experiments for cell survival and western blot analysis were always performed at day 6 *in vitro* (DIV 6). Cells were washed twice with serum-free DMEM and then incubated for 24 h in serum-free Neurobasal supplemented with 30 mM glucose, 2 mM L-Glutamine, and 0.25 mg/ml of penicillin/streptomycin. The experimental controls included sham treatments consisting of two washes with serum-free media and incubation with the same original conditioned media. BDNF (human Brain-Derived Neurotrophic Factor, Alomone #B-250) and IGF-1 (Millipore #GF138) were diluted in DMEM without any supplement. The inhibitors Akti-1/2 (Calbiochem #124018), PI-103 (Calbiochem #528100), SB-216763 (Millipore #361566), Staurosporine (Sigma #S4400), rapamycin (Calbiochem #553210) and BI-D1870

(kindly provided by Professor Dario R Alessi) were dissolved in dimethyl sulfoxide (DMSO, Sigma #D5879). For viability and apoptosis analysis, growth factors and inhibitors were added at the onset of trophic deprivation. For western blot analysis, cells were pre-treated for 30 min with inhibitors and then stimulated with BDNF as indicated.

4. PLASMID DNA TRANSFECTION

Hippocampal cells were plated onto 12-mm diameter glass cover slips in a 24-well plate at a density of 5 x 10^4 cells/ml in a final volume of 500 µl. 48 h later, cells were transfected using Lipofectamine® 2000 (Invitrogen #11668-027) according to the manufacturer´s instruction. Briefly, 250 µl of conditioned medium was removed from each well prior the transfection and kept in the bath at 37º C. Then the following mixtures were prepared in Opti-MEM®I Reduced Serum Medium (Gibco #31985-047):

1. 0.7 µl Lipofectamine® 2000 + 49 µl Opti-MEM medium per well.
2. 1 µg of DNA mixture (0.3 µg of plasmid of interest or empty vector plus 0.7 µg of GFP reporter plasmid) + 49 µl Opti-MEM medium per well.

Tubes were incubated at RT for 5 min, and then the content of tube 1 was transferred to tube 2 and further incubated for 20 min to form the DNA-liposome complex. The mixture was then added to the corresponding well and mixed gently by rocking the plate back and forth. The cells were incubated with the complexes for 1.5 h at 37ºC in the incubator (optimal incubation times had been determined previously by time course). The transfection mixture was then replaced with the kept 250 µl conditioned medium supplemented with 250 µl of complete fresh neuronal cell growth medium topping-up to 500 µl/well. Transfection efficiency was evaluated after 48 h by means of the fluorescent marker GFP.

The N-terminal HA-tagged human full length cDNAs of BRSK1 and BRSK2 (Lizcano *et al.*, 2004) were subcloned into pCMV and kindly provided by Gerard Ruiz from the Institut de Neurociències-Unitat de Bioquímica, whereas the pEGFP-C1 plasmid was from Invitrogen (#6084-1).

5. WESTERN BLOT ANALYSIS

5.1. GENERATION OF PROTEIN EXTRACTS FROM CELLS AND TISSUES

Primary cortical neurons were cultured for six days, then incubated for 4 h in DMEM without serum, and subsequently stimulated with the indicated agonists as described in the figure legends. The neurons were rapidly lysed in ice cold Lysis Buffer (50 mM Tris-HCl pH 7.5, 1 mM EGTA, 1 mM EDTA, 1 mM sodium orthovanadate, 50 mM sodium fluoride, 5 mM sodium pyrophosphate, 10 mM sodium beta glicerophosphate, 0.27 M sucrose, 1% (by mass) Triton-X 100, 0.1% (v/v) 2-mercaptoethanol, 1:100 Protease Inhibitor Cocktail) using the scraper for cell harvesting. The collected lysates were left on ice for 30 min and then centrifuged at 4^{o}C for 10 min at 13000 rpm. The supernatants were collected into fresh eppendorf tubes, frozen quickly in liquid nitrogen and finally kept at -20ºC.

LYSIS BUFFER	**REFERENCE**	**M.W.**	**grams/L**	**VOLUME FROM STOCK**
50 mM Tris-HCl, pH 7.5	Amresco 0497	121.14		50 ml Tris-HCl 1M pH 7.5
1 mM EGTA	Sigma E0396	380.35		4 ml EGTA 250 mM pH 7.5
1 mM EDTA	Sigma 443885	372.24		2 ml EDTA 500 mM pH 8.0
1 mM Na-orthovanadate	Sigma S6508	183.91		10 ml Na-OTV 100 mM
50 mM Na-fluoride	Sigma 7920	41.99	2.100	
5 mM Na-pyrophosphate	Sigma 221369	446.06	2.230	
10 mM Na-B-glycerol-P	Sigma G6501	216.11	2.161	
0.27 M sucrose	Sigma S9378	342.30	92.421	
1% (by mass) Triton X-100	Sigma X100	n.a	n.a	0.1 ml Triton X-100/10 ml buffer
0.1% 2-mercaptoethanol	Sigma M7154	n.a	n.a	0.01 ml 2-mercapto/10 ml buffer
Proteinase inhibitor	Sigma P8340	n.a	n.a	0.1 ml Prot. Inhibit/10 ml buffer

STOCK	**M.W.**	**PREPARATION**
Tris-HCl 1M, pH 7.5	121.14	60.7 g TRIS in 500 ml water, pH to 7.5 with HCl
EGTA 250 mM, pH 7.5	380.35	19.02 g EGTA in 200 ml water, pH to 7.5 with HCl
EDTA 500 mM, pH 8.0	372.24	93.06 g EDTA in 500 ml water, pH to 8.0 with HCl
Na-OTV 100 mM	183.91	3.68 g Na-OTV in 200 ml water, pH to 7.0 with HCl and microwaves to achieve yellow colour

TABLE 5. Lysis Buffer. The composition and procedure to prepare lysis buffer are provided.

Tissue extracts were prepared by homogenizing the tissue in a 10-fold mass excess of ice-cold Lysis Buffer using a pellet pestle for microcentrifuge tubes (Sigma-Aldrich #Z359955-1EA) for small size tissue pieces, like cortex, hippocampus and other brain parts of adult and embryonic mouse brains, or a Kinematica Polytron Homogenizer (PCU GmbH) for big size parts of the adult mouse, such as whole brain or liver. The tissue samples were directly transferred into a tube on ice containing ice-cold Lysis Buffer. The homogenates were left on ice for 30 min and then centrifuged at 4°C for 10 min at 13000 rpm to remove insoluble material. The supernatants were aliquoted, frozen in liquid nitrogen and stored at -20ºC until proceeding with protein analysis. Protein concentrations were determined by the Bradford method (Coomassie protein assay reagent, Pierce #23200) using bovine serum albumin (BSA) as a standard.

5.2. PROTEIN IMMUNOPRECIPITATION

For protein immunoprecipitation, 1 µg of the corresponding antibody was conjugated with 10 µl of beads (Streptavidin Sepharose, GE Healthcare, #71-5004-70). Sepharose beads and antibody were incubated at 4ºC for 30 min on a tube rotator mixer. Beads were washed three times with washing buffer (Lysis Buffer (See Table 5) plus 0.5 M NaCl). Then, the beads conjugated with the corresponding antibody were added to lysates containing 500 µg of protein and the immune complexes were allow to form overnight at 4ºC on a tube rotator mixer. Beads were collected by centrifugation and washed three times with washing buffer, while the supernatants were recovered and kept after the first centrifugation. Finally, the immune complexes were denatured by boiling 5 min in a Laemmli-SDS sample buffer (See Table 7, section 5.3.2) and resolved on a SDS-PAGE. Western blot analyses were carried out as described below. The supernatants depleted from a certain protein were loaded side by side with the immunoprecipitated samples, which served as a control of specificity of the procedure.

5.3. SODIUM DODECYL SULFATE-POLYACRYLAMIDE GEL ELECTROPHORESIS

5.3.1. SDS-PAGE gel preparation

Polyacrylamide gels were prepared in BIO-RAD mini PAGE (polyacrylamide gel electrophoresis) system (10 well, thickness 1 mm) using solutions listed in table 6.

SOLUTIONS (ml)	**RUNNING GEL**						**STACKING GEL**	
PERCENTAGE (%)	**5%**	**6%**	**7.5%**	**10%**	**12%**	**15%**	**3.6%**	**5%**
dH_2O	11.6	10.4	10	8.3	7	5	5.8	3.8
30% acryl 0.8 bis	3.4	4	5	6.7	8	10	1.3	0.85
1.5M Tris pH 8.8	5	5	5	5	5	5	-	-
0.5M Tris pH 6.8	-	-	-	-	-	-	2.5	0.325
20 % SDS	0.25	0.25	0.25	0.25	0.25	0.25	0.05	0.025
10 % APS	0.15	0.15	0.15	0.15	0.15	0.15	0.15	0.05
TEMED	0.03	0.03	0.03	0.03	0.03	0.03	0.03	0.005

TABLE 6. Table of solutions used in the preparation of SDS-PAGE running and stacking BIO-RAD gels. SDS: sodium dodecyl sulphate; TEMED: N, N, N', N'-tetramethylethylenediamine; APS: ammonium persulfate.

5.3.2. Running a SDS-PAGE gel

5X Laemmli sample buffer was added to normalized lysate samples, which were then boiled for 5 min at 95ºC before loaded on the SDS-PAGE gel alongside prestained protein markers (250-10kDa) from Bio-Rad (#161-0373). Gels were run on 1X Tris-Glycine Buffer 0.1% (w/v) SDS (see Table 7) at 160 V for 60-100 min depending on the nature of the gel and the protein of interest.

LAEMMLI-SDS SAMPLE BUFFER

CONCENTRATION	5X	1X	For 100 ml of 5X
Tris-HCl pH 6.8	125 mM	25 mM	25 ml Tris-HCl 0.5 M 6.8
Glycerol	50 %	10 %	50 ml
SDS	10 %	2 %	10 g
Bromophenol Blue	0.01 %	0.0025 %	12.5 mg
β-Mercaptoethanol		1 %	Freshly added

TRIS-GLYCINE SDS ELECTROPHORESIS BUFFER (10X)

CONCENTRATION	1X	10X	For 1 litter of 10X
Tris base	25 mM	250 mM	30.3 g
Glycine	192 mM	1.92 M	144.1 g
SDS	0.1 % (w/v)	1 % (w/v)	10 g

TRIS-GLYCINE TRANSFER BUFFER (10X)

CONCENTRATION	1X	10X	For 1 litter of 10X
Tris base	25 mM	250 mM	30.3 g
Glycine	192 mM	1.92 M	144.1 g

TBS BUFFER (10X)

CONCENTRATION	1X	10X	For 1 litter of 10X
NaCl	150 mM	1.5 M	87.6 g
Tris base	25 mM	250 mM	30.3 g

TABLE 7. Western Blot Buffers. Recipes of western blot buffers are provided as well as the concentrations of their components.

5.4. TRANSFER OF PROTEINS TO NITROCELLULOSE MEMBRANES

After SDS-PAGE, proteins were transferred to nitrocellulose membrane (Whatman®GmbH) using the wet transfer system (Bio-Rad). The paper/gel/membrane "sandwich" consisted, from the bottom to the front, on: three (Whatman™ #3030917) 3MM papers soaked in transfer buffer, membrane, gel and another three 3MM papers. Air bubbles were removed after each layer of the "sandwich" was added. The transfer was then performed at 100 V for 90 min.

Following the transfer, membranes were blocked in 10% skimmed milk/1X TBST for 45 min at room temperature. Primary antibodies were diluted in 5% milk/1X TBST (total protein antibodies) or in 0.5% BSA/1X TBST (phospho-protein antibodies) as indicated in Table 9 and incubated for 16 h at 4º C. Dilution factors of the primary antibodies were according to manufacturer's instructions. After 16 h incubation, the membrane was washed three times for 5 min in 1X TBST and then incubated with the appropriate secondary antibodies coupled to horseradish peroxidase diluted 1:5000 in 5% milk/1X TBST for 45 min at room temperature. The membrane was then washed three times for 10 min with 1X TBST. Detection of proteins was performed by the enhanced chemiluminescence (ECL) system (Table 8). Membranes were treated with the ECL reagent mixture for 1 min before exposed to Super RX Fujifilm (MTB) in the dark room. The film was developed to produce the images shown in the figures.

SOLUTION	REAGENTS	FOR 50 ml
ECL1	Tris-HCl 1M pH 8.5	5 ml
	Luminol 0.5M in DMSO	0.25 ml
	P-Coumaric Acid 79.2 mM in DMSO	0.25 ml
ECL2	Tris-HCl 1M pH 8.5	5 ml
	Hydrogen Peroxide 8.8M	0.32 ml

TABLE 8. Recipe of enhanced chemiluminescence (ECL) reagents.

5.4.1. Antibody detection

The following antibodies were kindly provided by Prof. Dario Alessi from the University of Dundee. All were raised in sheep and affinity purified on the appropriate antigen. The PKBα total antibody was raised against the sequence RPHFPQFSYSASGTA corresponding to residues 466–480 of rat PKBα; The total TSC2 antibody was raised against a sequence encompassing residues 1719-1814 of mouse TSC2; the total PRAS40 antibody was raised against the peptide DLPRPRLNTSDFQKLKRKY corresponding to residues 238-256 of human PRAS40; the total NDRG1 antibody was raised against the recombinant human NDRG1 protein expressed in *E.coli*. Affinity-purified polyclonal BRSK1 or BRSK2 specific antibodies were raised in sheep against the peptide SPRRGPPKDKKLLATNGTPLP corresponding to the C-terminal residues 774–794 of human BRSK1 and the peptide LSWGAGLKGQKVATSYESSL encompassing residues 655–674 of human BRSK2, as described (Rodriguez-Asiain *et al.*, 2011). The rest of the primary and secondary antibodies used for western blot and immunofluorescence analysis were of commercial origin and are listed below (Table 9).

PRIMARY ANTIBODY	HOST	SUPPLIER	REFERENCE	DILUTION
phospho-PKB Thr308	Rabbit	CST	#9275	1:1000
phospho-PKB Ser473	Rabbit	CST	#9271	1:1000
phospho-S6K Thr389	Rabbit	CST	#9205	1:1000
Phospho-S6K Thr229	Rabbit	CST	#9379	1:1000
total S6K	Rabbit	CST	#9202	1:1000
phospho-S6 Ser235/236	Rabbit	CST	#2211	1:1000
total S6	Rabbit	CST	#2217	1:1000
phospho-p44/42 Thr202/Tyr204	Rabbit	CST	#9101	1:1000
total p44/42 MAPK	Rabbit	CST	#9102	1:1000

phospho-GSK3α/β Ser21/9	Rabbit	CST	#9331	1:1000
total GSK3α/β	Mouse	SCB	#sc-7291	1:1000
phospho-FOXO-1 Thr24	Rabbit	CST	#9464	1:1000
phospho-FOXO-1 Ser256	Rabbit	CST	#9461	1:1000
total FOXO1	Rabbit	CST	#2880	1:1000
phospho-RSK Thr227	Rabbit	SCB	#sc-12445-R	1:1000
phospho-RSK Ser380	Rabbit	CST	#9335	1:1000
phospho-RSK Thr573	Rabbit	CST	#9346	1:1000
total RSK1/2/3	Rabbit	CST	#9355	1:1000
phospho-TSC2 Thr1462	Rabbit	CST	#3611	1:1000
phospho-PRAS40 Thr246	Rabbit	CST	#2997	1:1000
phospho-NDRG1 Thr346	Rabbit	CST	#5482	1:1000
phospho-TrkB Tyr706/707	Rabbit	CST	#4621	1:1000
total TrkB	Rabbit	CST	#4603	1:1000
Anti-Tau-1	Mouse	Millipore	#MAB3420	1:200
Anti Neurofilament H	Mouse	Covance	#SMI-312R	1:2000
Anti-MAP2	Rabbit	Sigma	#M3696	1:200

SECONDARY ANTIBODY	**HOST**	**SUPPLIER**	**REFERENCE**	**DILUTION**
Anti-Rabbit HRP-conjugated	Goat	Thermo	#31460	1:5000
Anti-Mouse HRP-conjugated	Goat	Thermo	#31430	1:5000
Anti-Sheep HRP-conjugated	Rabbit	Thermo	#31480	1:5000
Anti-Rabbit Alexa Fluor 594	Goat	Invitrogen	#A11072	1:400
Anti-Mouse Alexa Fluor 488	Goat	Invitrogen	#A11017	1:400

TABLE 9. Primary and secondary antibodies for western blot and immunofluorescence analysis. A list of primary and secondary antibodies is provided, as well as their source and the dilution that was used for western blot and immunofluorescence analysis. CST: Cell Signaling Technology, SCB, Santa Cruz Biotechnology.

6. EVALUATION OF CELL VIABILITY

6.1. MTT REDUCTION ASSAY

Cell viability was determined by the MTT reduction assay. Briefly, the 3-[4,5-dimethylthiazol-2-yl]-2,5-diphenyltetrazolium bromide salt (MTT, Sigma #M2128) was added to the cell culture at a final concentration of 0.5 mg/ml. Plates were then returned to the incubator for 45 min. After incubation, the medium was aspirated and the resulting formazan crystals were dissolved by mixing with 300 µl of DMSO. Absorbance intensity was measured at 570 nm, with background measured at 690 nm, using a spectrophotometer running the Labsystem Multiskan® software.

6.2. QUANTIFICATION OF APOPTOSIS

Cells were fixed in 2% paraformaldehyde, stained with 1 µg/ml of the DNA dye Hoechst 33342, and then visualized under the fluorescence microscope. Apoptosis was quantified at each condition point by scoring the percentage of apoptotic cells in the adherent cell population. Cells exhibiting fragmented or condensed nuclei were scored as apoptotic whilst cells showing uniformly stained nuclei were scored as viable. At least 300 cells from 5 to 6 randomly selected fields per well were counted.

7. MORPHOLOGICAL ANALYSIS

7.1. DETERMINATION OF ORGAN VOLUME AND CELL SIZE

Organ volume was determined using the Cavalieri method (Gundersen and Jensen, 1987) on brain paraffin sections of 8 µm collected at systematically spaced locations (k=96 µm) from a random starting position. The sections were photographed with a Nikon SMZ800 stereomicroscope at 2 X magnification using a digital camera. A square lattice grid was then overlaid on the picture using the program Photoshop version vCS5.1 and the number of intersections (P) hitting the organ was scored. The organ volume was then estimated using the equation $\sum P \times d^2 \times k$, in which d^2, the distance between each point of the square lattice grid squared was 0.14792 mm^2. The number and size of the cells was determined on E15,5 dissociated cortex and hippocampal tissues with the Scepter^{TM} 2.0 Handheld Automated Cell Counter (Millipore).

7.2-IMMUNOCYTOCHEMISTRY

Dissociated hippocampal cells were cultured on cover slips for the indicated experimental days *in vitro* and then fixed with 4% paraformaldehyde in PBS for 20 min at room temperature. Fixative solution was rinsed three times with PBS for 5 min, and then the cells were permeabilized with 0.02% saponin in PBS for 7 min at room temperature and blocked in 0.01% saponin, 5% BSA, 10 mM glycine in PBS for 1 hour. Primary antibodies were diluted 1:200 in PBS supplemented with 0.01% saponin, 1% normal goat serum and incubated overnight at 4ºC. Cells were then washed three times with PBS for 10 minutes. Appropriate secondary antibodies conjugated to Alexa594 or Alexa488 fluorescent dyes were used at a concentration of 1:400, and nuclei were stained with 1 µg/ml Hoechst 33342. Cover slips were then mounted with FluoroSave Reagent on microscope slides for further analysis.

7.3. IMMUNOHISTOCHEMISTRY

Three $PDK1^{+/+}$ and three $PDK1^{K465E/K465E}$ matched littermate mice were deeply anesthetized by intra-peritoneal injection with a ketamine/xylacine mixture and then intracardially perfused with 0.9% NaCl followed by 4% buffered paraformaldehyde. Brains were extracted and post-fixed with the same solution for 2 h, washed in phosphate buffer 0.1 M pH 6.0 for 2 h and preserved in a 70% ethanol solution at 4ºC. All the six specimens were then embedded in the same paraffin block and sliced into 5 µm thick coronal sections with a Leica RM2255 microtome. Paraffin-embedded sections were incubated for 2 h at 60ºC and then rehydrated through a series of 2 washes with xylene for 5 min, 2 washes with 100% ethanol for 3 min, 1 wash with 96% ethanol for 3 min, 1 wash with 70% ethanol for 3 min, 1 wash with 50% ethanol for 5 min and 1 wash with water for 1 min. Sections were then boiled 10 min in 10 mM sodium citrate pH 6 for antigen retrieval and cooled down for 30 min on ice. Samples were blocked in Tris Buffer Saline (TBS, 50 mM Tris pH 7.5, 150 mM NaCl) containing 0.02% Triton and 5% goat serum for 30 min, and incubated overnight at 4°C with primary antibodies diluted in the same blocking solution (1:300 for the rabbit anti-MAP2 antibody and 1:2000 for the mouse monoclonal anti-pan axonal marker SMI-312R). Sections were rinsed with TBS buffer and detected with the Alexa488-conjugated anti-mouse (1:400) and Alexa594-conjugated anti-rabbit (1:300) secondary antibodies for 1.5 h at room temperature. Tissue autofluorescence was removed by incubation with Sudan Black for 10 minutes (0.3% w/v Sudan Black in 70% ethanol). Sections were counterstained with Hoechst and mounted

with FluorSave Reagent. Immunostained sections were photographed with a Nikon Eclipse 90i epifluorescent microscope and the captured images analyzed and processed with the ImageJ 1.42q (Wayne Rasband, National Institutes of Health, USA) and the Fiji (http://pacific.mpi-cbg.de/wiki/index.php/Main_Page) softwares.

7.4. QUANTIFICATION OF DIFFERENTIATION

For differentiation analysis of the cortical neurons, cells were seeded at a reduced density of 37500 cells/ml. Under this condition most neurons did not contact with neighbouring cells, allowing the measurement of neurite development of individual neurons. Images were acquired at 20X magnification on random fields by using an inverted microscope equipped with a high sensibility camera Hamamatzu Orca-Er at the maximal resolution of the microscope. The total neurite length per cell was measured by tracing all the neurites on each individual neuron from the cell body to the tip with the Adobe Photoshop vCS5.1 software, and the number of pixels converted to micrometers. The cell diameter was defined using the same technique by measuring the major axis of the neuronal cell body. The number of neurites per cell and number of branching points per neurite were also determined by direct counting on the acquired images.

For differentiation analysis of the hippocampal cells, images were obtained with an epifluorescent microscope (Nikon Eclipse 90i) interfaced to a DXM 1200F camera at 20X magnification. Images for the red and green channels were taken simultaneously. Neuronal dendrites were identified by immunostaining with the dendritic marker MAP2, whereas the axon was defined as a neurite whose length is 2 times longer than the other neurites and also is immunoreactive for the axonal marker Tau-1. To measure the axonal elongation, each particular axon was manually traced followed by automatic length calculation with the MetaMorph® image analysis software v6.1.

8. STATISTICAL ANALYSIS

Statistical significance was determined using the Student's t test analysis. $*p < 0.05$, $**p < 0.005$ between categories or conditions as indicated in the figure legends.

RESULTS

1. THE PDK1$^{K465E/K465E}$ PH-DOMAIN KNOCK-IN MICE

Crystal structure resolution of the PDK1 PH domain in complex with PtdIns(3,4,5)P_3 demonstrated that it possesses a ligand-binding site that enables PDK1 to interact with phosphoinositides with high affinity. Among the different positively-charged lateral chains conforming this binding pocket, Lysine at position 465 establishes fundamental interactions with the phosphate groups at position D3 and D4 within the PtdIns(3,4,5)P_3 inositol ring, and the targeted mutagenesis of Lysine 465 to Glutamic acid abolished the PDK1-phosphoinositide interaction by disrupting the conformation of this lipid-binding pocket (Komander *et al.*, 2004, see Fig. 9). In the case of PKB, interaction with PtdIns(3,4,5)P_3 has been reportedly shown to play fundamental roles in PKB activation. First, it promotes the translocation of PKB to the plasma membrane (Andjelkovic *et al.*, 1997). Second, the PKB PH domain bound to phosphoinositides undergoes a conformational change that result in the switch of the kinase from the inactive to the active conformer, which can be then phosphorylated and activated by membrane-localized PDK1 (Calleja *et al.*, 2007;Milburn *et al.*, 2003;Thomas *et al.*, 2002). By contrast, the role that the PDK1-PtdIns(3,4,5)P_3 interaction plays in this pathway has not been well defined. In order to analyze the importance of the PDK1-PtdIns(3,4,5)P_3 interaction *in vivo*, the homozygous PDK1$^{K465E/K465E}$ knock-in mice were generated that express the PDK1 K465E mutant protein abrogating phosphoinositide binding and leading to an specific signaling lesion. As a direct consequence, the mutant mice were shown to be smaller than control littermates, hyperinsulinemic and insulin resistant (Bayascas *et al.*, 2008). Notably, this study constituted the first genetic evidence in an animal model to highlight the fact that the binding of PDK1 to phosphoinositides is required for optimal activation of PKB, since the homozygous PDK1$^{K465E/K465E}$ mice express a mutant form of PDK1 just incapable of phosphoinositide binding but with intact catalytic activity. Since the PI3K/PKB pathway is meant to control many essential physiological functions in the central nervous system, it was reasoned that this mouse model could be successfully employed to define the importance of this pathway in neurons. Besides, the fact that the PDK1 K465E knock-in mutation is not tissue-specific, but expressed in every single tissue including the brain, opened-up a good possibility to use this strain straight forward in order to focus on the effects of the PDK1 K465E mutation on several aspects of brain development.

1.1. GROWTH RETARDATION OF THE PDK1$^{K465E/K465E}$ MICE

The homozygous PDK1$^{K465E/K465E}$ mice are viable, fertile and display no severe defect except that they are smaller than their control littermates, in agreement with the phenotype which was observed previously (Bayascas *et al.*, 2008). However, in my hands this strain produced offspring from heterozygous breeding in which the homozygous PDK1$^{K465E/K465E}$ mice were detected at reduced Mendelian frequency, both at embryonic day E15 (19.8 %) and at birth (16.0 %), thereby indicating that the PDK1 K465E mutation resulted in partial embryonic lethality (Fig. 11A). No differences in the incidence of mortality were reported for the mutant PDK1$^{K465E/K465E}$ mice compared to the control PDK1$^{+/+}$ mice from birth and during the whole adulthood. The phenotype associated with the growth deficiency of the PDK1$^{K465E/K465E}$ mice might have arisen early during development, since I observed that at gestational day E15.5, the PDK1 knock-in embryos were already 20% smaller than their control littermates. The difference in size between PDK1$^{K465E/K465E}$ and PDK1$^{+/+}$ mice was acutely increased after two weeks of post gestational growth up to almost 35% difference in body weight by the third week of age (Fig. 11B) which was maintained throughout their adulthood. For example, the growth curve of the PDK1$^{K465E/K465E}$ male mice equalize the growth curve of the PDK1$^{+/+}$ female littermates, indicating the growth impediment of the PDK1$^{K465E/K465E}$ mice (Fig. 11C).

1.2 REDUCED BRAIN SIZE OF THE PDK1$^{K465E/K465E}$ MICE

I next compared the brain volume from the PDK1$^{K465E/K465E}$ and PDK1$^{+/+}$ E15,5 embryonic littermates using sections analyzed by the quantitative Cavalieri method, as described in Methods. Consistent with the reduced body weight of the PDK1$^{K465E/K465E}$ mice, the overall size of the brain in the PDK1$^{K465E/K465E}$ mice was strikingly reduced when compared with the PDK1$^{+/+}$ control littermates. A representative example is shown on figure 12. The average estimated volume was 20% smaller in the PDK1$^{K465E/K465E}$ mice compared with their PDK1$^{+/+}$ littermates (31.96 ± 1.68 mm^3 for the PDK1$^{+/+}$ brain compared to 25.54 ± 1.19 mm^3 for the PDK1$^{K465E/K465E}$ one). This 20% reduction in the brain volume together with the body weight reduction observed at E15,5 in the PDK1$^{K465E/K465E}$ mice indicates that brain size is reduced to scale (Fig. 12A). Overall, these data highlights the contributing role of the PDK1 interaction with phosphoinositides to growth and development.

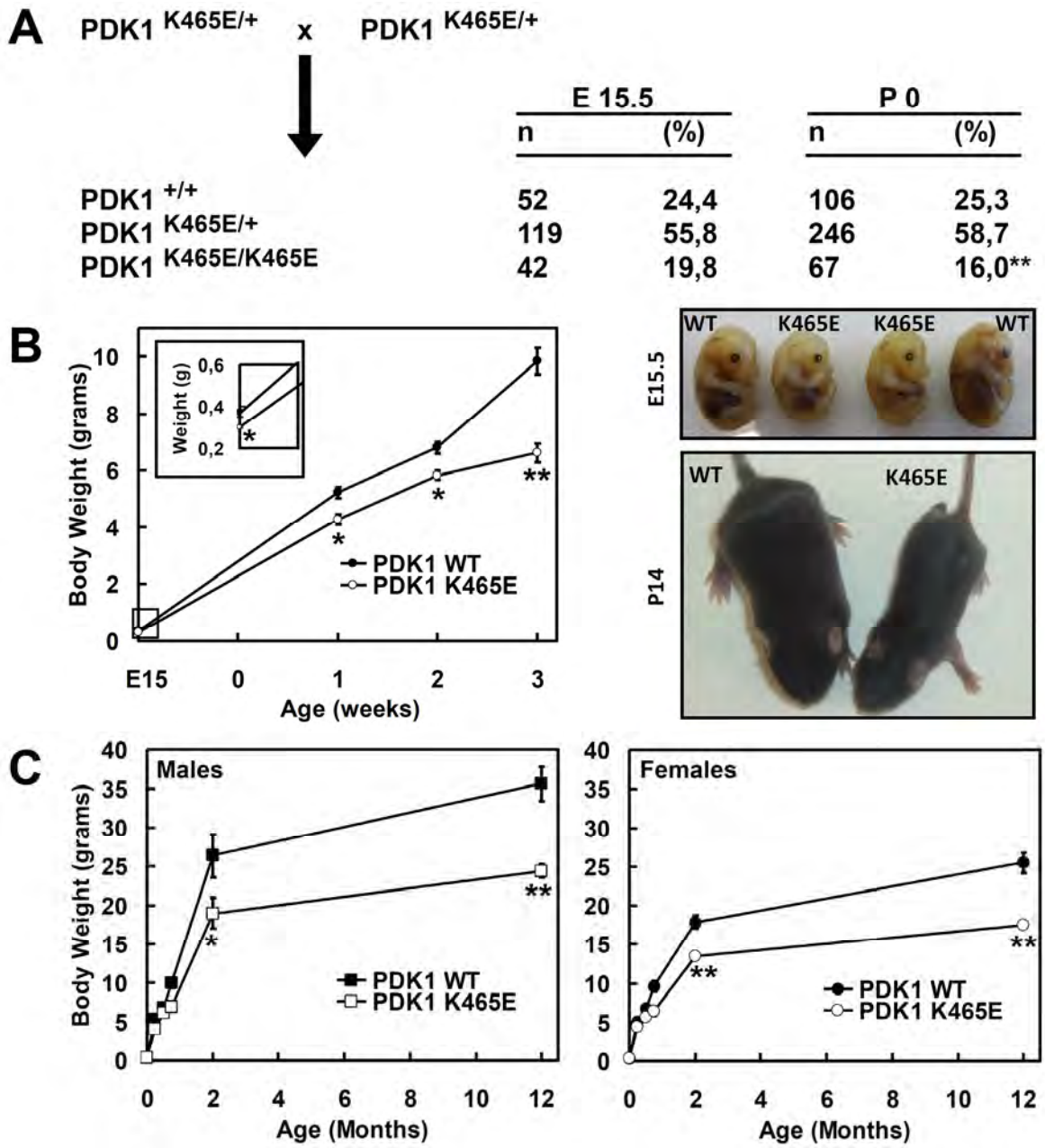

FIGURE 11. Reduced body size of the PDK1$^{K465E/K465E}$ mice. (A) The number (n) and proportion (%) of mice of the three different genotypes resulting from heterozygous breeding are indicated both at embryonic day 15.5 (E15,5) and at birth (P0). ** indicates that lower than expected frequency of PDK1$^{K465E/K465E}$ pups obtained is statistically significant ($\chi 2$ Test p <0.005). (B and C) The mean body weights of the indicated PDK1 wild type (PDK1 WT) and mutant (PDK1 K465E) male and female mice at the indicated age in weeks (B) or months (C) are shown. The values represent the mean ± SEM with each data point obtained from at least five embryos or pups (B) or ten mice (C) per genotype. Representative pictures of the indicated littermate wild type (WT) and mutant (K465E) E15,5 embryos (E15,5) or 14 days-old pups (P14) are shown in (B). * $p < 0.05$; *$p < 0.005$ compared with wild type controls as obtained by the Student's t test.

1.3. REDUCED NEURONAL CELL SIZE WITH NORMAL NUMBER OF NEURONS IN THE PDK1$^{K465E/K465E}$ MICE BRAIN

The reduced brain size in the PDK1$^{K465E/K465E}$ mice could be explained if the cells are of normal size but are fewer in number or if the cells are smaller but normal in number, or both. To distinguish between these two possibilities it was employed the quantitative unbiased method for determining neuronal cell soma volume and number of neuronal cells purified from both the embryonic cortex and hippocampus as it is described in methods.

Whilst the number of cortical and hippocampal neurons obtained from the E15,5 embryonic brain was not significantly different between genotypes, the volume of the neuronal cell soma was 20% reduced in the PDK1$^{K465E/K465E}$ mutant hippocampal and cortical cells when compared to PDK1$^{+/+}$ cells (Fig. 12B and C). These findings show that a reduced neuronal cell volume rather than a decrease in cell number caused the reduction in brain mass of the PDK1$^{K465E/K465E}$ mice, thereby pointing out to a specific growth defect.

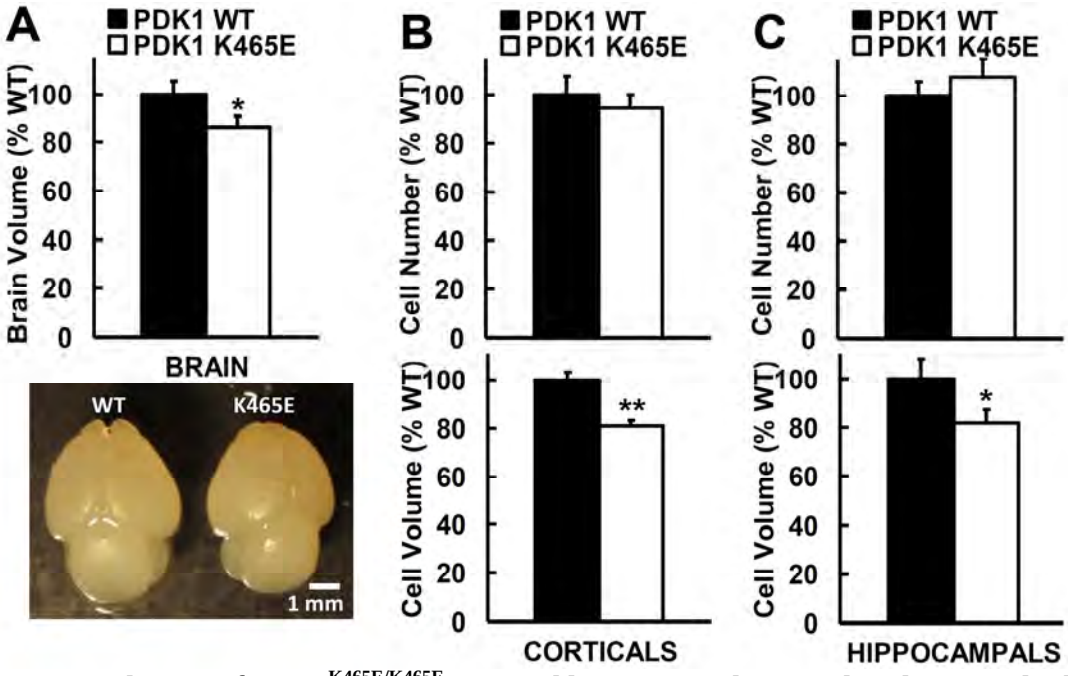

FIGURE 12. Reduction of PDK1$^{K465E/K465E}$ neuronal brain size is due to reduced neuronal cell size rather than cell number. (A) Upper panel, the volume of the brain was measured at E15,5 from histological sections using the Cavalieri method. The data are represented as the mean ± SEM for three different mice per genotype. Bottom panel, representative photographs of brains dissected from E15,5 PDK1 WT and PDK1 K465E embryo littermates; scale bar 1 mm. (B and C) The number of cells (upper panels) and the volume of the cell (bottom panels) were determined from E15,5 dissociated cortical (B) or hippocampal (C) neurons. The data are represented as the mean ± SEM for (B) twenty five wild type and twenty nine mutant embryonic cortical cultures obtained from eighteen independent litters, or (C) eight wild type and seven mutant embryonic hippocampal cultures obtained from six independent litters. * $p < 0.05$ and * $p < 0.005$ compared with wild types as obtained by the Student's t test.

2. MUTATION OF THE PDK1 PH-DOMAIN IMPAIRS BDNF-MEDIATED PKB ACTIVATION

In order to determine whether the impaired PDK1-PtdIns(3,4,5)P_3 interaction could affect PKB activation in neuronal cells, I evaluated the impact of the PDK1 K465E mutation on PKB phosphorylation and activation induced by growth factors such as BDNF. For this purpose, primary cultures of cortical neurons derived from littermate PDK1$^{+/+}$ and PDK1$^{K465E/K465E}$ embryos were deprived from serum for 4 hours and then stimulated with 50 ng/ml of BDNF for the indicated time points (Fig. 13A). As a control of the stimulation, it was first assessed the activation state of the BDNF receptor TrkB by measuring its phosphorylation at the residues Tyr706/707, corresponding to the activation loop, which demonstrated the equal phosphorylation levels in both PDK1$^{+/+}$ wild type and PDK1$^{K465E/K465E}$ mutant cortical cells in response to BDNF.

2.1. DEFFICIENT ACTIVATION OF PKB IS RATE LIMITING FOR SUBSTRATES SUCH AS PRAS40 AND TSC2, BUT NOT GSK3 OR FOXO1

In the PDK1$^{+/+}$ mice cortical neurons, BDNF induced a rapid activation of PKB, as judged by the level of phosphorylation of the two activating residues, Thr308 and Ser473, which reached the maximum after 5 minutes and was then sustained for up to 30 minutes. The phosphorylation of PKB at Thr308, the PDK1 site, was significantly reduced in the PDK1$^{K465E/K465E}$ mice neurons during the first 15 min of stimulation and was then detected at fairly normal levels after 30 min. By contrast, the phosphorylation of PKB at Ser473, the mTORC2 site, was not affected by the PDK1 mutation (Fig. 13A). Quantification of the immunoblot signals showed that the maximal difference in PKB Thr308 phosphorylation between the PDK1$^{+/+}$ and PDK1$^{K465E/K465E}$ neurons was reached at 5 min of BDNF treatment (Fig. 13B). The observed reduction of PKB phosphorylation was translated on reduced phosphorylation levels of some PKB substrates. For instance, phosphorylation of PRAS40 at Thr246 and TSC2 at Thr1462, corresponding to their specific PKB sites, were significantly reduced. By contrast, this deficient PKB phosphorylation at the activation loop seems not to be rate limiting in neurons for BDNF-mediated phosphorylation of FOXO1 or GSK3α/β, the more popular and ancient PKB substrate (Fig. 13A). It is worthy to mention that PKB is not the only kinase phosphorylating these sites in FOXO1 and GSK3α/β, since there are several AGC kinases including RSK, S6K and PKC responsible for this task. For example, while

BDNF-induced phosphorylation of GSK3α/β at Ser21/9 is totally abrogated by the PI 3-kinase specific inhibitor PI-103, either inhibition of PKB with the Akti-1/2 isoform specific inhibitor or RSK with the BI-D1870 specific inhibitory compound partially affected BDNF-induced phosphorylation of GSK3α/β at Ser21/9, therefore supporting the notion of RSK compensating for the PKB activation deficit in the $PDK1^{K465E/K465E}$ mice (Fig. 13C). However, GSK3 phosphorylation is still moderately decreased in the $PDK1^{K465E/K465E}$ mice samples under basal conditions (control and 1 minute time points) raising the possibility of PKB activity being rate limiting for this substrate in some particular conditions. All together, these western blot data demonstrate that mutation of the phosphoinositide binding site in PDK1 results in attenuated PKB activation.

2.2. PKB ACTIVATION DEFICIENCY IS TIME- AND DOSE-DEPENDENT

As mentioned in the previous section, lack of interaction of PDK1 with phosphoinositides resulted in deficient activation of PKB due to incomplete phosphorylation of the Thr308 residue within the T-loop. As shown in Figure 13A, this defect is clearly but transiently observed only at short time points of stimulation, but recover to normal levels at 30 min. I further explored the dynamic pattern of phosphorylation of PKB during a more detailed time course of BDNF stimulation, and confirmed that phosphorylation of PKB by PDK1 is in fact delayed in the $PDK1^{K465E/K465E}$ cortical cells (Fig. 14A). Next it was analyzed the response of the cortical cultures to a dose-curve of BDNF. Five minute time point was chosen for this experiment as it has been shown previously to represent the pick of PKB activation. In the $PDK1^{K465E/K465E}$ mice samples, BDNF-induced phosphorylation of PKB at the T-loop (Thr308) is reduced at all the indicated doses tested, being only detectable at a maximal dose of 50 ng/ml of BDNF, whereas the hydrophobic motif (Ser473) phosphorylation of PKB was indistinguishable between $PDK1^{+/+}$ and $PDK1^{K465E/K465E}$ cortical protein samples (Fig. 14B).

FIGURE 13. Deficient PKB phosphorylation and activation in the $PDK1^{K465E/K465E}$ cortical neurons. (A) Cortical neurons from two PDK1 wild type (WT) and two PDK1 mutant (K465E) mice embryos were cultured for 6 DIV, then serum starved for 4 hours and then either left unstimulated or stimulated with 50 ng/ml BDNF for the indicated time points. Lysates were immunoblotted with the indicated phospho and total antibodies. A representative Western blot of three independent experiments is shown. (B) The effect of the PDK1 K465E mutation on the phosphorylation of PKB at Thr308 and Ser473 was determined by quantitative western blot on cell extracts from cortical neurons

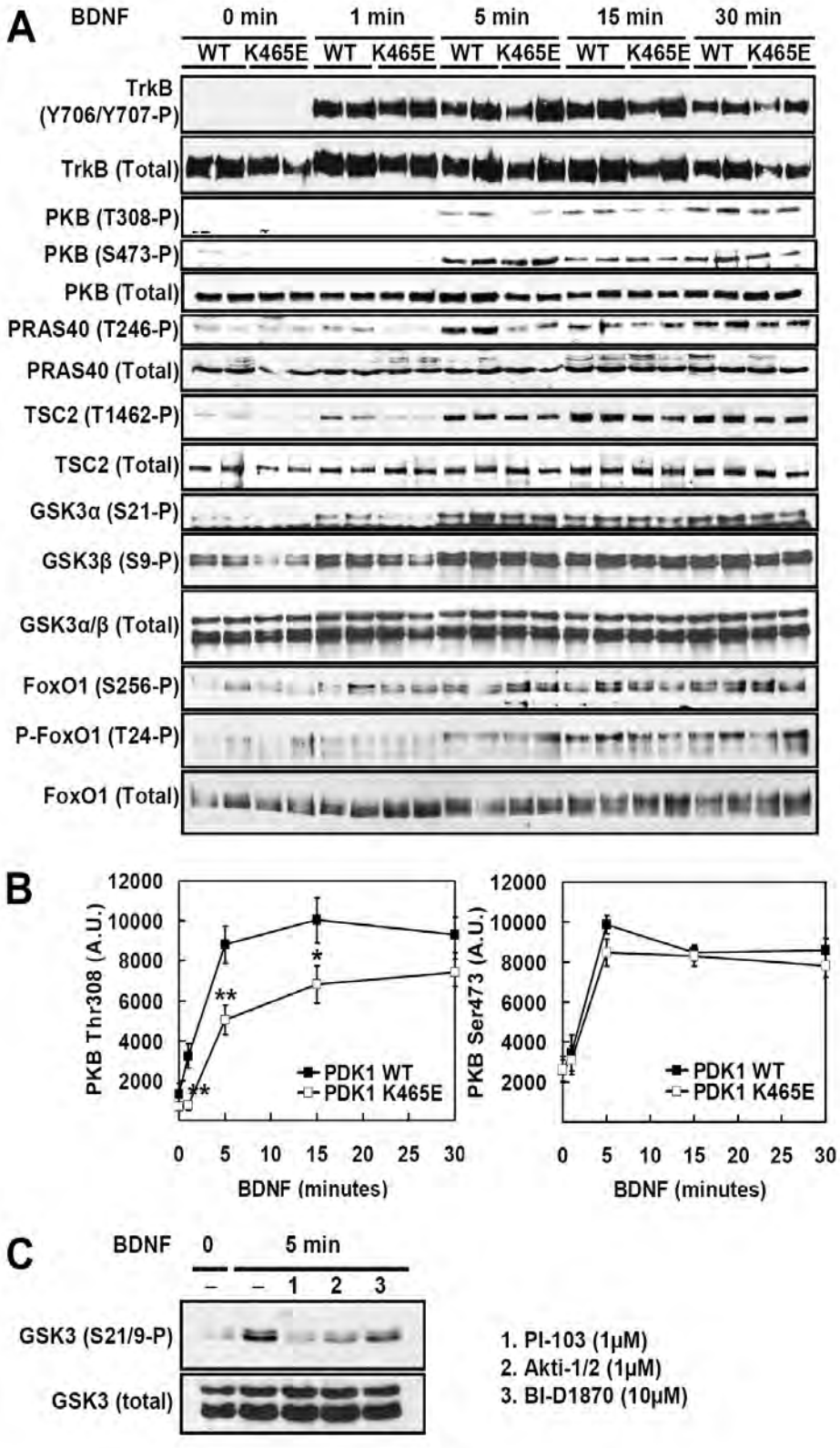

stimulated as in (A). Values are expressed as arbitrary units (A.U) and are presented as the mean ± SEM of protein extracts derived from three independent experiments. * $p < 0.05$; ** $p < 0.005$ (Student's t test) compared with wild type extracts. (C) Wild type cortical neurons were cultured for 6 DIV, serum starved for 4 hours, pretreated for 30 min with PI-103 and Akti-1/2 or 1 hour with BI-D1870 as indicated and then left unstimulated or stimulated with 50 ng/ml BDNF for 15 minutes. Lysates were immunoblotted with the indicated phospho and total antibodies.

Accordingly, PRAS40 phosphorylation at Ser246 and TSC2 phospholylation at Thr1462 were also reduced at all BDNF doses tested. By contrast, phosphorylation of GSK3α/β was not affected in the mutant samples (Fig. 14B).

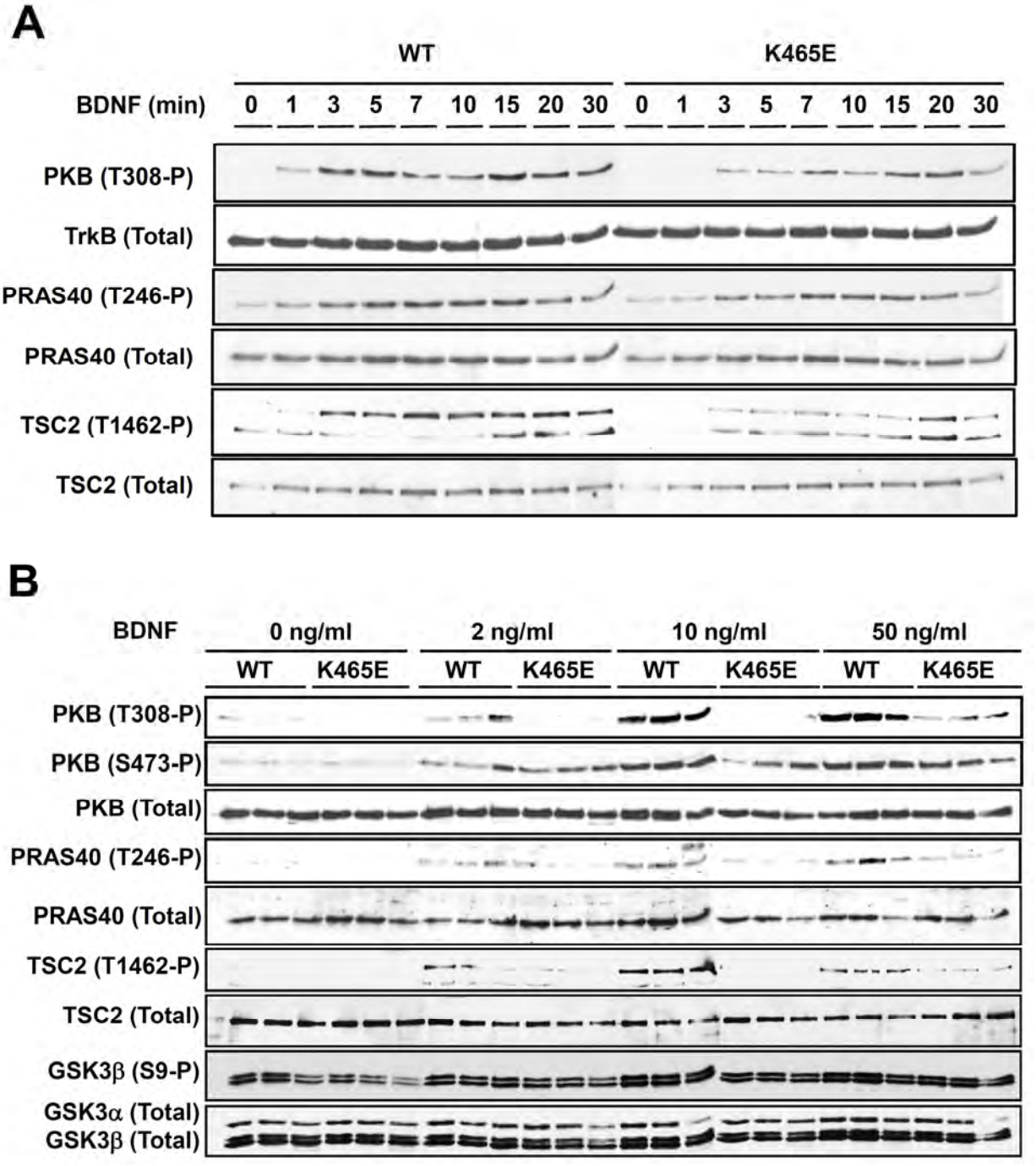

FIGURE 14. BDNF time and dose-dependent response in the PDK1$^{K465E/K465E}$ cultured cortical neurons. (A) Cortical cultures from PDK1 wild type (WT) and knock-in (K465E) embryos were cultured for 6 DIV, then serum starved for 4h and either left unstimulated or stimulated with 50 ng/ml BDNF for the indicated time points (min). (B) Cortical cultures from three PDK1 wild type (WT) and three knock-in (K465E) embryos were trophic deprived for 4h and then treated for 5 minutes with the indicated concentrations of BDNF. The phosphorylation of PKB and its substrates were determined by western blot using phospho-specific and total antibodies.

3. REDUCED ACTIVATION OF S6K IN THE PDK1$^{K465E/K465E}$ MICE CORTICAL NEURONS

PKB acts as an upstream kinase for S6K since PKB induces mTORC1 activation by inhibiting the tuberous sclerosis complex 2 (TSC2), which negatively regulates G protein Rheb (Inoki *et al.*, 2002). Once Rheb is active it promotes mTORC1 activation. PKB also phosphorylates PRAS40, thereby relieving the PRAS40-induced inhibition of mTORC1. Active mTORC1 phosphorylates S6K on Thr389, thereby creating a docking site for PDK1 and allowing the phosphorylation of the S6K Thr229 residue in the activation loop by PDK1. These concomitant mechanisms eventually allow S6K activation. Accordingly, although S6K is a docking site-dependent PDK1 substrate, the reduced phosphorylation of PKB, PRAS40 and TSC2 proteins observed in the BDNF-stimulated PDK1$^{K465E/K465E}$ cortical neurons (Fig. 13A) resulted in a deficient activation of mTORC1, as judged by the reduced phosphorylation of S6K at Thr389 detected at 5 minutes of BDNF treatment. As a consequence, PDK1 phosphorylation of Thr229 residue was also reduced, leading to decreased S6K activation and clear impairment of S6 protein phosphorylation at the Ser235 phosphorylation site. Phosphorylation of the S6 ribosomal protein at Ser235 serves as a good read out of S6K activity and fully parallels the phosphorylation of S6K at the two activation sites. By contrast, the phosphorylation of S6K at Thr421/Ser424 by ERK is intact in the BDNF-stimulated PDK1$^{K465E/K465E}$ cortical neurons (Fig. 15).

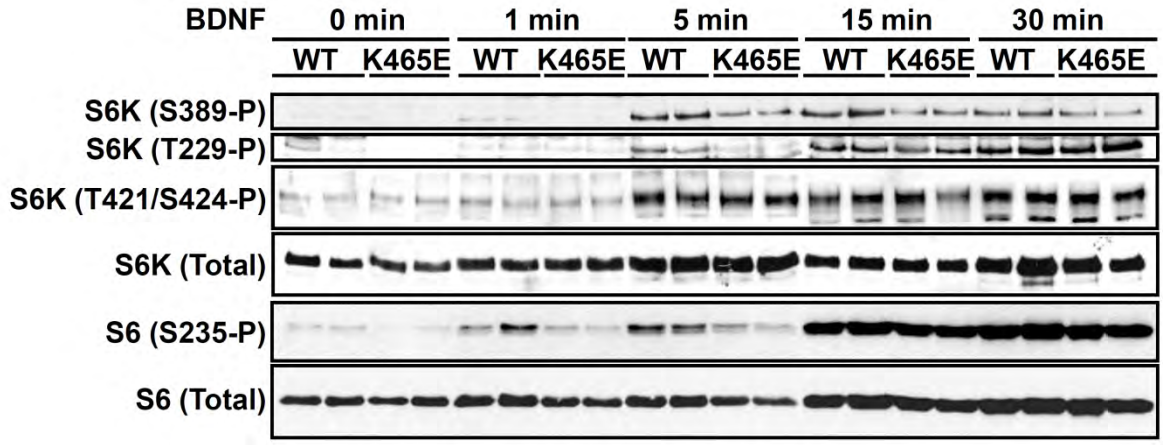

FIGURE 15. Phosphorylation of S6K by BDNF in the PDK1$^{K465E/K465E}$ cultured cortical neurons. Cortical neurons from two wild type (WT) and two knock-in mice (K465E) were cultured for 6 DIV, then serum starved for 4h and then either left unstimulated or stimulated with 50 ng/ml BDNF for the indicated time points (min). Lysates were immunoblotted with the indicated phospho and total antibodies.

The evidence that in the PDK1$^{K465E/K465E}$ mutant cells S6K phosphorylation is decreased both at the Ser389 mTORC1 and the Thr229 PDK1 regulatory sites at early time-points is in agreement with the fact that the maximal deficiency of PKB activation as well as PRAS40 and TSC2 phosphorylation is observed also at 5 min. These data suggests that the defective mTORC1/S6K activation associated with the PDK1 K465E mutation is relevant to BDNF-induced release of mTORC1 activity by PKB.

3.1. NUTRIENT-INDUCED ACTIVATION OF S6K BY GLUTAMINE IS PRESERVED IN THE PDK1$^{K465E/K465E}$ MICE CORTICAL NEURONS

mTORC1 acts in cells as a sophisticated cellular sensor of growth factors, intracellular energy levels and amino acids that can also be activated in a PKB-independent manner. The nutrient-stimulated pathway is triggered by a bidirectional transport of Glutamine and essential amino acids (Nicklin *et al.*, 2009) and promotes the targeting of mTORC1 to the lysosome by the Rag GTPases/Ragulator complexes, leading to mTORC1 activation (Sancak *et al.*, 2010;Sancak *et al.*, 2008).

Since activation of mTORC1 can also be achieved in response to nutrients, and in particular amino acids (Avruch *et al.*, 2006;Sancak *et al.*, 2008) in a PKB-independent manner, I wondered whether this pathway can compensate for PKB deficiency and guarantee in that way proper S6K activation and S6 protein phosphorylation in the PDK1$^{K465E/K465E}$ cells. For this reason, the same experiment depicted in Figure 15 was repeated in which the cortical cultures were deprived for four hours from both serum as well as Glutamine. As shown in Figure 16A, the deficiency in S6K activation and S6 ribosomal protein phosphorylation is more pronounced than that depicted on Figure 15 and parallels closely the deficient PKB Thr308 phosphorylation of the mutant extracts, thereby indicating that Glutamine as well as other essential aminoacids present in the culture media could have attenuated the requirement of proper PKB activation for adequate mTORC1 activation.

The detection of S6K phosphorylation at Thr229 has been proved elusive for years due to the lack of good antibodies. The Phospho-PKC pan gamma Thr514 Antibody from Cell Signaling Technology (#9379), which was meant to detects endogenous levels of PKC alpha, beta I, beta II, gamma, delta, epsilon, eta and theta isoforms only when phosphorylated by PDK1 at their activation loop residue homologous to threonine 514 of human PKC gamma, was shown to detect also S6K when phosphorylated at its activation loop Thr229 site (Collins *et al.*, 2003). In my hands, this antibody also was able to recognize PKB when phosphorylated at the

activation loop Thr308 site and therefore became an invaluable tool to analyze the activation levels of both S6K and PKB at the same time. As shown in Figure 16B, the stimulation of cells with BDNF induced two bands of around 70 and 65 kDa that were recognized by the above mentioned antibody, the upper being sensitive to the mTORC1 inhibitor rapamycin whilst the lower to the Akti-1/2 PKB inhibitor. Pre-treatment of cells with the PI 3-kinase inhibitor PI-103 totally inhibited both phosphorylation signals (Fig. 16B). To further evaluate the impact of the nutrient pathway in S6K activation, I next cultured in parallel the same cortical neurons from PDK1$^{+/+}$ and PDK1$^{K465E/K465E}$ embryos in minimal media in the presence or absence of 2 mM L-Glutamine. Stimulation with BDNF was performed at two time points as indicated in Figure 16C.

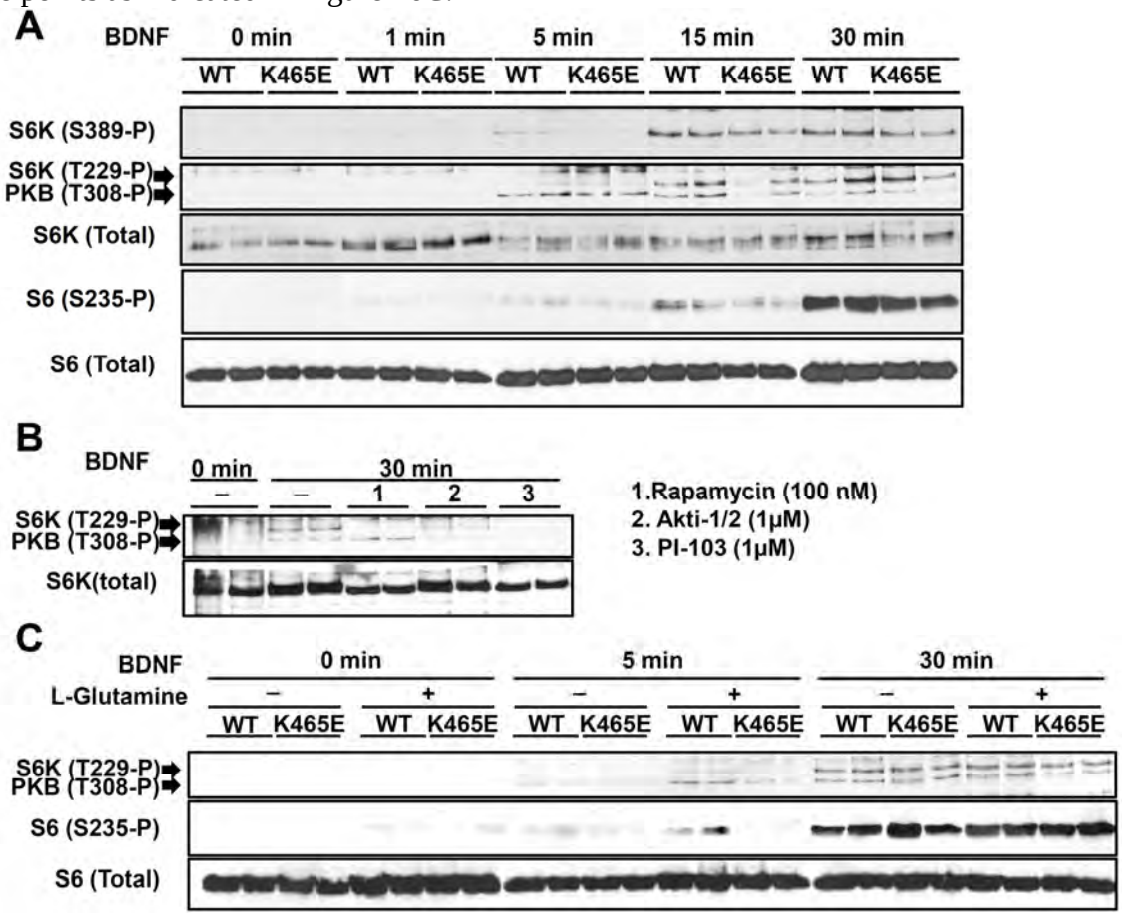

FIGURE 16. The nutrient supply is needed for BDNF-induced S6K activation. (A) Cortical neurons from two wild type (WT) and two knock-in mice (K465E) were cultured for 6 DIV, then starved from serum and Glutamine for 4 hours and stimulated with 50 ng/ml of BDNF for the indicated time points. (B) Cortical neurons from two wild type embryos were cultured for 6 DIV, then serum starved for 4h, next either left untreated or pre-treated with 100 nM Rapamycin, 1 μM PI-103, or 1 μM Akt-1/2 compounds for 30 min as indicated, and subsequently stimulated with 50 ng/ml BDNF for 30 min. (C) Cortical neurons from two wild type (WT) and two knock-in mice (K465E) were cultured for 6 DIV, then starved from serum in the presence or absence of Glutamine for 4 hours and then stimulated with 50 ng/ml of BDNF for the indicated time points. Lysates were immunoblotted with the indicated phospho and total antibodies.

The essential amino acid L-Glutamine had a strong influence on S6 phosphorylation in basal conditions in the absence of serum, so that basal phosphorylation of the S6 ribosomal protein at Ser235 was preserved during serum but not L-Glutamine deprivation conditions both in $PDK1^{+/+}$ and $PDK1^{K465E/K465E}$ cultures. By contrast, stimulation with BDNF for 5 minutes mildly increase the amino acid-induced phosphorylation of the ribosomal S6 protein, which was reduced in the $PDK1^{K465E/K465E}$ cell extracts, and failed to induce any further increase in the signal in the absence of L-Glutamine, whilst at 30 minutes BDNF induced a robust phosphorylation of S6K and S6 protein even in the absence of L-Glutamine which was not compromised in the $PDK1^{K465E/K465E}$ samples (Fig. 16C). These results indicate that amino acids, likely L-Glutamine, could account for the nearly normal activation of the mTORC1/S6K/S6-protein pathway detected in the mutant samples at 5 minutes, which is the window of time when the deficiency in PKB activity becomes more restrictive for S6K activity, whereas at 30 minutes of BDNF stimulation, in which activation of PKB is only moderately reduced in mutant samples, the PKB dependent activation of the mTORC1/S6K/S6-protein pathway seem to play a prominent role. Besides that, these data reveal that L-Glutamine sensitizes S6K to BDNF, integrating in this manner growth factor signals and nutrient signals upstream of mTORC1.

To confirm that the ability of PDK1 to interact with and activate S6K is independent of the PDK1 PH domain integrity, the phosphorylation of the ribosomal S6 protein at Ser235 was measured in cortical cultures deprived from serum and Glutamine, then pre-loaded or not with 2 mM Glutamine for 1 hour, and then stimulated with BDNF for the indicated times (Fig. 17A). I found that Glutamine induced the phosphorylation of the S6 protein at Ser235 to the same extent in both the $PDK1^{+/+}$ and $PDK1^{K465E/K465E}$ cortical cells, which compensated for the defective BDNF-induced activation of the S6K pathway detected in the mutant cells. These results suggest that the pre-loading of the $PDK1^{K465E/K465E}$ primary cortical cultures with L-Glutamine induces the activation of S6K by mTORC1, which can get over the defect caused by the PDK1 K465E mutation (see Fig. 15) and thereby bypass the requirement of BDNF-induced, PKB-dependent, mTORC1 activation.

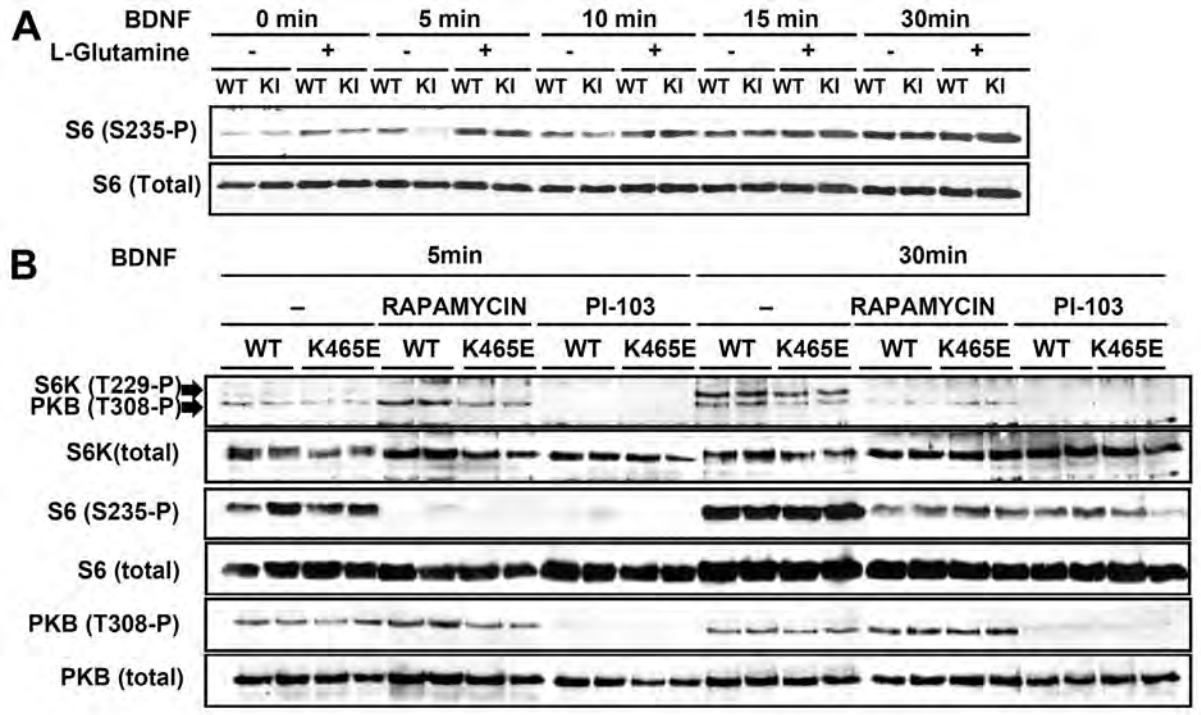

FIGURE 17. Normal nutrient-induced activation of S6K in the PDK1$^{K465E/K465E}$ knock-in mice. (A) Cortical neurons from matched PDK1 wild type (WT) and PDK1 mutant (KI) littermate mice embryos were cultured for 6 DIV, deprived from serum and Glutamine for 4 h, then either left in starved medium (-) or preloaded with 2 mM Glutamine (+) for 1 h, and then stimulated or not with 50 ng/ml of BDNF for the indicated time points. (B) Cortical neurons from two PDK1 wild type (WT) and two PDK1 knock-in embryos (K465E) were cultured for 6 DIV, then serum starved for 4 h, then either left untreated (-) or pre-treated with 100 nM rapamycin or 1 μM PI-103 compounds for 30 min, and then stimulated with 50 ng/ml of BDNF for indicated time points. Lysates were immunoblotted with the indicated phospho and total antibodies.

I further confirmed these observations by using the mTORC1 specific inhibitor rapamycin, which fully prevented mTORC1 activation and S6K phosphorylation at Thr229, but not PKB phosphorylation at Thr308, both at 5 min and 30 min of BDNF stimulation. By contrast, the PI3K inhibitor PI-103 totally wiped out both S6K and PKB phosphorylation signals at the two time-points analyzed (Fig. 17B). Rapamycin has been reportedly shown to induce the reactivation of the PI 3-kinase signaling pathway due to the inhibition of S6K (Laplante and Sabatini, 2012), which is involved in a negative signal loop against apical elements of the pathway such us the IRS1 protein (Zick, 2001). Interestingly, this rapamycin-induced feedback loop between mTORC1 and PI3K, leading to increased PKB phosphorylation, was clearly observed in control samples at 5 min of BDNF treatment, but it was not obvious in mutant samples, further emphasizing the difference between the PDK1$^{+/+}$ and the PDK1$^{K465E/K465E}$ cortical cells (Fig. 17B).

4. NORMAL ACTIVATION OF RSK IN THE PDK1$^{K465E/K465E}$ NEURONS

The p90 ribosomal S6 kinase (RSK) is an unusual serine-threonine protein kinase containing two kinase domains, one of them belonging to the AGC kinase family, and is activated downstream of the ERK signaling pathway. It phosphorylates and regulates a number of cellular substrates mediating growth factor-induced cell survival, proliferation and growth. ERK1/2 phosphorylates the T-loop Thr573 residue in the C-terminal kinase domain (CTKD) of RSK and activates it. Once the CTKD is active, it autophosphorylates the Ser380 within the hydrophobic motif, which in RSK is located in a linker region between the two kinase domains (Dalby *et al.*, 1998) and serves as a docking site for PDK1, which can then phosphorylate the T-loop residue Ser227 in the N-terminal kinase domain (NTKD), leading to its activation (Anjum and Blenis, 2008).

In the PDK1$^{K465E/K465E}$ mice, the knock-in mutation is affecting the PDK1 PH-domain function while the PDK1 PIF pocket mechanism is intact. The same samples depicted in figure 13 were analyzed by western blot with phospho specific antibodies monitoring the activation of ERK1/2, as well as RSK at Ser227, the PDK1 site. Since PKB is not involved in RSK activation, and activation of RSK kinase relies on the PDK1 PIF pocket function rather than the PH domain one, the PDK1-mediated phosphorylation of RSK was, as expected, not affected by the K465E mutation, which in turns serves as a control for the specificity of this mutant. BDNF induced a rapid phosphorylation of ERK1/2 at Thr202/Tyr204 that reached the maximum at five minutes and was sustained for thirty minutes. That was accompanied by a robust induction of RSK phosphorylation at the Thr573 by ERK1/2, Ser380 autophosphorylation site and Ser227-PDK1 site, which were indistinguishable between control and mutant cortical neurons (Fig. 18). Thus, RSK activation appears to not to be affected by the PDK1 K465E mutation and serves as a control of the specificity of this mutation.

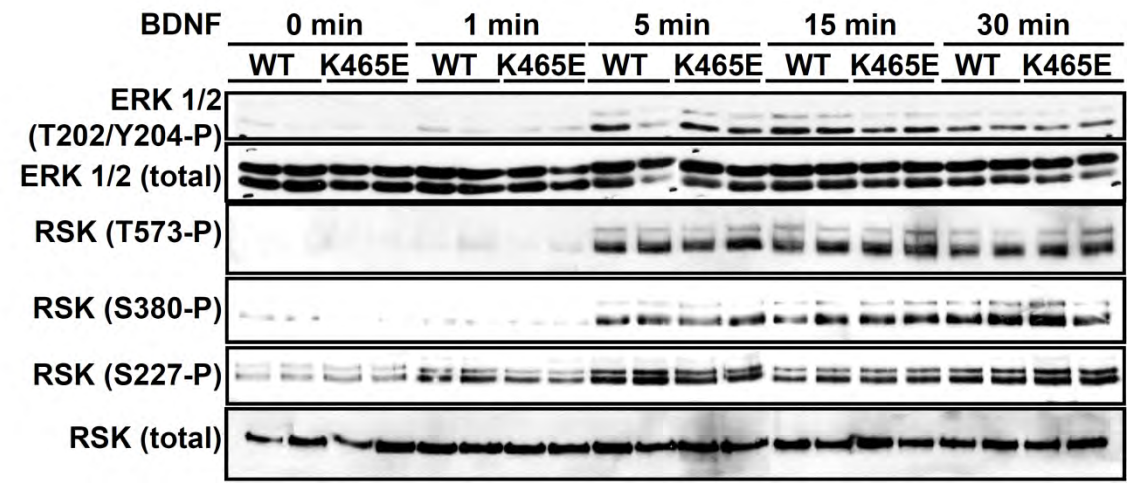

FIGURE 18. Phosphorylation of ERK1/2 and RSK induced by BDNF in the PDK1$^{K465E/K465E}$ cultured cortical neurons. Cortical neurons from two PDK1 wild type (WT) and two knock-in mice (K465E) were cultured for 6 DIV, then serum starved for 4 h and then either left unstimulated or stimulated with 50 ng/ml BDNF for the indicated time points. Lysates were immunoblotted with the indicated phospho and total antibodies.

5. REDUCED PHOSPHORYLATION OF THE SGK1 SUBSTRATE NDRG1 IN THE PDK1$^{K465E/K465E}$ KNOCK-IN NEURONS

Next I aimed to evaluate the impact of the PDK1 K465E mutation on SGK1 activation, as SGK1 is a member of the AGC family of protein kinases which is also regulated by PDK1. Indeed, SGK1 closely resembles PKB but entirely differs from PKB in the mechanism of activation (Murray *et al.*, 2004a). Activation of SGK1 involves the primary phosphorylation of the hydrophobic motif at Ser422 by mTORC2 (Garcia-Martinez *et al.*, 2008), which is then recognized by the PIF pocket within the PDK1 kinase domain, followed by the phosphorylation of the T-loop at Thr256 by PDK1 (Kobayashi and Cohen, 1999). It was relevant to investigate the role of the PDK1-phosphoinositide interaction in activating SGK1, by examining the phosphorylation of the SGK1 specific substrate NDRG1. The n-myc downstream-regulated gene (NDRG) family members were identified as the first specific physiological substrates of the SGK isoforms, and the phosphorylation of the NDRG1 protein at Thr346/356/366 sites, lying in a C-terminal decapeptide repeated sequence, is used as a specific read out of the SGK1 activity. The functional role of NDRG proteins in the mammal nervous system is significant and has been explored by numerous studies showing that NDRG proteins play important roles in the development of the central nervous system. For instance, mutation in the NDRG1 gene causes motor and sensory neuropathy in humans (Kalaydjieva *et*

al., 2000) whereas NDRG1 deficient mice exhibited Schwann cell dysfunction and peripheral nerve degeneration (Okuda *et al.*, 2004). The current evidence points out to a role of NDRG4 in spatial learning deficits and vulnerabilities to cerebral ischemia (Yamamoto *et al.*, 2011). However, the importance of the NDRG1 phosphorylation by SGK1 in neuronal development is largely undescribed. For all these reasons, it was of interest to establish whether SGK1 could be activated normally in the PDK1$^{K465E/K465E}$ mice neurons. I used specific antibodies recognizing the phosphorylated C-tail repeats of the NDRG1 protein, and found that BDNF rapidly induced the phosphorylation of NDRG1 at the SGK1 sites in cortical neurons, which was surprisingly reduced in the PDK1$^{K465E/K465E}$ neurons after 5 minutes of BDNF stimulation (Fig. 19).

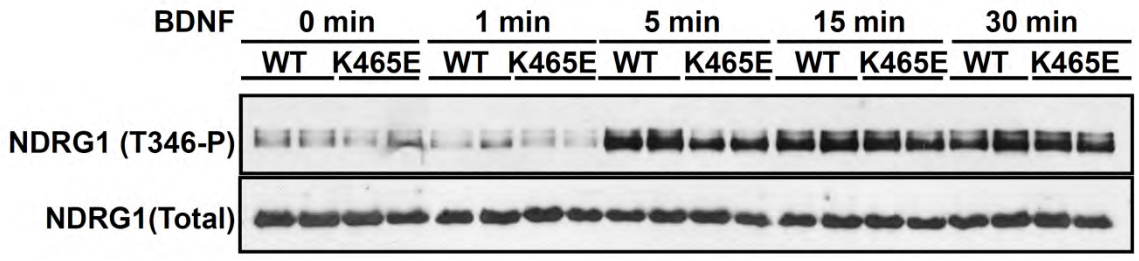

FIGURE 19. Analysis of NDRG1 in the PDK1$^{K465E/K465E}$ cortical neurons. Cortical neurons from two PDK1 wild type (WT) and two PDK1 mutant (K465E) mice embryos were cultured for 6 DIV, then serum starved for 4 hours and either left unstimulated or stimulated with 50 ng/ml BDNF for the indicated time points. Lysates were immunoblotted with the indicated phospho and total antibodies.

5.1. NDRG1 IS PHOSPHORYLATED BY PKB, AT LEAST IN NEURONS

The observation of NDRG1 phosphorylation being affected in the PDK1$^{K465E/K465E}$ mutant neurons was totally unexpected, because a role for the PDK1-phosphoinositide interaction in activating SGK1 could not be foreseen. Another scenario would be that the PKB isoforms, which are indeed specifically affected by the PDK1 K465E mutation, contributed to the phosphorylation of NDRG1 at Thr346/356/366, at least in neurons. However, insulin-induced phosphorylation of NDRG1 at the SGK1 sites was previously shown to be preserved in the liver of the PDK1$^{K465E/K465E}$ mice (Bayascas *et al.*, 2008 and also see Figure 20A). By contrast, SGK1 knockout mice exhibit severe impairment of NDRG1 phosphorylation at Thr346/356/366 sites in several tissues including spleen, lung, liver and skeletal muscle (Murray *et al.*, 2004a). Strikingly, reduced phosphorylation of NDRG1 is also observed in the PDK1$^{K465E/K465E}$ brain extracts (Fig. 20A). In fact, PKB was originally shown to be capable of marginally phosphorylating the NDRG2 isoform at Thr348 (Murray *et al.*, 2004a). In this regard, two of the residues in the NDRG1 sequence that conform to the specific SGK1

phosphorylation signature, namely Ser at position n+1 and Glu at n+2, which were probed to be deleterious to phosphorylation by PKB (Murray *et al.*, 2005), are not conserved in the NDRG2 sequence. By contrast, the PRAS40 Thr246 phosphorylation site, which is a bona fide PKB substrate, possesses Ser at position n+1 and Asp at n+2 (Fig. 20B). Thus, although NDRG1 possesses residues which are drawbacks to PKB phosphorylation, it may act as a substrate for PKB with the same success that PRAS40 does. This notion was tested by stimulating cortical neurons with BDNF in the presence of different kinase inhibitors, and found that BDNF-induced phosphorylation of NDRG1, as detected with the phospho-NDRG1 Thr346/356/366 specific antibody, was totally ablated by the PI3K inhibitor PI-103, greatly reduced by the PKB inhibitor Akti-1/2, and unaffected by the unrelated RSK inhibitor BI-D1870 (Fig. 20C).

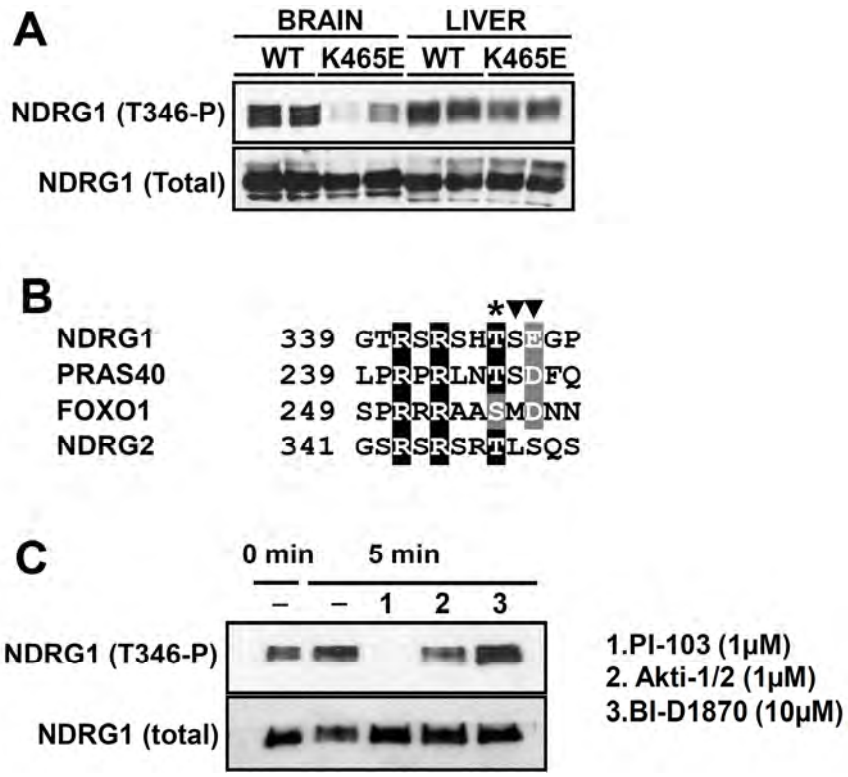

FIGURE 20. PKB phosphorylates NDRG1 at Thr346/356/366 sites in neurons. (A) Mouse brain and liver tissue extracts from the indicated genotypes were subjected to immunoblot analysis with the indicated antibodies. Each lane corresponds to a sample derived from a different mouse. (B) Multiple sequence alignment of the sequences flanking the indicated phosphorylation sites in NDRG1, NDRG2, PRAS40 and FOXO1. The positions of the first aminoacid aligned according to the mouse protein sequences are depicted. The black shadow indicates similarity, and the grey shadow corresponds to residues conserved in more than 50% of the aligned sequences. The phosphorylated threonine or serine residues are indicated with an asterisk. Flanking residues conserved between NDRG1 and PRAS40, but not NDRG2, are marked with an arrowhead. (C) Wild type cortical neurons were cultured for 6 DIV, serum starved for 4 hours, pretreated for 30 min with PI-103 and Akti-1/2 or 1 hour with BI-D1870 as indicated and then left unstimulated or stimulated with 50 ng/ml BDNF for 15 minutes. Lysates were immunoblotted with the indicated phospho and total antibodies.

Phosphorylation of NDRG1 at all the three Thr346/356/366 sites by SGK primes NDRG1 for phosphorylation by GSK3 at the corresponding (n-4) Thr342/352/362 sites (Murray *et al.*, 2004a). If in some particular circumstances GSK3 could not be properly phosphorylated and thereby inhibited by PKB in the PDK1$^{K465E/K465E}$ mice neurons, this may result in hiperphosphorylation of NDRG1 at the GSK3 sites. Since I detected reduced NDRG1 phosphorylation at the SGK1 three threonine sites in the PDK1$^{K465E/K465E}$ extracts, it was reasoned that this could be due to the artifactual masking of the Thr346/356/366 epitope by the hyperphosphorylated GSK3 sites in the NDRG1 protein. Inhibition of GSK3 with two independent inhibitors, lithium and SB-216763, increased the NDRG1 protein electrophoretic mobility, which can account for a decrease in the abundance of the hyperphosphorylated NDRG1 species, whereas the three threonine signal intensity was not changed (Fig. 21). Thus, the GSK3 phospho-sites are not masking the phosphoThr346/356/366 antibody epitope. Then, why SGK1 does not properly phosphorylate this site on NDRG1 in the PDK1$^{K465E/K465E}$ mice cortical neuronal cells after growth factor stimulation, given that the PDK1 K465E mutation is exclusively affecting PKB activitation? The notion about PKB being responsible for NDRG1 phosphorylation was further corroborated by the fact that the Akti-1/2 inhibitor reduced the Thr346/356/366 signal intensity detected after BDNF stimulation in wild type cells (Fig. 21) without affecting the electrophoretic mobility, similarly to what was observed in the PDK1$^{K465E/K465E}$ mice neuronal cultures (Fig. 19) and brain tissues (Fig. 20A), and therefore clearly state for the first time that NDRG1 is phosphorylated by PKB, at least in neurons.

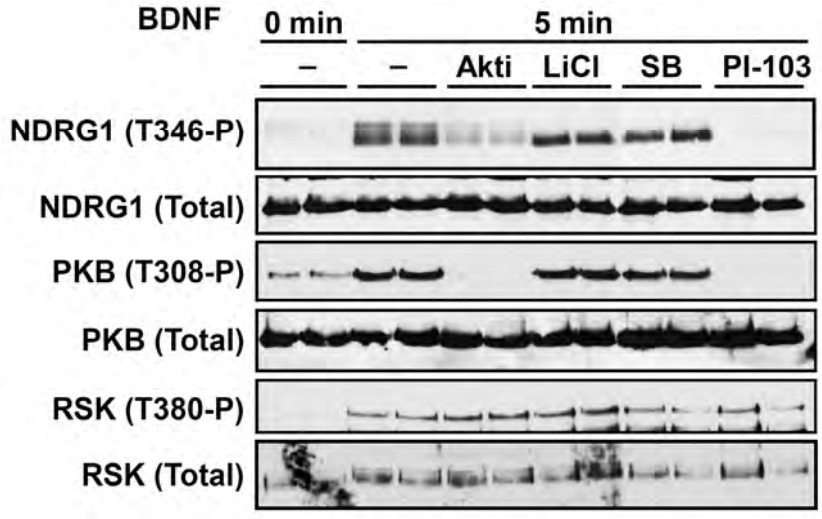

FIGURE 21. Further confirmation on the role of PKB in phosphorylating NDRG1 in neurons. Wild type cortical neurons were cultured for 6 DIV, serum starved for 4 hours, and then left untreated or pre-treated with the Akti-1/2 (1µM), LiCl (10mM), SB-216763 (3µM) or PI-103 (1µM) compounds for 30 min as indicated, following the stimulation with 50 ng/ml of BDNF for 5 minutes. The cell lysates were immunoblotted with the indicated phospho and total antibodies.

6. INTERACTION OF PDK1 WITH PtdIns(3,4,5)P_3 IS NOT ESSENTIAL FOR NEURONAL CELL SURVIVAL

During neuronal development, avoidance of programmed cell death depends on neurotrophins such as brain-derived neurotrophic factor (BDNF) (Arevalo and Wu, 2006;Kaplan and Miller, 2000). When cultured cortical neurons are treated with BDNF, they are relatively resistant to being damaged by a range of insults which are relevant to acute or chronic neurodegenerative conditions. The neurotrophins as well as their respective receptors are broadly expressed in various brain regions with a particular enrichment in cortical formation. The biological effects of BDNF are mediated by high affinity receptors leading to the activation of several signaling pathways including Ras/Raf/MAPK and PI3K/PKB, which are highly conserved signal transduction pathways that mediate neuronal survival responses. The activation of PI3K stimulates PDK1-regulated phosphorylation of several AGC kinases, including PKB. The PDK1 neuroprotective function is attributed to its role as a PI3K-dependent activator of PKB, which is mainly involved in survival promotion (Dudek *et al.,* 1997). Indeed, activated PKB in turn phosphorylates and inhibits several pro-apoptotic proteins and transcription factors leading to cell survival. However, the pro-survival effects of PDK1 may involve as well the other downstream targets rather than PKB, so this notion was assessed here and questioned whether PDK1-phosphoinositide interaction is relevant to growth factor-dependent survival of developing neuronal cells.

6.1. BINDING OF PDK1 TO PtdIns(3,4,5)P_3 IS NOT ESSENTIAL TO SUPPORT NEURONAL SURVIVAL

To determine whether BDNF can rescue trophic factor deprivation-induced neuronal cell death, primary cultures of cortical neurons derived from the $PDK1^{+/+}$ and $PDK1^{K465E/K465E}$ mice embryos at E15,5 were grown for 6 DIV and then cultured in serum-free medium in the absence or presence of BDNF for 24 h. Neuronal survival was determined by the MTT assay. Serum withdrawal equally compromised the viability of $PDK1^{+/+}$ and $PDK1^{K465E/K465E}$ cortical neuronal cultures, as measured by a decrease in the MTT reduction levels, and BDNF treatment rescued both the $PDK1^{+/+}$ and the $PDK1^{K465E/K465E}$ neurons from cell death to the same extend, as revealed by the recovery in the MTT reduction values. These results were confirmed by scoring the percentage of apoptotic nuclei after Hoechst staining. Apoptotic morphological characteristics such as chromatin condensation and nuclear fragmentation were

increased in serum starvation condition, which were partially reversed by BDNF treatment, as judged by the decrease in the number of nuclear apoptotic figures and the increase instead in the number of round, intact nuclei that closely resembled control, serum-maintained ones. Importantly, similar findings were obtained in both the $PDK1^{+/+}$ wild type and $PDK1^{K465E/K465E}$ mutant cortical neurons (Fig. 22). These data suggest that the PDK1 interaction to phosphoinositides is likely not essential for the neuroprotective actions of BDNF, at least in cultured embryonic cortical neurons.

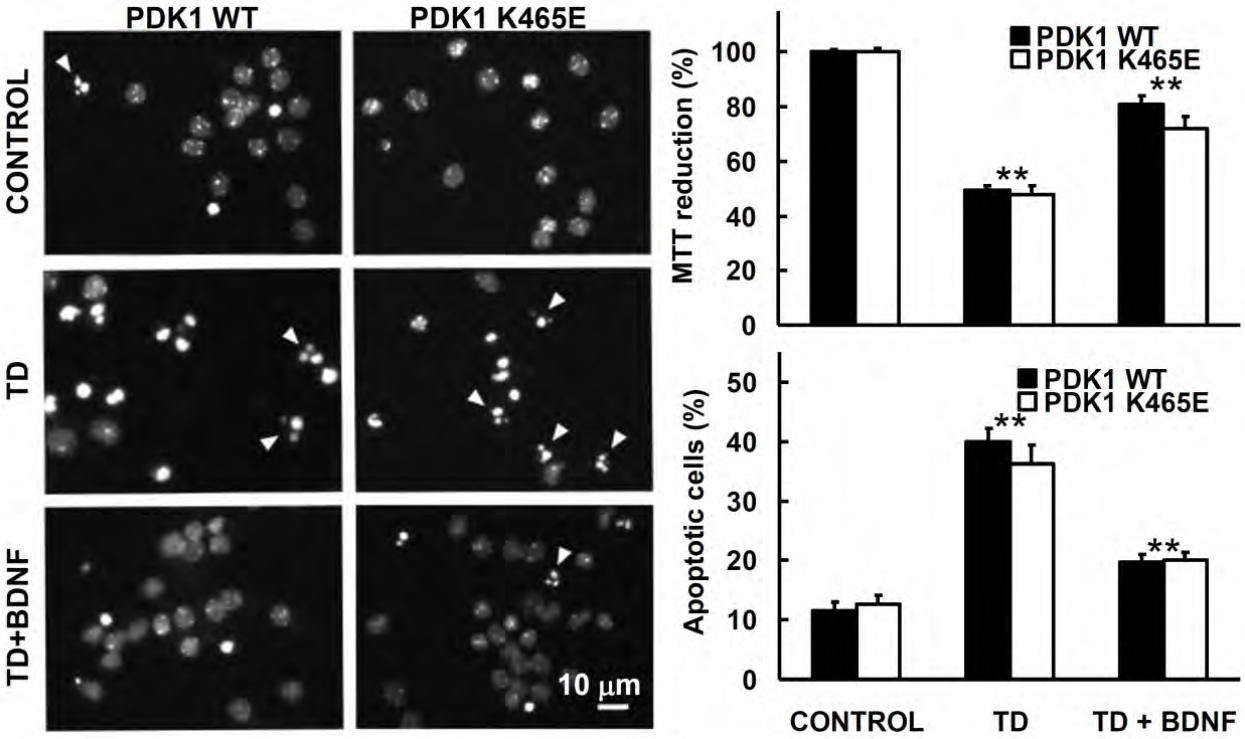

FIGURE 22. Neuronal survival responses are not impaired in the $PDK1^{K465E/K465E}$ mice. Cortical cells of the indicated genotypes were either sham treated (CONTROL), or deprived from trophic factors in the absence (TD) or presence of 50 ng/ml of BDNF (TD+BDNF) for 24 h. Left panel, representative micrographs of wild type (PDK1 WT) and mutant (PDK1 K465E) Hoechst-stained cortical neurons after 24 h of the indicated treatment; arrowheads indicate apoptotic nuclei, scale bar 10 μm; right upper panel, the cell viability was determined with the MTT reduction assay and is expressed as a percentage of the untreated cells; data represents the mean ± SEM for at least twenty independent mice embryos per genotype from seven different litters, with each sample assayed in triplicate. Right bottom panel, the percentage of apoptotic cells was obtained by scoring the number of nuclei exhibiting chromatin fragmentation divided by the total; data represents the mean ± SEM for at least nine independent mice embryos per genotype from four independent litters. * $p < 0.05$; ** $p < 0.005$ as obtained with the Student's t test between trophic deprivation and controls, or BDNF stimulation and trophic deprivation.

6.2-SURVIVAL-PROMOTING EFFECTS OF BDNF AND IGF-1 ARE PRESERVED IN THE IN THE PDK1$^{K465E/K465E}$ CORTICAL CULTURES

Insulin-like growth factor (IGF-1) is a polypeptidic trophic factor playing important roles during the development of the central nervous system. Its biological actions are mediated by the IGF-1 receptor, which is similar to the insulin receptor both in structure and function. Binding of IGF-1 to its receptor leads to activation of various intracellular proteins like the insulin receptor substrate 1 (IRS-1) and Shc, leading to the activation of multiple signaling pathways including the PI3K/PKB and Ras/Raf/MAPK pathways. Moreover, the survival-promoting effect of IGF-1 was shown to be further stronger than that of BDNF in serum deprivation-induced death of rat cultured cortical neurons (Yamada *et al.*, 2001). I hypothesized that the deficient PDK1/PKB signaling pathway in the PDK1$^{K465E/K465E}$ mutant cortical cells may distinctly respond to the strength of the survival-promoting effect of IGF-1 rather than BDNF, and also I wondered to observe whether IGF-1 is indeed more potent than BDNF in protecting cortical neurons against serum withdrawal-induced cell death. To test this assumption, the efficacy of IGF-1 and BDNF in promoting the survival of serum-deprived cultures of cortical neurons in the presence and absence of optimal and suboptimal doses of either IGF-1 or BDNF was compared (Fig. 23).

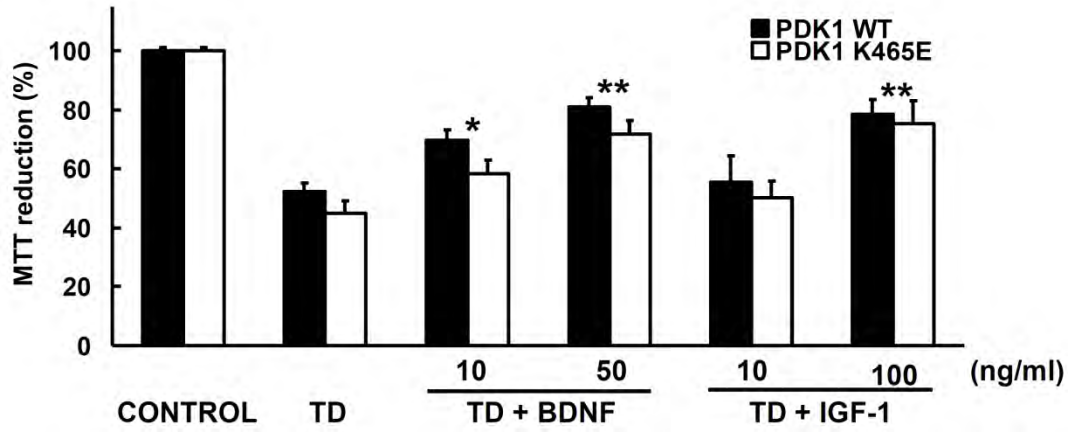

FIGURE 23. BDNF and IGF-1-induced embryonic cortical neuronal cell survival in the PDK1$^{K465E/K465E}$ mice. Cortical cells of the indicated genotypes were either sham treated (CONTROL), or deprived from trophic factors (TD) in the presence of the indicated concentrations of BDNF or IGF-1 for 24 h. The cell viability was determined on samples of at least five independent mice embryos per genotype, with each sample assayed in triplicate. * $p < 0.05$; ** $p < 0.005$ as obtained with the Student's t test between BDNF or IGF-1 stimulation and trophic deprivation.

The results show that both growth factors protected cortical cells from serum deprivation-induced cell death. Serum deprivation caused the death of around 50 % of cells, as determined by the MTT assay. BDNF at 10 ng/ml partially rescued the neuronal cell culture, while IGF-1 at the same dose almost had no survival benefit during the whole incubation period, thus in comparison with BDNF, IGF-1 demonstrated weaker survival-promoting effects at suboptimal doses. By contrast, at maximal doses both growth factors equally rescued from death 60% of the dying cells. Importantly, the neuroprotective actions elicited by the two trophic factors were similar in both the $PDK1^{+/+}$ and $PDK1^{K465E/K465E}$ embryonic cortical neuronal cells in culture.

6.3. THE PKB INHIBITOR Akti-1/2 DOES NOT COMPROMISE NEURONAL CELL VIABILITY

PKB is widely believed to be involved in the survival-promoting effects of growth factors in various cell types (Dudek *et al.*, 1997). However, in the $PDK1^{K465E/K465E}$ mice, the survival promoting effects of neurotrophic factors are preserved, despite the PDK1-phosphoinositide interaction is important for PKB activation. To further investigate the role of the PKB kinase in mediating the survival-promoting effects of BDNF, it was analyzed the impact of the Akti-1/2 inhibitor, which specifically targets the PKBα and PKBβ isoforms, and the PI 3-kinase inhibitor PI-103, on cultured $PDK1^{+/+}$ and $PDK1^{K465E/K465E}$ embryonic cortical cells. Cells were thus cultured for 6 DIV and then switched or not to a serum-free culture medium supplemented with BDNF in the presence or absence of the Akti-1/2 or the PI-103 compounds. After 24 h, the neuronal culture cell viability was determined by the MTT assay and the percentage of apoptotic figures scored (Fig. 24). The PI 3-kinase PI-103 inhibitor, but not the Akti-1/2 PKB inhibitor, prevented the survival-promoting effects mediated by BDNF. Indeed, serum deprivation induced 50% of cell loss and at the same time it completely blunted PKB signal at both phosphorylation sites. BDNF rescued trophic factor deprivation-induced cell death, as revealed by the recovery in the MTT reduction and percentage of apoptosis values and at the same time induced PKB phosphorylation at both regulatory sites. The treatment of cortical cultures with the Akti-1/2 compound at specific doses that does not affect other closely related kinases (Logie *et al.*, 2007) had no effect on growth factor-induced neuroprotection against serum withdrawal, whereas the PI-103 inhibitor fully blocked the protective effects of BDNF. Parallel studies on the phosphorylation of PKB revealed that the Akti-1/2 compound significantly prevented the BDNF-induced increase in the PKB

phosphorylation levels at both Thr308 and Ser473 sites, whereas the PI-103 inhibitor totally wiped out the PKB phosphorylation signal at both sites (Fig. 24). Altogether, these results suggest that some effectors activated downstream of the PI 3-kinase pathway others than PKB are key elements involved in the control of neuronal survival induced by growth factors.

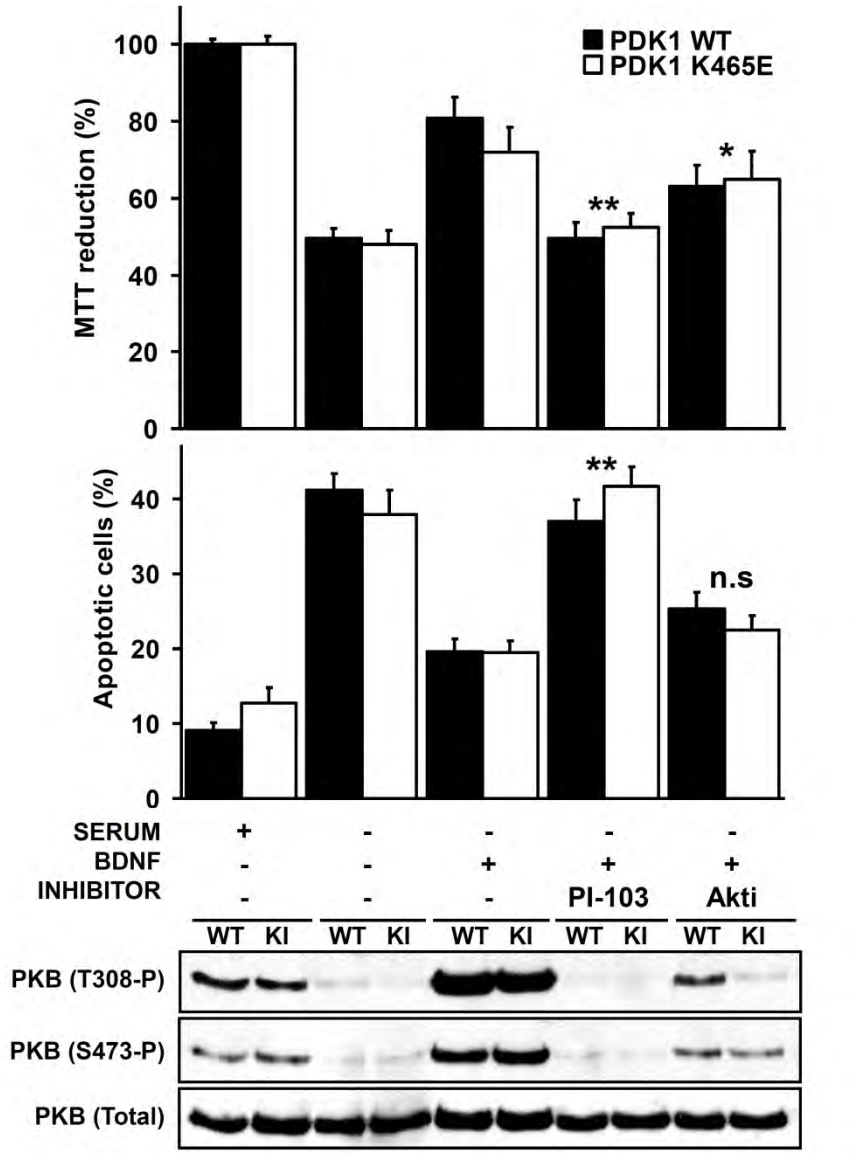

FIGURE 24. The PKB inhibitor Akti-1/2 does not impair neuronal survival. Cortical cells of the indicated genotypes were cultured in complete media or deprived from serum for 24 h in the absence or presence of 50 ng/ml of BDNF, 1 μM of PI-103 or 1 μM of Akti-1/2, as depicted. The MTT reduction and the percentage of apoptotic nuclei were determined and represented as the mean ± SEM for at least five independent embryos per genotype from two separate experiments, with each sample assayed in triplicate. As a control of the different treatments, cell lysates from matched PDK1 wild type (WT) and PDK1 mutant (KI) littermate mice were immunoblotted with the indicated antibodies. n.s. not significant; *$p < 0.05$; **$p < 0.005$ (Student's t test) between samples treated with BDNF plus the indicated inhibitor and samples treated with BDNF alone.

6.4. SENSITIVITY TO STAUROSPORINE-INDUCED DEATH IS NOT ENHANCED IN THE PDK1$^{K465E/K465E}$ PRIMARY CORTICAL NEURONS

The sensitivity to staurosporine-evoked cell death of the PDK1$^{+/+}$ wild type and the PDK1$^{K465E/K465E}$ mutant mice embryonic cortical neurons was next assessed. Staurosporine is known as an apoptotic agent inducing apoptosis via the mitochondrial apoptotic pathway (Budd *et al.*, 2000). To determine whether the PDK1$^{K465E/K465E}$ mutant neuronal cells are more prone to apoptosis than their controls, primary cortical cultures of the PDK1$^{+/+}$ and PDK1$^{K465E/K465E}$ embryos were exposed to increasing doses of staurosporine for 24 h, and the neurotoxicity determined by the MTT assay. The neurotoxic effects of staurosporine were strongly concentration-dependent, with the neuronal cell viability decreasing in a dose-dependent manner with increasing concentrations of staurosporine, ranking from 10 nM concentrations, which produced little detrimental effects, to 50 and 500 nM which resulted in markedly decreased viability (Fig. 25A). Interestingly, the PDK1$^{K465E/K465E}$ mutant cells are not more sensitive to the toxic effects of staurosporine than PDK1$^{+/+}$ wild type neurons, indicating that the PDK1$^{K465E/K465E}$ mutant mice neurons are equally susceptible to cell death insults as the PDK1$^{+/+}$ wild type neurons.

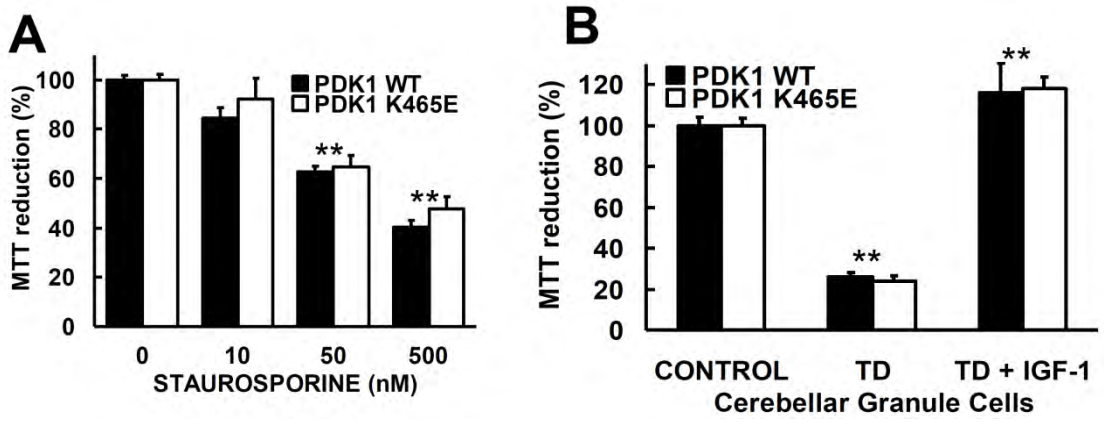

FIGURE 25. Normal sensitivity to staurosporine of the PDK1$^{K465E/K465E}$ cortical neurons and normal growth factor response of the PDK1$^{K465E/K465E}$ CGCs neurons. (A) Cortical cell cultures of the indicated genotypes were treated with the indicated doses of staurosporine in complete media for 24 h, and then the cell viability determined by the MTT assay. **(**B) Cerebellar granule cells were either sham treated (CONTROL), or deprived from serum and potassium in the absence (TD) or presence of 100 ng/ml of IGF-1 (TD+IGF-1) for 24 h; the cell viability was measured as in (A) from three different mice pups each genotype assayed in quadruplicate. * $p < 0.05$; ** $p < 0.005$ as obtained with the Student's t test between staurosporine compared to untreated controls (A), or trophic deprivation versus controls and IGF-1 stimulation versus trophic deprivation (B).

6.5. IGF-1 PROTECTS PDK1$^{K465E/K465E}$ CEREBELLAR GRANULE CELLS AGAINST LOW POTASSIUM AND TROPHIC DEPRIVATION-INDUCED CELL DEATH

It was previously demonstrated that the neuronal survival responses were not affected in the PDK1$^{K465E/K465E}$ mice embryonic cortical neuronal cells. Therefore, we used cerebellar granule cells (CGCs) to examine the reproducibility of the data obtained in cortical neurons and the extent of these observations. CGCs require excitatory inputs for proper differentiation and development. Cultured CGCs undergo spontaneous apoptosis if grown in physiological KCl concentration (5 mM, K5). However, they survive in the presence of depolarizing concentration of KCl (25 mM, K25). The trophic factor effect on the survival of cultured CGCs has been proposed to mimic the excitatory inputs required for the survival of CGCs in the cerebellum through the activation of the PI3K/PKB pathway (Dudek *et al.*, 1997;Shimoke *et al.*, 1997). Switching of mature CGCs at DIV6 from a culture medium containing 10% serum and 25 mM potassium to a serum-free medium containing 25 mM potassium did not decrease neuronal viability when compared with that of non-treated cells (D'Mello *et al.*, 1997). Consistent with this finding, challenging the CGCs culture by incubating them in serum-free medium containing 5 mM KCl (K5) decreased cell viability (Fig. 25B). IGF-1 elicited a maximal protection against trophic factor and potassium-deprivation in both PDK1$^{+/+}$ and PDK1$^{K465E/K465E}$ CGCs cultures.

Altogether, these data strongly suggest that the PKB branch of the PDK1 pathway seems to be dispensable in neurons for growth factor-induced survival and protection against neurotoxic insults. This conclusion appears to be against a number of findings using different models of neuroprotection. However, the PDK1 K465E mutation still allows the activation of other PDK1 substrates downstream of PI 3-kinase that are not phosphoinositide binding-dependent but are PIF pocket-dependent and that might be involved in transducing the BDNF-mediated survival signals in neurons.

7. CONTRIBUTION OF PDK1-PHOSPHOINOSITIDE INTERACTION TO NEURONAL MORPHOGENESIS

The biochemical analysis on the PDK1$^{K465E/K465E}$ mice demonstrated reduced PKB activation accompanied with comparable inhibition of the downstream signaling pathways. In particular, the defect in mTORC1/S6K activation observed in the neurons of the PDK1$^{K465E/K465E}$ homozygous mice was shown to be relevant to growth factor stimulation. mTORC1 is sensitive to rapamycin and is broadly known to be involved in the control of cell size. Recent studies state for the requirement of mTORC1 activity also in neuronal cell morphogenesis (Swiech *et al.*, 2008;Tavazoie *et al.*, 2005). This raised the question of whether the observed reduced mTORC1/S6K activity plays a direct role in neuronal cell morphology in the PDK1$^{K465E/K465E}$ mice. Since primary cultures make individual living neurons more easily accessible to both manipulation and observation and, besides that, the time-course of neuronal cell development often parallels the one displayed by neurons *in vivo*, we took advantage of the primary cortical and hippocampal neuronal cultures in order to evaluate the impact of the PDK1 K465E mutation on neuronal morphogenesis.

To determine whether the PDK1$^{K465E/K465E}$ mice cortical neurons exhibited alterations in neuritogenesis, three distinct morphological parameters of differentiation, namely the average neuritic process length, the number of neurites and the number of branching points, were analyzed in the primary culture of cortical neurons derived from PDK1$^{+/+}$ and PDK1$^{K465E/K465E}$ E15,5 embryos at different days *in vitro* (DIV). I could clearly demonstrate the existence of morphological defects in the PDK1$^{K465E/K465E}$ isolated cortical neurons that prompted to move the analysis on the hippocampal cells as a highly valuable research tool to expand the understanding on neuronal differentiation. For this purpose, the ability of the PDK1$^{K465E/K465E}$ mutant hippocampal cells to achieve their polarized morphology and undergo axon elongation was also evaluated.

7.1. DEFECTIVE PKB ACTIVATION DISRUPTS NEURITE OUTGROWTH IN THE PDK1$^{K465E/K465E}$ MICE CORTICAL CELLS

Primary cultures of cortical neurons derived from the PDK1$^{+/+}$ and PDK1$^{K465E/K465E}$ E15,5 embryos were grown in complete media and then photographed alive at different days *in vitro* under bright field microscopy. Neurite length was measured as it is described in the Methods section. Estimated average neurite length was significantly reduced at DIV3, which was

further aggravated at DIV4, in the PDK1$^{K465E/K465E}$ mice cortical neurons (Fig. 26A). Indeed, the neurites from the PDK1$^{K465E/K465E}$ mice embryonic cortical neurons were 20% shorter when compared to the PDK1$^{+/+}$ cortical neurites at DIV3. No further increase in neurite length was observed in the PDK1$^{K465E/K465E}$ mutant cortical cultures from DIV3 to DIV4, resulting in neurites that were as much as 40% shorter by DIV4 (Fig. 26B). The next question that was addressed was whether reduced length of the PDK1$^{K465E/K465E}$ mice cortical neurites was the consequence of the reduced size of the mutant cells. To that end, I measured the major axis of the cortical cell soma. The estimated cortical cell soma diameter was only 10% shorter in the PDK1$^{K465E/K465E}$ mutant neurons when compared to the control ones, and remained constantly reduced at the two time points analyzed (Fig. 26C). These results indicate that deficient activation of PKB affects the neurite outgrowth in the mutant cortical neurons.

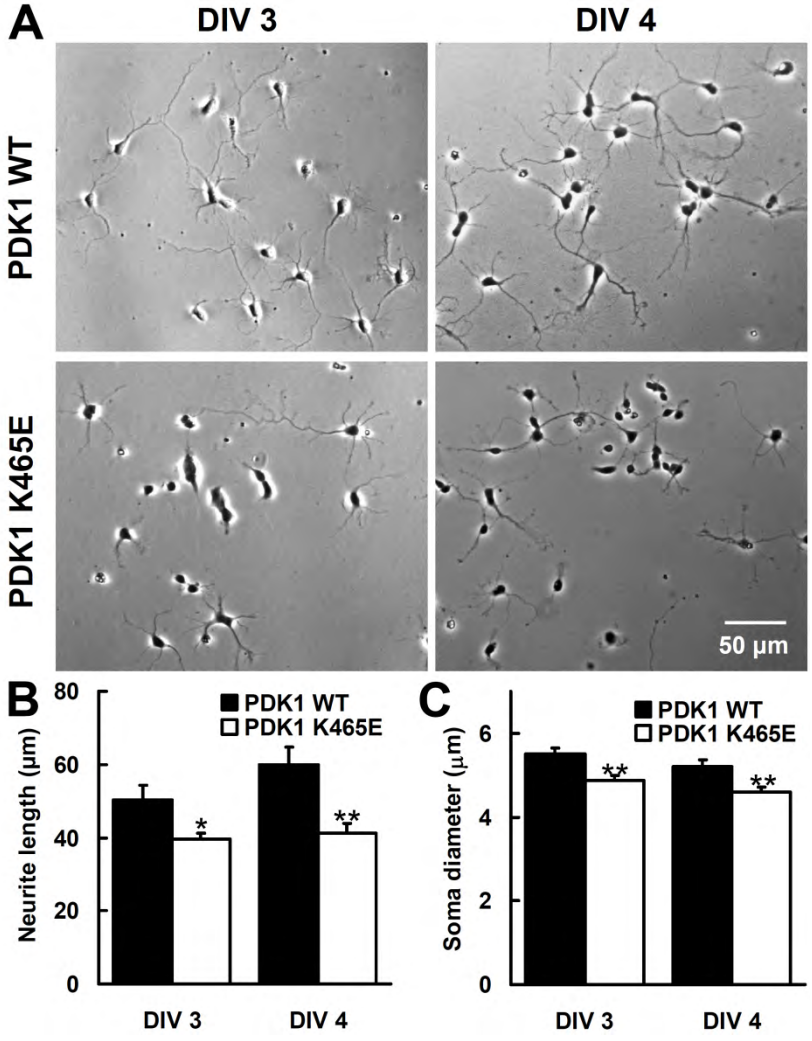

FIGURE 26. Deficient cortical neuritogenesis in the PDK1$^{K465E/K465E}$ mice. (A) Representative micrographs of the PDK1 WT and the PDK1 K465E cortical neurons at 3 and 4 days *in vitro* (DIV). Scale bar 50 µm. (B) The total length of the neurites and (C) the soma diameter were measured on digitally acquired images. Each bar represents the mean ± SEM of 200-300 neurons per embryo and four embryos per genotype. *$p < 0.05$; **$p < 0.005$ (Student's t test) compared to wild type controls.

7.1.1. Alteration in neurite initiation process, but not arborization, in the PDK1$^{K465E/K465E}$ mice cortical cells

Both the number of neurites and its arborization (measured as branching point per neurite) of the PDK1$^{+/+}$ and PDK1$^{K465E/K465E}$ mutant cortical neurons were found to be similar. By contrast, the percentage of undifferentiated cells possessing not a single neurite was significantly higher in the PDK1$^{K465E/K465E}$ mice cortical cultures when compared to the PDK1$^{+/+}$ controls (Fig. 27), thereby suggesting that PKB activation is likely involved in the initial events of neuronal differentiation. These observations show that PKB/mTORC1/S6K axis impairment in the PDK1$^{K465E/K465E}$ mutant neurons is correlated with both altered neurite formation, as inferred from the increase in the number of cells without processes, and neurite extension as denoted by the reduced average neurite length. By contrast, the PDK1 K465E mutation did not produce any obvious alterations in the neurite branching patterns.

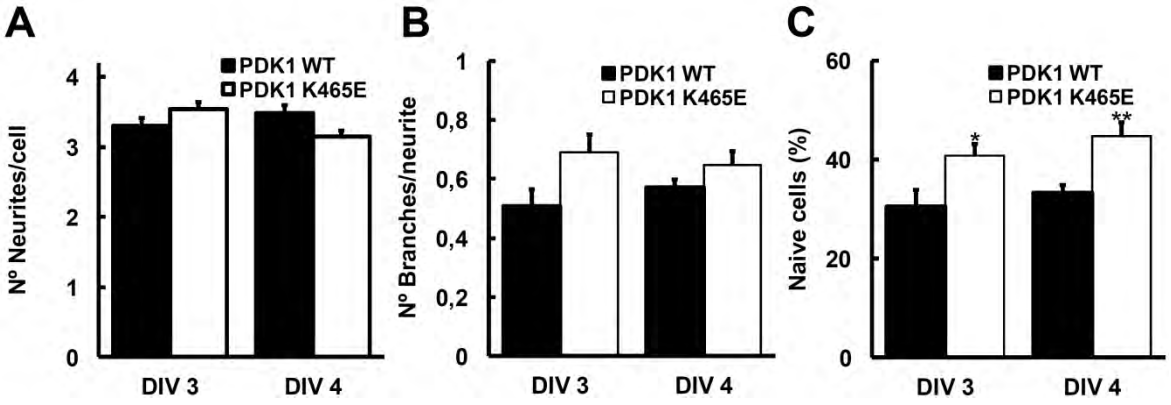

FIGURE 27.- Increased number of undifferentiated neurons in the PDK1$^{K465E/K465E}$ mice cortical primary cultures. (A) The total number of neurites per cell, (B) the number of branching points per neurite and (C) the percentage of cells possessing no neurites were measured on digitally acquired images from PDK1 WT and PDK1 K465E cortical cultures at three and four days *in vitro* (DIV). Each bar represents the mean ± SEM of 200 to 300 neurons per embryo and four embryos per genotype. *p < 0.05; **p < 0.005 (Student's t test) compared to wild type controls.

7.2. DELAYED HIPPOCAMPAL CELL POLARIZATION IN THE PDK1$^{K465E/K465E}$ HIPPOCAMPAL NEURONS

The TSC1/2 protein complex is presumed to be a major regulator of the cell polarity, since the deletion of TSC1/2 was shown to induce the initiation of axon-specific marker, Tau-1-positive, multiple axon formation (Choi *et al.*, 2008). Having observed the morphological alterations exhibited by the cortical cells, it was questioned whether the insufficient phosphorylation and thereby lack of inhibition of the protein complex TSC1/2 observed in the

PDK1$^{K465E/K465E}$ mice is critical for polarization and axonogenesis of the PDK1$^{K465E/K465E}$ mutant hippocampal neuronal cells.

Much effort has been dedicated towards the understanding of the process of neuronal differentiation, using dissociated hippocampal neurons in culture which establishes the ideal *in vitro* system (Dotti *et al.*, 1988). The advantage of this culture is that dissociated hippocampal cells plated at very low densities are rapidly polarized and form distinctive axon and dendrite. Cultured hippocampal neurons progress through multiple stages of morphological transition, starting with lamellipodial protrusions (Stage 1), followed shortly by growth of simple, immature neurites (Stage 2). One of these neurites initiates a rapid and persistent outgrowth to become an axon (Stage 3), other processes develop into dendrites, whereas the axon continues its elongation (Stage 4) and ultimately, both sets of processes develop further specifications characteristics of neuronal cells (Baas *et al.*, 1989). I also took advantage of this widely and extensively used model for studying neuronal polarization. The experiments have focused on all the transition stages of axon development *in vitro*, starting with the very early visual detection of developing process till the appearance of a mature axon. Axonogenesis was determined during the differentiation of PDK1$^{+/+}$ and PDK1$^{K465E/K465E}$ hippocampal primary cultures at different days *in vitro* after immunostaining of these neurons with antibodies to microtubule-associated proteins (MAPs) that are selectively localized in either axons (Tau-1) or dendrites (MAP2). Hippocampal neuronal cell polarity phenotypes were categorized into three groups: no axon, single axon and multiple axons.

The polarity defect of the PDK1$^{K465E/K465E}$ mice hippocampal neurons comprised the retarded ability in the dendrite/axon fate decision. At DIV2, corresponding to the onset of neuronal polarization, the PDK1$^{K465E/K465E}$ hippocampal neuronal cultures displayed significantly higher number of neurons displaying short neurites which were negative for the axonal marker Tau-1, whereas the PDK1$^{+/+}$ hippocampal cells, despite the early stage of differentiation, were already characterized with a higher number of neurons possessing axonal marker Tau-1-positive neurites (Fig 28A and B). The percentage of cells displaying a single axon was significantly lower in the PDK1$^{K465E/K465E}$ mutant cells when compared to control ones also at DIV3 and DIV4 (Fig. 28B). These experimental data shows that the PDK1 K465E mutation resulted in an early failure to initiate axon specification of hippocampal neuronal cells in culture, which was manifested by the reduced ability to establish the typical bipolar neuronal morphology. The observed phenotypic abnormalities of the PDK1$^{K465E/K465E}$ mice neuronal cells is interpreted as the consequence of the PDK1 K465E mutation deficiencies on

regulatory proteins which harbor responsibilities in axonal polarization, such as the TSC1/2 complex.

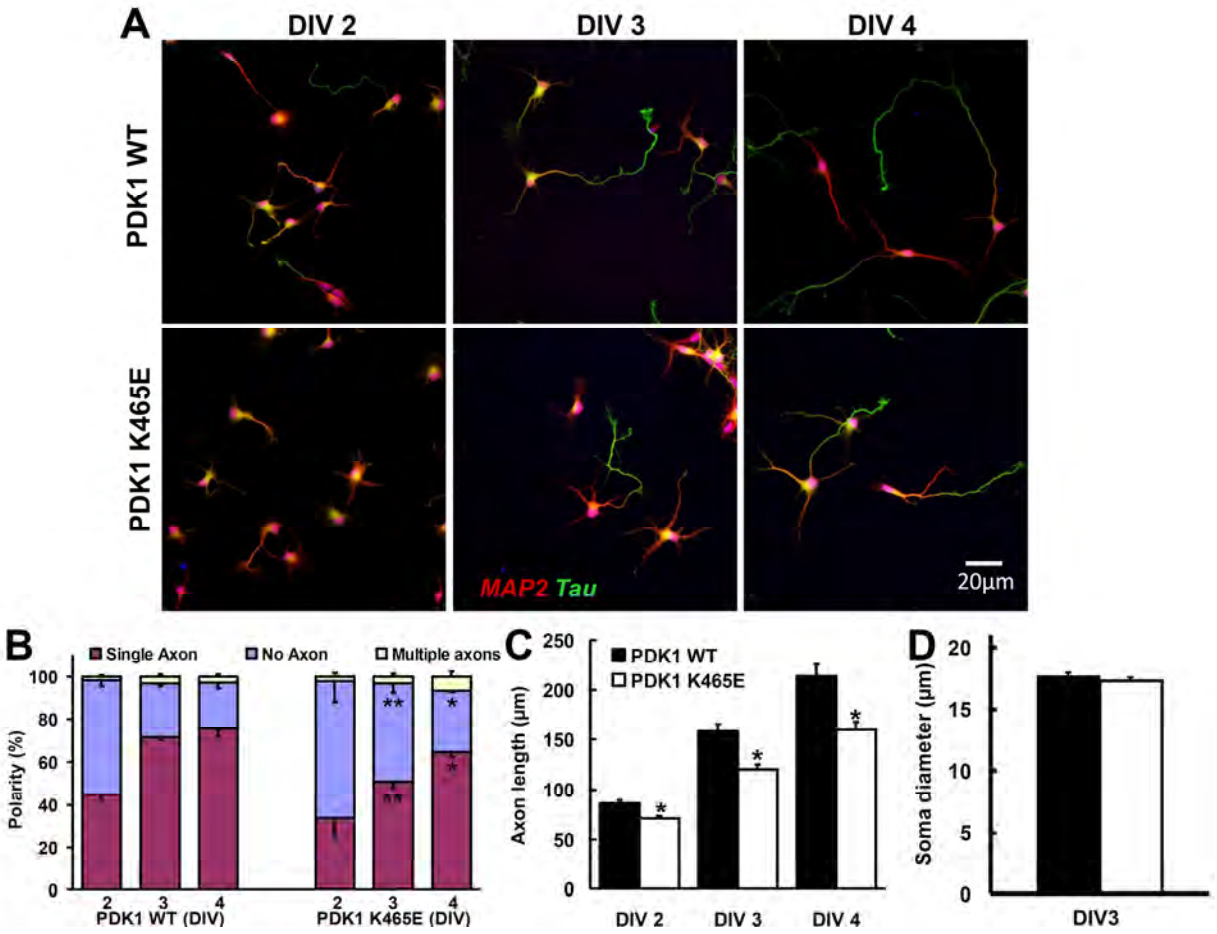

FIGURE 28.-Deficient hippocampal axon formation and growth in the PDK1$^{K465E/K465E}$ mice (A) Representative micrographs of PDK1 WT and PDK1 K465E hippocampal neurons at 2, 3 and 4 days *in vitro* (DIV) stained with antibodies against the MAP2 dendrite-specific marker (red) and the Tau-1 axonal-specific marker (green). Scale bar 20 µm. (B) The percentage of polarization, (C) the axon elongation and (D) the hippocampal cell diameter of the PDK1 WT and the PDK1 K465E hippocampal neurons measured at the indicated time points. Each bar represents the mean ± SEM of 300-500 neurons from five different embryos per condition. *$p < 0.05$; **$p < 0.005$ as obtained with the Student's t test compared to controls.

7.3. DEFICIENT AXON ELONGATION IN THE PDK1$^{K465E/K465E}$ HIPPOCAMPAL NEURONS

The observed aspects of altered polarity in the PDK1$^{K465E/K465E}$ mice neurons raised the possibility that PKB might also regulate the neuronal elongation process, through which a single neurite is differentiated to become an axon.

We found alterations in axon formation and growth in mutant cells (Fig. 28A and C). By DIV2, axons were already 25% reduced in length in the PDK1$^{K465E/K465E}$ mice hippocampal

cells compared to PDK1$^{+/+}$ cells and remained constantly reduced also at DIV3 and DIV4 (Fig. 28C). In order to identify that the observed axon elongation defect was not a reduction to scale phenomenon, I measured the major axis of hippocampal cell soma and found almost no difference while comparing PDK1$^{+/+}$ and PDK1$^{K465E/K465E}$ neurons. (Fig. 28D), thereby reinforcing the notion that the decrease in the length of PDK1$^{K465E/K465E}$ mutant axons is due to a specific growth defect.

7.4. THE SHORT AXON PHENOTYPE OF THE PDK1$^{K465E/K465E}$ HIPPOCAMPAL NEURONS IS DUE TO THE INHIBITION OF PKB-MEDIATED mTORC1 ACTIVATION

PKB phosphorylates TSC2 at conserved consensus phosphorylation sequences, inhibiting in this way its GTP-ase activating protein (GAP) activity, which results in increased GTP-bound Rheb levels in the cell that has a stimulatory effect on mTORC1 activity. mTORC1 is sensitive to rapamycin and controls cell growth through multiple actions by enhancing protein translation in the cell (Inoki *et al.*, 2002;Manning *et al.*, 2002a). On the other hand, PKB can induce mTORC1 activity directly phosphorylating PRAS40, which is a negative regulator of mTORC1 (Sancak *et al.*, 2007). In the PDK1$^{K465E/K465E}$ mice neuronal primary cultures, deficiency in PKB activity was translated on reduced phosphorylation on its downstream substrates TSC2 and PRAS40 (Fig. 13 and 14). Since TSC2 is not properly phosphorylated, thereby inhibited, by PKB in the PDK1$^{K465E/K465E}$ mice neuronal cells, it converts active Rheb into the inactive state, which is no longer able to activate mTORC1. To assess whether reduced PKB activity directly affected neuronal differentiation and, if so, whether it occurs through the decreased mTORC1 activity, primary cultures of wild type hippocampal neurons were allowed to differentiate *in vitro* for four days in the presence or absence of the Akti-1/2 isoform specific inhibitor. It was measured the axon specification and growth at different time-points, and found that the Akti-1/2 compound phenocopied the deficient PKB activity of the PDK1$^{K465E/K465E}$ neurons in wild type hippocampal cultures, resulting in axons about 20% shorter than in control, non-treated cultures, similar to what was demonstrated previously in the PDK1$^{K465E/K465E}$ mice hippocampal neurons (Fig. 29A). It was also found that treatment with the Akti-1/2 compound markedly affected the ability of the neurons to acquire the polarity that endows axon and dendrite with different properties. Indeed, the percentage of cells exhibiting one differentiated axon was significantly reduced in the neuronal cultures treated with the inhibitor compared to the control ones at all time-points analyzed (Fig. 29B).

To ask whether PKB-dependent impairment of mTORC1 activation play a direct role in hippocampal neuronal cell polarization, we assessed axonal growth and neuronal polarization in hippocampal cultures grown in the presence of rapamycin, a potent and specific inhibitor of mTORC1, which is predicted to act downstream of the TSC1/2 complex. It was found that the complete inhibition of the mTORC1 pathway prevented axonal growth even more strongly than the treatment with the Akti-1/2 compound. In fact, rapamycin-treated hippocampal neurons possessed Tau-1-positive neurites than were as much as 50% shorter when compared to the untreated controls (Fig. 29A). Inhibition of mTORC1 also compromised hippocampal cell polarization to a similar extends to that observed in the Akti-1/2 inhibitor-treated cells (Fig. 29B).

In summary, these results show that the characteristic changes in the PKB/TSC2/mTORC1 pathway correlate with specific alterations in neuronal differentiation and polarization.

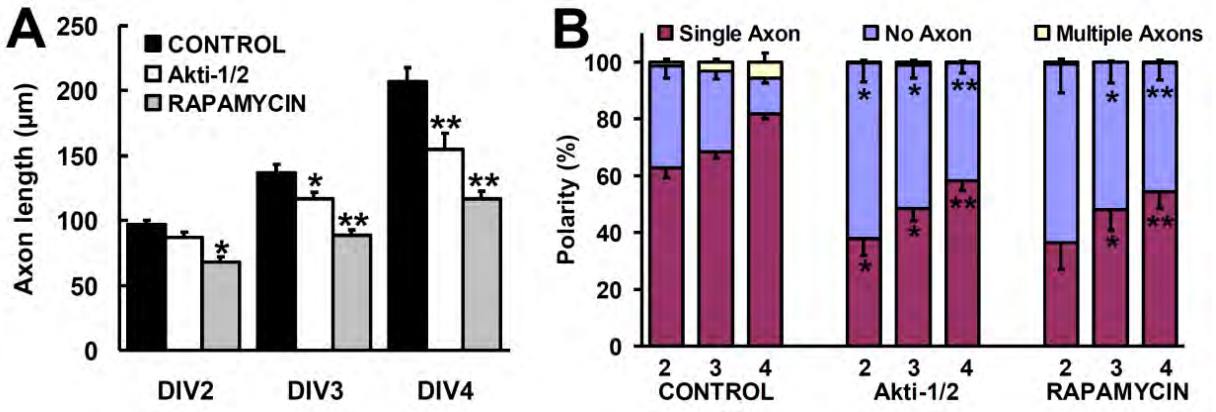

FIGURE 29.-Pharmacological inhibition of hippocampal axon formation and growth. Wild type hippocampal neurons were cultured either in the absence (CONTROL) or presence of the inhibitors Akti-1/2 and RAPAMYCIN, fixed at 2, 3 and 4 days *in vitro* (DIV) and stained with antibodies against the MAP2 dendrite-specific marker and the Tau-1 axonal-specific marker. The axon elongation (A) and the percentage of polarization (B) of the cells were measured at the indicated time points. Each bar represents the mean ± SEM of 300-500 neurons from five different embryos per condition. *$p < 0.05$; **$p < 0.005$ as obtained with the Student's t test compared to untreated controls.

7.5. THE DEVELOPING PDK1$^{K465E/K465E}$ NEURONS DISPLAY REDUCED BRSK1/2 EXPRESSION LEVELS

I searched for proteins that were regulated by TSC1/2 during axon growth by focusing on molecules that have been implicated in neuronal polarity. The tuberous sclerosis complex proteins TSC1 and TSC2 have been shown to act upstream of mTORC1 and the synthesis of specific proteins that are required for neuronal polarization, such as the brain-specific kinase (BRSK)-1 and -2. The synthesis of BRSK proteins is specifically up-regulated by the

inactivation of TSC1/2 and activation of mTORC1 signaling (Choi *et al.*, 2008). There is growing evidence of BRSK1 and BRSK2 kinases being the main determinants in establishing neuronal polarity (Crump *et al.*, 2001;Kishi *et al.*, 2005). Based on these results and on the current experimental evidences regarding the defective PKB/TSC2/mTORC1 pathway described in the PDK1$^{K465E/K465E}$ mice, I hypothesized that PKB might regulate the polarization of neurons and might do so by acting on BRSK kinases. All these prompted to further define the pattern of expression of both the BRSK1 and BRSK2 proteins in primary neuronal culture samples. Western blot analysis of BRSK1 and BRSK2 protein levels clearly demonstrated reduced expression of BRSK proteins in the PDK1$^{K465E/K465E}$ embryonic cortical cells in culture compared to either PDK1$^{+/+}$ or PDK1$^{+/K465E}$ samples at all the time points analyzed (Fig. 30A). Then both the BRSK1 and BRSK2 protein expression levels were further monitored from the first day in culture, and it was observed that they both were clearly induced from DIV3 in control extracts. By contrast, the PDK1$^{K465E/K465E}$ mice cortical neurons showed significantly low levels of BRSKs proteins compared to PDK1$^{+/+}$ controls from the first day in culture, with delayed induction profile which progressively recovered to nearly normal levels along the *in vitro* differentiation period (Fig. 30B).

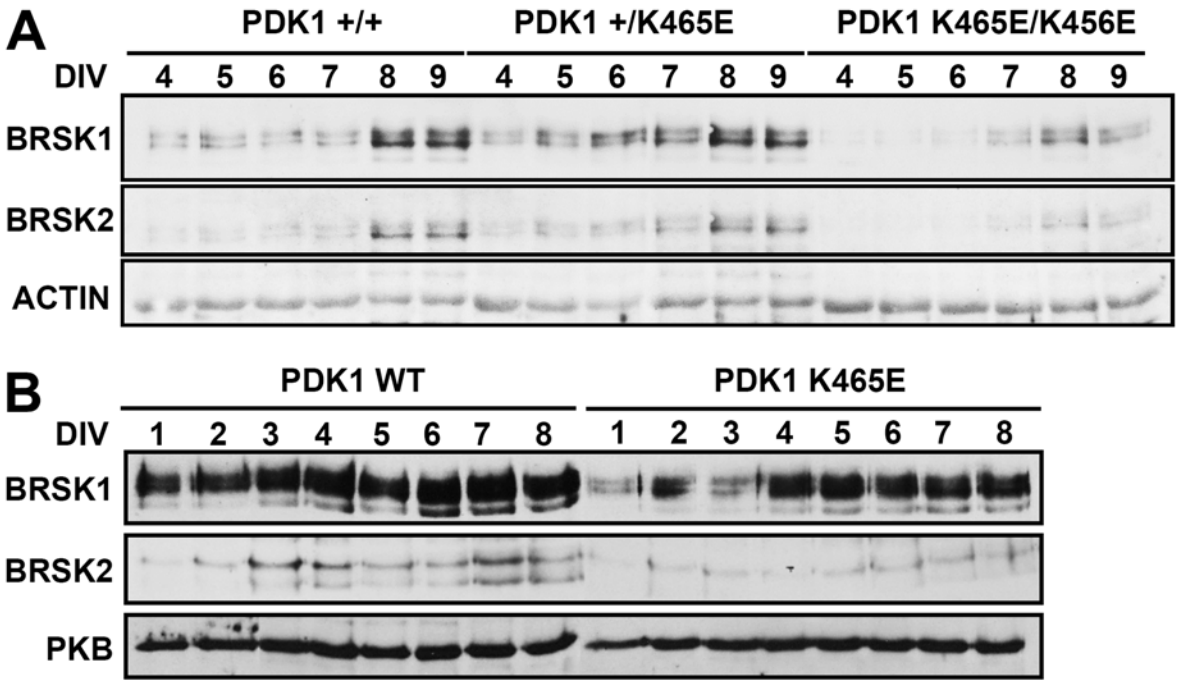

FIGURE 30. Reduced BRSK1/2 expression levels in the PDK1$^{K465E/K465E}$ cortical cells. Cortical neurons from PDK1$^{+/+}$, PDK1$^{+/K465E}$ and PDK1$^{K465E/K465E}$ embryos were cultured in complete media for the indicated time points. Lysates were immunoblotted with the indicated antibodies. Representative western blot of two independent experiments are shown.

Reduced BRSK1 protein levels were also observed in the PDK1$^{K465E/K465E}$ hippocampal neuronal cells compared to the PDK1$^{+/+}$ ones. Moreover, the treatment of PDK1$^{+/+}$ neurons with rapamycin clearly decreased the levels of BRSK1 protein and also hugely reduced the phosphorylation of the S6 ribosomal protein at the Ser235 S6K phosphorylation site, which serves as a control of the treatment (Fig. 31B). Altogether, these results suggest that PKB regulates BRSK protein levels in neurons, since their expression is reduced in neuronal cell cultures with the defective PKB signaling pathway that at the same time display morphological abnormalities, and also indicates that regulation of BRSKs levels is mTORC1 activation-dependent, since it is prevented by rapamycin in wild type neuronal cells.

Previous studies have demonstrated that BRSK1 and BRSK2 are expressed predominantly in brain (Kishi *et al.*, 2005). After having established that BRSKs expression levels were blunted in the neuronal cells cultured *in vitro*, it was analyzed the levels of BRSK1 and BRSK2 proteins by western blot in both the developing and adult PDK1$^{K465E/K465E}$ and PDK1$^{+/+}$ mice whole brain tissues extracts. The results showed that both BRSK1 and BRSK2 protein levels were markedly reduced in the brain from the PDK1$^{K465E/K465E}$ embryos compared with the PDK1$^{+/+}$ mice at E15,5, whereas BRSK1 and BRSK2 proteins were equally expressed in the adult brain of both PDK1$^{+/+}$ and PDK1$^{K465E/K465E}$ mutant mice. By contrast, PKB phosphorylation at Thr308, PRAS40 at Thr246 and TSC2 at Thr1462 were clearly reduced in both embryonic and adult brains (Fig. 31A), suggesting that BRSKs expression deficiencies are transient, at least in that narrow window which was analyzed from embryo to adult. In order to better monitor the dynamic patterns of BRSK protein expression, I checked their levels during different developmental stages. Similar to the previously results (Fig. 31A) the developing PDK1$^{K465E/K465E}$ and PDK1$^{+/+}$ mice whole brain as well as hippocampal protein extracts showed that BRSK protein expression levels were gradually augmenting during embryonic development. Whilst the expression of both proteins was notably blunted in the PDK1$^{K465E/K465E}$ mice embryonic neuronal tissues, a clear recovery of the signal was achieved in the adult, which exhibited no differences between wild type and mutant samples (Fig. 31D). An analogous trend towards the recovery of BRSK levels was also observed during the differentiation of the PDK1$^{K465E/K465E}$ mice primary cultures *in vitro* (Fig. 30). Taken together, these data suggest that the signaling defects associated with the PDK1 K465E mutation somehow affect the onset of BRSK protein expression, since it reaches normal levels in post-mitotic neurons despite the reduced PKB activation. Overall, this indicates that in neuronal tissues the moderate decrease in PKB activity affected the normal profile of expression of

BRSKs, and that the observations obtained *in vitro* are relevant to the ones observed in the mouse intact brain.

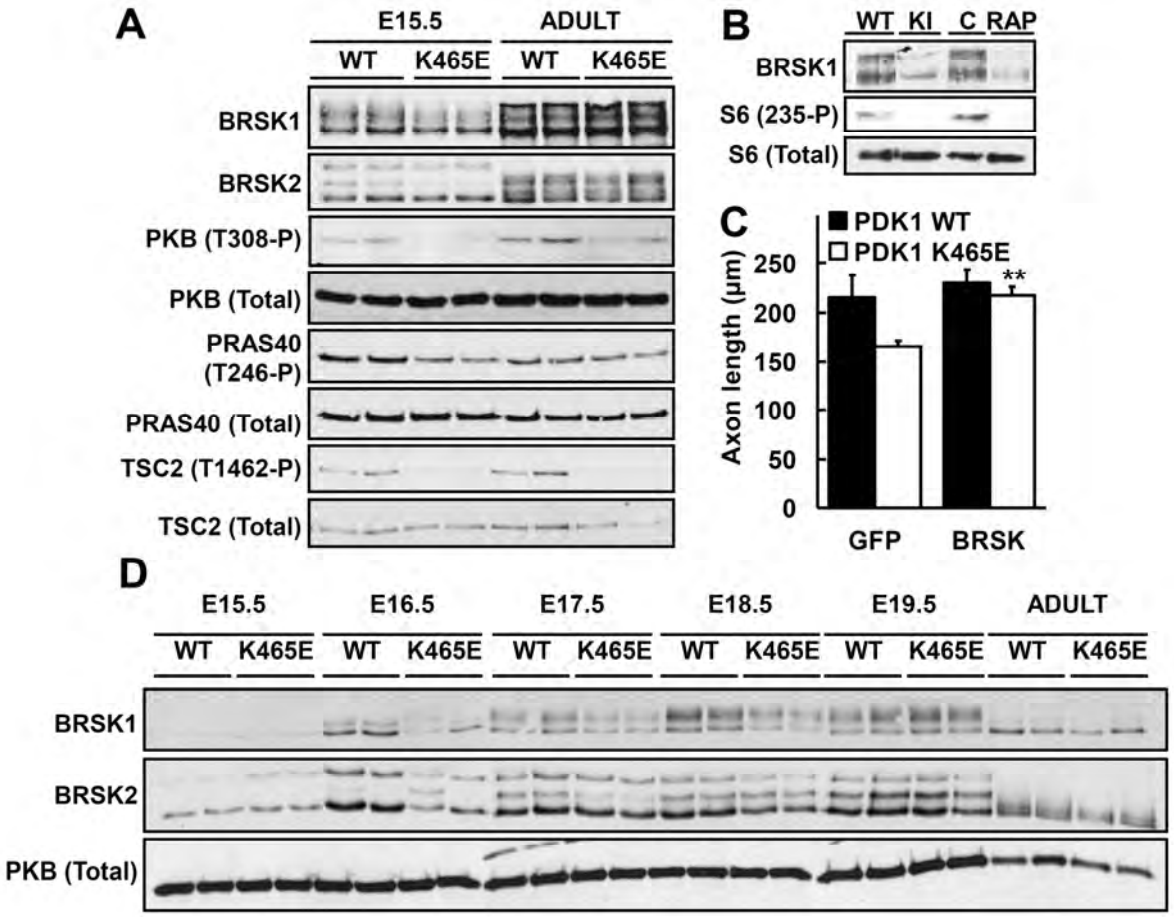

FIGURE 31. PDK1 promotes hippocampal axonogenesis through the PKB/mTORC1/BRSK pathway. (A) Brain whole protein extracts from PDK1 WT and PDK1 K465E mice of the indicated age were subjected to immunoblot analysis with the indicated antibodies. Each lane corresponds to a sample derived from a different embryo or mouse. (B) Hippocampal neurons from PDK1 wild type (WT) and PDK1 mutant (KI) mice embryos were cultured for four days in the presence (RAP) or absence (CON) of rapamycin. Lysates were immunoblotted with the indicated antibodies. A representative western blot of three independent experiments is shown. (C) PDK1 WT and PDK1 K465E hippocampal cells were transfected with the indicated expression vectors at DIV2, and the axon length determined at DIV4. Each bar represents the mean ± SEM of 100-200 neurons from three different embryos per condition. $^{**}p < 0.005$ as obtained with the Student's t test compared to controls. (D) Hippocampal tissue protein extracts from PDK1 WT and PDK1 K465E mice of the indicated age were subjected to immunoblot analysis with the indicated antibodies. Each lane corresponds to a sample derived from a different embryo or mouse.

7.6. BRSK1/2 RE-EXPRESSION RESCUE THE SHORT AXON PHENOTYPE IN THE PDK1$^{K465E/K465E}$ MICE HIPPOCAMPAL CELLS

Recent studies show that the overexpression of TSC1/2 suppresses axon formation, where lack of its function induces ectopic axons *in vitro* and in mouse brain (Choi *et al.*, 2008). BRSK

kinases are the important proteins required for neurons to acquire polarity, since the loss of both BRSK proteins in the BRSK1/2 double mutant mice resulted in alterations of neuronal polarization with aberrant neuronal morphology and severe neuronal defects causing the death within two hours of birth (Kishi *et al.*, 2005). Therefore, it was asked whether increasing BRSK1/2 expression would overcome the deficient axon specification described in the $PDK1^{K465E/K465E}$ hippocampal cells. If the low levels of expression of BRSK1 and BRSK2 are critical for the $PDK1^{K465E/K465E}$ axonal defects, re-expression of BRSK1 and BRSK2 should recover the axonal elongation process in mutant cells. To address this question, BRSK1 and BRSK2 were co-expressed in the $PDK1^{K465E/K465E}$ hippocampal neuronal cells, and found that this rescued the growth deficiencies of the $PDK1^{K465E/K465E}$ mutant neurons, whereas it had little effect on the axonal elongation of wild type cells (Fig. 31C). The $PDK1^{K465E/K465E}$ neuronal cells expressing only GFP (green fluorescent protein) displayed impaired axonogenesis compared to its control $PDK1^{+/+}$ cells as it was observed before. This result indicates that an increase in BRSK1/2 levels rescued the defective axonal phenotype in the $PDK1^{K465E/K465E}$ mice hippocampal cells. Thus, the PDK1-phosphoinositide interaction is essential for correct BRSK-dependent axon-inducing effects.

8. NORMAL LAYERING AND CONNECTIVITY IN THE $PDK1^{K465E/K465E}$ ADULT BRAIN

The generation, differentiation and migration of newborn neurons are the critical features of normal brain development which are controlled by intracellular and extracellular regulatory mechanisms. Here we show that the BRSK protein levels are regulated downstream of the PKB signaling pathway during neuronal development, since their expression levels were declined in the $PDK1^{K465E/K465E}$ mutant embryonic neurons with impaired PKB activation compared with the $PDK1^{+/+}$ ones. Expression of BRSK proteins at low levels in the embryonic differentiating neurons significantly affected axonal outgrowth. However, as development proceeds, the BRSK protein expression levels in the $PDK1^{K465E/K465E}$ mice embryonic brains were progressively achieving the normal levels observed in the adult $PDK1^{+/+}$ mice. Therefore, BRSK isoforms were overexpressed in the $PDK1^{K465E/K465E}$ mutant E15 embryonic hippocampal cells, and the axonal outgrowth consequently recovered by DIV4.

Mice lacking both BRSK isoforms exhibited immobility and poor responsiveness and died shortly after birth. Close examination of the central nervous system demonstrated a smaller forebrain with a thinner cortex and neurons failing to form axons (Kishi *et al.*, 2005). As

mentioned above, the PDK1$^{K465E/K465E}$ mice are nearly viable and exhibited neither an overt phenotype nor growth abnormalities in the architecture of the central nervous system, which exhibited normal cortical layering and connectivity (Fig. 32, experiment performed by Lluís Cordón-Barris). This finding is in agreement with the fact that the transient character of the PDK1 K465E mutation may allow the accumulation of sufficient levels of BRSK proteins in the adult tissue. However, it would be interesting to explore whether the hypomorphic reduction of PKB/mTORC1 activation, causing a delayed and/or reduced onset of BRSK protein synthesis and altered neuronal morphogenesis in the PDK1$^{K465E/K465E}$ embryo, would lead to more subtle alterations in the patterning of the central nervous system that could ultimately translate into abnormal behavioural phenotypes.

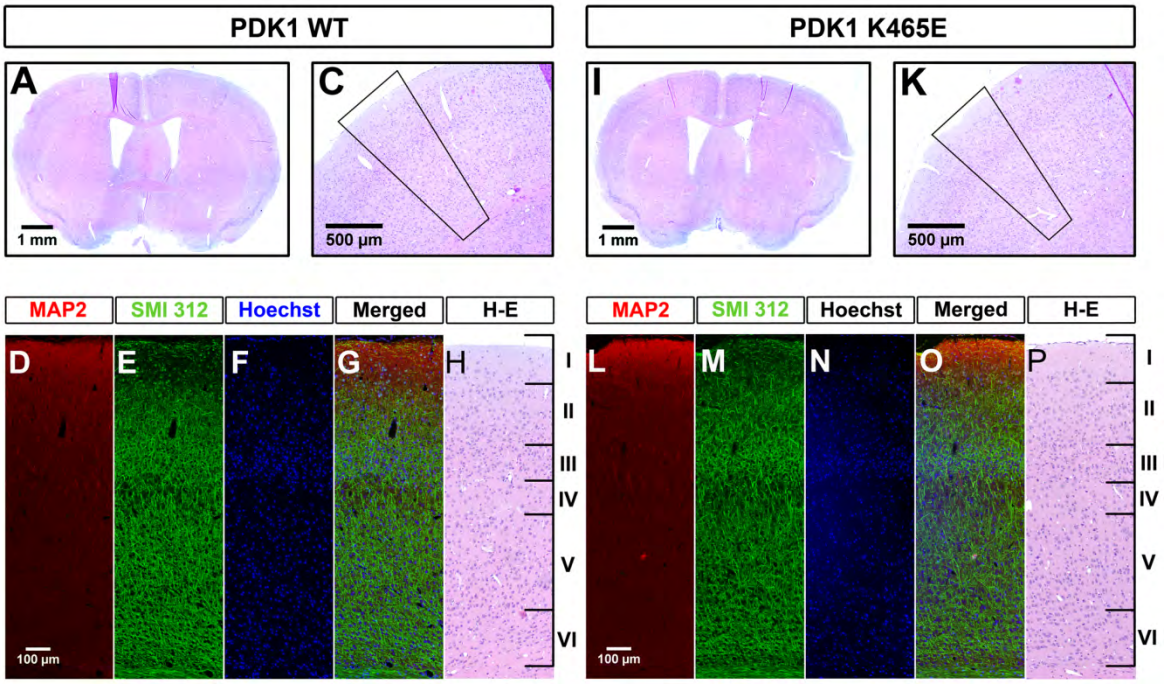

FIGURE 32. Normal layering and connectivity in the PDK1$^{K465E/K465E}$ adult brain. (Top) Five-micrometer-thick coronal brain sections from PDK1 wild-type (WT) (A and C) and PDK1 K465E (I and K) mice stained with hematoxylin and eosin showing the overall architecture of the rostral adult brain. (Bottom) Epifluorescence microscopy images of PDK1 wild-type (D to H) and PDK1 K465E (L to P) cortexes stained with the dendrite-specific marker MAP2 (D and L), the general axonal marker SMI-312 (E and M), and nuclear Hoechst dye (F and N). The merged signals (G and O) as well as adjacent hematoxylin-and-eosin (H-E)-stained sections (H and P) are also shown. Cortical layers are indicated on the right from I to VI.

DISCUSSION

The present study has explored the importance of the binding of the PtdIns(3,4,5)P_3 second messenger to the PH domain of PDK1 for the development of neuronal cells. The findings derived from the work in this thesis suggest that the integrity of the PDK1 PH domain is essential for the optimal activation of PKB and that this is required for maximal phosphorylation of some of its downstream substrates in neuronal cells. Indeed, the low levels of PKB activation caused by the loss of a functional PDK1 PH domain were sufficient to support the normal phosphorylation of GSK3 and FOXO, which possibly explain the retained capacity of the PDK1$^{K465E/K465E}$ neuronal cells to adequately respond to BDNF and survive in the absence of trophic support. Collectively, these studies suggest that the binding of PDK1 to PtdIns(3,4,5)P_3 is therefore not essential to support neuronal survival.

It is also shown that there was normal phosphorylation of RSK on the PDK1 site Ser227 in the PDK1$^{K465E/K465E}$ neurons, which is clear evidence that the PDK1 K465E mutation exclusively affected the PDK1 PH domain function and not the PDK1 catalytic function. This is in accordance with the fact that no differences in the protein expression levels or the catalytic activity of the PDK1 K465E mutant protein expressed from tissues were detected when compared to that of wild type PDK1 (Bayascas *et al.*, 2008).

This study also provides evidence suggesting that NDRG1 is phosphorylated by PKB at the Thr346/356/366 sites, at least in the BDNF-stimulated cortical neurons. Furthermore, reduced phosphorylation of NDRG1 in the PDK1$^{K465E/K465E}$ mice brain extracts was also observed that most likely arise from incomplete PKB activation.

However, the PDK1 PH domain-PtdIns(3,4,5)P_3 binding was shown to be essential for normal phosphorylation and thereby inactivation of PRAS40 and TSC2, which act as intermediate partners in mTORC1 activation downstream of PDK1. Reduced mTORC1 activation was indeed observed in the PDK1$^{K465E/K465E}$ mice neuronal cells. Importantly, the findings in this study demonstrated impaired neuritogenesis, cell polarity and axon growth in the PDK1$^{K465E/K465E}$ knock-in mice primary neuronal cell cultures. The loss of the mTORC1 arm of the downstream PKB signaling pathway caused a noticeable decrease in the expression of neuronal polarity important regulators, such as the BRSK1/2 protein kinases, both in the primary neuronal cultures and in the developing brain of the PDK1$^{K465E/K465E}$ knock-in mice. Another important finding is that the defective PKB/TSC2/mTORC1/BRSK pathway appears to limit axon formation and to restrain the polarization in the PDK1$^{K465E/K465E}$ knock-in neuronal cells, while re-expression of BRSK1/2 rescued the short axon phenotype. Accordingly, the observations described in this study support the concept of TSC2/mTORC1

governing the neuronal cell differentiation/polarity. In addition to that, the findings from this work shed light on the link connecting the upstream signals activating mTORC1 to the downstream mediators of neuronal polarity/axon formation process.
Specific discussions focusing on the different implications depicted in this thesis are described below in their respective sections.

1. MUTATION OF THE PDK1 PH-DOMAIN ONLY MODERATELY AFFECTED PKB ACTIVATION IN NEURONS

PDK1 uses different mechanisms to modulate the activation of its downstream targets that include isoforms of PKB, S6K or SGK. PDK1 phosphorylates the T-loop of all these kinases. Maximal activation of these kinases requires also phosphorylation of a residue lying C-terminal to the kinase domain, known as the hydrophobic motif. The hydrophobic motif of S6K is phosphorylated by mTORC1 (Hara *et al.*, 2002;Kim *et al.*, 2002), whereas mTORC2 phosphorylates the hydrophobic motif of PKB (Sarbassov *et al.*, 2005b) and SGK (Garcia-Martinez *et al.*, 2008). Activation of PKB is dependent on prior activation of PI3K and generation of the second messenger PtdIns(3,4,5)P_3 (Alessi *et al.*, 1997a). Binding of PKB to PtdIns(3,4,5)P_3 induces a conformational change that facilitates the phosphorylation of the kinase domain by PDK1 at Thr308 (Currie *et al.*, 1999). Both PKB and PDK1 possess PH-domains that bind PtdIns(3,4,5)P_3 and promote in this manner the interaction of these enzymes at the plasma membrane, where PKB is phosphorylated and activated by PDK1.
In order to study the effect of inhibiting the ability of PDK1 to interact with PtdIns(3,4,5)P_3, the targeted mutagenesis of Lysine 465 to Glutamic acid abolishing the PDK1-phosphoinositide interaction by disrupting the conformation of the lipid-binding pocket was designed (Komander *et al.*, 2004). Actually, when the PDK1 K465E knock-in mutation was first designed, the PKB phosphorylation at Thr308 in the absence of PDK1-PtdIns(3,4,5)P_3 interaction was totally excluded. The first animal model which provided the evidence that the PDK1 interaction to phosphoinositides is required for optimal activation of PKB *in vivo* was the homozygous PDK1$^{K465E/K465E}$ mice expressing this mutant form of PDK1 just incapable of phosphoinositide binding but with intact catalytic activity (Bayascas *et al.*, 2008).
Indeed, BDNF-induced activation of PKB is partially inhibited in the PDK1$^{K465E/K465E}$ mice embryonic cortical neurons. The phosphorylation of PKB at the Thr308 residue, the PDK1 site, was shown to be reduced in the PDK1$^{K465E/K465E}$ mutant neuronal cells compared with the

$PDK1^{+/+}$ wild type neurons, while PKB phosphorylation at the Ser473 residue, mTORC2 phospho-site, proceeded normally. The findings in this study show that the impact of the PDK1 K465E knock-in mutation on PKB activation in neuronal cells is not as potent as it was observed previously in the $PDK1^{K465E/K465E}$ mice insulin-responsive tissues, in which PDK1 phosphorylation of the PKB Thr308 site and PKB activation were reduced by three-to four-fold (Bayascas *et al.*, 2008). Quantification of the immunoblot signals obtained here showed that the BDNF-induced phosphorylation of PKB at Thr308 was reduced by less than two-fold in the $PDK1^{K465E/K465E}$ mutant mice cortical neurons, and that the maximal difference in PKB Thr308 phosphorylation between the $PDK1^{+/+}$ and $PDK1^{K465E/K465E}$ neurons was reached at 5 min, which appears to attain nearly total recovery after 30 min of BDNF stimulation.

Thus, preventing the interaction of PDK1 with phosphoinositides in the $PDK1^{K465E/K465E}$ mutant mice embryonic cortical neurons did not fully abolish PKB activation by PDK1. This phenomenon could be explained by the existence of a pool of the PDK1 protein at the membrane, which is not dependent on the phosphoinositide binding neither on agonist stimulation, but still capable of phosphorylating PKB at the T-loop, since the catalytic activity of PDK1 is fully preserved in the $PDK1^{K465E/K465E}$ knock-in mutant mice in all the tissues analyzed including brain (Bayascas *et al.*, 2008). Indeed, the experimental data clearly demonstrate that PDK1 is constitutively associated with membrane in the resting cells, which is not further enriched by stimulation and importantly, is preserved to the same level in the $PDK1^{K465E/K465E}$ mutant cells (Fig. 33A).

However, as PKB has three isoforms, the possibility of one PKB isoform accounting for the observed remaining PKB activation cannot be excluded. Since the third isoform PKBγ is abundantly expressed in neuronal tissue, it is intriguing to speculate that the poor impact that the PDK1 K465E mutation impinges on PKB Thr308 phosphorylation in neurons could be due to a reduced sensitivity of the neuronal PKBγ isoform to the PDK1 PH domain knock-in mutation. In this regard, a structural-based mechanism accounting for the lower sensitivity of the PKBγ isoform to the allosteric inhibitory compound Akti-1/2, which specifically targets the inactive conformer of PKBα and PKBβ, but not PKBγ, has been proposed (Calleja *et al.*, 2011;Calleja *et al.*, 2009). Because both PDK1 and PKB have been evidenced to exist in a cytosolic pre-activation complex in the cells (Calleja *et al.*, 2007), it is intriguing to speculate that the same structural particularities of the PKBγ isoform could explain both the insensitivity to the Akti-1/2 inhibitor and to the PDK1-phosphoinositide interaction.

Recently, in favour to this investigation study, Najafov et al proposed an alternative mechanism of PKB activation that might account for the resistance of PKB to PDK1 inhibitors. This second mechanism entails the recruitment of PDK1 at PKB via the PDK1 substrate docking motif, termed PIF pocket, upon PKB phosphorylation at Ser473 by mTORC2. Treatment of PDK1 K465E mutant ES cells with the mTORC2 inhibitor AZD8055 to suppress Ser473 phosphorylation inhibited Thr308 phosphorylation more potently compared with the wild type, control ES cells. Comparable inhibition trends were observed in the phosphorylation of the PKB substrate PRAS40 (Najafov *et al.*, 2012). The current data suggests that the residual phosphorylation of PKB at Thr308 observed in the $PDK1^{K465E/K465E}$ mice cortical neurons in the absence of PDK1-PtdIns(3,4,5)P_3 binding is likely to be dependent on the PDK1 PIF pocket mechanism. Then a potential interpretation of the current data would be that this PIF pocket-dependent mechanism of PKB phosphorylation at Thr308 is much more potent in neuronal cells that it is in other cell types.

PDK1 strongly binds to the PIF (PDK1 interacting fragment) peptide, a peptide resembling the substrate docking site of S6K that interacts with the catalytic domain of PDK1 independently of the PH domain, both in the $PDK1^{+/+}$ and the $PDK1^{K465E/K465E}$ mice liver extracts (Bayascas *et al.*, 2008) and muscle samples (Fig. 33B) with the same efficiency, whereas interestingly this binding is much more enhanced in the $PDK1^{K465E/K465E}$ mutant mice brain lysates than in control samples (Fig. 33B). By contrast, the PDK1 K465E protein from either muscle or brain extracts totally failed to bind PtdIns(3,4,5)P_3-coated agarose beads, further emphasizing the validity of the PDK1 PH domain mutation expressed in the $PDK1^{K465E/K465E}$ knock-in mice (Fig. 33B). Moreover, whilst the PDK1 catalytic activity against a peptide encompassing the PKB phosphorylation site of PKB, termed T308tide, is similar in $PDK1^{+/+}$ and $PDK1^{K465E/K465E}$ tissue extracts, the activity against a peptide encompassing the PDK1 phosphorylation site on PKB plus the docking site, termed PDKtide, is enhanced in the $PDK1^{K465E/K465E}$ mutant extracts when compared to $PDK1^{+/+}$ controls (Fig. 33C). I further favour the explanation that in the absence of PDK1-PtdIns(3,4,5)P3 interaction, PKB phosphorylation at Thr308 can still be efficiently achieved due to the binding of PDK1 to the phospho-Ser473 docking site in the $PDK1^{K465E/K65E}$ mutant mice, a phenomenon which might operate more efficiently in neurons that in insulin-responsive tissues such as liver or muscle (Fig. 33).

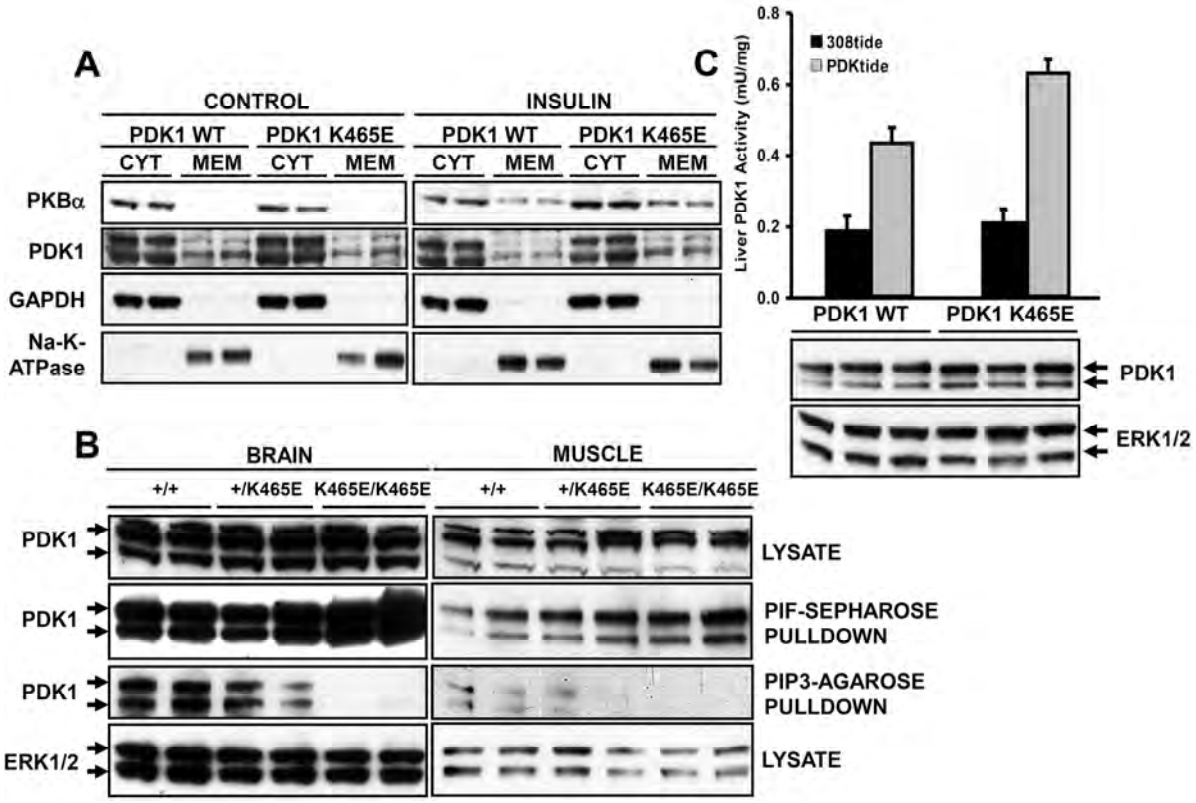

FIGURE 33. (A) Two PDK1 WT and two PDK1 K465E mice cytosolic (CYT) and membrane (MEM) muscle fractions stimulated or not with insulin were analyzed with the indicated antibodies. (B) Two PDK1 wild type (+/+), heterozygous (+/K465E) and homozygous (K465E/K465E) mice brain and muscle tissue extracts were incubated with Sepharose conjugated to PIFtide or Agarose conjugated with PtdIns(3,4,5)P_3. Pull downs were subjected to immunoblot analysis with the indicated antibodies. (C) The PDK1 activity of three PDK1 wild type and three PDK1 K465E mutant mice liver lysates was determined using a peptide encompassing only the substrate phosphorylation site (308tide) or a peptide encompassing the substrate phosphorylation site plus the docking site (PDKtide). As a control, immunoblot analysis was performed with the indicated antibodies. Each lane represents a sample derived from a different mouse.

Accordingly, the stronger effect of the Akti-1/2 inhibitor on Thr308 phosphorylation in the PDK1$^{K465E/K465E}$ mutant neurons compared to the PDK1$^{+/+}$ wild type ones (Fig. 24), also supports the concept of the PDK1 PIF pocket-dependent mechanism of PKB activation operating in neurons. The interpretation of this data is that since the Akti-1/2 compound acts as an allosteric inhibitor targeting the inactive conformation of PKB and preventing in this way phosphorylation of the two PKB activation sites, the reduced phosphorylation of Ser473 caused by the Akti-1/2 treatment will trigger a further reduction in the phosphorylation of Thr308 on mutant cells, which rely solely on the ability of PDK1 to bind to the phospho-Ser473 site, whilst the wild type cells could take advantage of the more efficient phosphoinositide-mediated mechanism to phosphorylate phospho-Thr308 in a Ser473 independent manner. All these together raises the possibility that the PDK1-PtdIns(3,4,5)P_3 binding may instead act as a crucial mechanism in PKB activation by targeting PDK1 to a

particular location within the cell and/or by presenting PKB to PDK1 as a target for phosphorylation.

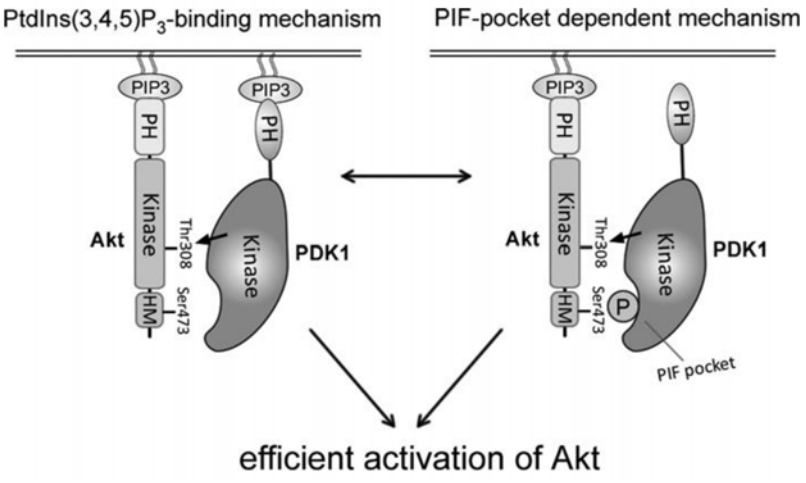

FIGURE 34. Two alternative PtdIns(3,4,5)P_3 binding and PIF pocket-dependent mechanisms enabling PKB to be efficiently activated, which account for the resistance to PDK1 K465E knock-in mutation in neurons. Figure is adapted from (Najafov *et al.*, 2012)

In order to further confirm the observed reduced PKB phosphorylation at Thr308, a BDNF dose-response experiment was performed. Treatment with BDNF starting with minimal concentrations of 2 ng/ml to maximal of 50 ng/ml of BDNF was found to be additive for PKB phosphorylation, demonstrating a robust difference in Thr308 phospho-levels between the PDK1$^{+/+}$ wild type and the PDK1$^{K465E/K465E}$ knock-in samples at lower doses of BDNF (Fig. 14A).

The reduced level of PKB activation in the PDK1$^{K465E/K465E}$ neuronal cells is rate limiting for PRAS40 and TSC2 phosphorylation at early times of BDNF stimulation similar to PKB, resulting in incomplete BDNF-mediated activation of mTORC1. The reduced mTORC1 activation leads to impaired phosphorylation of the S6K Ser389 hydrophobic motif residue which proportionally compromised the interaction of PDK1 with S6K, resulting in reduced S6K phosphorylation at Thr229 within the T-loop, leading to decreased S6K activation. These observations served to clarify the mechanism by which the non PH-domain dependent substrate of PDK1 S6K is also affected by the PDK1 PH domain mutation.

By contrast, the analyzed mutation still allows the activation of other PDK1 substrates that are not PtdIns(3,4,5)P_3 binding dependent but are PIF pocket dependent. Indeed, the activitation of the PDK1/RSK1/2 pathway proceeded normally in the PDK1$^{K465E/K465E}$ mutant mice neurons.

The reduced PKB activation turns out not to be rate limiting in neurons for BDNF-mediated phosphorylation of FOXO1 or GSK3, the more popular and ancient PKB substrate. Indeed,

whereas attention has been largely focused on the regulation of GSK3 activity by the PKB pathway, evidence exists for the role of other signaling pathways in GSK3 regulation (Sutherland *et al.*, 1993). In this regard, a role for RSK in phosphorylating GSK3 has been evidenced in these studies by using specific kinase inhibitors (Fig. 13C). GSK3 regulates a wide range of substrates favouring differentiation/survival state of the neuronal cell (Cole, 2012). On the other hand, FOXO appears to serve as a point of convergence of molecular mechanisms implicated in cell survival in response to growth factors (Tran *et al.*, 2003). However, GSK3 and FOXO1 phosphorylation are still moderately decreased in the PDK1$^{K465E/K465E}$ mice samples under basal conditions, raising the possibility of deficient PKB activity being rate limiting for those substrates in some particular conditions.

2. DEFECTIVE S6K ACTIVATION IN THE PDK1$^{K465E/K465E}$ KNOCK-IN NEURONS

This study clearly shows that TSC2 and PRAS40 are not properly phosphorylated and thereby inhibited by PKB in the PDK1$^{K465E/K465E}$ mice embryonic cortical neurons, which are characterized with the reduced mTORC1 pathway activity. Collectively, the general findings from this study about mTORC1/S6K activation suggest that (i) in the primary culture of cortical neurons, BDNF-induced S6K activation, as a readout of mTORC1 activity downstream of the PI3K/PDK1 pathway, is highly dependent on the nutrient status of the cell. (ii) S6K phosphorylation at two regulatory sites, Ser389 at the hydrophobic motif and Thr229, the PDK1 phospho-site, is reduced in the PDK1$^{K465E/K465E}$ mice cortical neurons compared with the PDK1$^{+/+}$ wild type ones. (iii) This deficient S6K activation in response to BDNF is due to defective PKB/mTORC1 activation, since mTORC1 capacity to sense amino acids, which occurs independently of PKB/TSC2, is preserved in the PDK1$^{K465E/K465E}$ mice cortical neurons.

S6K activation is much more rapid (1 min) after serum deprivation than after double serum and L-Glutamine deprivation conditions in the BDNF stimulation time-course experiment (Fig 15 and 16A). Consistent with this, in serum deprived cortical cells, BDNF treatment showed a significant difference in S6K activation between the PDK1$^{+/+}$ and PDK1$^{K465E/K465E}$ mutant neurons at 5 min, which is the optimal time-window for PKB maximal activation (Fig. 15 and 16C). L-Glutamine withdrawal from the neuronal cell culture medium disables S6K to adequately respond to BDNF stimulation, since its activation is very weak, with reduced phosphorylation at both activation sites even in the PDK1 wild type neurons (Fig. 16A and C), indicating that L-Glutamine is required for growth factor-induced S6K activation. At 30 min,

BDNF induced a robust S6 phospho-signal even in the absence of L-Glutamine which was not compromised in the PDK1$^{K465E/K465E}$ mice cortical cell samples. These observations reveal that amino acids, likely L-Glutamine, support S6K activation in the mutant samples in the basal and at early times of BDNF stimulation conditions, which is the window of time when the deficiency in PKB activity becomes more restrictive, whereas at 30 min of BDNF stimulation, when PKB activation is almost indistinguishable between wild type and mutant samples, the PKB-dependent activation of the mTORC1/S6K/S6-protein pathway seems to play a prominent role.

The preloading with L-Glutamine prior the growth factor stimulation induced S6 phosphorylation to the same extent in both PDK1$^{+/+}$ and PDK1$^{K465E/K465E}$ cortical cells, which compensated for the defective BDNF-induced activation of the S6K pathway detected in the PDK1$^{K465E/K465E}$ mice neuronal cells. Thus, the preloading of cells with L-Glutamine accelerates mTORC1/S6K activation, which abrogates the defective mTORC1/S6K activity downstream of PDK1/PKB (Fig. 17A).

These experimental observations indicate that the mTORC1 pathway remains sensitive to amino acids in the PDK1$^{K465E/K465E}$ mutant cells lacking PKB activity, and importantly, that the amino acid-induced S6K activation is indistinguishable between PDK1$^{+/+}$ and PDK1$^{K465E/K465E}$ mutant neurons (Fig. 17A, lanes 3 and 4) further supporting the notion of mTORC1 capacity to sense amino acids independently from PKB/TSC2. By contrast, BDNF-induced S6K activation upon double starvation conditions, but not in L-Glutamine preloaded samples, is compromised at 5 minutes in the PDK1$^{K465E/K465E}$ mice cortical cells (Fig. 17A, lanes 5 and 6). This deficient S6K activation in the PDK1$^{K465E/K465E}$ mutant cortical cells was compensated by preloading for 1 h with L-Glutamine. Compared to the pharmacological inhibitory data, withdrawal of serum and L-Glutamine from the cell culture medium causes reduction in mTORC1 activity almost to the same extent as the mTORC1 specific inhibitor does. In the rapamycin pretreated neuronal cell culture, BDNF stimulation failed to activate S6K whilst induced a robust activation of PKB. Moreover, upon 5 min of BDNF stimulation, full inhibition of mTORC1 resulted in a clear inhibition of the negative feedback loop to IRS/PI3K, further increasing the activation of the PDK1/PKB signaling pathway, which was reflected in the further phosphorylation of PKB at Thr308, which was defective in the PDK1$^{K465E/K465E}$ mutant cortical cells.

Although normal levels of S6K activation are equally observed in the PDK1$^{+/+}$ and PDK1$^{K465E/K465E}$ mutant cultured neuronal cells by 30 min of BDNF stimulation, the rate of

S6K activation differs in the PDK1$^{K465E/K465E}$ samples compared to controls, which might be physiologically relevant to the reduced size, delayed neuronal polarization and axonal growth deficiency of the PDK1$^{K465E/K465E}$ mice, since S6K is broadly involved in cell growth control. Consistent with this observation, the inhibition of mTORC1 signaling by rapamycin mimicked the S6K activity inhibition as well as the phenotype of the neuronal cells.

Since the cellular processes controlled by mTORC1 are nutrient-demanding, mTORC1 inhibition upon amino acid deprivation is of great importance for the cell to maintain the balance between metabolic consumption and supply, which ultimately contributes to the cell vital processes to stay alive during nutrient starvation. On the other hand, mTORC1 is broadly regulated by growth factors and the signaling pathways linking the growth receptors to mTORC1 regulation are also highly demanded. The PKB/TSC2 independent, amino acid-sensitive mechanism of mTORC1 activation seems to be quite potent, since I provide the evidence that 1 h preloading with L-Glutamine compensated for the PDK1 K465E knock-in mutation-induced impediment of S6K phosphorylation. Here it is clearly shown the defective BDNF-induced mTORC1 activation, as judged by S6K phosphorylation, of the PDK1$^{K465E/K465E}$ mutant cortical cells in the presence of L-Glutamine but absence of serum. All these suggest that growth factors and PDK1/PKB signaling pathway are highly important in mTORC1 activation. On the other hand, the inability of growth factors to induce mTORC1 activation in the L-Glutamine starvation conditions is also evident from experiments described in here, suggesting that amino acid supply is also relevant for BDNF-induced mTORC1 activation.

Depicting the relationship between amino acid and growth factor mechanisms of mTORC1 activation helps to understand how they interact with each other in order to determine the cell fate. Thus, cell growth impediment in the PDK1$^{K465E/K465E}$ mutant cells is likely to be mediated by defective PDK1/PKB signaling pathway, which normally impinges on TSC2 to stimulate mTORC1.

Taken together, the above findings suggest that the PDK1 PH domain is required for the optimal activation of PKB, for the maximal phosphorylation and inactivation of PRAS40 and TSC2 to achieve the efficient mTORC1 activity in the cell. Also this study clearly shows that the PDK1 PH domain integrity is not required for the L-Glutamine-regulated activation of mTORC1 and subsequently, S6K phosphorylation on Thr389.

3. PKB REGULATES NDRG1 PHOSPHORYLATION IN NEURONAL CELLS

Another member of the AGC family of kinases regulated by PDK1 that does not possess the PH domain to directly sense the phosphoinositides is SGK. SGK is phosphorylated at its hydrophobic motif by mTORC2, and this phosphorylation does not directly activate SGK1, but enables PDK1 to interact with SGK1 through its PIF pocket docking site, thereby allowing T-loop phosphorylation and activation of SGK1. The SGK isoforms are widely expressed and are reported to possess distinct, as well as overlapping roles with other AGC kinases. In particular, SGK1 shares structural identity with PKB and can account for some of the PKB functions in the cell. For example, both PKB and SGK coordinately regulate the function of transcription factors of the forkhead family, preventing cell from entering in apoptosis (Jones *et al.*, 2009). Since SGK1 phosphorylation is not PH domain dependent, it was not expected to be affected by the PDK1 K465E mutation. SGK1 might as well be involved in transducing the BDNF-mediated survival signals on cultured cortical neurons. One of the best characterized substrates of SGK is NDRG1 (Murray *et al.*, 2004a), and although NDRG1 might play important roles in the nervous system, the regulation of this protein by SGK1 is not well described.

The phosphorylation of the NDRG1 protein at Thr346/356/366 sites, lying in a C-terminal decapeptide repeated sequence, is used as a read out of the SGK1 activity (Garcia-Martinez *et al.*, 2008). BDNF-stimulated cortical cell extracts and tissue extracts from the adult were analyzed by western blot using a phospho-specific antibody recognizing the phosphorylated C-tail repeats of the NDRG1 protein. As expected, phosphorylation of NDRG1 is preserved in the liver tissue extracts from the $PDK1^{K465E/K465E}$ mice (Fig 20A) as reported previously (Bayascas *et al.*, 2008). By contrast, BDNF-induced phosphorylation of NDRG1 in the $PDK1^{K465E/K465E}$ mice neurons as well as in the $PDK1^{K465E/K465E}$ mice brain extracts was found to be clearly reduced (Fig. 19 and 20). NDRG1 alteration at the SGK1 phospho-sites was totally unexpected, since SGK1 is not a PH domain-dependent substrate of PDK1. Strikingly, the PKB inhibitor Akti-1/2 also greatly reduced NDRG1 phosphorylation at a dose that did not affect other closely related kinases such as RSK (Fig 21). The phosphorylation of NDRG1 at three threonine sites by SGK1 transforms it into an excellent substrate for GSK3, allowing the latter to phosphorylate NDRG1 at Ser342/352/362. To rule out the possibility that the observed altered NDRG1 phosphorylation at Thr346/356/366 sites was due to the masking of the corresponding epitope by GSK3-hyperphosphorylated NDRG1 protein, next experiment was designed in order to define the responsible kinase for this phospho-site in neurons.

Inhibition of GSK3 with two independent GSK3 inhibitors induced an electrophoretic band-shift in the BDNF-induced three phospho-threonine signal, which accounts for the reduced phosphorylation of NDRG1. In parallel, Akti-1/2 inhibitor caused the reduction of the NDRG1 signal intensity but did not increase the electrophoretic mobility, similarly to what was observed in the PDK1$^{K465E/K465E}$ mice neuronal cells (Fig. 21). All this suggest that PKB inhibition by the specific inhibitory compound is equivalent to the reduced PKB activation observed in the PDK1$^{K465E/K465E}$ knock-in neuronal cells, and that both the treatment with the inhibitor and the defective PKB activation resulting from the PDK1 K465E knock-in mutation are responsible for the reduced NDRG1 phosphorylation on Thr346/356/366 sites in neurons. Also, the Akti-1/2 compound-induced release of GSK3 activity from the PKB inhibitory effect should be equivalent to the inefficient inhibition of GSK3 resulting from deficient PKB activation in the PDK1$^{K465E/K465E}$ mice, which in both cases are responsible for the band-shift which is characteristic of the NDRG1 protein when phosphorylated on the three phospho-threonine and three phospho-serine residues at the same time. Although this confronts what is stated in this study regarding GSK3 normal phosphorylation in the PDK1$^{K465E/K465E}$ mice mutant neurons, at the same time it leaves open the possibility that GSK3 might not be properly phosphorylated, thereby inhibited, due to the deficient PKB activation of the PDK1$^{K465E/K465E}$ mutant neurons in some particular circumstances in the living organism, which is not always accessible to be validated *in vitro*. Moreover, it cannot be fully ignored the finding that the PDK1 K465E mutation indeed do have impact on GSK3 phosphorylation in basal and early time (1 min) points of BDNF stimulation conditions. All these together indicate that GSK3 phosphorylation of NDRG1 is not an obstacle for the antibody which recognizes the Thr346/356/366 sites and strongly suggest that PKB governs this phosphorylation site in neurons.

The notion of PKB being responsible for Thr346/356/366 site phosphorylation on the NDRG1 protein in neuronal cells was further supported by the finding that NDRG1 phosphorylation at Thr346/356/366 site was not affected in the PDK1 L155E neuronal specific conditional knock-in mice cortical cells (data not shown). That was also surprising, since mutation of Leucine at position 155 in the hydrophobic groove of the PIF-pocket to Glutamic acid disrupts the function of the PIF pocket of PDK1, resulting in lack of activity of the PIF pocket-dependent substrates RSK and S6K, whereas PKB was normally active in PDK1 L155E ES cells (Collins *et al.*, 2003) and in BDNF-stimulated cortical cells obtained from the PDK1

L155E neuronal specific conditional knock-in mice (Lluís Cordon-Barris, personal communication).

Several aspects of this finding deserve additional comments; among them is the identification of the NDRG1 residues which are designated for SGK phosphorylation. Within the NDRG1 nonapeptide that conform to the specific SGK1 phosphorylation signature, there are two residues, Ser at position n+1 and Glu at n+2, which are probed to be the drawbacks for PKB phosphorylation (Murray *et al.*, 2005), whereas these two residues are not conserved in NDRG2, an isoform that was indeed shown to be phosphorylated at Thr348 residue by PKB (Murray *et al.*, 2004a). However, the bona fide substrate of PKB PRAS40 possesses Ser at position n+1 and Asp at position n+2, thereby suggesting that NDRG1 can be phosphorylated by PKB with the same success as PRAS40 does (Fig. 20C).

4. INTERACTION OF PDK1 WITH PHOSPHOINOSITIDES IS NOT ESSENTIAL FOR NEURONAL SURVIVAL

One of the main goals of this study was to test the hypothesis that the inhibition of PDK1 binding to phosphoinositides is one of the downstream mechanisms that mediate PI3K-dependent neuronal survival. Using cultured primary neurons, it was observed that the cell viability was not compromised in the $PDK1^{K465E/K465E}$ mutant neuronal cells compared with the $PDK1^{+/+}$ wild type ones in different tested paradigms of cell death. The two genotypes equally die and respond to BDNF after trophic factor deprivation in the culture. Furthermore, these results were reinforced when specific cell death nuclear markers characteristic of apoptosis were scored, suggesting that PKB is not essential for neuronal cell survival.

Active PKB serves as a general mediator of cell survival by phosphorylating and inactivating a number of cytoplasmic substrates. Among them are the pro-apoptotic Bcl-2 family member Bad (Datta *et al.*, 1997) and the metabolic regulator glycogen synthase kinase-3 (GSK3) (Cross *et al.*, 1995). GSK3 is critical for the normal function of the central nervous system, where it regulates a variety of neuronal functions including neurogenesis and apoptosis. Some of the GSK3 substrates implicated in apoptosis so far are pro-survival factors and their negative regulation by GSK3 compromise the cell survival. Thus, when GSK3 activity is low, reduced phosphorylation of its substrates protects them against proteasome-mediated degradation and promote survival of the cell (Cole, 2012). Also, the direct phosphorylation of the Forkhead family of transcription factors represents a link between the PKB signaling

pathway and the transcriptional regulation of cell survival. Indeed, overexpression of a constitutively active form of FOXO in which all the three PKB regulatory sites are converted to alanines promotes apoptosis in a number of cell types in culture (Brunet *et al.*, 1999;Tang *et al.*, 1999).

This study shows that the reduced levels of PKB activation in the PDK1$^{K465E/K465E}$ mutant mice neurons are still sufficient to support the phosphorylation of GSK3 and FOXO. In fact, GSK3 and FOXO phosphorylation by PKB were expected to be affected in the PDK1 K465E knock-in neuronal cells. However, in the growth factor stimulated PDK1$^{K465E/K465E}$ mice neurons, phosphorylation of the PKB substrates GSK3 and FOXO is not compromised. Consistent with this, the cell survival process was not affected by the PDK1 K465E mutation.

To further explore the initial findings, the cultured primary cortical neurons were exposed to the PKB specific inhibitor Akti-1/2. This revealed that the direct inhibition of PKB did not further compromise the cell viability induced by serum deprivation, whereas in parallel experiments the PI3K inhibitor PI-103 totally abolished the recovery of the cell viability induced by BDNF equally in the PDK1$^{K465E/K465E}$ and PDK1$^{+/+}$ cortical neurons. In fact, the PKB inhibitor Akti-1/2 still allowed some GSK3 activation on neuronal cells at the same dose as it was applied for the viability test (Fig. 13C). But despite GSK3, which is supposed to be liberated from the PKB inhibitory effect, the Akti-1/2 still allowed the normal survival responses both in the PDK1$^{K465E/K465E}$ and PDK1$^{+/+}$ wild type neurons (Fig. 24). These experiments suggested that BDNF-mediated protection against trophic deprivation involves other PDK1 substrates rather than PKB.

In the PDK1 PH domain, Lys465 is the central residue conforming the phosphoinositide-binding pocket, and its mutation to Glu prevents the association of PDK1 with PtdIns(3,4,5)P_3, thereby affecting PKB phosphorylation. By contrast, this mutation still allows the activation of other PDK1 substrates that are not PIP3 binding dependent but are PIF pocket dependent. As mentioned before, in the BDNF-treated cortical neurons, PKB phosphorylation at the PDK1 site is not completely abrogated but is significantly reduced, whereas the phosphorylation of the PDK1 PIF pocket-dependent targets proceeded normally.

The activity of the PDK1/RSK1/2 pathway could be estimated by determining the phosphorylation of RSK and ERK. BDNF equally stimulated RSK both in the PDK1$^{K465E/K465E}$ knock-in and PDK1$^{+/+}$ wild type cells. In cultured cortical cells, the BDNF-mediated pro-survival effect seems to be dependent on PDK1-dependent RSK activation. Indeed, it has been already described that RSK1/2 play prominent roles in BDNF-mediated neuronal survival.

Knockdown of RSK1/2 abolished BDNF protective effect against trophic deprivation. The electroporation of rat cortical neurons with the mutant form of PDK1 A280V, mutation that greatly increases PDK1 activity, reduced trophic deprivation-induced apoptosis. In contrast, the antiapoptotic effects of PDK1A280V were abolished by RSK1/2 knockdown (Kharebava *et al.*, 2008). Increased protein levels of RSK1/2 were reported in the striatum of mice models of Huntington Disease which were proved protective against mutant huntingtin toxicity (Xifro *et al.*, 2011). Thus, clear evidences were provided from these studies about RSK1/2 requirement for BDNF antiapoptotic activity in cortical neurons and for protection against huntingtin toxicity is striatal neurons.

Another substrate of PDK1 that is involved in cell survival is SGK1. The activation of SGK1 is dependent on the PI3K pathway and PDK1 activity but, as mentioned before, it is different from PKB as SGK1 does not contain any PtdIns(3,4,5)P_3 binding domain. SGK1 is phosphorylated at its hydrophobic motif by mTORC2 and next activated by PDK1 by phosphorylation of the T-loop residue. Since SGK1 phosphorylation is therefore not PH domain dependent, it is not expected to be affected by the PDK1 K465E mutation, and might as well be involve in transducing the BDNF-mediated survival signals on cultured cortical neurons.

The analysis was expanded to other neurotrophic factors and other neuronal cell types with the ultimate goal of determining the role of the PDK1-PtdIns(3,4,5)P_3 interaction in neuronal cell viability, with all the obtained results strongly supporting the notion of the PDK1-PtdIns(3,4,5)P_3 binding being dispensable for neuronal survival. Taken together all the above findings, they raise the possibility of the other PDK1 substrates playing a major role in controlling neuronal survival rather than PKB. Preliminary findings about the role of other PDK1 targets responsibility rather than PKB in mediating survival were provided by this study. Indeed, the cortical cells viability was strongly affected by the PI3K inhibitor, but not by the PKB inhibitor, which strongly support the notion that the other AGC kinases regulated by PDK1 mediate neuronal cell survival.

5. IMPACT OF THE PDK1 K465E KNOCK-IN MUTATION ON NEURONAL GROWTH, DEVELOPMENT AND NEURONAL MORPHOLOGY

The $PDK1^{K465E/K465E}$ mutant mice are smaller than the $PDK1^{+/+}$ wild type ones, with reduced cell volume resulting from deficient activation of the PKB/mTORC1/S6K signaling axis

(Bayascas *et al.*, 2008). In agreement with this previous observations, a growth deficiency phenotype of the PDK1$^{K465E/K465E}$ knock-in mice compared with the PDK1$^{+/+}$ wild type mice has been detected from early stages during development in this study as well. In the PDK1$^{K465E/K465E}$ mice, the volume of the embryonic brain at E15,5 was 20% reduced when compared to PDK1$^{+/+}$ control mice. Similar growth retardation observations were observed in mice lacking different elements of this signaling network. For instance, the PKBγ-deficient mice demonstrated 25% reduction in brain size than those of their wild type littermates, whereas the body and the other organs were normally sized in the PKBγ knockout mice. Thus, the reduced organ mass of the PKBγ$^{-/-}$ mice was specific to the brain and was not proportional to the body size (Easton *et al.*, 2005). It is worth to mention that among the three PKB isoforms encoded by three separate genes in mammals, PKBγ is mostly abundant in the brain (Brodbeck *et al.*, 1999). Moreover, the reduced brain volume observed in the PKBγ knockout mice was proposed to be mainly due to the presence of smaller cells, whereas the cell number was not affected. The same study provided with evidence that mice lacking the PKBα gene showed reduction of organ mass including the brain, which was proportional to the body size, and that the mechanism of organ mass reduction involved was tissue-depended. For instance, reduced heart and brain organ mass was attributed to a decrease in the both number and size of cells in the PKBα knockout mice (Easton *et al.*, 2005). These data together with the present study observations, clearly demonstrating the reduced brain size of the PDK1$^{K465E/K465E}$ mice due to a reduction of the cell size, whereas the number of neurons is unaffected, serve to further emphasize the critical role of PKB in controlling cell growth.

Neurons undergo morphological transformations during development. Starting from being simple symmetric spheres, they develop into highly elaborate cells with distinct axonal and dendritic compartments. One of the aims of the this study was to investigate the role of the PDK1-PtdIns(3,4,5)P_3 binding in neurite outgrowth. The understanding of the mechanisms controlling neuritogenesis in the developing brain may offer insights into pathological situations and potential therapeutic approaches. This work reports that deficient activation of PKB affects the neurite outgrowth process. Indeed, both by eye and based on careful measurements, the PDK1$^{K465E/K465E}$ mice cortical cells displayed altered neurite elongation compared with their controls, whereas the cell soma diameter remained constantly reduced. Thus, the PDK1$^{K465E/K465E}$ mice cortical cell neurites are shorter due to a specific neuronal defect affecting neurite outgrowth rather than to a general cell growth deficiency. However, no obvious defect was detected while scoring both the branching per neurite and the number

of neurites per cell in the PDK1 mutant cortical cultures, whereas considerable differences existed in the number of non-differentiated cortical cells between the $PDK1^{+/+}$ and $PDK1^{K465E/K465E}$ mice cultures.

Analysis of the role of the PKB/mTORC1/S6K signaling pathway in neuronal morphology may highlight a number of challenges in targeting this pathway. The further investigation on the role of the PDK1-PtdIns(3,4,5)P_3 binding in neuronal morphology raised a number of important implications and this is the focus of the following discussion section.

6. THE PDK1-PtdIns(3,4,5)P_3 BINDING AND PKB ACTIVATION IN NEURONAL CELL POLARIZATION AND AXON ELONGATION

This study provides evidence that normal activation of PKB is required for neuronal polarity and axon elongation. The $PDK1^{K465E/K465E}$ knock-in mice cortical and hyppocampal neurons deficient for PKB activation exhibit alterations on diverse parameters of neurogenesis. What downstream effectors are regulated by the PKB signaling during neuronal polarization? Actually, it has been suggested that PKB promotes axon formation by phosphorylating and inhibiting GSK3 (Jiang *et al.*, 2005;Yoshimura *et al.*, 2005). However, the double knock-in mice neurons in which Ser9/21 were replaced by Ala thereby abolishing PKB phosphorylation sites were normally developed with neurons properly polarized independently of the phosphorylation at these residues (Gartner *et al.*, 2006). Recently, Choi et al demonstrated that phosphorylated, thereby inhibited, TSC2 at the PKB phosphorylation site Thr1462 was specifically localized along the axon of hippocampal cells, whereas total TSC2 was distributes throughout the neurons. This observation was further confirmed by using the PI3K inhibitor, which significantly reduced phospho TSC2 staining. PKB is among the multiple protein kinases downstream of PI3K blocked by the inhibitor the one that may dictate TSC2 inactivation along the axon. In the same study, the TSC/mTORC1 downstream target S6K phosphorylated at the mTORC1 site was also found specifically enriched in the axon, suggesting that the inactivation of TSC2 and activation of mTORC1 takes place on the axon (Choi *et al.*, 2008).

The present study clearly shows that TSC2 and PRAS40 are not properly phosphorylated and thereby are not inactivated by PKB in the $PDK1^{K465E/K465E}$ mice embryonic and adult neurons, which are characterized by PKB deficiency leading to reduced mTORC1 pathway activity.

Moreover, delayed hippocampal cell polarization and deficient axon elongation in the PDK1$^{K465E/K465E}$ hippocampal neurons are described also in this work.

BRSK protein kinases are essential for specifying the axon/dendrite identity in the developing neurons, which is a cardinal feature of neuronal morphology (Kim *et al.*, 2008;Kishi *et al.*, 2005). BRSKs phosphorylate the microtubule-associated protein Tau on Ser262 residue within the tubulin binding domain (Kishi *et al.*, 2005). Tau is implicated in axon specification and neuronal polarization by regulating cytoskeletal dynamics during the process of axon specification (Kempf *et al.*, 1996). Thus, this is one way in which BRSK kinases may affect neuronal polarization. After investigating the expression levels of BRSK1/2 proteins, this study presented a clear evidence that the loss of PKB activation was associated with the decrease in BRSK1/2 protein expression levels both in the embryonic primary culture and in the developing brain of the PDK1$^{K465E/K465E}$ mice, which was however recovered in the adult and may explain the normal layering and connectivity attained in the PDK1$^{K465E/K465E}$ knock-in mice adult brain. Interestingly, there was a partial reduction of BSRK1/2 protein expression levels in the embryonic brain extracts of the PDK1$^{+/K465E}$ compared with the PDK1$^{+/+}$ mice and that was more pronounced in the PDK1$^{K465E/K465E}$ knock-in mice embryos. Importantly, the BRSK1/2 re-expression rescued the observed short axon phenotype in the PDK1$^{K465E/K465E}$ mice neurons.

In order to investigate the potential causal relationship between PKB activity and axon formation, pharmacological inhibition of PKB in neurons was carried out, and its effect on neuronal polarity analyzed. The specific Akti-1/2 inhibitor caused deficient axonal elongation and impaired polarization of the PDK1 wild type cells, indicating the importance of PKB and its downstream substrates in the axon formation process. Moreover, the PDK1 wild type hippocampal neurons grown in the presence of the mTORC1 specific inhibitor rapamycin also showed impaired polarization and stronger prevention of axon growth than the Akti-1/2 treated ones. The results derived from these two independent pharmacological inhibitors treatments encouraged the above proposed hypothesis about TSC2 being a target of PKB in polarizing neurons through the mTORC1/S6K pathway.

Previous studies suggesting PKB as an upstream kinase controlling neuronal polarity were so far just informative, since no evidence in terms of PKB mediating neuronal polarity and moreover axon growth were provided. Likewise, the reported evidence showed that perturbing the PI3K function disrupted axon guidance (Akiyama and Kamiguchi, 2010), but the role of downstream effectors likely PKB remained to be defined. Furthermore, the finding revealing

that the elevation of PtdIns(3,4,5)P_3 levels and PKB activation are essential in mediating the growth cone guidance process (Henle *et al.*, 2011) fails to dissect the specific molecular interactions implicated in neuronal polarity.

The current study aimed to identify the role of PKB in the regulation of neuronal polarization. The obtained results firmly designate PKB as an upstream kinase in the axis of TSC2/mTORC1/BRSK in both neuronal polarization and axon elongation. Furthermore, using the PDK1 PH domain specific knock-in approach makes these observations more solid, suggesting that the PtdIns(3,4,5)P_3/PDK1/PKB signaling pathway may hold therapeutic promise for enhancing functional axon regeneration and treatment of neurological disorders.

This work also aimed to understand the contributable role of PKB in neuronal cell survival and differentiation, to provide both the basis and also stimulation for future studies to identifying downstream PKB specific substrates that can be targeted without potential adverse consequences that currently confounds efforts to target PKB dysfunction in human pathologies. The PKB signaling pathway has many vital physiological roles including metabolic actions as well as proliferation, differentiation and survival. There is a current major focus towards the development of chemical compounds inhibiting the PKB signaling pathway for the treatment of diverse human somatic pathologies. In the best scenario, these compounds would be in the future able to modestly inhibit PKB activity *in vivo*. It would be beneficial to take a profit from the here described resultant neuronal phenotypes from the PDK1 K465E knock-in mutation, which genetically blunts PKB kinase activation mildly leading to small changes in its signaling network, for the drug compound compliance in the design of therapeutic trials with less side effects.

CONCLUSIONS

V-CONCLUSIONS

1-The PDK1 K465E knock-in mutation preventing the interaction of PDK1 with phosphoinositides does not fully abolish, but moderately impairs, PKB activation. The phosphorylation of PKB at Thr308, the PDK1 phospho-site, is reduced in the BDNF-stimulated PDK1$^{K465E/K465E}$ knock-in mice cortical neurons compared to the PDK1$^{+/+}$ wild type cells in time and dose-dependent manner. By contrast Ser473, the mTORC2 site, is normally phosphorylated in both the PDK1$^{+/+}$ and PDK1 $^{K465E/K465E}$ neuronal cells.

2-The deficient activation of PKB is rate limiting for some substrates such as PRAS40 and TSC2 in the PDK1$^{K465E/K465E}$ knock-in mice cortical neurons, which is translated into incomplete activation of mTORC1 in response to BDNF, paralleling in this manner the reduced PKB activation profile of the mutant neurons at early time points.

3-The moderately reduced PKB activation in the PDK1$^{K465E/K465E}$ knock-in mice neurons does not affect the phosphorylation of GSK3 and FOXO.

4-The deficient mTORC1 activation results in reduced S6K hydrophobic motif phosphorylation at Ser389, leading to reduced phosphorylation of S6K at Thr229, the PDK1 phospho-site, in the PDK1$^{K465E/K465E}$ knock-in mice cortical neurons stimulated with BDNF.

5-Nutrient-induced activation of S6K is preserved in the PDK1$^{K465E/K465E}$ knock-in mice neurons and is independent of the PDK1-PtdIns(3,4,5)P_3 interaction.

6-The non PH-domain dependent, but PIF pocket-dependent PDK1 substrate RSK is normally activated in the PDK1$^{K465E/K465E}$ knock-in mice neurons, validating in this way the specificity of the PDK1 K465E mutation.

7-The phosphorylation of NDRG1 at Thr346/356/366 sites, lying in a C-terminal decapeptide repeated sequence, is under the control of PKB in neurons.

8-The interaction of PDK1 with phosphoinositides is not essential for neuronal cell survival. The PDK1$^{K465E/K465E}$ knock-in and PDK1$^{+/+}$ wild type neurons exhibit similar survival responses either to cell death inducers or to growth factors.

9-The interaction of PDK1 with phosphoinositides is important for growth and development. Consistent with the reduced body size, the PDK1$^{K465E/K465E}$ mice brain is 20% smaller compared with that of the PDK1$^{+/+}$ mice. The observed brain phenotype in the PDK1$^{K465E/K465E}$ mice is due to reduced cell volume rather than decreased cell number.

10-The PDK1 K465E knock-in mutation has an impact on neuritogenesis. The PDK1$^{K465E/K465E}$ mice cortical cells display altered neurite outgrowth compared with their controls. Deficient activation of PKB also leads to alterations in the neurite initiation process but not in the arborisation of the PDK1$^{K465E/K465E}$ mice cortical neurons.

11-The PKB/mTORC1/S6K activity is critical for neuronal cell polarization and axon elongation. The marked deficiency in the PKB/mTORC1/S6K axis is manifested by axonal specific growth defects and delayed cell polarization in the PDK1$^{K465E/K465E}$ mice hippocampal neurons.

12-The alteration in the process of axon formation observed in the PDK1$^{K465E/K465E}$ mice hippocampal cells is due to the reduced expression of the BRSK1/2 protein kinases in both the embryonic primary cultures and the developing brain of the PDK1$^{K465E/K465E}$ mutant mice. The re-expression of BRSK isoforms rescues the short axon phenotype. The deficient BRSK1/2 expression levels recovered in the adult, what may explain the normal layering and connectivity observed in the PDK1$^{K465E/K465E}$ knock-in mice adult brain.

REFERENCE LIST

REFERENCES

1. Akiyama H and Kamiguchi H (2010) Phosphatidylinositol 3-kinase facilitates microtubule-dependent membrane transport for neuronal growth cone guidance. *J Biol Chem,* **285,** 41740-41748.

2. Alessi DR, Caudwell FB, Andjelkovic M, Hemmings BA, and Cohen P (1996) Molecular basis for the substrate specificity of protein kinase B; comparison with MAPKAP kinase-1 and p70 S6 kinase. *FEBS Lett,* **399,** 333-338.

3. Alessi DR, Deak M, Casamayor A, Caudwell FB, Morrice N, Norman DG, Gaffney P, Reese CB, MacDougall CN, Harbison D, Ashworth A, and Bownes M (1997a) 3-Phosphoinositide-dependent protein kinase-1 (PDK1): structural and functional homology with the Drosophila DSTPK61 kinase. *Curr Biol,* **7,** 776-789.

4. Alessi DR, James SR, Downes CP, Holmes AB, Gaffney PR, Reese CB, and Cohen P (1997b) Characterization of a 3-phosphoinositide-dependent protein kinase which phosphorylates and activates protein kinase Balpha. *Curr Biol,* **7,** 261-269.

5. Alessi DR, Kozlowski MT, Weng QP, Morrice N, and Avruch J (1998) 3-Phosphoinositide-dependent protein kinase 1 (PDK1) phosphorylates and activates the p70 S6 kinase in vivo and in vitro. *Curr Biol,* **8,** 69-81.

6. Allan LA and Clarke PR (2009) Apoptosis and autophagy: Regulation of caspase-9 by phosphorylation. *FEBS J,* **276,** 6063-6073.

7. Allan LA, Morrice N, Brady S, Magee G, Pathak S, and Clarke PR (2003) Inhibition of caspase-9 through phosphorylation at Thr 125 by ERK MAPK. *Nat Cell Biol,* **5,** 647-654.

8. Anderson KE, Coadwell J, Stephens LR, and Hawkins PT (1998) Translocation of PDK-1 to the plasma membrane is important in allowing PDK-1 to activate protein kinase B. *Curr Biol,* **8,** 684-691.

9. Andjelkovic M, Alessi DR, Meier R, Fernandez A, Lamb NJ, Frech M, Cron P, Cohen P, Lucocq JM, and Hemmings BA (1997) Role of translocation in the activation and function of protein kinase B. *J Biol Chem,* **272,** 31515-31524.

10. Anjum R and Blenis J (2008) The RSK family of kinases: emerging roles in cellular signalling. *Nat Rev Mol Cell Biol,* **9,** 747-758.

11. Arbour N, Vanderluit JL, Le Grand JN, Jahani-Asl A, Ruzhynsky VA, Cheung EC, Kelly MA, MacKenzie AE, Park DS, Opferman JT, and Slack RS (2008) Mcl-1 is a key regulator of apoptosis during CNS development and after DNA damage. *J Neurosci,* **28,** 6068-6078.

12. Arevalo JC and Wu SH (2006) Neurotrophin signaling: many exciting surprises! *Cell Mol Life Sci,* **63,** 1523-1537.

13. Arimura N and Kaibuchi K (2007) Neuronal polarity: from extracellular signals to intracellular mechanisms. *Nat Rev Neurosci,* **8,** 194-205.

14. Avruch J, Hara K, Lin Y, Liu M, Long X, Ortiz-Vega S, and Yonezawa K (2006) Insulin and amino-acid regulation of mTOR signaling and kinase activity through the Rheb GTPase. *Oncogene,* **25,** 6361-6372.

15. Baas PW, Black MM, and Banker GA (1989) Changes in microtubule polarity orientation during the development of hippocampal neurons in culture. *J Cell Biol,* **109,** 3085-3094.

16. Barde YA, Edgar D, and Thoenen H (1982) Purification of a new neurotrophic factor from mammalian brain. *EMBO J,* **1,** 549-553.

17. Barnes AP, Lilley BN, Pan YA, Plummer LJ, Powell AW, Raines AN, Sanes JR, and Polleux F (2007) LKB1 and SAD kinases define a pathway required for the polarization of cortical neurons. *Cell,* **129,** 549-563.

18. Barnes AP and Polleux F (2009) Establishment of axon-dendrite polarity in developing neurons. *Annu Rev Neurosci,* **32,** 347-381.

19. Basu A, Castle VP, Bouziane M, Bhalla K, and Haldar S (2006) Crosstalk between extrinsic and intrinsic cell death pathways in pancreatic cancer: synergistic action of estrogen metabolite and ligands of death receptor family. *Cancer Res,* **66,** 4309-4318.

20. Bayascas JR (2008) Dissecting the role of the 3-phosphoinositide-dependent protein kinase-1 (PDK1) signalling pathways. *Cell Cycle,* **7,** 2978-2982.

21. Bayascas JR (2010) PDK1: the major transducer of PI 3-kinase actions. *Curr Top Microbiol Immunol,* **346,** 9-29.

22. Bayascas JR, Leslie NR, Parsons R, Fleming S, and Alessi DR (2005) Hypomorphic mutation of PDK1 suppresses tumorigenesis in PTEN(+/-) mice. *Curr Biol,* **15,** 1839-1846.

23. Bayascas JR, Sakamoto K, Armit L, Arthur JS, and Alessi DR (2006) Evaluation of approaches to generation of tissue-specific knock-in mice. *J Biol Chem,* **281,** 28772-28781.

24. Bayascas JR, Wullschleger S, Sakamoto K, Garcia-Martinez JM, Clacher C, Komander D, Van Aalten DM, Boini KM, Lang F, Lipina C, Logie L, Sutherland C, Chudek JA, van Diepen JA, Voshol PJ, Lucocq JM, and Alessi DR (2008) Mutation of the PDK1 PH domain inhibits protein kinase B/Akt, leading to small size and insulin resistance. *Mol Cell Biol,* **28,** 3258-3272.

25. Beaulieu JM, Gainetdinov RR, and Caron MG (2009) Akt/GSK3 signaling in the action of psychotropic drugs. *Annu Rev Pharmacol Toxicol,* **49,** 327-347.

26. Becker EB and Bonni A (2004) Cell cycle regulation of neuronal apoptosis in development and disease. *Prog Neurobiol,* **72,** 1-25.

27. Bellacosa A, Franke TF, Gonzalez-Portal ME, Datta K, Taguchi T, Gardner J, Cheng JQ, Testa JR, and Tsichlis PN (1993) Structure, expression and chromosomal mapping of c-akt: relationship to v-akt and its implications. *Oncogene,* **8,** 745-754.

28. Bernal-Mizrachi E, Wen W, Stahlhut S, Welling CM, and Permutt MA (2001) Islet beta cell expression of constitutively active Akt1/PKB alpha induces striking hypertrophy, hyperplasia, and hyperinsulinemia. *J Clin Invest,* **108,** 1631-1638.

29. Biondi RM, Cheung PC, Casamayor A, Deak M, Currie RA, and Alessi DR (2000) Identification of a pocket in the PDK1 kinase domain that interacts with PIF and the C-terminal residues of PKA. *EMBO J,* **19,** 979-988.

30. Biondi RM, Kieloch A, Currie RA, Deak M, and Alessi DR (2001) The PIF-binding pocket in PDK1 is essential for activation of S6K and SGK, but not PKB. *EMBO J,* **20,** 4380-4390.

31. Biondi RM, Komander D, Thomas CC, Lizcano JM, Deak M, Alessi DR, and Van Aalten DM (2002) High resolution crystal structure of the human PDK1 catalytic domain defines the regulatory phosphopeptide docking site. *EMBO J,* **21,** 4219-4228.

32. Birkenkamp KU and Coffer PJ (2003) Regulation of cell survival and proliferation by the FOXO (Forkhead box, class O) subfamily of Forkhead transcription factors. *Biochem Soc Trans,* **31,** 292-297.

33. Blendy JA, Kaestner KH, Weinbauer GF, Nieschlag E, and Schutz G (1996) Severe impairment of spermatogenesis in mice lacking the CREM gene. *Nature,* **380,** 162-165.

34. Boyd JM, Gallo GJ, Elangovan B, Houghton AB, Malstrom S, Avery BJ, Ebb RG, Subramanian T, Chittenden T, Lutz RJ, et al. (1995) Bik, a novel death-inducing protein shares a distinct sequence motif with Bcl-2 family proteins and interacts with viral and cellular survival-promoting proteins. *Oncogene,* **11,** 1921-1928.

35. Brennan P, Babbage JW, Burgering BM, Groner B, Reif K, and Cantrell DA (1997) Phosphatidylinositol 3-kinase couples the interleukin-2 receptor to the cell cycle regulator E2F. *Immunity,* **7,** 679-689.

36. Brodbeck D, Cron P, and Hemmings BA (1999) A human protein kinase Bgamma with regulatory phosphorylation sites in the activation loop and in the C-terminal hydrophobic domain. *J Biol Chem,* **274,** 9133-9136.

37. Brognard J, Sierecki E, Gao T, and Newton AC (2007) PHLPP and a second isoform, PHLPP2, differentially attenuate the amplitude of Akt signaling by regulating distinct Akt isoforms. *Mol Cell,* **25,** 917-931.

38. Brunet A, Bonni A, Zigmond MJ, Lin MZ, Juo P, Hu LS, Anderson MJ, Arden KC, Blenis J, and Greenberg ME (1999) Akt promotes cell survival by phosphorylating and inhibiting a Forkhead transcription factor. *Cell,* **96,** 857-868.

39. Brunet A, Datta SR, and Greenberg ME (2001) Transcription-dependent and -independent control of neuronal survival by the PI3K-Akt signaling pathway. *Curr Opin Neurobiol,* **11,** 297-305.

40. Budd SL, Tenneti L, Lishnak T, and Lipton SA (2000) Mitochondrial and extramitochondrial apoptotic signaling pathways in cerebrocortical neurons. *Proc Natl Acad Sci U S A,* **97,** 6161-6166.

41. Buss RR, Sun W, and Oppenheim RW (2006) Adaptive roles of programmed cell death during nervous system development. *Annu Rev Neurosci,* **29,** 1-35.

42. Caceres A, Ye B, and Dotti CG (2012) Neuronal polarity: demarcation, growth and commitment. *Curr Opin Cell Biol*. **24**, 547-53.

43. Calleja V, Alcor D, Laguerre M, Park J, Vojnovic B, Hemmings BA, Downward J, Parker PJ, and Larijani B (2007) Intramolecular and intermolecular interactions of protein kinase B define its activation in vivo. *PLoS Biol,* **5,** e95.

44. Calleja V, Laguerre M, and Larijani B (2011) Role of the C-terminal regulatory domain in the allosteric inhibition of PKB/Akt. *Adv Enzyme Regul*. **52**, 46-57.

45. Calleja V, Laguerre M, Parker PJ, and Larijani B (2009) Role of a novel PH-kinase domain interface in PKB/Akt regulation: structural mechanism for allosteric inhibition. *PLoS Biol,* **7,** e17.

46. Cardone MH, Roy N, Stennicke HR, Salvesen GS, Franke TF, Stanbridge E, Frisch S, and Reed JC (1998) Regulation of cell death protease caspase-9 by phosphorylation. *Science,* **282,** 1318-1321.

47. Casamayor A, Morrice NA, and Alessi DR (1999) Phosphorylation of Ser-241 is essential for the activity of 3-phosphoinositide-dependent protein kinase-1: identification of five sites of phosphorylation in vivo. *Biochem J,* **342 (Pt 2),** 287-292.

48. Castro AF, Rebhun JF, Clark GJ, and Quilliam LA (2003) Rheb binds tuberous sclerosis complex 2 (TSC2) and promotes S6 kinase activation in a rapamycin- and farnesylation-dependent manner. *J Biol Chem,* **278,** 32493-32496.

49. Cecconi F, Alvarez-Bolado G, Meyer BI, Roth KA, and Gruss P (1998) Apaf1 (CED-4 homolog) regulates programmed cell death in mammalian development. *Cell,* **94,** 727-737.

50. Chalhoub N, Zhu G, Zhu X, and Baker SJ (2009) Cell type specificity of PI3K signaling in Pdk1- and Pten-deficient brains. *Genes Dev,* **23,** 1619-1624.

51. Chao MV (2003) Neurotrophins and their receptors: a convergence point for many signalling pathways. *Nat Rev Neurosci,* **4,** 299-309.

52. Chen WS, Xu PZ, Gottlob K, Chen ML, Sokol K, Shiyanova T, Roninson I, Weng W, Suzuki R, Tobe K, Kadowaki T, and Hay N (2001) Growth retardation and increased apoptosis in mice with homozygous disruption of the Akt1 gene. *Genes Dev,* **15,** 2203-2208.

53. Cheng EH, Wei MC, Weiler S, Flavell RA, Mak TW, Lindsten T, and Korsmeyer SJ (2001) BCL-2, BCL-X(L) sequester BH3 domain-only molecules preventing BAX- and BAK-mediated mitochondrial apoptosis. *Mol Cell,* **8,** 705-711.

54. Cho H, Mu J, Kim JK, Thorvaldsen JL, Chu Q, Crenshaw EB, III, Kaestner KH, Bartolomei MS, Shulman GI, and Birnbaum MJ (2001a) Insulin resistance and a diabetes mellitus-like syndrome in mice lacking the protein kinase Akt2 (PKB beta). *Science,* **292,** 1728-1731.

55. Cho H, Thorvaldsen JL, Chu Q, Feng F, and Birnbaum MJ (2001b) Akt1/PKBalpha is required for normal growth but dispensable for maintenance of glucose homeostasis in mice. *J Biol Chem,* **276,** 38349-38352.

56. Cho KS, Lee JH, Kim S, Kim D, Koh H, Lee J, Kim C, Kim J, and Chung J (2001c) Drosophila phosphoinositide-dependent kinase-1 regulates apoptosis and growth via the phosphoinositide 3-kinase-dependent signaling pathway. *Proc Natl Acad Sci U S A,* **98,** 6144-6149.

57. Choi YJ, Di NA, Kramvis I, Meikle L, Kwiatkowski DJ, Sahin M, and He X (2008) Tuberous sclerosis complex proteins control axon formation. *Genes Dev,* **22,** 2485-2495.

58. Chou MM, Hou W, Johnson J, Graham LK, Lee MH, Chen CS, Newton AC, Schaffhausen BS, and Toker A (1998) Regulation of protein kinase C zeta by PI 3-kinase and PDK-1. *Curr Biol,* **8,** 1069-1077.

59. Coffer PJ and Woodgett JR (1991) Molecular cloning and characterisation of a novel putative protein-serine kinase related to the cAMP-dependent and protein kinase C families. *Eur J Biochem,* **201,** 475-481.

60. Cole AR (2012) GSK3 as a Sensor Determining Cell Fate in the Brain. *Front Mol Neurosci,* **5,** 4.

61. Collins BJ, Deak M, Arthur JS, Armit LJ, and Alessi DR (2003) In vivo role of the PIF-binding docking site of PDK1 defined by knock-in mutation. *EMBO J,* **22,** 4202-4211.

62. Collins BJ, Deak M, Murray-Tait V, Storey KG, and Alessi DR (2005) In vivo role of the phosphate groove of PDK1 defined by knockin mutation. *J Cell Sci,* **118,** 5023-5034.

63. Courchesne SL, Karch C, Pazyra-Murphy MF, and Segal RA (2011) Sensory neuropathy attributable to loss of Bcl-w. *J Neurosci,* **31,** 1624-1634.

64. Craig AM, Jareb M, and Banker G (1992) Neuronal polarity. *Curr Opin Neurobiol,* **2,** 602-606.

65. Cross DA, Alessi DR, Cohen P, Andjelkovich M, and Hemmings BA (1995) Inhibition of glycogen synthase kinase-3 by insulin mediated by protein kinase B. *Nature,* **378,** 785-789.

66. Crowell JA, Steele VE, and Fay JR (2007) Targeting the AKT protein kinase for cancer chemoprevention. *Mol Cancer Ther,* **6,** 2139-2148.

67. Crump JG, Zhen M, Jin Y, and Bargmann CI (2001) The SAD-1 kinase regulates presynaptic vesicle clustering and axon termination. *Neuron,* **29,** 115-129.

68. Currie RA, Walker KS, Gray A, Deak M, Casamayor A, Downes CP, Cohen P, Alessi DR, and Lucocq J (1999) Role of phosphatidylinositol 3,4,5-trisphosphate in regulating the activity and localization of 3-phosphoinositide-dependent protein kinase-1. *Biochem J,* **337 (Pt 3),** 575-583.

69. D'Mello SR, Borodezt K, and Soltoff SP (1997) Insulin-like growth factor and potassium depolarization maintain neuronal survival by distinct pathways: possible involvement of PI 3-kinase in IGF-1 signaling. *J Neurosci,* **17,** 1548-1560.

70. Dalby KN, Morrice N, Caudwell FB, Avruch J, and Cohen P (1998) Identification of regulatory phosphorylation sites in mitogen-activated protein kinase (MAPK)-activated protein kinase-1a/p90rsk that are inducible by MAPK. *J Biol Chem,* **273,** 1496-1505.

71. Dan HC, Cooper MJ, Cogswell PC, Duncan JA, Ting JP, and Baldwin AS (2008) Akt-dependent regulation of NF-{kappa}B is controlled by mTOR and Raptor in association with IKK. *Genes Dev,* **22,** 1490-1500.

72. Danial NN and Korsmeyer SJ (2004) Cell death: critical control points. *Cell,* **116,** 205-219.

73. Datta SR, Dudek H, Tao X, Masters S, Fu H, Gotoh Y, and Greenberg ME (1997) Akt phosphorylation of BAD couples survival signals to the cell-intrinsic death machinery. *Cell,* **91,** 231-241.

74. Datta SR, Katsov A, Hu L, Petros A, Fesik SW, Yaffe MB, and Greenberg ME (2000) 14-3-3 proteins and survival kinases cooperate to inactivate BAD by BH3 domain phosphorylation. *Mol Cell,* **6,** 41-51.

75. Datta SR, Ranger AM, Lin MZ, Sturgill JF, Ma YC, Cowan CW, Dikkes P, Korsmeyer SJ, and Greenberg ME (2002) Survival factor-mediated BAD phosphorylation raises the mitochondrial threshold for apoptosis. *Dev Cell,* **3,** 631-643.

76. Davies AM (2003) Regulation of neuronal survival and death by extracellular signals during development. *EMBO J,* **22,** 2537-2545.

77. de Anda FC, Pollarolo G, Da Silva JS, Camoletto PG, Feiguin F, and Dotti CG (2005) Centrosome localization determines neuronal polarity. *Nature,* **436,** 704-708.

78. de la Rosa EJ and de Pablo F (2000) Cell death in early neural development: beyond the neurotrophic theory. *Trends Neurosci,* **23,** 454-458.

79. Deckwerth TL, Elliott JL, Knudson CM, Johnson EM, Jr., Snider WD, and Korsmeyer SJ (1996) BAX is required for neuronal death after trophic factor deprivation and during development. *Neuron,* **17,** 401-411.

80. Dettori R, Sonzogni S, Meyer L, Lopez-Garcia LA, Morrice NA, Zeuzem S, Engel M, Piiper A, Neimanis S, Frodin M, and Biondi RM (2009) Regulation of the interaction between protein kinase C-related protein kinase 2 (PRK2) and its upstream kinase, 3-phosphoinositide-dependent protein kinase 1 (PDK1). *J Biol Chem,* **284,** 30318-30327.

81. Dijkers PF, Medema RH, Lammers JW, Koenderman L, and Coffer PJ (2000) Expression of the pro-apoptotic Bcl-2 family member Bim is regulated by the forkhead transcription factor FKHR-L1. *Curr Biol,* **10,** 1201-1204.

82. Dotti CG, Sullivan CA, and Banker GA (1988) The establishment of polarity by hippocampal neurons in culture. *J Neurosci,* **8,** 1454-1468.

83. Drewes G, Ebneth A, Preuss U, Mandelkow EM, and Mandelkow E (1997) MARK, a novel family of protein kinases that phosphorylate microtubule-associated proteins and trigger microtubule disruption. *Cell,* **89,** 297-308.

84. Du K and Montminy M (1998) CREB is a regulatory target for the protein kinase Akt/PKB. *J Biol Chem,* **273,** 32377-32379.

85. Dudek H, Datta SR, Franke TF, Birnbaum MJ, Yao R, Cooper GM, Segal RA, Kaplan DR, and Greenberg ME (1997) Regulation of neuronal survival by the serine-threonine protein kinase Akt. *Science,* **275,** 661-665.

86. Dummler B, Tschopp O, Hynx D, Yang ZZ, Dirnhofer S, and Hemmings BA (2006) Life with a single isoform of Akt: mice lacking Akt2 and Akt3 are viable but display impaired glucose homeostasis and growth deficiencies. *Mol Cell Biol,* **26,** 8042-8051.

87. Dutil EM, Toker A, and Newton AC (1998) Regulation of conventional protein kinase C isozymes by phosphoinositide-dependent kinase 1 (PDK-1). *Curr Biol,* **8,** 1366-1375.

88. Earnshaw WC (1995) Nuclear changes in apoptosis. *Curr Opin Cell Biol,* **7,** 337-343.

89. Earnshaw WC, Martins LM, and Kaufmann SH (1999) Mammalian caspases: structure, activation, substrates, and functions during apoptosis. *Annu Rev Biochem,* **68,** 383-424.

90. Easton RM, Cho H, Roovers K, Shineman DW, Mizrahi M, Forman MS, Lee VM, Szabolcs M, De JR, Oltersdorf T, Ludwig T, Efstratiadis A, and Birnbaum MJ (2005) Role for Akt3/protein kinase Bgamma in attainment of normal brain size. *Mol Cell Biol,* **25,** 1869-1878.

91. Encinas M, Rozen EJ, Dolcet X, Jain S, Comella JX, Milbrandt J, and Johnson EM, Jr. (2008) Analysis of Ret knockin mice reveals a critical role for IKKs, but not PI 3-K, in neurotrophic factor-induced survival of sympathetic neurons. *Cell Death Differ,* **15,** 1510-1521.

92. Fayard E, Gill J, Paolino M, Hynx D, Hollander GA, and Hemmings BA (2007) Deletion of PKBalpha/Akt1 affects thymic development. *PLoS One,* **2,** e992.

93. Field SJ, Tsai FY, Kuo F, Zubiaga AM, Kaelin WG, Jr., Livingston DM, Orkin SH, and Greenberg ME (1996) E2F-1 functions in mice to promote apoptosis and suppress proliferation. *Cell,* **85,** 549-561.

94. Flynn P, Mellor H, Casamassima A, and Parker PJ (2000) Rho GTPase control of protein kinase C-related protein kinase activation by 3-phosphoinositide-dependent protein kinase. *J Biol Chem,* **275,** 11064-11070.

95. Frade JM, Rodriguez-Tebar A, and Barde YA (1996) Induction of cell death by endogenous nerve growth factor through its p75 receptor. *Nature,* **383,** 166-168.

96. Fraser MM, Zhu X, Kwon CH, Uhlmann EJ, Gutmann DH, and Baker SJ (2004) Pten loss causes hypertrophy and increased proliferation of astrocytes in vivo. *Cancer Res,* **64,** 7773-7779.

97. Friedman WJ (2000) Neurotrophins induce death of hippocampal neurons via the p75 receptor. *J Neurosci,* **20,** 6340-6346.

98. Frodin M, Jensen CJ, Merienne K, and Gammeltoft S (2000) A phosphoserine-regulated docking site in the protein kinase RSK2 that recruits and activates PDK1. *EMBO J,* **19,** 2924-2934.

99. Fujita E, Jinbo A, Matuzaki H, Konishi H, Kikkawa U, and Momoi T (1999) Akt phosphorylation site found in human caspase-9 is absent in mouse caspase-9. *Biochem Biophys Res Commun,* **264,** 550-555.

100. Gagliardini V, Fernandez PA, Lee RK, Drexler HC, Rotello RJ, Fishman MC, and Yuan J (1994) Prevention of vertebrate neuronal death by the crmA gene. *Science,* **263,** 826-828.

101. Gao T, Furnari F, and Newton AC (2005) PHLPP: a phosphatase that directly dephosphorylates Akt, promotes apoptosis, and suppresses tumor growth. *Mol Cell,* **18,** 13-24.

102. Garcia I, Martinou I, Tsujimoto Y, and Martinou JC (1992) Prevention of programmed cell death of sympathetic neurons by the bcl-2 proto-oncogene. *Science,* **258,** 302-304.

103. Garcia-Martinez JM and Alessi DR (2008) mTOR complex 2 (mTORC2) controls hydrophobic motif phosphorylation and activation of serum- and glucocorticoid-induced protein kinase 1 (SGK1). *Biochem J,* **416,** 375-385.

104. Garofalo RS, Orena SJ, Rafidi K, Torchia AJ, Stock JL, Hildebrandt AL, Coskran T, Black SC, Brees DJ, Wicks JR, McNeish JD, and Coleman KG (2003) Severe diabetes, age-dependent loss of adipose tissue, and mild growth deficiency in mice lacking Akt2/PKB beta. *J Clin Invest,* **112,** 197-208.

105. Gartner A, Huang X, and Hall A (2006) Neuronal polarity is regulated by glycogen synthase kinase-3 (GSK-3beta) independently of Akt/PKB serine phosphorylation. *J Cell Sci,* **119,** 3927-3934.

106. Gonzalez E and McGraw TE (2009) The Akt kinases: isoform specificity in metabolism and cancer. *Cell Cycle,* **8,** 2502-2508.

107. Gonzalez-Garcia M, Garcia I, Ding L, O'Shea S, Boise LH, Thompson CB, and Nunez G (1995) bcl-x is expressed in embryonic and postnatal neural tissues and functions to prevent neuronal cell death. *Proc Natl Acad Sci U S A,* **92,** 4304-4308.

108. Gundersen HJ and Jensen EB (1987) The efficiency of systematic sampling in stereology and its prediction. *J Microsc,* **147,** 229-263.

109. Hara K, Maruki Y, Long X, Yoshino K, Oshiro N, Hidayat S, Tokunaga C, Avruch J, and Yonezawa K (2002) Raptor, a binding partner of target of rapamycin (TOR), mediates TOR action. *Cell,* **110,** 177-189.

110. Hara K, Yonezawa K, Kozlowski MT, Sugimoto T, Andrabi K, Weng QP, Kasuga M, Nishimoto I, and Avruch J (1997) Regulation of eIF-4E BP1 phosphorylation by mTOR. *J Biol Chem,* **272,** 26457-26463.

111. Harada T, Morooka T, Ogawa S, and Nishida E (2001) ERK induces p35, a neuron-specific activator of Cdk5, through induction of Egr1. *Nat Cell Biol,* **3,** 453-459.

112. Hashimoto N, Kido Y, Uchida T, Asahara S, Shigeyama Y, Matsuda T, Takeda A, Tsuchihashi D, Nishizawa A, Ogawa W, Fujimoto Y, Okamura H, Arden KC, Herrera PL, Noda T, and Kasuga M (2006) Ablation of PDK1 in pancreatic beta cells induces diabetes as a result of loss of beta cell mass. *Nat Genet,* **38,** 589-593.

113. He C and Klionsky DJ (2009) Regulation mechanisms and signaling pathways of autophagy. *Annu Rev Genet,* **43,** 67-93.

114. Henle SJ, Wang G, Liang E, Wu M, Poo MM, and Henley JR (2011) Asymmetric PI(3,4,5)P3 and Akt signaling mediates chemotaxis of axonal growth cones. *J Neurosci,* **31,** 7016-7027.

115. Hetman M, Cavanaugh JE, Kimelman D, and Xia Z (2000) Role of glycogen synthase kinase-3beta in neuronal apoptosis induced by trophic withdrawal. *J Neurosci,* **20,** 2567-2574.

116. Hinton HJ, Alessi DR, and Cantrell DA (2004) The serine kinase phosphoinositide-dependent kinase 1 (PDK1) regulates T cell development. *Nat Immunol,* **5,** 539-545.

117. Hirotani M, Zhang Y, Fujita N, Naito M, and Tsuruo T (1999) NH2-terminal BH4 domain of Bcl-2 is functional for heterodimerization with Bax and inhibition of apoptosis. *J Biol Chem,* **274,** 20415-20420.

118. Holgado-Madruga M, Moscatello DK, Emlet DR, Dieterich R, and Wong AJ (1997) Grb2-associated binder-1 mediates phosphatidylinositol 3-kinase activation and the promotion of cell survival by nerve growth factor. *Proc Natl Acad Sci U S A,* **94,** 12419-12424.

119. Holz MK, Ballif BA, Gygi SP, and Blenis J (2005) mTOR and S6K1 mediate assembly of the translation preinitiation complex through dynamic protein interchange and ordered phosphorylation events. *Cell,* **123,** 569-580.

120. Hongisto V, Smeds N, Brecht S, Herdegen T, Courtney MJ, and Coffey ET (2003) Lithium blocks the c-Jun stress response and protects neurons via its action on glycogen synthase kinase 3. *Mol Cell Biol,* **23,** 6027-6036.

121. Hsu SY, Kaipia A, McGee E, Lomeli M, and Hsueh AJ (1997) Bok is a pro-apoptotic Bcl-2 protein with restricted expression in reproductive tissues and heterodimerizes with selective anti-apoptotic Bcl-2 family members. *Proc Natl Acad Sci U S A,* **94,** 12401-12406.

122. Huang EJ and Reichardt LF (2003) Trk receptors: roles in neuronal signal transduction. *Annu Rev Biochem,* **72,** 609-642.

123. Huang HM, Huang CJ, and Yen JJ (2000) Mcl-1 is a common target of stem cell factor and interleukin-5 for apoptosis prevention activity via MEK/MAPK and PI-3K/Akt pathways. *Blood,* **96,** 1764-1771.

124. Hur EM and Zhou FQ (2010) GSK3 signalling in neural development. *Nat Rev Neurosci,* **11,** 539-551.

125. Ibrado AM, Liu L, and Bhalla K (1997) Bcl-xL overexpression inhibits progression of molecular events leading to paclitaxel-induced apoptosis of human acute myeloid leukemia HL-60 cells. *Cancer Res,* **57,** 1109-1115.

126. Ikenoue T, Inoki K, Yang Q, Zhou X, and Guan KL (2008) Essential function of TORC2 in PKC and Akt turn motif phosphorylation, maturation and signalling. *EMBO J,* **27,** 1919-1931.

127. Inoki K, Li Y, Zhu T, Wu J, and Guan KL (2002) TSC2 is phosphorylated and inhibited by Akt and suppresses mTOR signalling. *Nat Cell Biol,* **4,** 648-657.

128. Jensen CJ, Buch MB, Krag TO, Hemmings BA, Gammeltoft S, and Frodin M (1999) 90-kDa ribosomal S6 kinase is phosphorylated and activated by 3-phosphoinositide-dependent protein kinase-1. *J Biol Chem,* **274,** 27168-27176.

129. Jiang H, Guo W, Liang X, and Rao Y (2005) Both the establishment and the maintenance of neuronal polarity require active mechanisms: critical roles of GSK-3beta and its upstream regulators. *Cell,* **120,** 123-135.

130. Jones KT, Greer ER, Pearce D, and Ashrafi K (2009) Rictor/TORC2 regulates Caenorhabditis elegans fat storage, body size, and development through sgk-1. *PLoS Biol,* **7,** e60.

131. Jones PF, Jakubowicz T, and Hemmings BA (1991) Molecular cloning of a second form of rac protein kinase. *Cell Regul,* **2,** 1001-1009.

132. Kalaydjieva L, Gresham D, Gooding R, Heather L, Baas F, de JR, Blechschmidt K, Angelicheva D, Chandler D, Worsley P, Rosenthal A, King RH, and Thomas PK

(2000) N-myc downstream-regulated gene 1 is mutated in hereditary motor and sensory neuropathy-Lom. *Am J Hum Genet,* **67,** 47-58.

133. Kaplan DR and Miller FD (2000) Neurotrophin signal transduction in the nervous system. *Curr Opin Neurobiol,* **10,** 381-391.

134. Kempf M, Clement A, Faissner A, Lee G, and Brandt R (1996) Tau binds to the distal axon early in development of polarity in a microtubule- and microfilament-dependent manner. *J Neurosci,* **16,** 5583-5592.

135. Kerr JF, Wyllie AH, and Currie AR (1972) Apoptosis: a basic biological phenomenon with wide-ranging implications in tissue kinetics. *Br J Cancer,* **26,** 239-257.

136. Kharebava G, Makonchuk D, Kalita KB, Zheng JJ, and Hetman M (2008) Requirement of 3-phosphoinositide-dependent protein kinase-1 for BDNF-mediated neuronal survival. *J Neurosci,* **28,** 11409-11420.

137. Kiefer MC, Brauer MJ, Powers VC, Wu JJ, Umansky SR, Tomei LD, and Barr PJ (1995) Modulation of apoptosis by the widely distributed Bcl-2 homologue Bak. *Nature,* **374,** 736-739.

138. Kim DH, Sarbassov DD, Ali SM, King JE, Latek RR, Erdjument-Bromage H, Tempst P, and Sabatini DM (2002) mTOR interacts with raptor to form a nutrient-sensitive complex that signals to the cell growth machinery. *Cell,* **110,** 163-175.

139. Kim J, Kundu M, Viollet B, and Guan KL (2011) AMPK and mTOR regulate autophagy through direct phosphorylation of Ulk1. *Nat Cell Biol,* **13,** 132-141.

140. Kim JS, Lilley BN, Zhang C, Shokat KM, Sanes JR, and Zhen M (2008) A chemical-genetic strategy reveals distinct temporal requirements for SAD-1 kinase in neuronal polarization and synapse formation. *Neural Dev,* **3,** 23.

141. Kishi M, Pan YA, Crump JG, and Sanes JR (2005) Mammalian SAD kinases are required for neuronal polarization. *Science,* **307,** 929-932.

142. Kobayashi T and Cohen P (1999) Activation of serum- and glucocorticoid-regulated protein kinase by agonists that activate phosphatidylinositide 3-kinase is mediated by 3-phosphoinositide-dependent protein kinase-1 (PDK1) and PDK2. *Biochem J,* **339 (Pt 2),** 319-328.

143. Kobayashi T, Deak M, Morrice N, and Cohen P (1999) Characterization of the structure and regulation of two novel isoforms of serum- and glucocorticoid-induced protein kinase. *Biochem J,* **344 Pt 1,** 189-197.

144. Komander D, Fairservice A, Deak M, Kular GS, Prescott AR, Peter DC, Safrany ST, Alessi DR, and Van Aalten DM (2004) Structural insights into the regulation of PDK1 by phosphoinositides and inositol phosphates. *EMBO J,* **23,** 3918-3928.

145. Kozma SC, Ferrari S, and Thomas G (1989) Unmasking a growth factor/oncogene-activated S6 phosphorylation cascade. *Cell Signal,* **1,** 219-225.

146. Kuida K, Haydar TF, Kuan CY, Gu Y, Taya C, Karasuyama H, Su MS, Rakic P, and Flavell RA (1998) Reduced apoptosis and cytochrome c-mediated caspase activation in mice lacking caspase 9. *Cell,* **94,** 325-337.

147. Kuida K, Zheng TS, Na S, Kuan C, Yang D, Karasuyama H, Rakic P, and Flavell RA (1996) Decreased apoptosis in the brain and premature lethality in CPP32-deficient mice. *Nature,* **384,** 368-372.

148. Kwiatkowski DJ and Manning BD (2005) Tuberous sclerosis: a GAP at the crossroads of multiple signaling pathways. *Hum Mol Genet,* **14 Spec No. 2,** R251-R258.

149. Laplante M and Sabatini DM (2012) mTOR signaling in growth control and disease. *Cell,* **149,** 274-293.

150. Lawlor MA, Mora A, Ashby PR, Williams MR, Murray-Tait V, Malone L, Prescott AR, Lucocq JM, and Alessi DR (2002) Essential role of PDK1 in regulating cell size and development in mice. *EMBO J,* **21,** 3728-3738.

151. Le Good JA, Ziegler WH, Parekh DB, Alessi DR, Cohen P, and Parker PJ (1998) Protein kinase C isotypes controlled by phosphoinositide 3-kinase through the protein kinase PDK1. *Science,* **281,** 2042-2045.

152. Lee R, Kermani P, Teng KK, and Hempstead BL (2001) Regulation of cell survival by secreted proneurotrophins. *Science,* **294,** 1945-1948.

153. Lee-Fruman KK, Kuo CJ, Lippincott J, Terada N, and Blenis J (1999) Characterization of S6K2, a novel kinase homologous to S6K1. *Oncogene,* **18,** 5108-5114.

154. Leenders F, Mopert K, Schmiedeknecht A, Santel A, Czauderna F, Aleku M, Penschuck S, Dames S, Sternberger M, Rohl T, Wellmann A, Arnold W, Giese K, Kaufmann J, and Klippel A (2004) PKN3 is required for malignant prostate cell growth downstream of activated PI 3-kinase. *EMBO J,* **23,** 3303-3313.

155. Leonard JR, D'Sa C, Cahn BR, Korsmeyer SJ, and Roth KA (2001) Bid regulation of neuronal apoptosis. *Brain Res Dev Brain Res,* **128,** 187-190.

156. Levi-Montalcini R (1983) The nerve growth factor-target cells interaction: a model system for the study of directed axonal growth and regeneration. *Birth Defects Orig Artic Ser,* **19,** 3-22.

157. Levi-Montalcini R (1987) The nerve growth factor 35 years later. *Science,* **237,** 1154-1162.

158. Li Z, Theus MH, and Wei L (2006) Role of ERK 1/2 signaling in neuronal differentiation of cultured embryonic stem cells. *Dev Growth Differ,* **48,** 513-523.

159. Limon JJ and Fruman DA (2012) Akt and mTOR in B Cell Activation and Differentiation. *Front Immunol,* **3,** 228.

160. Lindsten T, Ross AJ, King A, Zong WX, Rathmell JC, Shiels HA, Ulrich E, Waymire KG, Mahar P, Frauwirth K, Chen Y, Wei M, Eng VM, Adelman DM, Simon MC, Ma

A, Golden JA, Evan G, Korsmeyer SJ, MacGregor GR, and Thompson CB (2000) The combined functions of proapoptotic Bcl-2 family members bak and bax are essential for normal development of multiple tissues. *Mol Cell,* **6,** 1389-1399.

161. Linseman DA, Butts BD, Precht TA, Phelps RA, Le SS, Laessig TA, Bouchard RJ, Florez-McClure ML, and Heidenreich KA (2004) Glycogen synthase kinase-3beta phosphorylates Bax and promotes its mitochondrial localization during neuronal apoptosis. *J Neurosci,* **24,** 9993-10002.

162. Liu H, Perlman H, Pagliari LJ, and Pope RM (2001) Constitutively activated Akt-1 is vital for the survival of human monocyte-differentiated macrophages. Role of Mcl-1, independent of nuclear factor (NF)-kappaB, Bad, or caspase activation. *J Exp Med,* **194,** 113-126.

163. Lizcano JM, Goransson O, Toth R, Deak M, Morrice NA, Boudeau J, Hawley SA, Udd L, Makela TP, Hardie DG, and Alessi DR (2004) LKB1 is a master kinase that activates 13 kinases of the AMPK subfamily, including MARK/PAR-1. *EMBO J,* **23,** 833-843.

164. Logie L, Ruiz-Alcaraz AJ, Keane M, Woods YL, Bain J, Marquez R, Alessi DR, and Sutherland C (2007) Characterization of a protein kinase B inhibitor in vitro and in insulin-treated liver cells. *Diabetes,* **56,** 2218-2227.

165. Lopez-Pajares V, Kim MM, and Yuan ZM (2008) Phosphorylation of MDMX mediated by Akt leads to stabilization and induces 14-3-3 binding. *J Biol Chem,* **283,** 13707-13713.

166. Luo X, Budihardjo I, Zou H, Slaughter C, and Wang X (1998) Bid, a Bcl2 interacting protein, mediates cytochrome c release from mitochondria in response to activation of cell surface death receptors. *Cell,* **94,** 481-490.

167. Manning BD and Cantley LC (2007) AKT/PKB signaling: navigating downstream. *Cell,* **129,** 1261-1274.

168. Manning BD, Tee AR, Logsdon MN, Blenis J, and Cantley LC (2002a) Identification of the tuberous sclerosis complex-2 tumor suppressor gene product tuberin as a target of the phosphoinositide 3-kinase/akt pathway. *Mol Cell,* **10,** 151-162.

169. Manning G, Whyte DB, Martinez R, Hunter T, and Sudarsanam S (2002b) The protein kinase complement of the human genome. *Science,* **298,** 1912-1934.

170. Marino S, Krimpenfort P, Leung C, van der Korput HA, Trapman J, Camenisch I, Berns A, and Brandner S (2002) PTEN is essential for cell migration but not for fate determination and tumourigenesis in the cerebellum. *Development,* **129,** 3513-3522.

171. Martin DP, Schmidt RE, DiStefano PS, Lowry OH, Carter JG, and Johnson EM, Jr. (1988) Inhibitors of protein synthesis and RNA synthesis prevent neuronal death caused by nerve growth factor deprivation. *J Cell Biol,* **106,** 829-844.

172. Martinou JC, Dubois-Dauphin M, Staple JK, Rodriguez I, Frankowski H, Missotten M, Albertini P, Talabot D, Catsicas S, Pietra C, et al. (1994) Overexpression of BCL-2

in transgenic mice protects neurons from naturally occurring cell death and experimental ischemia. *Neuron,* **13,** 1017-1030.

173. Matsuda N, Lu H, Fukata Y, Noritake J, Gao H, Mukherjee S, Nemoto T, Fukata M, and Poo MM (2009) Differential activity-dependent secretion of brain-derived neurotrophic factor from axon and dendrite. *J Neurosci,* **29,** 14185-14198.

174. Mattson MP (2006) Neuronal life-and-death signaling, apoptosis, and neurodegenerative disorders. *Antioxid Redox Signal,* **8,** 1997-2006.

175. Maurer U, Charvet C, Wagman AS, Dejardin E, and Green DR (2006) Glycogen synthase kinase-3 regulates mitochondrial outer membrane permeabilization and apoptosis by destabilization of MCL-1. *Mol Cell,* **21,** 749-760.

176. Mayo LD and Donner DB (2001) A phosphatidylinositol 3-kinase/Akt pathway promotes translocation of Mdm2 from the cytoplasm to the nucleus. *Proc Natl Acad Sci U S A,* **98,** 11598-11603.

177. McManus EJ, Collins BJ, Ashby PR, Prescott AR, Murray-Tait V, Armit LJ, Arthur JS, and Alessi DR (2004) The in vivo role of PtdIns(3,4,5)P3 binding to PDK1 PH domain defined by knockin mutation. *EMBO J,* **23,** 2071-2082.

178. Menager C, Arimura N, Fukata Y, and Kaibuchi K (2004) PIP3 is involved in neuronal polarization and axon formation. *J Neurochem,* **89,** 109-118.

179. Michaelidis TM, Sendtner M, Cooper JD, Airaksinen MS, Holtmann B, Meyer M, and Thoenen H (1996) Inactivation of bcl-2 results in progressive degeneration of motoneurons, sympathetic and sensory neurons during early postnatal development. *Neuron,* **17,** 75-89.

180. Miguel-Aliaga I and Thor S (2009) Programmed cell death in the nervous system--a programmed cell fate? *Curr Opin Neurobiol,* **19,** 127-133.

181. Milburn CC, Deak M, Kelly SM, Price NC, Alessi DR, and Van Aalten DM (2003) Binding of phosphatidylinositol 3,4,5-trisphosphate to the pleckstrin homology domain of protein kinase B induces a conformational change. *Biochem J,* **375,** 531-538.

182. Momand J, Zambetti GP, Olson DC, George D, and Levine AJ (1992) The mdm-2 oncogene product forms a complex with the p53 protein and inhibits p53-mediated transactivation. *Cell,* **69,** 1237-1245.

183. Mora A, Davies AM, Bertrand L, Sharif I, Budas GR, Jovanovic S, Mouton V, Kahn CR, Lucocq JM, Gray GA, Jovanovic A, and Alessi DR (2003) Deficiency of PDK1 in cardiac muscle results in heart failure and increased sensitivity to hypoxia. *EMBO J,* **22,** 4666-4676.

184. Mora A, Lipina C, Tronche F, Sutherland C, and Alessi DR (2005) Deficiency of PDK1 in liver results in glucose intolerance, impairment of insulin-regulated gene expression and liver failure. *Biochem J,* **385,** 639-648.

185. Morgan JL, Dhingra A, Vardi N, and Wong RO (2006) Axons and dendrites originate from neuroepithelial-like processes of retinal bipolar cells. *Nat Neurosci,* **9,** 85-92.

186. Movassagh M and Foo RS (2008) Simplified apoptotic cascades. *Heart Fail Rev,* **13,** 111-119.

187. Muchmore SW, Sattler M, Liang H, Meadows RP, Harlan JE, Yoon HS, Nettesheim D, Chang BS, Thompson CB, Wong SL, Ng SL, and Fesik SW (1996) X-ray and NMR structure of human Bcl-xL, an inhibitor of programmed cell death. *Nature,* **381,** 335-341.

188. Murray JT, Campbell DG, Morrice N, Auld GC, Shpiro N, Marquez R, Peggie M, Bain J, Bloomberg GB, Grahammer F, Lang F, Wulff P, Kuhl D, and Cohen P (2004a) Exploitation of KESTREL to identify NDRG family members as physiological substrates for SGK1 and GSK3. *Biochem J,* **384,** 477-488.

189. Murray JT, Cummings LA, Bloomberg GB, and Cohen P (2005) Identification of different specificity requirements between SGK1 and PKBalpha. *FEBS Lett,* **579,** 991-994.

190. Murray SS, Perez P, Lee R, Hempstead BL, and Chao MV (2004b) A novel p75 neurotrophin receptor-related protein, NRH2, regulates nerve growth factor binding to the TrkA receptor. *J Neurosci,* **24,** 2742-2749.

191. Najafov A, Shpiro N, and Alessi DR (2012) Akt is efficiently activated by PIF-pocket- and PtdIns(3,4,5)P3-dependent mechanisms leading to resistance to PDK1 inhibitors. *Biochem J,* **448,** 285-295.

192. Nakagawa T, Zhu H, Morishima N, Li E, Xu J, Yankner BA, and Yuan J (2000) Caspase-12 mediates endoplasmic-reticulum-specific apoptosis and cytotoxicity by amyloid-beta. *Nature,* **403,** 98-103.

193. Nicklin P, Bergman P, Zhang B, Triantafellow E, Wang H, Nyfeler B, Yang H, Hild M, Kung C, Wilson C, Myer VE, MacKeigan JP, Porter JA, Wang YK, Cantley LC, Finan PM, and Murphy LO (2009) Bidirectional transport of amino acids regulates mTOR and autophagy. *Cell,* **136,** 521-534.

194. Nijhawan D, Fang M, Traer E, Zhong Q, Gao W, Du F, and Wang X (2003) Elimination of Mcl-1 is required for the initiation of apoptosis following ultraviolet irradiation. *Genes Dev,* **17,** 1475-1486.

195. O'Connor L, Strasser A, O'Reilly LA, Hausmann G, Adams JM, Cory S, and Huang DC (1998) Bim: a novel member of the Bcl-2 family that promotes apoptosis. *EMBO J,* **17,** 384-395.

196. Okuda T, Higashi Y, Kokame K, Tanaka C, Kondoh H, and Miyata T (2004) Ndrg1-deficient mice exhibit a progressive demyelinating disorder of peripheral nerves. *Mol Cell Biol,* **24,** 3949-3956.

197. Oltvai ZN, Milliman CL, and Korsmeyer SJ (1993) Bcl-2 heterodimerizes in vivo with a conserved homolog, Bax, that accelerates programmed cell death. *Cell,* **74,** 609-619.

198. Oppenheim RW (1989) The neurotrophic theory and naturally occurring motoneuron death. *Trends Neurosci,* **12,** 252-255.

199. Oppenheim RW (1991) Cell death during development of the nervous system. *Annu Rev Neurosci,* **14,** 453-501.

200. Pap M and Cooper GM (2002) Role of translation initiation factor 2B in control of cell survival by the phosphatidylinositol 3-kinase/Akt/glycogen synthase kinase 3beta signaling pathway. *Mol Cell Biol,* **22,** 578-586.

201. Paradis S, Ailion M, Toker A, Thomas JH, and Ruvkun G (1999) A PDK1 homolog is necessary and sufficient to transduce AGE-1 PI3 kinase signals that regulate diapause in Caenorhabditis elegans. *Genes Dev,* **13,** 1438-1452.

202. Park J, Leong ML, Buse P, Maiyar AC, Firestone GL, and Hemmings BA (1999) Serum and glucocorticoid-inducible kinase (SGK) is a target of the PI 3-kinase-stimulated signaling pathway. *EMBO J,* **18,** 3024-3033.

203. Pazyra-Murphy MF, Hans A, Courchesne SL, Karch C, Cosker KE, Heerssen HM, Watson FL, Kim T, Greenberg ME, and Segal RA (2009) A retrograde neuronal survival response: target-derived neurotrophins regulate MEF2D and bcl-w. *J Neurosci,* **29,** 6700-6709.

204. Pearce LR, Huang X, Boudeau J, Pawlowski R, Wullschleger S, Deak M, Ibrahim AF, Gourlay R, Magnuson MA, and Alessi DR (2007) Identification of Protor as a novel Rictor-binding component of mTOR complex-2. *Biochem J,* **405,** 513-522.

205. Pearce LR, Komander D, and Alessi DR (2010) The nuts and bolts of AGC protein kinases. *Nat Rev Mol Cell Biol,* **11,** 9-22.

206. Peng XD, Xu PZ, Chen ML, Hahn-Windgassen A, Skeen J, Jacobs J, Sundararajan D, Chen WS, Crawford SE, Coleman KG, and Hay N (2003) Dwarfism, impaired skin development, skeletal muscle atrophy, delayed bone development, and impeded adipogenesis in mice lacking Akt1 and Akt2. *Genes Dev,* **17,** 1352-1365.

207. Petros AM, Medek A, Nettesheim DG, Kim DH, Yoon HS, Swift K, Matayoshi ED, Oltersdorf T, and Fesik SW (2001) Solution structure of the antiapoptotic protein bcl-2. *Proc Natl Acad Sci U S A,* **98,** 3012-3017.

208. Pettmann B and Henderson CE (1998) Neuronal cell death. *Neuron,* **20,** 633-647.

209. Pullen N, Dennis PB, Andjelkovic M, Dufner A, Kozma SC, Hemmings BA, and Thomas G (1998) Phosphorylation and activation of p70s6k by PDK1. *Science,* **279,** 707-710.

210. Ranger AM, Zha J, Harada H, Datta SR, Danial NN, Gilmore AP, Kutok JL, Le Beau MM, Greenberg ME, and Korsmeyer SJ (2003) Bad-deficient mice develop diffuse large B cell lymphoma. *Proc Natl Acad Sci U S A,* **100,** 9324-9329.

211. Ray R, Chen G, Vande VC, Cizeau J, Park JH, Reed JC, Gietz RD, and Greenberg AH (2000) BNIP3 heterodimerizes with Bcl-2/Bcl-X(L) and induces cell death

independent of a Bcl-2 homology 3 (BH3) domain at both mitochondrial and nonmitochondrial sites. *J Biol Chem,* **275,** 1439-1448.

212. Reichardt LF (2006) Neurotrophin-regulated signalling pathways. *Philos Trans R Soc Lond B Biol Sci,* **361,** 1545-1564.

213. Richards SA, Fu J, Romanelli A, Shimamura A, and Blenis J (1999) Ribosomal S6 kinase 1 (RSK1) activation requires signals dependent on and independent of the MAP kinase ERK. *Curr Biol,* **9,** 810-820.

214. Rinkenberger JL, Horning S, Klocke B, Roth K, and Korsmeyer SJ (2000) Mcl-1 deficiency results in peri-implantation embryonic lethality. *Genes Dev,* **14,** 23-27.

215. Rintelen F, Stocker H, Thomas G, and Hafen E (2001) PDK1 regulates growth through Akt and S6K in Drosophila. *Proc Natl Acad Sci U S A,* **98,** 15020-15025.

216. Robinson MJ and Cobb MH (1997) Mitogen-activated protein kinase pathways. *Curr Opin Cell Biol,* **9,** 180-186.

217. Rodriguez-Asiain A, Ruiz-Babot G, Romero W, Cubi R, Erazo T, Biondi RM, Bayascas JR, Aguilera J, Gomez N, Gil C, Claro E, and Lizcano JM (2011) Brain specific kinase-1 BRSK1/SAD-B associates with lipid rafts: modulation of kinase activity by lipid environment. *Biochim Biophys Acta,* **1811,** 1124-1135.

218. Roth KA, Kuan C, Haydar TF, D'Sa-Eipper C, Shindler KS, Zheng TS, Kuida K, Flavell RA, and Rakic P (2000) Epistatic and independent functions of caspase-3 and Bcl-X(L) in developmental programmed cell death. *Proc Natl Acad Sci U S A,* **97,** 466-471.

219. Roth KA, Motoyama N, and Loh DY (1996) Apoptosis of bcl-x-deficient telencephalic cells in vitro. *J Neurosci,* **16,** 1753-1758.

220. Sancak Y, Bar-Peled L, Zoncu R, Markhard AL, Nada S, and Sabatini DM (2010) Ragulator-Rag complex targets mTORC1 to the lysosomal surface and is necessary for its activation by amino acids. *Cell,* **141,** 290-303.

221. Sancak Y, Peterson TR, Shaul YD, Lindquist RA, Thoreen CC, Bar-Peled L, and Sabatini DM (2008) The Rag GTPases bind raptor and mediate amino acid signaling to mTORC1. *Science,* **320,** 1496-1501.

222. Sancak Y, Thoreen CC, Peterson TR, Lindquist RA, Kang SA, Spooner E, Carr SA, and Sabatini DM (2007) PRAS40 is an insulin-regulated inhibitor of the mTORC1 protein kinase. *Mol Cell,* **25,** 903-915.

223. Sarbassov DD, Ali SM, and Sabatini DM (2005a) Growing roles for the mTOR pathway. *Curr Opin Cell Biol,* **17,** 596-603.

224. Sarbassov DD, Guertin DA, Ali SM, and Sabatini DM (2005b) Phosphorylation and regulation of Akt/PKB by the rictor-mTOR complex. *Science,* **307,** 1098-1101.

225. Sattler M, Liang H, Nettesheim D, Meadows RP, Harlan JE, Eberstadt M, Yoon HS, Shuker SB, Chang BS, Minn AJ, Thompson CB, and Fesik SW (1997) Structure of Bcl-xL-Bak peptide complex: recognition between regulators of apoptosis. *Science,* **275,** 983-986.

226. Saunders JW, Jr. (1966) Death in embryonic systems. *Science,* **154,** 604-612.

227. Savill J and Fadok V (2000) Corpse clearance defines the meaning of cell death. *Nature,* **407,** 784-788.

228. Sedlak TW, Oltvai ZN, Yang E, Wang K, Boise LH, Thompson CB, and Korsmeyer SJ (1995) Multiple Bcl-2 family members demonstrate selective dimerizations with Bax. *Proc Natl Acad Sci U S A,* **92,** 7834-7838.

229. Segal RA (2003) Selectivity in neurotrophin signaling: theme and variations. *Annu Rev Neurosci,* **26,** 299-330.

230. Seilicovich A (2010) Cell life and death in the anterior pituitary gland: role of oestrogens. *J Neuroendocrinol,* **22,** 758-764.

231. Shelly M, Cancedda L, Heilshorn S, Sumbre G, and Poo MM (2007) LKB1/STRAD promotes axon initiation during neuronal polarization. *Cell,* **129,** 565-577.

232. Shi SH, Jan LY, and Jan YN (2003) Hippocampal neuronal polarity specified by spatially localized mPar3/mPar6 and PI 3-kinase activity. *Cell,* **112,** 63-75.

233. Shimizu S, Eguchi Y, Kosaka H, Kamiike W, Matsuda H, and Tsujimoto Y (1995) Prevention of hypoxia-induced cell death by Bcl-2 and Bcl-xL. *Nature,* **374,** 811-813.

234. Shimoke K, Kubo T, Numakawa T, Abiru Y, Enokido Y, Takei N, Ikeuchi T, and Hatanaka H (1997) Involvement of phosphatidylinositol-3 kinase in prevention of low K(+)-induced apoptosis of cerebellar granule neurons. *Brain Res Dev Brain Res,* **101,** 197-206.

235. Shindler KS, Latham CB, and Roth KA (1997) Bax deficiency prevents the increased cell death of immature neurons in bcl-x-deficient mice. *J Neurosci,* **17,** 3112-3119.

236. Shitamukai A and Matsuzaki F (2012) Control of asymmetric cell division of mammalian neural progenitors. *Dev Growth Differ,* **54,** 277-286.

237. Snider WD (1994) Functions of the neurotrophins during nervous system development: what the knockouts are teaching us. *Cell,* **77,** 627-638.

238. Staal SP (1987) Molecular cloning of the akt oncogene and its human homologues AKT1 and AKT2: amplification of AKT1 in a primary human gastric adenocarcinoma. *Proc Natl Acad Sci U S A,* **84,** 5034-5037.

239. Stokoe D, Stephens LR, Copeland T, Gaffney PR, Reese CB, Painter GF, Holmes AB, McCormick F, and Hawkins PT (1997) Dual role of phosphatidylinositol-3,4,5-trisphosphate in the activation of protein kinase B. *Science,* **277,** 567-570.

240. Sutherland C, Leighton IA, and Cohen P (1993) Inactivation of glycogen synthase kinase-3 beta by phosphorylation: new kinase connections in insulin and growth-factor signalling. *Biochem J,* **296 (Pt 1),** 15-19.

241. Swiech L, Perycz M, Malik A, and Jaworski J (2008) Role of mTOR in physiology and pathology of the nervous system. *Biochim Biophys Acta,* **1784,** 116-132.

242. Tang ED, Nunez G, Barr FG, and Guan KL (1999) Negative regulation of the forkhead transcription factor FKHR by Akt. *J Biol Chem,* **274,** 16741-16746.

243. Tavazoie SF, Alvarez VA, Ridenour DA, Kwiatkowski DJ, and Sabatini BL (2005) Regulation of neuronal morphology and function by the tumor suppressors Tsc1 and Tsc2. *Nat Neurosci,* **8,** 1727-1734.

244. Thomas CC, Deak M, Alessi DR, and Van Aalten DM (2002) High-resolution structure of the pleckstrin homology domain of protein kinase b/akt bound to phosphatidylinositol (3,4,5)-trisphosphate. *Curr Biol,* **12,** 1256-1262.

245. Tompa P and Friedrich P (1998) Synaptic metaplasticity and the local charge effect in postsynaptic densities. *Trends Neurosci,* **21,** 97-102.

246. Tran H, Brunet A, Griffith EC, and Greenberg ME (2003) The many forks in FOXO's road. *Sci STKE,* **2003,** RE5.

247. Tschopp O, Yang ZZ, Brodbeck D, Dummler BA, Hemmings-Mieszczak M, Watanabe T, Michaelis T, Frahm J, and Hemmings BA (2005) Essential role of protein kinase B gamma (PKB gamma/Akt3) in postnatal brain development but not in glucose homeostasis. *Development,* **132,** 2943-2954.

248. Tsujimoto Y, Yunis J, Onorato-Showe L, Erikson J, Nowell PC, and Croce CM (1984) Molecular cloning of the chromosomal breakpoint of B-cell lymphomas and leukemias with the t(11;14) chromosome translocation. *Science,* **224,** 1403-1406.

249. Tuttle RL, Gill NS, Pugh W, Lee JP, Koeberlein B, Furth EE, Polonsky KS, Naji A, and Birnbaum MJ (2001) Regulation of pancreatic beta-cell growth and survival by the serine/threonine protein kinase Akt1/PKBalpha. *Nat Med,* **7,** 1133-1137.

250. Vander HE, Lee SI, Bandhakavi S, Griffin TJ, and Kim DH (2007) Insulin signalling to mTOR mediated by the Akt/PKB substrate PRAS40. *Nat Cell Biol,* **9,** 316-323.

251. Vanhaesebroeck B and Alessi DR (2000) The PI3K-PDK1 connection: more than just a road to PKB. *Biochem J,* **346 Pt 3,** 561-576.

252. Vanhaesebroeck B, Leevers SJ, Ahmadi K, Timms J, Katso R, Driscoll PC, Woscholski R, Parker PJ, and Waterfield MD (2001) Synthesis and function of 3-phosphorylated inositol lipids. *Annu Rev Biochem,* **70,** 535-602.

253. Vanhaesebroeck B, Leevers SJ, Panayotou G, and Waterfield MD (1997) Phosphoinositide 3-kinases: a conserved family of signal transducers. *Trends Biochem Sci,* **22,** 267-272.

254. Veis DJ, Sorenson CM, Shutter JR, and Korsmeyer SJ (1993) Bcl-2-deficient mice demonstrate fulminant lymphoid apoptosis, polycystic kidneys, and hypopigmented hair. *Cell,* **75,** 229-240.

255. Walker KS, Deak M, Paterson A, Hudson K, Cohen P, and Alessi DR (1998) Activation of protein kinase B beta and gamma isoforms by insulin in vivo and by 3-phosphoinositide-dependent protein kinase-1 in vitro: comparison with protein kinase B alpha. *Biochem J,* **331 (Pt 1),** 299-308.

256. Wang K, Yin XM, Chao DT, Milliman CL, and Korsmeyer SJ (1996) BID: a novel BH3 domain-only death agonist. *Genes Dev,* **10,** 2859-2869.

257. Wang X (2001) The expanding role of mitochondria in apoptosis. *Genes Dev,* **15,** 2922-2933.

258. Wang X, Li W, Williams M, Terada N, Alessi DR, and Proud CG (2001) Regulation of elongation factor 2 kinase by p90(RSK1) and p70 S6 kinase. *EMBO J,* **20,** 4370-4379.

259. Watcharasit P, Bijur GN, Song L, Zhu J, Chen X, and Jope RS (2003) Glycogen synthase kinase-3beta (GSK3beta) binds to and promotes the actions of p53. *J Biol Chem,* **278,** 48872-48879.

260. Watson FL, Heerssen HM, Bhattacharyya A, Klesse L, Lin MZ, and Segal RA (2001) Neurotrophins use the Erk5 pathway to mediate a retrograde survival response. *Nat Neurosci,* **4,** 981-988.

261. Waugh C, Sinclair L, Finlay D, Bayascas JR, and Cantrell D (2009) Phosphoinositide (3,4,5)-triphosphate binding to phosphoinositide-dependent kinase 1 regulates a protein kinase B/Akt signaling threshold that dictates T-cell migration, not proliferation. *Mol Cell Biol,* **29,** 5952-5962.

262. Wei MC, Zong WX, Cheng EH, Lindsten T, Panoutsakopoulou V, Ross AJ, Roth KA, MacGregor GR, Thompson CB, and Korsmeyer SJ (2001) Proapoptotic BAX and BAK: a requisite gateway to mitochondrial dysfunction and death. *Science,* **292,** 727-730.

263. Williams MR, Arthur JS, Balendran A, van der KJ, Poli V, Cohen P, and Alessi DR (2000) The role of 3-phosphoinositide-dependent protein kinase 1 in activating AGC kinases defined in embryonic stem cells. *Curr Biol,* **10,** 439-448.

264. Willis SN, Fletcher JI, Kaufmann T, van Delft MF, Chen L, Czabotar PE, Ierino H, Lee EF, Fairlie WD, Bouillet P, Strasser A, Kluck RM, Adams JM, and Huang DC (2007) Apoptosis initiated when BH3 ligands engage multiple Bcl-2 homologs, not Bax or Bak. *Science,* **315,** 856-859.

265. Wodarz A (2002) Establishing cell polarity in development. *Nat Cell Biol,* **4,** E39-E44.

266. Wu GY, Deisseroth K, and Tsien RW (2001) Spaced stimuli stabilize MAPK pathway activation and its effects on dendritic morphology. *Nat Neurosci,* **4,** 151-158.

267. Wullschleger S, Loewith R, and Hall MN (2006) TOR signaling in growth and metabolism. *Cell,* **124,** 471-484.

268. Wullschleger S, Sakamoto K, Johnstone L, Duce S, Fleming S, and Alessi DR (2011) How moderate changes in Akt T-loop phosphorylation impact on tumorigenesis and insulin resistance. *Dis Model Mech,* **4,** 95-103.

269. Xifro X, Anglada-Huguet M, Rue L, Saavedra A, Perez-Navarro E, and Alberch J (2011) Increased 90-kDa ribosomal S6 kinase (Rsk) activity is protective against mutant huntingtin toxicity. *Mol Neurodegener,* **6,** 74.

270. Yamada M, Tanabe K, Wada K, Shimoke K, Ishikawa Y, Ikeuchi T, Koizumi S, and Hatanaka H (2001) Differences in survival-promoting effects and intracellular signaling properties of BDNF and IGF-1 in cultured cerebral cortical neurons. *J Neurochem,* **78,** 940-951.

271. Yamaguchi H and Wang HG (2001) The protein kinase PKB/Akt regulates cell survival and apoptosis by inhibiting Bax conformational change. *Oncogene,* **20,** 7779-7786.

272. Yamamoto H, Kokame K, Okuda T, Nakajo Y, Yanamoto H, and Miyata T (2011) NDRG4 protein-deficient mice exhibit spatial learning deficits and vulnerabilities to cerebral ischemia. *J Biol Chem,* **286,** 26158-26165.

273. Yang E, Zha J, Jockel J, Boise LH, Thompson CB, and Korsmeyer SJ (1995) Bad, a heterodimeric partner for Bcl-XL and Bcl-2, displaces Bax and promotes cell death. *Cell,* **80,** 285-291.

274. Yang K, Cao F, Sheikh AM, Malik M, Wen G, Wei H, Ted BW, and Li X (2012) Up-regulation of Ras/Raf/ERK1/2 signaling impairs cultured neuronal cell migration, neurogenesis, synapse formation, and dendritic spine development. *Brain Struct Funct*. [Epub ahead of print] DOI: 10.1007/s00429-012-0420-7

275. Yang ZZ, Tschopp O, Di-Poi N, Bruder E, Baudry A, Dummler B, Wahli W, and Hemmings BA (2005) Dosage-dependent effects of Akt1/protein kinase Balpha (PKBalpha) and Akt3/PKBgamma on thymus, skin, and cardiovascular and nervous system development in mice. *Mol Cell Biol,* **25,** 10407-10418.

276. Yang ZZ, Tschopp O, Hemmings-Mieszczak M, Feng J, Brodbeck D, Perentes E, and Hemmings BA (2003) Protein kinase B alpha/Akt1 regulates placental development and fetal growth. *J Biol Chem,* **278,** 32124-32131.

277. Yoshimura T, Arimura N, Kawano Y, Kawabata S, Wang S, and Kaibuchi K (2006) Ras regulates neuronal polarity via the PI3-kinase/Akt/GSK-3beta/CRMP-2 pathway. *Biochem Biophys Res Commun,* **340,** 62-68.

278. Yoshimura T, Kawano Y, Arimura N, Kawabata S, Kikuchi A, and Kaibuchi K (2005) GSK-3beta regulates phosphorylation of CRMP-2 and neuronal polarity. *Cell,* **120,** 137-149.

279. Zaidi AU, D'Sa-Eipper C, Brenner J, Kuida K, Zheng TS, Flavell RA, Rakic P, and Roth KA (2001) Bcl-X(L)-caspase-9 interactions in the developing nervous system: evidence for multiple death pathways. *J Neurosci,* **21,** 169-175.

280. Zha J, Harada H, Yang E, Jockel J, and Korsmeyer SJ (1996) Serine phosphorylation of death agonist BAD in response to survival factor results in binding to 14-3-3 not BCL-X(L). *Cell,* **87,** 619-628.

281. Zick Y (2001) Insulin resistance: a phosphorylation-based uncoupling of insulin signaling. *Trends Cell Biol,* **11,** 437-441.

APPENDIX

MCB
Journals.ASM.org

Interaction of PDK1 with Phosphoinositides Is Essential for Neuronal Differentiation but Dispensable for Neuronal Survival

Tinatin Zurashvili,[a] Lluís Cordón-Barris,[a] Gerard Ruiz-Babot,[a] Xiangyu Zhou,[a] Jose M. Lizcano,[a] Nestor Gómez,[a] Lydia Giménez-Llort,[b] Jose R. Bayascas[a]

Institut de Neurociències and Departament de Bioquímica i Biologia Molecular, Universitat Autònoma de Barcelona, Barcelona, Spain[a]; Institut de Neurociències and Departament de Psiquiatria i de Medicina Legal, Universitat Autònoma de Barcelona, Barcelona, Spain[b]

3-Phosphoinositide-dependent protein kinase 1 (PDK1) operates in cells in response to phosphoinositide 3-kinase activation and phosphatidylinositol-3,4,5-trisphosphate [PtdIns(3,4,5)P_3] production by activating a number of AGC kinases, including protein kinase B (PKB)/Akt. Both PDK1 and PKB contain pleckstrin homology (PH) domains that interact with the PtdIns(3,4,5)P_3 second messenger. Disrupting the interaction of the PDK1 PH domain with phosphoinositides by expressing the PDK1 K465E knock-in mutation resulted in mice with reduced PKB activation. We explored the physiological consequences of this biochemical lesion in the central nervous system. The PDK1 knock-in mice displayed a reduced brain size due to a reduction in neuronal cell size rather than cell number. Reduced BDNF-induced phosphorylation of PKB at Thr308, the PDK1 site, was observed in the mutant neurons, which was not rate limiting for the phosphorylation of those PKB substrates governing neuronal survival and apoptosis, such as FOXO1 or glycogen synthase kinase 3 (GSK3). Accordingly, the integrity of the PDK1 PH domain was not essential to support the survival of different embryonic neuronal populations analyzed. In contrast, PKB-mediated phosphorylation of PRAS40 and TSC2, allowing optimal mTORC1 activation and brain-specific kinase (BRSK) protein synthesis, was markedly reduced in the mutant mice, leading to impaired neuronal growth and differentiation.

During the development of the nervous system, among all the neuronal precursors initially produced during the neurogenesis stage, only those encountering the appropriate set of neurotrophic factors along with a complex set of extracellular positional signals will be further selected to survive and differentiate (1). The phosphoinositide 3-kinase (PI3K)/protein kinase B (PKB) axis is one of the critical intracellular signaling pathways that promotes neuronal survival by inhibiting the apoptotic cell death machinery in response to a number of extracellular stimuli (2). Thus, pharmacological inhibition of PI3K catalytic activity causes neuronal cell death, while forced expression of constitutively active forms of the PKB/Akt kinase promotes the survival of many neuronal cell types (3). PI3K also plays fundamental roles in regulating neuronal differentiation by defining the axon-dendrite axis through the activation of PKB (4). PKB promotes axon specification by inhibiting glycogen synthase kinase 3β (GSK3β) (5). PKB also inhibits the TSC1-TSC2 complex, which antagonizes axon formation by inhibiting mTORC1 and in this way restricting the expression of the brain-specific kinase (BRSK)/SAD kinases (6), which are known to play fundamental roles in neuronal polarization *in vivo* (7, 8).

However, mice lacking the neuronal Akt3/PKBγ isoform are viable and do not exhibit any overt phenotype, although they display a reduced brain size, with neurons more sensitive to apoptotic insults (9, 10). Therefore, the contribution of kinases activated downstream of the PI3K cascade besides PKB cannot be overlooked. In this regard, a role for the closely related kinase serum- and glucocorticoid-induced kinase (SGK) (11) or p90 ribosomal S6 kinase (RSK) (12) in promoting neuronal survival, and for RSK in promoting neurite outgrowth (13), has also been proposed.

3-Phosphoinositide-dependent protein kinase 1 (PDK1) elicits cellular responses to growth factors, hormones, and many other agonists that signal through PI3K activation and phosphatidylinositol-3,4,5-trisphosphate [PtdIns(3,4,5)P_3] production by directly activating as many as 23 protein kinases of the AGC family. These protein kinases include PKB/Akt, p70 ribosomal S6 kinase (S6K), SGK, RSK, and protein kinase C (PKC) isoforms, which in turn regulate cell growth, proliferation, survival, as well as metabolism (14, 15). All these AGC kinases share structural homology and a common mechanism of activation based on the dual phosphorylation of two residues lying within two highly conserved motifs, namely, the T loop (Thr308 residue for PKBα) and the hydrophobic motif (Ser473 residue for PKBα). PDK1 acts as the master upstream kinase activating this set of AGC kinases by phosphorylating their T-loop sites (16). The hydrophobic motif kinase is different among the different AGC family members, although a prominent role for mTOR complexes has emerged (17). Thus, the mTORC1 complex phosphorylates the hydrophobic motif of S6K isoforms (18, 19) and novel PKC isoforms (20), while the mTORC2 complex is the hydrophobic motif kinase for PKB (21), PKCα (22), and SGK (23) isoforms.

PDK1 is expressed in cells as a constitutively active enzyme which is not modulated by any stimuli. Regulation of this intricate signaling network relies instead on the ability of PDK1 to specifically recognize and interact with its substrates (24). The interaction of PDK1 with most AGC kinases needs the previous phosphorylation of their hydrophobic motifs, which in this manner become a substrate docking site for PDK1 binding (25). Activa-

Received 1 August 2012 **Returned for modification** 28 August 2012
Accepted 19 December 2012
Published ahead of print 28 December 2012
Address correspondence to Jose R. Bayascas, joseramon.bayascas@uab.cat.

doi:10.1128/MCB.01052-12

tion of PKB/Akt isoforms represents an exception to this general mechanism. Among all the PDK1-activated kinases, PKB isoforms are the only ones possessing pleckstrin homology domains, a phosphoinositide binding domain that is also present in the PDK1 protein (26, 27). The specific binding of the pleckstrin homology domain of PKB with PtdIns(3,4,5)P_3 becomes rate limiting for the translocation of PKB to the plasma membrane and colocalization with PDK1, where PDK1 can then efficiently phosphorylate PKB at Thr308 (28, 29), while mTORC2 phosphorylates the Ser473 site in the hydrophobic motif (21), resulting in maximal activation of the enzyme. The significance of the interaction of the PDK1 PH domain with phosphoinositides in the activation of PKB has been evaluated *in vivo* using PDK1$^{K465E/K465E}$ knock-in mice (30), which express a rationally designed point mutant form of PDK1 that retains catalytic activity but is incapable of phosphoinositide binding (27). In tissues derived from these mice, PKB is still activated by growth factors albeit to a reduced level (30–32), whereas the activation of the rest of the PDK1 substrates proceeds normally. As a consequence, these mice are smaller, prone to diabetes (30), and protected from PTEN-induced tumorigenesis (32). The PDK1$^{K465E/K465E}$ mouse is a genuine model in which PKB activation is only moderately reduced, which might originate from the ability of PDK1 to recognize the PKB Ser473 phospho-docking site in the absence of phosphoinositide binding (33). This genetic model has proven instrumental in dissecting PDK1 signaling (34) and has revealed that in T cells a PKB/Akt signaling threshold depending on PDK1-phosphoinositide interactions dictates specific cellular responses such as cell migration but not cell proliferation (31).

In the present study, we have employed PDK1$^{K465E/K465E}$ knock-in mice to explore the role that the interaction of the PDK1 PH domain with phosphoinositides plays in neuronal tissues. We found that the brain of homozygous PDK1$^{K465E/K465E}$ knock-in mice was reduced in size due to a reduction in cell size rather than cell number. In agreement with the maintenance of the number of cells, both the sensitivity of the mutant neurons to apoptosis induced by serum withdrawal as well as the ability of different growth factors to support neuronal survival in the absence of serum were preserved in the mutant neurons. The deficient activation of PKB and incomplete phosphorylation and inactivation of PRAS40 and TSC2 observed in the mutant neurons caused decreased mTORC1 activation, leading to reduced BRSK protein synthesis and deficient neuronal differentiation.

MATERIALS AND METHODS

Materials and constructs. Protease inhibitor cocktail, thiazolyl blue tetrazolium bromide [3-(4,5-dimethylthiazol-2-yl)-2,5-diphenyltetrazolium bromide (MTT)], staurosporine, Dulbecco's modified Eagle's medium (DMEM), basal medium Eagle (BME), and fetal bovine serum (FBS) were purchased from Sigma. Human recombinant BDNF was obtained from Alomone, and human recombinant IGF-1 was obtained from Millipore. The Calbiochem inhibitors Akti-1/2 (catalog number 124018), PI-103 (catalog number 528100), rapamycin (catalog number 553210), and SB-216763 (catalog number 361566) were purchased from Merck Millipore. Neurobasal medium, B27 supplement, Opti-MEM, and Lipofectamine 2000 were obtained from Invitrogen. Hemagglutinin (HA)-tagged human BRSK1 and BRSK2 (35) were subcloned into a pEIGW lentiviral vector that allows the expression of both green fluorescent protein (GFP) and BRSK1/2 from a bicistronic messenger.

Antibodies. The following antibodies were kindly provided by Dario Alessi from the University of Dundee. All antibodies were raised in sheep and affinity purified on the appropriate antigen. The PKBα total antibody was raised against the sequence RPHFPQFSYSASGTA, corresponding to residues 466 to 480 of rat PKBα; the total TSC2 antibody was raised against a sequence encompassing residues 1719 to 1814 of mouse TSC2; the total PRAS40 antibody was raised against the peptide DLPRPRLNTS DFQKLKRKY, corresponding to residues 238 to 256 of human PRAS40; and the total NDRG1 antibody was raised against the recombinant human NDRG1 protein expressed in *Escherichia coli*. Affinity-purified polyclonal BRSK1- or BRSK2-specific antibodies were raised in sheep against the peptide SPRRGPPKDKKLLATNGTPLP, corresponding to C-terminal residues 774 to 794 of human BRSK1, and the peptide LSWGAGLKGQK VATSYESSL, encompassing residues 655 to 674 of human BRSK2, as described previously (36). Phospho-PKB Thr308 (catalog number 9275), phospho-PKB Ser473 (catalog number 9271), phospho-S6K Thr389 (catalog number 9205), total S6K (catalog number 9202), phospho-S6 ribosomal protein Ser235/236 (catalog number 2211), total S6 ribosomal protein (catalog number 2217), phospho-p44/42 mitogen-activated protein kinase (MAPK) Thr202/Tyr204 (catalog number 9101), total p44/42 MAPK (catalog number 9102), phospho-GSK3α/β Ser21/9 (catalog number 9331), phospho-FOXO1 Ser256 (catalog number 9461), phospho-FOXO1 Thr24 (catalog number 9464), total FOXO1 (catalog number 2880), phospho-RSK Ser380 (catalog number 9335), phospho-RSK Thr573 (catalog number 9346), total RSK1/2/3 (catalog number 9355), phospho-TSC2 Thr1462 (catalog number 3611), phospho-PRAS40 Thr246 (catalog number 2997), phospho-NDRG1 Thr346 (catalog number 5482), phospho-TrkB Tyr706/707 (catalog number 4621), and total TrkB (catalog number 4603) antibodies were purchased from Cell Signaling Technology. The pan-PDK1 site antibody from Cell Signaling Technology (catalog number 9379) recognizes phosphorylated Thr229 of S6K in cell extracts (37). Total GSK3α/β (sc-7291) and phospho-RSK Thr227 (sc-12445) antibodies were purchased from Santa Cruz Biotechnology. Appropriate secondary antibodies coupled to horseradish peroxidase were obtained from Pierce. For the immunofluorescence analysis, the anti-Tau-1 monoclonal antibody (MAB3420) was purchased from Millipore, the pan-axonal anti-neurofilament H monoclonal antibody (SMI-312R) was obtained from Covance, and the rabbit anti-MAP2 polyclonal antibody (M3696) was obtained from Sigma; Alexa Fluor 594-conjugated goat anti-rabbit (catalog number A11072) and Alexa Fluor 488-conjugated goat anti-mouse (catalog number A11017) fluorescent secondary antibodies were obtained from Invitrogen.

Mice. The generation and genotyping of PDK1$^{K465E/K465E}$ knock-in mice expressing the single-amino-acid substitution of lysine 465 to glutamic acid in the PDK1 PH domain were described previously (30). Mice were maintained in the Animal House Facility of the Universitat de Lleida under standard husbandry conditions. All animal studies and breeding were approved by the Universitat Autònoma de Barcelona ethical committee and performed under a Generalitat de Catalunya project license.

Primary cultures. Cerebral cortical or hippocampal tissues were dissected from PDK1$^{+/+}$ and PDK1$^{K465E/K465E}$ littermate mice at embryonic day 15.5 (E15.5), and the cells were enzymatically dissociated in Krebs Ringer buffer (120 mM NaCl, 4.8 mM KCl, 1.2 mM KH_2PO_4, 25 mM $NaHCO_3$, 14.3 mM glucose) containing 0.25 mg/ml of trypsin for 10 min at 37°C and were then mechanically dissociated in Krebs Ringer buffer containing 0.08 mg/ml DNase and 0.52 mg/ml trypsin inhibitor by gentle pipetting using a fire-polished Pasteur pipette to produce a single-cell suspension. Cells were then centrifuged and resuspended, counted with the Scepter 2.0 handheld automated cell counter (Millipore), and finally diluted in DMEM complemented with 2 mM L-glutamine, 0.25 mg/ml penicillin-streptomycin, and 10% FBS. The cortical cells were then plated onto poly-D-lysine (50 μg/ml)-coated 24-well plates for cell viability studies, or 6-well plates for Western blot analysis, at a density of 15×10^4 cells/ml, whereas the hippocampal cells were plated onto poly-D-lysine (150 μg/ml)-coated 12-mm-diameter glass coverslips at a density of 5×10^4 cells/ml. The cells were allowed to attach to the plate for 2 h, and the medium was then replaced by Neurobasal medium complemented with 2

mM L-glutamine, 0.25 mg/ml of penicillin-streptomycin, and 2% B27 supplement. Cells were maintained at 37°C in a humidified incubator containing 5% CO_2 under normoxia conditions.

Cerebellar granule cell cultures were prepared from dissociated cerebella of 8-day-old mice by mechanically chopping the cerebellum, followed by trypsin digestion and triturating, as described above. Cells were plated onto BME supplemented with 25 mM KCl, 10% FBS, and 0.25 mg/ml of penicillin-streptomycin. Cytosine-β-D-arabinofuranoside (10 μM) was added to the culture after 24 h of seeding to prevent the proliferation of nonneuronal cells. Cells were plated onto 48-well culture plates coated with 10 μg/ml poly-L-lysine at a density of 1.35×10^6 cells/ml.

Trophic deprivation and drug treatment. Survival experiments were performed at day 6 *in vitro* (DIV6). Cells were washed twice with serum-free DMEM and then incubated for 24 h in serum-free Neurobasal medium supplemented with 2 mM L-glutamine and 0.25 mg/ml of penicillin-streptomycin. The experimental controls included sham treatments consisting of two washes with serum-free medium and incubation with the same conditioned medium. BDNF and IGF-1 were diluted in DMEM without any supplement. The inhibitors Akti-1/2, PI-103, SB-216763, staurosporine, and rapamycin were dissolved in dimethyl sulfoxide (DMSO). For viability and apoptosis analysis, growth factors and inhibitors were added at the onset of trophic deprivation. For Western blot analysis, cells were pretreated with inhibitors for 30 min and then stimulated with BDNF, as indicated.

Evaluation of cell viability. Cell viability was determined by an MTT reduction assay. Briefly, MTT salt was added to the cell culture at a final concentration of 0.5 mg/ml. Plates were then returned to the incubator for 45 min. After incubation, the medium was aspirated, and the resulting formazan crystals were dissolved by mixing with 300 μl of DMSO. Absorbance intensity was measured at 570 nm, with the background measured at 690 nm, using a spectrophotometer running Labsystem Multiskan software.

Quantification of apoptosis. Cells were fixed in 2% paraformaldehyde, stained with 1 μg/ml of the DNA dye Hoechst 33342, and then visualized under a fluorescence microscope. Apoptosis was quantified at each condition point by scoring the percentage of apoptotic cells in the adherent cell population. Cells exhibiting fragmented or condensed nuclei were scored as apoptotic, while cells showing uniformly stained nuclei were scored as viable. At least 300 cells from 6 randomly selected fields per well were counted.

Transfection. A total of 2.5×10^4 embryonic hippocampal neurons grown for 2 days in 12-mm-diameter 24-well plates were transfected with 0.7 μl of Lipofectamine 2000 reagent diluted in 50 μl of Opti-MEM plus 1 μg of the indicated DNA diluted again in 50 μl of Opti-MEM. After 3 h, the transfection medium was replaced by conditioned medium, and the axon length of the GFP-expressing cells was evaluated at day 4 *in vitro*, as described above.

Generation of protein extracts and Western blot analysis. Primary cortical neurons were cultured for 6 days and then incubated for 4 h in Neurobasal medium without B27 and subsequently stimulated with the indicated agonists, as described in the figure legends. The neurons were lysed at the indicated time points in ice-cold lysis buffer (50 mM Tris-HCl [pH 7.5], 1 mM EGTA, 1 mM EDTA, 1 mM sodium orthovanadate, 50 mM sodium fluoride, 5 mM sodium pyrophosphate, 10 mM sodium β-glycerophosphate, 0.27 M sucrose, 1% [wt/vol] Triton X-100, 0.1% [vol/vol] 2-mercaptoethanol, and a 1:100 dilution of protease inhibitor cocktail) and centrifuged at 4°C for 10 min at 13,000 × *g*. Tissue extracts were prepared by homogenizing the frozen tissue on ice in a 10-fold excess volume of ice-cold lysis buffer using the Polytron homogenizer and then centrifuged at 4°C for 10 min at 13,000 × *g* to remove insoluble material. The supernatants were aliquoted, frozen in liquid nitrogen, and stored at −20°C until use. Protein concentrations were determined by the Bradford method (38), using bovine serum albumin (BSA) as a standard. The activation state of the different pathways analyzed was assessed by immunoblotting the extracts (10 μg) with the indicated antibodies and detected with the appropriate horseradish peroxidase-conjugated secondary antibodies. Membranes were incubated with enhanced chemiluminescence (ECL) reagent, either exposed to Super RX Fujifilm and developed or detected by using a GeneGnome HR detection system (Syngene, Cambridge, United Kingdom), and quantified by using ImageJ software.

Determination of organ volume and cell size. Organ volume was determined by using the Cavalieri method (39) on 8-μm brain paraffin sections collected at systematically spaced locations ($k = 96$ μm) from a random starting position. The sections were photographed with a Nikon SMZ800 stereomicroscope at a ×2 magnification using a digital camera. A square lattice grid was then overlaid onto the picture by using the program Photoshop, version vCS5.1, and the number of intersections (P) hitting the organ was scored. The organ volume was then estimated by using the equation $\Sigma P \times d^2 \times k$, in which d^2, the distance between each point of the square lattice grid squared, was 0.14792 mm^2. The number and size of the cells in E15.5 dissociated cortex and hippocampal tissues were determined with the Scepter 2.0 handheld automated cell counter (Millipore).

Immunocytochemistry. Dissociated hippocampal cells were cultured on coverslips for the indicated number of experimental days *in vitro* and then fixed with 4% paraformaldehyde in phosphate-buffered saline (PBS) for 20 min at room temperature. Fixative solution was rinsed 3 times with PBS for 5 min, and the cells were then permeabilized with 0.02% saponin in PBS for 7 min at room temperature and blocked in a solution containing 0.01% saponin, 5% BSA, and 10 mM glycine in PBS for 1 h. Primary antibodies were diluted 1:200 in PBS supplemented with 0.01% saponin and 1% normal goat serum and incubated overnight at 4°C. Cells were then washed three times with PBS for 10 min. Appropriate secondary antibodies conjugated to Alexa Fluor 594 or Alexa Fluor 488 fluorescent dye were used at a concentration of 1:400, and nuclei were stained with 1 μg/ml Hoechst 33342. Coverslips were then mounted onto microscope slides with FluorSave reagent for further analysis.

Immunohistochemistry. Three $PDK1^{+/+}$ and three $PDK1^{K465E/K465E}$ matched littermate mice were anesthetized by intraperitoneal injection of a ketamine-xylazine mixture and then intracardially perfused with 0.9% NaCl followed by 4% buffered paraformaldehyde. Brains were extracted and postfixed with the same solution for 2 h, washed in phosphate buffer (0.1 M, pH 6.0) for 2 h, and preserved in a 70% ethanol solution at 4°C. All six specimens were then embedded in the same paraffin block and sliced into 5-μm-thick coronal sections with a Leica RM2255 microtome. Paraffin-embedded sections were incubated for 2 h at 60°C and then rehydrated through a series of 2 washes with xylene for 5 min, 2 washes with 100% ethanol for 3 min, 1 wash with 96% ethanol for 3 min, 1 wash with 70% ethanol for 3 min, 1 wash with 50% ethanol for 5 min, and 1 wash with water for 1 min. Sections were then boiled for 10 min in 10 mM sodium citrate (pH 6) for antigen retrieval and cooled down for 30 min on ice. Samples were blocked in Tris-buffered saline (TBS) (50 mM Tris [pH 7.5], 150 mM NaCl) containing 0.02% Triton and 5% goat serum for 30 min and incubated overnight at 4°C with primary antibodies diluted in the same blocking solution (1:300 dilution for the rabbit anti-MAP2 antibody and 1:2,000 for the mouse monoclonal anti-pan-axonal marker SMI-312R). Sections were rinsed with TBS buffer and detected with Alexa Fluor 488-conjugated anti-mouse (dilution, 1:400) and Alexa Fluor 594-conjugated anti-rabbit (1:300) secondary antibodies for 1.5 h at room temperature. Tissue autofluorescence was removed by incubation with Sudan Black for 10 min (0.3% [wt/vol] Sudan Black in 70% ethanol). Sections were counterstained with Hoechst dye and mounted with FluorSave reagent. Immunostained sections were photographed with a Nikon Eclipse 90i epifluorescence microscope, and the captured images were analyzed and processed with ImageJ 1.42q (Wayne Rasband, National Institutes of Health) and Fiji (http://pacific.mpi-cbg.de/wiki/index.php/Main_Page) software.

Evaluation of differentiation. For differentiation analysis of the cortical neurons, cells were seeded at a reduced density of 75,000 cells/ml. Under this condition, most neurons did not contact neighboring cells,

allowing the measurement of neurite development of individual neurons. Images were acquired from random fields at a ×20 magnification by using an inverted microscope equipped with a Hamamatsu Orca-Er high-sensibility camera at the maximal resolution of the microscope. The total neurite length per cell was measured by tracing all the neurites on each individual neuron from the cell body to the tip with Adobe Photoshop, version vCS5.1, software, and the number of pixels was converted to micrometers. The cell diameter was defined by using the same technique, by measuring the major axis of the neuronal cell body. The number of neurites per cell and the number of branching points per neurite were also determined by direct counting on the acquired images.

For differentiation analysis of hippocampal cells, images were obtained with an epifluorescence microscope (Nikon Eclipse 90i) interfaced with a DXM 1200F camera at a ×20 magnification. Images for the red and green channels were taken simultaneously. Neuronal dendrites were identified by immunostaining with the dendritic marker MAP2, whereas the axon was defined as a neurite whose length is 2 times longer than that of the other neurites and is also immunoreactive for the axonal marker Tau-1. To measure axonal elongation, each particular axon was manually traced, followed by automatic length calculation with MetaMorph image analysis software, v6.1.

Statistical analysis. Statistical significance was determined by using Student *t* test analysis. *P* values of <0.05 and <0.005 between categories or conditions are indicated in the figures.

RESULTS

Reduced brain size of PDK1$^{K465E/K465E}$ mice. Mice homozygous for the PDK1 K465E knock-in alleles were previously reported to be viable, fertile, and healthy, although they displayed a 35% reduction in body weight compared to wild-type mice (30). We observed the homozygous PDK1$^{K465E/K465E}$ genotype at a reduced Mendelian distribution from heterozygous crosses, both at embryonic day 15 and at birth (19.8% and 16.0%, respectively), thereby indicating that the PDK1 K465E mutation resulted in partial embryonic lethality (Fig. 1A). The growth deficiency of the PDK1$^{K465E/K465E}$ mice might initiate early during development, as we observed that at E15.5, the PDK1 knock-in embryos were already 20% smaller than their control littermates (Fig. 1B), with brain size also reduced to scale (Fig. 1C). The small phenotype was further exacerbated after the second week of age, as the body weight of the PDK1$^{K465E/K465E}$ mice was 30 to 35% reduced compared to that of the PDK1$^{+/+}$ mice from 3 weeks of age (Fig. 1B) and during their adulthood (data not shown). To establish whether the reduction in the embryonic brain volume could be attributed to a reduction in cell size or number, the volume of the neuronal soma and the number of neuronal cells purified at E15.5 from both the embryonic cortex and the hippocampus were determined. While the number of cortical and hippocampal neurons was not significantly different between genotypes, the soma was 20% reduced in volume in the cortical (Fig. 1D) and hippocampal (Fig. 1E) mutant cells compared to controls, thereby demonstrating that the small size of the PDK1$^{K465E/K465E}$ mouse brain is due mostly to a reduction in cell size rather than cell number.

Binding of PDK1 to PtdIns(3,4,5)P_3 is not essential to support neuronal survival. We next compared the protective effects that BDNF elicited on the survival of PDK1$^{+/+}$ and PDK1$^{K465E/K465E}$ cortical neurons deprived of growth factors. In control cultures, trophic factor deprivation compromised cell viability, as denoted by a 50% decrease in the MTT reduction values, which was accompanied by a 3-fold increase in the number of apoptotic cells compared to that in the untreated cultures. BDNF stimulation markedly recovered cell viability and decreased the number of apoptotic dying cells of the serum-deprived cortical cultures (Fig. 2A). Unexpectedly, trophic factor withdrawal compromised neuronal viability to the same extent in the PDK1$^{+/+}$ and the PDK1$^{K465E/K465E}$ cultures, which was equally rescued by BDNF treatment for the two genotypes, thereby suggesting that the interaction of PDK1 with phosphoinositides is not essential for the neuroprotective actions of BDNF, at least in cortical neurons. We extended our observations to other neuronal populations and found that IGF-1 prompted the survival of cerebellar granule cells deprived of serum and potassium to the same level in the PDK1$^{+/+}$ and the PDK1$^{K465E/K465E}$ cultures (Fig. 2B). Moreover, the PDK1$^{+/+}$ and the PDK1$^{K465E/K465E}$ cortical neurons exhibited the same sensitivity to apoptotic stimuli such as staurosporine (Fig. 2C). We also cultured cortical neurons in the presence of suboptimal doses of either BDNF or IGF-1 and found that the two trophic factors elicited a dose-dependent neuroprotective action that was similar in both control and mutant cultures (Fig. 2D). Because the interaction of PDK1 with phosphoinositides is important for PKB activation (30), and PKB/Akt is a major regulator of neuronal survival (2), but the neuronal survival responses were still not affected in the PDK1$^{K465E/K465E}$ mice (Fig. 2), we assessed whether inhibition of PKB compromised the protective role of BDNF against serum deprivation. To that end, we employed the inhibitor Akti-1/2, which specifically targets PKBα and PKBβ. The treatment of cortical cultures with the Akti-1/2 compound at specific doses that markedly prevented PKB phosphorylation at both the Thr308 and Ser473 sites did not affect the survival responses elicited by BDNF. As a control, cortical cultures were also treated with the PI3K-specific inhibitor PI-103, and we found that the inhibition of PI3K totally abolished both the recovery of cell viability and the inhibition of apoptosis induced by BDNF (Fig. 3).

Mutation of the PDK1 PH domain impairs BDNF-mediated PKB activation. To define the importance of the PDK1-PtdIns(3,4,5)P_3 interaction in the ability of PDK1 to activate PKB, primary cultures of cortical neurons derived from littermate PDK1$^{+/+}$ and PDK1$^{K465E/K465E}$ embryos were stimulated with BDNF for the indicated times (Fig. 4A). As a control for stimulation, the activation of the BDNF receptor TrkB was monitored by measuring its phosphorylation at the activation loop residues Tyr706/707, which was very rapid and sustained in both control and mutant cell extracts. In PDK1$^{+/+}$ cells, BDNF induced a clear activation of PKB, as judged by the level of phosphorylation of the two activating residues, Thr308 and Ser473, which reached the maximum after 5 min and was then sustained for up to 30 min. In contrast, the phosphorylation of PKB at Thr308, the PDK1 site, was significantly reduced in the PDK1$^{K465E/K465E}$ mutant neurons during the first 15 min of stimulation and was then detected at nearly normal levels after 30 min, whereas the phosphorylation of PKB at Ser473, the mTORC2 site, was not affected in the mutant cells (Fig. 4A and C). Consistent with a reduction in the ability of the PDK1 K465E mutant protein to activate PKB, the phosphorylation levels of some PKB substrates at their specific PKB sites, namely, PRAS40 at Thr246 and TSC2 at Thr1462, were also significantly reduced in the mutant extracts. In contrast, the PKB-specific phosphorylation of GSK3α/β at Ser21/9 and FOXO1 at Thr24 and Ser256 was not affected by the PDK1 mutation (Fig. 4A). The moderate changes to the PKB downstream signaling pathways that the PDK1 PH domain mutation causes were

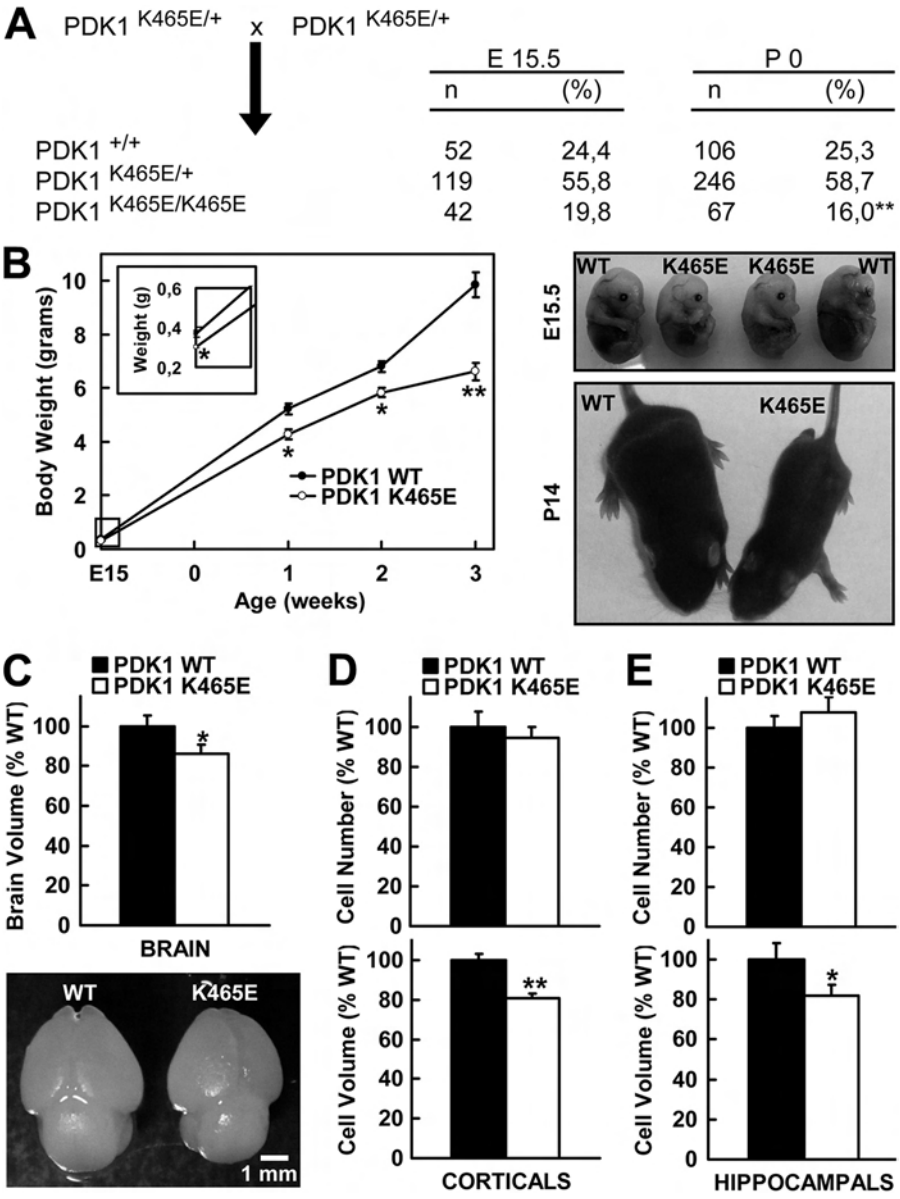

FIG 1 Reduced embryonic brain size in PDK1$^{K465E/K465E}$ mice. (A) The number and proportion (percentage) of mice of different genotypes resulting from heterozygous breeding are indicated both at embryonic day 15.5 (E15.5) and at birth (P0). ** indicates that the lower-than-expected frequency of PDK1$^{K465E/K465E}$ pups is statistically significant ($P < 0.005$ by χ^2 test). (B) The mean body weights of the indicated PDK1 wild-type (WT) and PDK1 K465E mice at the indicated ages in weeks are shown. The values represent the means ± standard errors of the means, with each data point obtained for at least five mice per genotype. Representative pictures of the indicated littermate PDK1 wild-type and PDK1 K465E embryos (E15.5) or 14-day-old pups (P14) are shown in the right panels. (C, top) The volume of the brain was measured at E15.5 from histological sections by using the Cavalieri method. The data are represented as the means ± standard errors of the means for three different mice per genotype. (Bottom) Representative photographs of brains dissected from E15.5 PDK1 wild-type and PDK1 K465E embryo littermates. Bar, 1 mm. (D and E) The number of cells (top) and the volume of the cell (bottom) were determined for E15.5 dissociated cortical (D) or hippocampal (E) neurons. The data are represented as the means ± standard errors of the means for 25 wild-type and 29 mutant embryonic cortical cultures obtained from 18 independent litters (D) or 8 wild-type and 7 mutant embryonic hippocampal cultures obtained from 6 independent litters (E). *, $P < 0.05$; **, $P < 0.005$ (compared with the wild type, as determined by the Student *t* test).

time and dose dependent and were better observed at low concentrations of BDNF (Fig. 4B).

Reduced activation of S6K in PDK1$^{K465E/K465E}$ cortical neurons. Activation of S6K involves the phosphorylation of the Thr389 residue within the S6K hydrophobic motif by mTORC1, followed by the phosphorylation of the Thr229 residue in the S6K activation loop by PDK1. Therefore, mTORC1 regulation greatly dictates S6K activation. PKB itself contributes to the activation of mTORC1 by phosphorylating and inhibiting two mTORC1-inhibitory proteins, namely, PRAS40 and TSC2. Accordingly, although S6K is a docking site-dependent PDK1 substrate, the reduced phosphorylation of PKB, PRAS40, and TSC2 proteins observed in the BDNF-stimulated PDK1$^{K465E/K465E}$ cortical neurons (Fig. 4) resulted in deficient activation of mTORC1, as

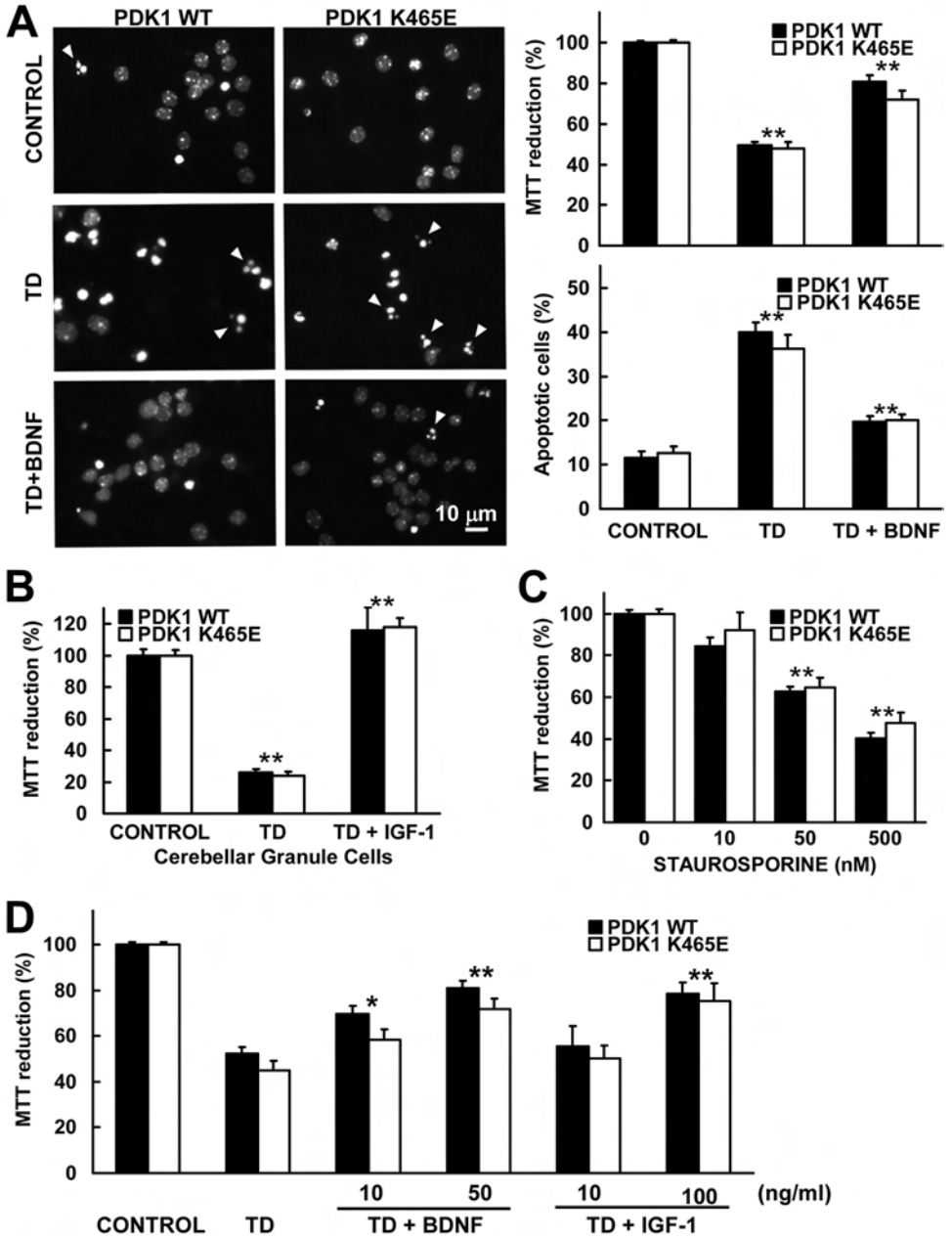

FIG 2 Neuronal survival responses are not impaired in PDK1$^{K465E/K465E}$ mice. (A) Cortical cells of the indicated genotypes were either sham treated (CONTROL) or deprived of trophic factors in the absence (TD) or presence of 50 ng/ml of BDNF (TD+BDNF) for 24 h. (Left) Representative micrographs of PDK1 wild-type (WT) and PDK1 K465E Hoechst-stained cortical neurons after 24 h of the indicated treatment; arrowheads indicate apoptotic nuclei. Bar, 10 μm. (Top right) Cell viability was determined with the MTT reduction assay and is expressed as a percentage of the untreated cells; data represent the means ± standard errors of the means for at least 20 independent mouse embryos per genotype from seven different litters, with each sample assayed in triplicate. (Bottom right) The percentage of apoptotic cells was obtained by scoring the number of nuclei exhibiting chromatin fragmentation divided by the total; data represent the means ± standard errors of the means for at least nine independent mouse embryos per genotype from four independent litters. (B) Cerebellar granule cells were either sham treated (CONTROL) or deprived of serum and potassium in the absence (TD) or presence of 100 ng/ml of IGF-1 (TD + IGF-1) for 24 h. Cell viability was measured, as described above for panel A, from three different mouse pups of each genotype assayed in quadruplicate. (C) Cortical cell cultures in complete medium were treated with the indicated doses of staurosporine for 24 h, and cell viability was then determined, as described above for panel A, from samples of at least seven independent embryos per genotype from four independent pregnancies, with each sample assayed in triplicate. (D) Cortical cells of the indicated genotypes were treated as described above for panel A, in the presence of the indicated concentrations of BDNF or IGF-1 for 24 h. Cell viability was determined from samples of at least five independent mouse embryos per genotype, with each sample assayed in triplicate. *, $P < 0.05$; **, $P < 0.005$ (between trophic deprivation and controls [A and B], BDNF or IGF-1 stimulation and trophic deprivation [A, B, and D], and staurosporine treatment and untreated controls [C], as determined by the Student *t* test).

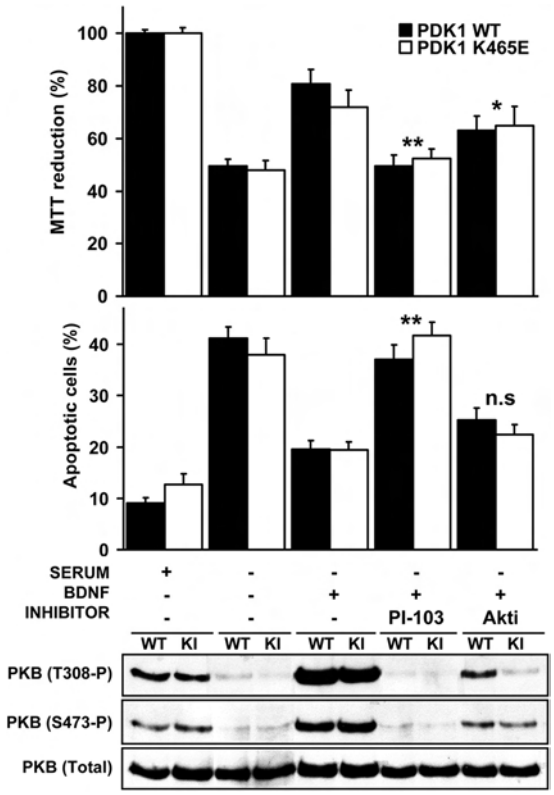

FIG 3 The PKB inhibitor Akti-1/2 does not impair neuronal survival. Cortical cells of the indicated genotypes were cultured in complete medium or deprived of serum for 24 h in the absence or presence of 50 ng/ml of BDNF, 1 μM PI-103, or 1 μM Akti-1/2, as indicated. MTT reduction and the percentage of apoptotic nuclei were determined and are represented as the means ± standard errors of the means for at least five independent embryos per genotype from two separate experiments, with each sample assayed in triplicate. As a control for the different treatments, cell lysates from matched PDK1 wild-type (WT) and PDK1 mutant (knock-in [KI]) littermate mice were immunoblotted with the indicated antibodies. n.s., not significant; *, $P < 0.05$; ** $P < 0.005$ (between samples treated with BDNF plus the indicated inhibitor and samples treated with BDNF alone, as determined by Student's *t* test).

judged by the reduced phosphorylation of S6K at Thr389, although this defect was very transient and detectable only at 5 min of BDNF treatment. As a consequence, PDK1 phosphorylation of the Thr229 residue was also reduced, leading to decreased S6K activation, as revealed by the impaired phosphorylation of the ribosomal S6 protein at Ser235 (Fig. 5A).

Normal activation of RSK in PDK1$^{K465E/K465E}$ neurons. RSK is activated downstream of the extracellular signal-regulated kinase (ERK) signaling pathway in a multistep phosphorylation sequence. ERK activates the C-terminal kinase domain (CTKD) of RSK by phosphorylating the T-loop Thr573 residue. Activated CTKD autophosphorylates the RSK hydrophobic motif at Ser380, thereby creating the docking site for PDK1, which can then phosphorylate the T-loop residue Ser227 in the N-terminal kinase domain (NTKD), leading to its activation (40). BDNF induced a rapid phosphorylation of ERK1/2 at Thr202/Tyr204 in cortical cells, which reached the maximum at 5 min and was sustained for 30 min. As expected, this was not affected by the PDK1 K465E mutation. This was accompanied by a robust induction of RSK phosphorylation at Thr573, Ser380, and Ser227, which was similar in both control and mutant cells (Fig. 5B).

Reduced phosphorylation of the SGK1 substrate NDRG1. Activation of SGK1 encompasses the phosphorylation of the hydrophobic motif at Ser422 by mTORC2, which primes the phosphorylation of the T loop at Thr256 by PDK1. The n-myc downstream-regulated gene (NDRG) family members were identified as the first specific physiological substrates of the SGK isoforms (41), and the phosphorylation of the NDRG1 protein at Thr346/356/366 sites, lying in a C-terminal decapeptide repeated sequence, is used as a readout of SGK1 activity (23). The NDRG proteins play important roles in the development of the central nervous system. Mutations in the NDRG1 gene cause motor and sensory neuropathy in humans (42), whereas NDRG1-deficient mice exhibited peripheral nerve degeneration (43). NDRG2 levels are upregulated in Alzheimer disease (44), and NDRG4-deficient mice exhibit spatial learning deficits and vulnerabilities to cerebral ischemia (45). However, the physiological relevance of NDRG phosphorylation by SGK1 in neurons is largely undefined. We used antibodies that recognize the phosphorylated C-tail repeats of the NDRG1 protein and found that BDNF rapidly induced the phosphorylation of NDRG1 at the SGK1 sites in PDK1$^{+/+}$ cortical neurons, which was significantly reduced in the PDK1$^{K465E/K465E}$ cells at 5 min of BDNF treatment (Fig. 6A). This observation was puzzling, because a role for the PDK1-phosphoinositide interaction in the activation of SGK1 could not be envisaged. Another scenario would be that the PKB isoforms contributed to the phosphorylation of NDRG1 at Thr346/356/366, at least in neurons. We tested this notion by stimulating cortical neurons with BDNF in the presence of the inhibitor Akti-1/2 and found that BDNF-induced phosphorylation of NDRG1 at Thr346/356/366 was greatly reduced by the Akti-1/2 compound at doses that did not affect other closely related kinases, such as RSK (Fig. 6B). Since SGK1 phosphorylation primes NDRG1 for GSK3 phosphorylation four amino acids N terminal to the residues phosphorylated by SGK1 (positions $n - 4$) (41), the phosphorylation of NDRG1 at Ser342/352/362 by GSK3, which could have been enhanced by the PDK1 K465E mutation, might have interfered with the recognition of NDRG1 by the phospho-Thr346/356/366 antibody. Treatment of BDNF-stimulated cells with two independent GSK3 inhibitors, namely, lithium and SB-216763, caused an increase in the electrophoretic mobility of the NDRG1 protein, which was compatible with a decrease in the abundance of the hyperphosphorylated NDRG1 species. In contrast, inhibitors of GSK3 did not significantly affect the intensity of the phospho-Thr346/356/366 signal (Fig. 6B), thereby indicating that the phosphorylation of the GSK3 sites was not masking the NDRG1 phospho-Thr346/356/366 antibody epitope and further suggesting a direct role of PKB in phosphorylating neuronal NDRG1 at the SGK1 sites.

PtdIns(3,4,5)P_3 binding to PDK1 promotes neuronal differentiation through the PKB/mTORC1/BRSK pathway. We showed that disruption of the interaction of PDK1 with PtdIns(3,4,5)P_3 in PDK1$^{K465E/K465E}$ mice affected the activation of PKB by BDNF, leading to the inhibition of the downstream mTORC1 and S6K signaling pathways. Since mTORC1 plays fundamental roles in regulating neuronal morphogenesis (46), we aimed to determine whether PDK1$^{K465E/K465E}$ mice exhibited alterations in neuronal morphology. To that end, primary cortical neurons derived from PDK1$^{+/+}$ and PDK1$^{K465E/K465E}$ E15.5 embryos were allowed to differentiate in culture, and the complexity

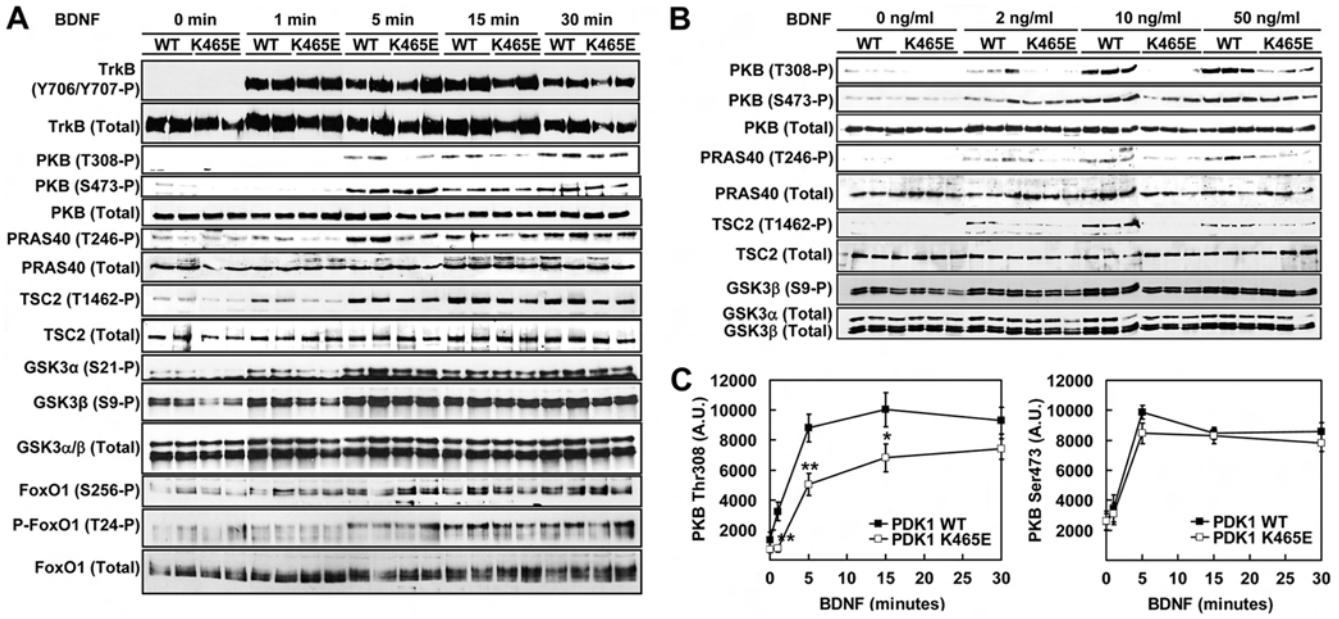

FIG 4 Deficient PKB phosphorylation and activation in PDK1$^{K465E/K465E}$ cortical neurons. (A and B) Cortical neurons from PDK1 wild-type (WT) and PDK1 K465E mouse embryos were cultured for 6 DIV and then serum starved for 4 h and either left unstimulated or stimulated with 50 ng/ml BDNF for the indicated times (A) or for 5 min with the indicated concentrations of BDNF (B). Lysates were immunoblotted with the indicated antibodies. A representative Western blot out of three independent experiments is shown, where each lane represents a sample derived from a different embryo. (C) The effect of the PDK1 K465E mutation on the phosphorylation of PKB at Thr308 and Ser473 was determined by quantitative Western blotting of cell extracts from cortical neurons stimulated as described above for panel A. Values are expressed as arbitrary units (A.U.) and are presented as the means ± standard errors of the means for protein extracts derived from three independent experiments. *, $P < 0.05$; **, $P < 0.005$ (compared with wild-type extracts, as determined by Student's *t* test).

of the neuronal processes was measured at different days *in vitro* (DIV) by scoring the length of the neurites, the number of neurites, and the number of branching points. The ability of the PDK1$^{K465E/K465E}$ embryonic cortical neurons to differentiate in culture was significantly reduced at DIV3, which was further aggravated at DIV4 (Fig. 7A). Indeed, the neurites from the PDK1$^{K465E/K465E}$ embryonic cortical neurons were 20% shorter than control PDK1$^{+/+}$ cells at DIV3; the rate of neurite outgrowth was then nearly null in the PDK1$^{K465E/K465E}$ cultures from DIV3 to DIV4, resulting in neurites that were as much as 40% shorter in the PDK1$^{K465E/K465E}$ cultures by DIV4 (Fig. 7B). To confirm than the reduced length of the PDK1$^{K465E/K465E}$ cortical neurons could not be the consequence of the reduced size of the mutant cells, we also measured the major axis of the neuronal soma and found that this was only 10% shorter in the mutant neurons (Fig. 7C). We also found that the number of neurites and branching points of the mutant neurons was similar to that of the controls, whereas the percentage of undifferentiated cells was significantly higher in the mutant cultures than in the controls (data not shown).

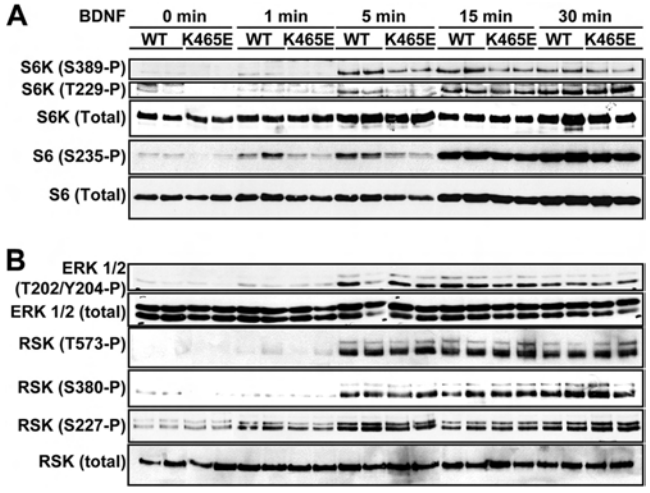

FIG 5 Analysis of S6K and RSK isoforms in PDK1$^{K465E/K465E}$ cortical neurons. Cortical neurons from two PDK1 wild-type (WT) and two PDK1 K465E mouse embryos were cultured for 6 DIV and then serum starved for 4 h and either left unstimulated or stimulated with 50 ng/ml of BDNF for the indicated times. Lysates were immunoblotted with the indicated antibodies to monitor the activation of S6K (A) and RSK (B). A representative Western blot of three independent experiments is shown.

We also took advantage of the widely used model of dissociated hippocampal neurons in culture for studying neuronal polarization (47). We determined axonogenesis during the differentiation of hippocampal primary cultures, as detected by immunocytochemistry with the specific axonal marker Tau-1 and the dendritic marker MAP2. Axon formation and growth were markedly impaired in PDK1$^{K465E/K465E}$ cells (Fig. 8A). While most of the PDK1$^{+/+}$ hippocampal neurons exhibited a differentiated axon by DIV3, the PDK1$^{K465E/K465E}$ hippocampal neurons did not reach this stage of differentiation until DIV4, and the percentage of cells exhibiting one axon was still significantly lower in the mutant cultures than the control ones, at both DIV3 and DIV4 (Fig. 8B). Moreover, the length of the axons was consistently reduced by 25% in PDK1$^{K465E/K465E}$ hippocampal neurons compared to the PDK1$^{+/+}$ controls at all the time points analyzed (Fig. 8C), while the cellular soma was only 5% shorter in the mutant hippocampal cells (data not shown). These results reveal that the interaction of

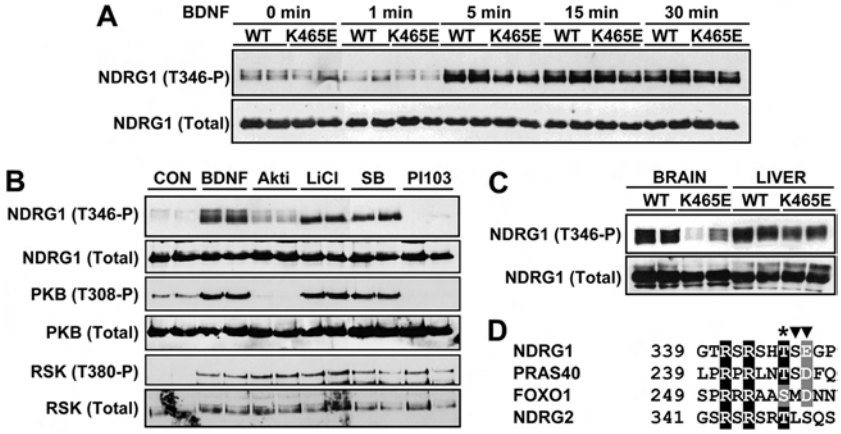

FIG 6 Analysis of SGK in PDK1$^{K465E/K465E}$ cortical neurons. (A and B) Cortical neurons from two PDK1 wild-type (WT) (A and B) and two PDK1 K465E (A) mouse embryos were cultured for 6 DIV and then serum starved for 4 h and either left untreated; stimulated with 50 ng/ml BDNF for the indicated times (A); or pretreated with the SB-216763 (3 μM), Akti-1/2 (1 μM), PI-103 (1 μM), or LiCl (10 mM) compound for 30 min, as indicated, and then stimulated with 50 ng/ml of BDNF for 5 min (B). Lysates were immunoblotted with the indicated antibodies. (C) Mouse brain and liver tissue extracts from the indicated genotypes were subjected to immunoblot analysis with the indicated antibodies. Each lane corresponds to a sample derived from a different mouse. (D) Multiple-sequence alignment of the sequence flanking the indicated phosphorylation sites in NDRG1, NDRG2, PRAS40, and FOXO1. The positions of the first amino acid aligned according to the mouse protein sequences are indicated. The black shading indicates similarity, and the gray shading indicates conservation in more than 50% of the sequences. The phosphorylated threonine or serine residues are labeled with an asterisk. Flanking residues conserved between NDRG1 and PRAS40, but not NDRG2, are marked with an arrowhead.

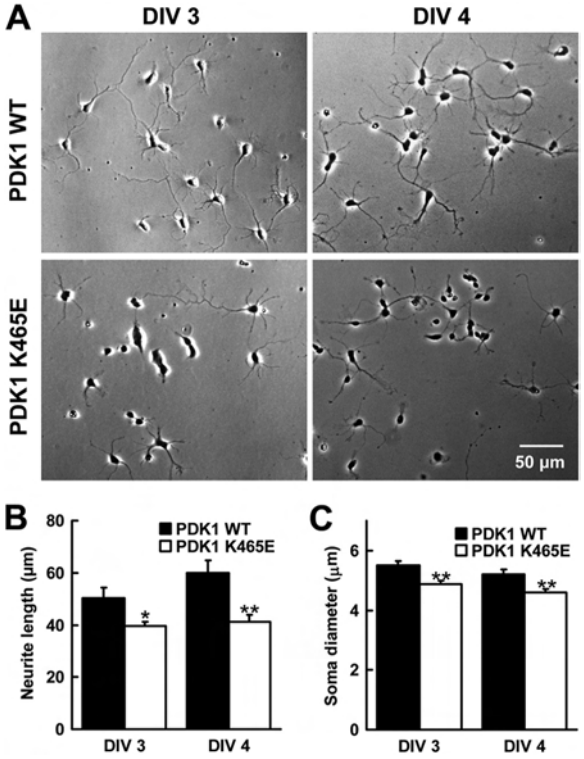

FIG 7 Deficient cortical neuritogenesis in PDK1$^{K465E/K465E}$ mice. (A) Representative micrographs of PDK1 wild-type (WT) and PDK1 K465E cortical neurons at 3 and 4 days *in vitro* (DIV). Bar, 50 μm. (B and C) The total length of the neurites (B) and the soma diameter (C) were measured on digitally acquired images. Each bar represents the mean ± standard error of the mean for 200 to 300 neurons per embryo and four embryos per genotype. *, $P < 0.05$; **, $P < 0.005$ (compared to wild-type controls, as determined by Student's *t* test).

PDK1 with phosphoinositides is required for both cortical and hippocampal neuronal morphogenesis.

To assess whether modulation of PKB activity affected neuronal differentiation directly, primary cultures of hippocampal neurons were allowed to differentiate *in vitro* for 4 days in the presence or absence of the Akti-1/2 isoform-specific inhibitor, and the axon specification and length were measured at different time points. Axon formation and growth were drastically impaired by the Akti-1/2 compound, with the percentage of cells exhibiting one differentiated axon being significantly reduced in the treated cultures compared to the control ones (Fig. 8D). Moreover, the length of the axons was also reduced in the Akti-1/2-treated hippocampal neurons to a similar extent as that observed for the PDK1$^{K465E/K465E}$ mutant cells (compare Fig. 8E and C).

In order to assess whether PKB-dependent deficient mTORC1 activation was mainly responsible for the described phenotypes, we also treated hippocampal primary cultures with the mTORC1-specific inhibitor rapamycin and found that complete inhibition of the mTORC1 pathway compromised neuronal polarization to an extent similar to that observed for the Akti-1/2-treated cells (Fig. 8D). In contrast, axonal elongation was even more severely impaired by rapamycin than by the inhibitor Akti-1/2, resulting in axons that were as much as 50% shorter than those of the untreated cells (Fig. 8E).

The tuberous sclerosis complex proteins TSC1 and TSC2 have been shown to control axon formation by modulating mTORC1 activity and the synthesis of specific proteins that are required for neuronal polarization, such as brain-specific kinase 1 (BRSK1) and BRSK2 (6). BRSK1 and BRSK2 are expressed during the differentiation of the cortex and the hippocampus, where they play fundamental roles in establishing proper neuronal polarity (7, 8). In agreement with that notion, we observed that both the BRSK1 and BRSK2 proteins were expressed at low levels in primary cultures of cortical neurons from the first day *in vitro* and that the

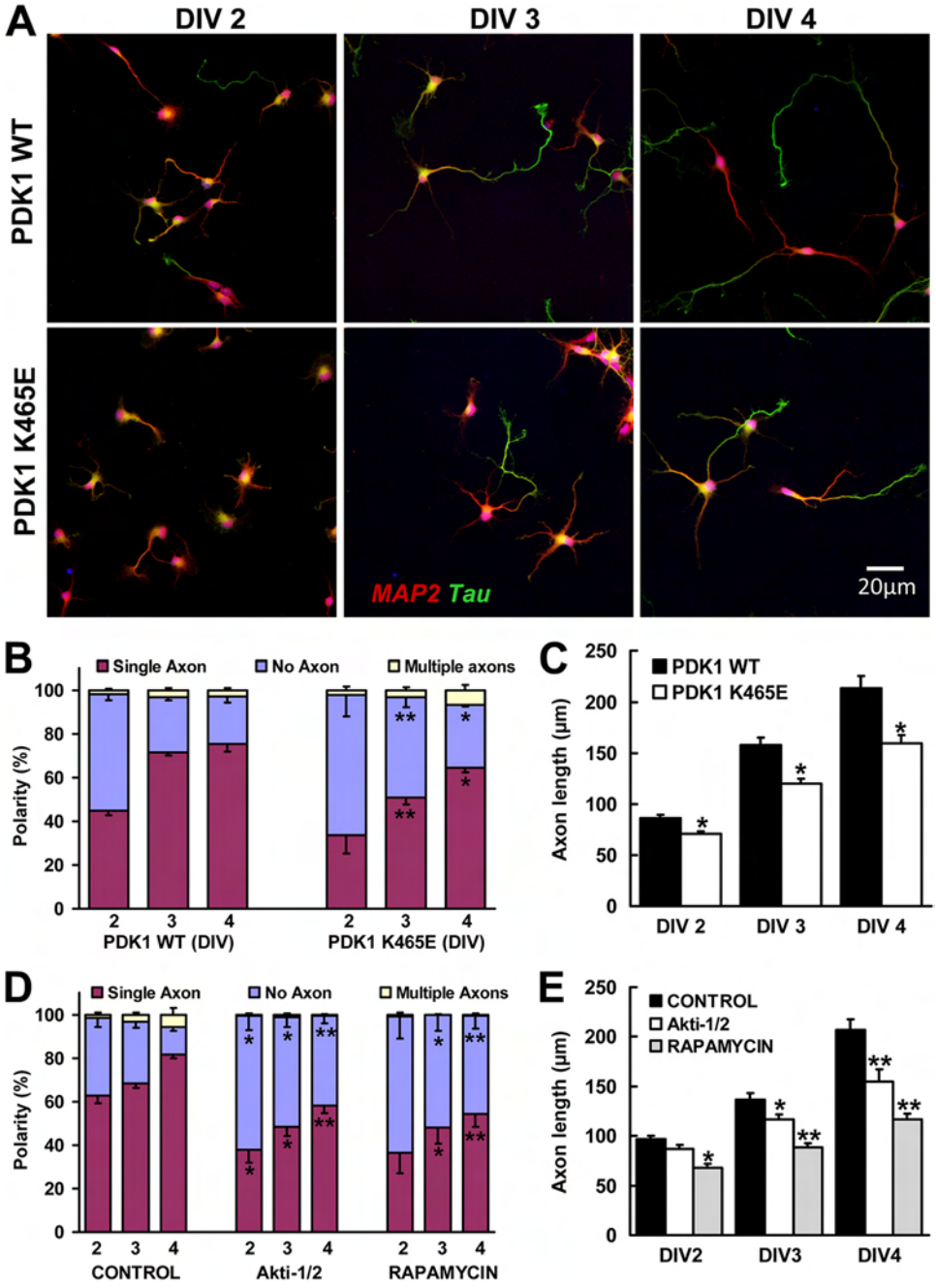

FIG 8 Deficient hippocampal axon formation and growth in PDK1$^{K465E/K465E}$ mice. (A) Representative micrographs of PDK1 wild-type (WT) and PDK1 K465E hippocampal neurons at 2, 3, and 4 days *in vitro* (DIV) stained with antibodies against the dendrite-specific marker MAP2 (red) and the specific axonal marker Tau-1 (green). Bar, 20 μm. (B to E) The percentage of polarization (B and D) and the axon elongation (C and E) of the PDK1 wild-type and the PDK1 K465E hippocampal neurons (B and C) or wild-type cells treated with the indicated inhibitors (D and E) were measured at the indicated time points. Each bar represents the mean ± standard error of the mean for 300 to 500 neurons from five different embryos per condition. *, $P < 0.05$; **, $P < 0.005$ (compared to controls, as determined by the Student *t* test).

levels of expression were then induced by day 3 *in vitro*. Strikingly, expression of the BRSK proteins was significantly reduced in the PDK1$^{K465E/K465E}$ cortical neurons from the first day in culture, which progressively recovered to nearly normal levels throughout the *in vitro* differentiation period (Fig. 9A). In agreement with this observation, BRSK1 and BRSK2 protein levels were also markedly reduced in brain extracts from PDK1$^{K465E/K465E}$ E15.5 embryos, while BRSK1 and BRSK2 protein expression was found to be similar in the adult brains of both the PDK1$^{K465E/K465E}$ and the PDK1$^{+/+}$ mice. In contrast, phosphorylation of PKB at Thr308, PRAS40 at Thr246, and TSC2 at Thr1462 was consistently reduced in the mutant protein extracts during development and in the adult (Fig. 9B). The BRSK1 expression level was also reduced in PDK1$^{K465E/K465E}$ hippocampal neurons compared to that in

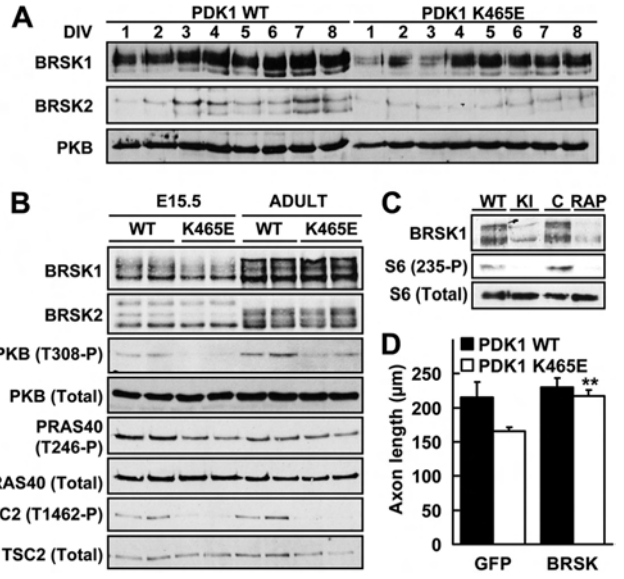

FIG 9 PDK1 promotes hippocampal axonogenesis through the PKB/mTORC1/BRSK pathway. (A) Cortical neurons from PDK1 wild-type (WT) and PDK1 K465E embryos were cultured in complete medium for the indicated times. Lysates were immunoblotted with the indicated antibodies. A representative Western blot of two independent experiments is shown. (B) Brain whole-protein extracts from PDK1 wild-type and PDK1 K465E mice of the indicated age were subjected to immunoblot analysis with the indicated antibodies. Each lane corresponds to a sample derived from a different embryo or mouse. (C) Hippocampal neurons from PDK1 wild-type and PDK1 mutant (KI) mouse embryos were cultured for 4 days in the presence (RAP) or absence (CON) of rapamycin. Lysates were immunoblotted with the indicated antibodies. A representative Western blot of three independent experiments is shown. (D) PDK1 wild-type and PDK1 K465E hippocampal cells were transfected with the indicated expression vectors at DIV2, and the axon length was determined at DIV4. Each bar represents the mean ± standard error of the mean for 100 to 200 neurons from three different embryos per condition. **, $P < 0.005$ compared to controls, as determined by the Student *t* test.

PDK1$^{+/+}$ control cells, and the treatment of these neurons with rapamycin clearly decreased the levels of BRSK1 protein (Fig. 9C). Altogether, these data suggest that the axonal phenotype observed for the PDK1$^{K465E/K465E}$ neurons is likely due to deficient PKB-mediated mTORC1 activation and blunted stimulation of BRSK expression. We tested this notion by reexpressing BRSK1 and BRSK2 in PDK1$^{K465E/K465E}$ hippocampal neurons and found that this rescued the growth deficiencies of the knock-in neurons, whereas it had little effect on the axonal elongation of wild-type cells (Fig. 9D), thereby providing strong evidence that the BRSK isoforms are key downstream targets mediating the actions of PDK1-phosphoinositide interactions in axon morphogenesis.

DISCUSSION

In the PDK1$^{K465E/K465E}$ mouse neurons, activation of PKB was partially inhibited due to an incomplete phosphorylation of PKB at the PDK1 site. Phosphorylation of the PKB Thr308 site was previously shown to be reduced 3- to 4-fold in the insulin-responsive tissues of PDK1$^{K465E/K465E}$ mice (30). We found that the impact of the PDK1 K465E mutation on PKB Thr308 phosphorylation was less severe in neuronal tissues than in insulin-responsive tissues, since BDNF-induced phosphorylation of PKB at Thr308 was reduced by only 2-fold in PDK1$^{K465E/K465E}$ cortical neurons (Fig. 4C). When the PDK1 K465E knock-in mutation was first characterized, the observation that PKB was still phosphorylated at Thr308 in the absence of a PDK1-PtdIns(3,4,5)P_3 interaction was unexpected. More recently, it was proposed that the phosphorylation of PKB at Thr308 detected in PDK1$^{K465E/K465E}$ knock-in embryonic stem (ES) cells relies on the phospho-docking site mechanism (33). It would be interesting to study whether this phospho-docking site-dependent activation of PKB operates more efficiently in neurons than in other cell types. In this regard, the activation of the docking site-dependent kinase S6K, RSK, or SGK, which occurs more slowly than the activation of PKB in several cell types, parallels the activation of PKB in neurons and reaches the maximum at 5 min of BDNF treatment.

We show that the reduced levels of PKB activation are sufficient to support the phosphorylation and inhibition of some cellular targets promoting apoptosis, such as the FOXO1 transcription factor (48) or the GSK3 kinase (49). In contrast, the reduced levels of PKB activation achieved in PDK1$^{K465E/K465E}$ neurons are rate limiting for PRAS40 and TSC2 phosphorylation. The inefficient phosphorylation of PRAS40 and TSC2 resulted in a reduced activation of mTORC1, leading to impaired phosphorylation of S6K at Thr389 within the hydrophobic motif. This most likely compromised the interaction of PDK1 with S6K, resulting in reduced S6K phosphorylation at Thr229 in the activation loop and diminished S6 protein phosphorylation, thereby explaining why the activation of a docking site-dependent kinase appears to be affected by PDK1-phosphoinositide binding. Moreover, we could bypass this requirement by stimulating mTORC1 with amino acids, which rendered normal levels of S6K and S6 protein phosphorylation in the mutant cells (data not shown).

The SGK isoforms are phosphorylated by PDK1 following the phosphorylation of their hydrophobic motif by mTORC2 (23). Because agonist-stimulated mTORC2 activation, as inferred from the levels of PKB Ser473 phosphorylation detected in the PDK1$^{K465E/K465E}$ neurons, is not affected by the PDK1 mutation, and PDK1 can phosphorylate and activate SGK in a PtdIns(3,4,5)P_3-independent manner (50), SGK1 activation was not expected to be affected in the mutant cells. In this regard, insulin-induced phosphorylation of NDRG1 at the SGK1 sites was previously shown to be preserved in the muscle and the liver of PDK1$^{K465E/K465E}$ mice (30). In contrast, phosphorylation of NDRG1 at Thr346/356/366 was reported previously to be severely impaired in several tissues of SGK1 knockout mice, including spleen, lung, liver, and muscle (41). However, we found reduced BDNF-induced phosphorylation of NDRG1 at Thr346/356/366 in PDK1$^{K465E/K465E}$ neurons. Although we failed to detect the phosphorylation of SGK1 at the Thr256 and Ser422 sites, it is unlikely that the phosphorylation of these activation sites by PDK1 or mTORC2 requires the binding of PDK1 to phosphoinositides. In contrast, we provided evidence to suggest that NDRG1 can be phosphorylated by PKB, at least in BDNF-stimulated cortical neurons. Moreover, we observed a reduced phosphorylation of NDRG1 in PDK1$^{K465E/K465E}$ brain extracts (Fig. 6C). In fact, PKB was originally shown to be capable of marginally phosphorylating the NDRG2 isoform at the Thr348 residue (41). In this regard, two of the residues in the NDRG1 sequence that conform to the specific SGK1 phosphorylation signature, namely, Ser at position $n + 1$ and Glu at position $n + 2$ C terminal from the SGK1 phosphorylation site, which were found to be deleterious to phosphorylation by PKB (51), are not conserved in the NDRG2 sequence. In contrast, PRAS40 Thr246, which is a bona fide PKB phos-

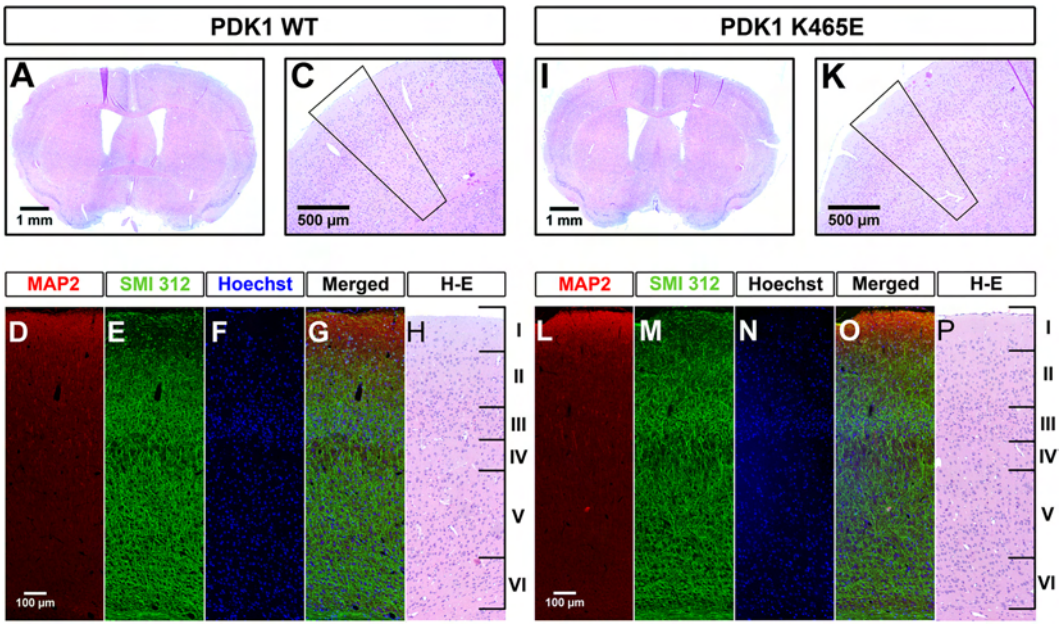

FIG 10 Normal layering and connectivity in the PDK1$^{K465E/K465E}$ adult brain. (Top) Five-micrometer-thick coronal brain sections from PDK1 wild-type (WT) (A and C) and PDK1 K465E (I and K) mice stained with hematoxylin and eosin showing the overall architecture of the rostral adult brain. (Bottom) Epifluorescence microscopy images of PDK1 wild-type (D to H) and PDK1 K465E (L to P) cortexes stained with the dendrite-specific marker MAP2 (D and L), the general axonal marker SMI-312 (E and M), and nuclear Hoechst dye (F and N). The merged signals (G and O) as well as adjacent hematoxylin-and-eosin (H-E)-stained sections (H and P) are also shown. Cortical layers are indicated on the right from I to VI.

phorylation site, possesses Ser at position $n + 1$ and Asp at position $n + 2$ C terminal from the PKB phosphorylation site (Fig. 6D).

Activation of RSK by PDK1 also relies on a phospho-docking site interaction in which the phosphorylation of the RSK hydrophobic motif is under the control of the ERK pathway. BDNF triggers the activation of both the PI3K and the ERK signaling pathways in neurons. As expected, the activation of RSK isoforms by BDNF, as monitored by the phosphorylation of the ERK site, the hydrophobic motif autophosphorylation site, and the T-loop PDK1 site, proceeded normally in the PDK1$^{K465E/K465E}$ neurons.

PDK1$^{K465E/K465E}$ mice are smaller, with a reduced cell volume resulting from deficient activation of the PKB/mTORC1/S6K signaling axis (30). The small-size phenotype is common in mice lacking different elements of this signaling network, including PKBα-deficient mice (52, 53), mTOR hypomorphic mice (54), S6K1-deficient mice (55), or S6K1 and S6K2 double knockout mice (56). In PDK1$^{K465E/K465E}$ mice, the volume of the brain was 20% reduced compared to that of the PDK1$^{+/+}$ controls. Mice lacking the PKBγ gene, which is expressed mainly in neuronal cells, displayed a selective 20 to 25% reduction of the brain size, whereas the rest of the organs analyzed were of a normal size (9, 10). In the PKBα knockout mice, a general reduction in body size that was accompanied by a proportional reduction in the sizes of different organs, including the brain, was also demonstrated (9). While the reduced brain size was attributed mainly to a decrease in the number of cells in the PKBα knockout mice, the reduced brain volume observed for the PKBγ knockout mice was proposed previously to be due mainly to the presence of smaller cells (9). Likewise, our data clearly demonstrate that the reduced brain size of the PDK1$^{K465E/K465E}$ mice is due to a reduction of the cell size, whereas the number of neurons is unaffected. It would be interesting to define whether the number and size of the neurons are specifically controlled by different PKB isoforms or whether the differences observed among the different transgenic mice could be explained in terms of whole PKB activation levels.

One salient finding derived from these studies is that in PDK1$^{K465E/K465E}$ knock-in mice, the survival responses of cortical, hippocampal, and cerebellar neurons to different neurotrophic factors are not compromised. Consistent with this conclusion, the number of neurons in the cortex and hippocampus is similar in PDK1$^{K465E/K465E}$ and control mice. PKB is a central regulator of survival and apoptosis in many neuronal types under many different stimuli. Therefore, the reduced activation of PKB observed in the PDK1$^{K465E/K465E}$ neurons might not be limiting to support the neuroprotective role of this kinase. Consistent with this, we show that the phosphorylation of some key PKB substrates that promote neuronal survival, including GSK3 and FOXO1, was not impaired in the mutant cells. Moreover, inhibition of PKBα and PKBβ, but not PKBγ, by using the Akti-1/2 compound did not compromise the neuroprotective actions of BDNF on cortical neurons deprived of serum, a situation that might resemble that of the PDK1$^{K465E/K465E}$ neurons. Because PKBγ accounts for about 40% of the total PKB protein in brain, these data suggest either that the PKBγ isoform is responsible for BDNF-mediated neuronal survival or that as little as 40% of total PKB activation is sufficient to support the survival of cortical neurons. Another scenario would be that other PDK1-activated AGC kinases different from PKB might also contribute to the neuroprotective functions of BDNF. In this regard, a specific role for SGK1 in mediating survival signals in cerebellar granule cells (11) or for RSK in cortical neurons (12) has also been proposed. Mice expressing specifically the PDK1 L155E mutation, disrupting the PDK1 substrate docking site recognition motif, in the nervous system are being generated by conditional knock-in methodologies (57). These mice will

help much in elucidating the contribution of the docking site-dependent branch of the PDK1 signaling pathway in promoting neuronal survival.

The observation that binding of PDK1 to phosphoinositides contributes to neuronal differentiation is particularly important, because deficient neuronal morphogenesis might result in a reduced ability of neurons to integrate and transmit information within the adult central nervous system, a condition which underlies many neurological and mental conditions in human disease. The differentiation of neuronal precursors onto mature neurons involves several stages that can be recapitulated *in vitro* by using dissociated mouse cortical as well as hippocampal neurons (47, 58). Here we demonstrated that the ability of cortical and hippocampal PDK1$^{K465E/K465E}$ neurons to differentiate *in vitro* was markedly impaired. This conclusion was sustained on the observations that in the PDK1$^{K465E/K465E}$ cortical neurons, the length of the neurites was significantly reduced, while axon formation and growth were diminished in the PDK1$^{K465E/K465E}$ hippocampal neurons. Interestingly, the treatment of wild-type hippocampal cultures with the PKB inhibitor Akti-1/2 or the mTORC1 inhibitor rapamycin mimicked the phenotypes of the PDK1$^{K465E/K465E}$ neurons, thereby suggesting that optimal activation of mTORC1 by PKB is required for the formation and outgrowth of the axon. We also show that the profile of expression of the BRSK isoforms throughout the *in vitro* differentiation period was blunted in PDK1$^{K465E/K465E}$ mice and that reexpression of BRSKs successfully rescued the axonal defects of the mutant hippocampal cultures. The BRSK1 and BRSK2 kinases are required for the polarization of cortical and hippocampal neurons (7, 8). Activation of BRSK isoforms by their upstream kinase LKB1 plays essential roles in neuronal polarization (8). Regulation of BRSK protein expression by TSC2/mTORC1 also influences neuronal polarity (6). Altogether, our data suggest that binding of PDK1 to phosphoinositides, acting through the PDK1/PKB/TSC2/mTORC1/BRSK pathway, is essential to efficiently transmit the extracellular signals that ultimately modulate neuronal polarization and axon outgrowth. Mice lacking both BRSK isoforms exhibited immobility and poor responsiveness and died shortly after birth. Close examination of the central nervous system demonstrated a smaller forebrain with a thinner cortex and neurons failing to form axons (7). As mentioned above, PDK1$^{K465E/K465E}$ mice are nearly viable and exhibited neither an overt phenotype nor gross abnormalities in the architecture of the central nervous system, which exhibited normal cortical layering and connectivity (Fig. 10). This finding is in agreement with the fact that the transient character of the PDK1 K465E mutation may allow the accumulation of sufficient levels of BRSK proteins in the adult tissue. However, it would be interesting to explore whether the hypomorphic reduction of PKB/mTORC1 activation, causing a delayed and/or reduced onset of BRSK protein synthesis and altered neuronal morphogenesis in the PDK1$^{K465E/K465E}$ embryo, would lead to more subtle alterations in the patterning of the central nervous system that could ultimately translate into abnormal behavioral phenotypes.

ACKNOWLEDGMENTS

We thank Dario Alessi (MRC Protein Phosphorylation Unit, Dundee, Scotland) for the mice and the antibodies. We thank Cristina Gutierrez, Mar Castillo, and Núria Barba from the Institut de Neurociencies Cell Culture, Histology, and Microscopy Facilities for technical assistance and Roser Pané, Jessica Pairada, and Nuria Riera from the SCC Estabulari de Rosegadors of the Universitat de Lleida for animal care. We also thank Arnaldo Parra and Carles Saura for their expert advice with the immunohistochemical analysis.

A Ramon y Cajal contract from the Spanish Ministerio de Educación y Ciencia supported J.R.B. T.Z. was supported by a UAB predoctoral fellowship, and X.Z. was supported by a Chinese Scholarship Council predoctoral fellowship. This work was supported by the Ministerio de Sanidad y Consumo (grant FIS-PI070101) and the Ministerio de Ciencia y Innovación (grant AES-PI10/00333).

REFERENCES

1. **Oppenheim RW.** 1989. The neurotrophic theory and naturally occurring motoneuron death. Trends Neurosci. **12**:252–255.
2. **Brunet A, Datta SR, Greenberg ME.** 2001. Transcription-dependent and -independent control of neuronal survival by the PI3K-Akt signaling pathway. Curr. Opin. Neurobiol. **11**:297–305.
3. **Datta SR, Brunet A, Greenberg ME.** 1999. Cellular survival: a play in three Akts. Genes Dev. **13**:2905–2927.
4. **Shi SH, Jan LY, Jan YN.** 2003. Hippocampal neuronal polarity specified by spatially localized mPar3/mPar6 and PI 3-kinase activity. Cell **112**:63–75.
5. **Jiang H, Guo W, Liang X, Rao Y.** 2005. Both the establishment and the maintenance of neuronal polarity require active mechanisms: critical roles of GSK-3beta and its upstream regulators. Cell **120**:123–135.
6. **Choi YJ, Di NA, Kramvis I, Meikle L, Kwiatkowski DJ, Sahin M, He X.** 2008. Tuberous sclerosis complex proteins control axon formation. Genes Dev. **22**:2485–2495.
7. **Kishi M, Pan YA, Crump JG, Sanes JR.** 2005. Mammalian SAD kinases are required for neuronal polarization. Science **307**:929–932.
8. **Barnes AP, Lilley BN, Pan YA, Plummer LJ, Powell AW, Raines AN, Sanes JR, Polleux F.** 2007. LKB1 and SAD kinases define a pathway required for the polarization of cortical neurons. Cell **129**:549–563.
9. **Easton RM, Cho H, Roovers K, Shineman DW, Mizrahi M, Forman MS, Lee VM, Szabolcs M, De Jong R, Oltersdorf T, Ludwig T, Efstratiadis A, Birnbaum MJ.** 2005. Role for Akt3/protein kinase Bgamma in attainment of normal brain size. Mol. Cell. Biol. **25**:1869–1878.
10. **Tschopp O, Yang ZZ, Brodbeck D, Dummler BA, Hemmings-Mieszczak M, Watanabe T, Michaelis T, Frahm J, Hemmings BA.** 2005. Essential role of protein kinase B gamma (PKB gamma/Akt3) in postnatal brain development but not in glucose homeostasis. Development **132**:2943–2954.
11. **Brunet A, Park J, Tran H, Hu LS, Hemmings BA, Greenberg ME.** 2001. Protein kinase SGK mediates survival signals by phosphorylating the forkhead transcription factor FKHRL1 (FOXO3a). Mol. Cell. Biol. **21**:952–965.
12. **Kharebava G, Makonchuk D, Kalita KB, Zheng JJ, Hetman M.** 2008. Requirement of 3-phosphoinositide-dependent protein kinase-1 for BDNF-mediated neuronal survival. J. Neurosci. **28**:11409–11420.
13. **Silverman E, Frodin M, Gammeltoft S, Maller JL.** 2004. Activation of p90 Rsk1 is sufficient for differentiation of PC12 cells. Mol. Cell. Biol. **24**:10573–10583.
14. **Mora A, Komander D, Van Aalten DM, Alessi DR.** 2004. PDK1, the master regulator of AGC kinase signal transduction. Semin. Cell Dev. Biol. **15**:161–170.
15. **Bayascas JR.** 2010. PDK1: the major transducer of PI 3-kinase actions. Curr. Top. Microbiol. Immunol. **346**:9–29.
16. **Pearce LR, Komander D, Alessi DR.** 2010. The nuts and bolts of AGC protein kinases. Nat. Rev. Mol. Cell Biol. **11**:9–22.
17. **Alessi DR, Pearce LR, Garcia-Martinez JM.** 2009. New insights into mTOR signaling: mTORC2 and beyond. Sci. Signal. **2**:e27. doi:10.1126/scisignal.267pe27.
18. **Hara K, Maruki Y, Long X, Yoshino K, Oshiro N, Hidayat S, Tokunaga C, Avruch J, Yonezawa K.** 2002. Raptor, a binding partner of target of rapamycin (TOR), mediates TOR action. Cell **110**:177–189.
19. **Kim DH, Sarbassov DD, Ali SM, King JE, Latek RR, Erdjument-Bromage H, Tempst P, Sabatini DM.** 2002. mTOR interacts with raptor to form a nutrient-sensitive complex that signals to the cell growth machinery. Cell **110**:163–175.
20. **Parekh D, Ziegler W, Yonezawa K, Hara K, Parker PJ.** 1999. Mammalian TOR controls one of two kinase pathways acting upon nPKCdelta and nPKCepsilon. J. Biol. Chem. **274**:34758–34764.
21. **Sarbassov DD, Guertin DA, Ali SM, Sabatini DM.** 2005. Phosphoryla-

tion and regulation of Akt/PKB by the rictor-mTOR complex. Science **307**:1098–1101.
22. **Guertin DA, Stevens DM, Thoreen CC, Burds AA, Kalaany NY, Moffat J, Brown M, Fitzgerald KJ, Sabatini DM.** 2006. Ablation in mice of the mTORC components raptor, rictor, or mLST8 reveals that mTORC2 is required for signaling to Akt-FOXO and PKCalpha, but not S6K1. Dev. Cell **11**:859–871.
23. **Garcia-Martinez JM, Alessi DR.** 2008. mTOR complex 2 (mTORC2) controls hydrophobic motif phosphorylation and activation of serum- and glucocorticoid-induced protein kinase 1 (SGK1). Biochem. J. **416**: 375–385.
24. **Biondi RM.** 2004. Phosphoinositide-dependent protein kinase 1, a sensor of protein conformation. Trends Biochem. Sci. **29**:136–142.
25. **Biondi RM, Kieloch A, Currie RA, Deak M, Alessi DR.** 2001. The PIF-binding pocket in PDK1 is essential for activation of S6K and SGK, but not PKB. EMBO J. **20**:4380–4390.
26. **Currie RA, Walker KS, Gray A, Deak M, Casamayor A, Downes CP, Cohen P, Alessi DR, Lucocq J.** 1999. Role of phosphatidylinositol 3,4,5-trisphosphate in regulating the activity and localization of 3-phosphoinositide-dependent protein kinase-1. Biochem. J. **337**(Part 3):575–583.
27. **Komander D, Fairservice A, Deak M, Kular GS, Prescott AR, Peter DC, Safrany ST, Alessi DR, Van Aalten DM.** 2004. Structural insights into the regulation of PDK1 by phosphoinositides and inositol phosphates. EMBO J. **23**:3918–3928.
28. **Alessi DR, Deak M, Casamayor A, Caudwell FB, Morrice N, Norman DG, Gaffney P, Reese CB, MacDougall CN, Harbison D, Ashworth A, Bownes M.** 1997. 3-Phosphoinositide-dependent protein kinase-1 (PDK1): structural and functional homology with the Drosophila DSTPK61 kinase. Curr. Biol. **7**:776–789.
29. **Stokoe D, Stephens LR, Copeland T, Gaffney PR, Reese CB, Painter GF, Holmes AB, McCormick F, Hawkins PT.** 1997. Dual role of phosphatidylinositol-3,4,5-trisphosphate in the activation of protein kinase B. Science **277**:567–570.
30. **Bayascas JR, Wullschleger S, Sakamoto K, Garcia-Martinez JM, Clacher C, Komander D, Van Aalten DM, Boini KM, Lang F, Lipina C, Logie L, Sutherland C, Chudek JA, van Diepen JA, Voshol PJ, Lucocq JM, Alessi DR.** 2008. Mutation of the PDK1 PH domain inhibits protein kinase B/Akt, leading to small size and insulin resistance. Mol. Cell. Biol. **28**: 3258–3272.
31. **Waugh C, Sinclair L, Finlay D, Bayascas JR, Cantrell D.** 2009. Phosphoinositide (3,4,5)-triphosphate binding to phosphoinositide-dependent kinase 1 regulates a protein kinase B/Akt signaling threshold that dictates T-cell migration, not proliferation. Mol. Cell. Biol. **29**:5952–5962.
32. **Wullschleger S, Sakamoto K, Johnstone L, Duce S, Fleming S, Alessi DR.** 2011. How moderate changes in Akt T-loop phosphorylation impact on tumorigenesis and insulin resistance. Dis. Model. Mech. **4**:95–103.
33. **Najafov A, Shpiro N, Alessi DR.** 2012. Akt is efficiently activated by PIF-pocket- and PtdIns(3,4,5)P3-dependent mechanisms leading to resistance to PDK1 inhibitors. Biochem. J. **448**:285–295.
34. **Bayascas JR.** 2008. Dissecting the role of the 3-phosphoinositide-dependent protein kinase-1 (PDK1) signalling pathways. Cell Cycle **7**:2978–2982.
35. **Lizcano JM, Goransson O, Toth R, Deak M, Morrice NA, Boudeau J, Hawley SA, Udd L, Makela TP, Hardie DG, Alessi DR.** 2004. LKB1 is a master kinase that activates 13 kinases of the AMPK subfamily, including MARK/PAR-1. EMBO J. **23**:833–843.
36. **Rodriguez-Asiain A, Ruiz-Babot G, Romero W, Cubi R, Erazo T, Biondi RM, Bayascas JR, Aguilera J, Gomez N, Gil C, Claro E, Lizcano JM.** 2011. Brain specific kinase-1 BRSK1/SAD-B associates with lipid rafts: modulation of kinase activity by lipid environment. Biochim. Biophys. Acta **1811**:1124–1135.
37. **Collins BJ, Deak M, Arthur JS, Armit LJ, Alessi DR.** 2003. In vivo role of the PIF-binding docking site of PDK1 defined by knock-in mutation. EMBO J. **22**:4202–4211.
38. **Bradford MM.** 1976. A rapid and sensitive method for the quantitation of microgram quantities of protein utilizing the principle of protein-dye binding. Anal. Biochem. **72**:248–254.
39. **Gundersen HJ, Jensen EB.** 1987. The efficiency of systematic sampling in stereology and its prediction. J. Microsc. **147**:229–263.
40. **Anjum R, Blenis J.** 2008. The RSK family of kinases: emerging roles in cellular signalling. Nat. Rev. Mol. Cell Biol. **9**:747–758.
41. **Murray JT, Campbell DG, Morrice N, Auld GC, Shpiro N, Marquez R, Peggie M, Bain J, Bloomberg GB, Grahammer F, Lang F, Wulff P, Kuhl D, Cohen P.** 2004. Exploitation of KESTREL to identify NDRG family members as physiological substrates for SGK1 and GSK3. Biochem. J. **384**:477–488.
42. **Kalaydjieva L, Gresham D, Gooding R, Heather L, Baas F, de Jonge R, Blechschmidt K, Angelicheva D, Chandler D, Worsley P, Rosenthal A, King RH, Thomas PK.** 2000. N-myc downstream-regulated gene 1 is mutated in hereditary motor and sensory neuropathy-Lom. Am. J. Hum. Genet. **67**:47–58.
43. **Okuda T, Higashi Y, Kokame K, Tanaka C, Kondoh H, Miyata T.** 2004. Ndrg1-deficient mice exhibit a progressive demyelinating disorder of peripheral nerves. Mol. Cell. Biol. **24**:3949–3956.
44. **Mitchelmore C, Buchmann-Moller S, Rask L, West MJ, Troncoso JC, Jensen NA.** 2004. NDRG2: a novel Alzheimer's disease associated protein. Neurobiol. Dis. **16**:48–58.
45. **Yamamoto H, Kokame K, Okuda T, Nakajo Y, Yanamoto H, Miyata T.** 2011. NDRG4 protein-deficient mice exhibit spatial learning deficits and vulnerabilities to cerebral ischemia. J. Biol. Chem. **286**:26158–26165.
46. **Swiech L, Perycz M, Malik A, Jaworski J.** 2008. Role of mTOR in physiology and pathology of the nervous system. Biochim. Biophys. Acta **1784**:116–132.
47. **Dotti CG, Sullivan CA, Banker GA.** 1988. The establishment of polarity by hippocampal neurons in culture. J. Neurosci. **8**:1454–1468.
48. **Tran H, Brunet A, Griffith EC, Greenberg ME.** 2003. The many forks in FOXO's road. Sci. STKE **2003**:RE5. doi:10.1126/stke.2003.172.re5.
49. **Cole AR.** 2012. GSK3 as a sensor determining cell fate in the brain. Front. Mol. Neurosci. **5**:4. doi:10.3389/fnmol.2012.00004.
50. **Kobayashi T, Cohen P.** 1999. Activation of serum- and glucocorticoid-regulated protein kinase by agonists that activate phosphatidylinositide 3-kinase is mediated by 3-phosphoinositide-dependent protein kinase-1 (PDK1) and PDK2. Biochem. J. **339**(Part 2):319–328.
51. **Murray JT, Cummings LA, Bloomberg GB, Cohen P.** 2005. Identification of different specificity requirements between SGK1 and PKBalpha. FEBS Lett. **579**:991–994.
52. **Cho H, Thorvaldsen JL, Chu Q, Feng F, Birnbaum MJ.** 2001. Akt1/PKBalpha is required for normal growth but dispensable for maintenance of glucose homeostasis in mice. J. Biol. Chem. **276**:38349–38352.
53. **Chen WS, Xu PZ, Gottlob K, Chen ML, Sokol K, Shiyanova T, Roninson I, Weng W, Suzuki R, Tobe K, Kadowaki T, Hay N.** 2001. Growth retardation and increased apoptosis in mice with homozygous disruption of the Akt1 gene. Genes Dev. **15**:2203–2208.
54. **Zhang S, Readinger JA, DuBois W, Janka-Junttila M, Robinson R, Pruitt M, Bliskovsky V, Wu JZ, Sakakibara K, Patel J, Parent CA, Tessarollo L, Schwartzberg PL, Mock BA.** 2011. Constitutive reductions in mTOR alter cell size, immune cell development, and antibody production. Blood **117**:1228–1238.
55. **Shima H, Pende M, Chen Y, Fumagalli S, Thomas G, Kozma SC.** 1998. Disruption of the p70(s6k)/p85(s6k) gene reveals a small mouse phenotype and a new functional S6 kinase. EMBO J. **17**:6649–6659.
56. **Pende M, Um SH, Mieulet V, Sticker M, Goss VL, Mestan J, Mueller M, Fumagalli S, Kozma SC, Thomas G.** 2004. S6K1(−/−)/S6K2(−/−) mice exhibit perinatal lethality and rapamycin-sensitive 5′-terminal oligopyrimidine mRNA translation and reveal a mitogen-activated protein kinase-dependent S6 kinase pathway. Mol. Cell. Biol. **24**:3112–3124.
57. **Bayascas JR, Sakamoto K, Armit L, Arthur JS, Alessi DR.** 2006. Evaluation of approaches to generation of tissue-specific knock-in mice. J. Biol. Chem. **281**:28772–28781.
58. **Craig AM, Banker G.** 1994. Neuronal polarity. Annu. Rev. Neurosci. **17**:267–310.